Variation in Cortical Bone Distribution in the Aging Adult Appendicular Skeleton

A Dissertation Presented for the

Doctor of Philosophy

Degree

The University of Tennessee, Knoxville

Alice Fazlollah Gooding

December 2017

Copyright © by Alice Fazlollah Gooding
All rights reserved.

ACKNOWLEDGEMENTS

The author would like to acknowledge her doctoral committee for their support, guidance, and patience with this project. Many thanks to Dr. Dawnie Steadman for her professionalism and quiet support. Her consistency in advice kept me grounded at many times when the wheels were falling off. I appreciate her patience and flexibility when working together long-distance. Thank you to Dr. Benjamin Auerbach for being a solid rock of support and guidance through a field I was just entering. His supervision of the mechanics of the document, the quality of the study, and the development of its analysis made this possible. Many thanks to Drs. Amy Mundorff and Zhang Songning for their feedback, editing, and thoughtful suggestions for future work.

I am very thankful to Dr. Adam Sylvester who guided me through data collection for this project. He devoted a great deal of time and effort to ensure the integrity of the project. I look forward to working together again in future and giving him credit for his hard work. Many thanks also to my friends and colleagues who supported this study in its very early stages, including Dr. Donald Chapman, many colleagues at Kennesaw State University, and my closest cohort at UT.

Most importantly, I would like to acknowledge the unending support of my family and friends, particularly my mother, grandmother, and husband, Grant Gooding. They provided a sanctuary to which I could retreat over the years, and the confidence in me to finish the project.

Finally, I thank the donors to the William M. Bass Donated Skeletal Collection. Your selfless act at the end of life has and will continue to support important research in this field and many others.

ABSTRACT

This study considers the effects of age on the distribution of bone in the adult skeleton. Age effects on the skeleton have been studied for diagnosis of osteoporosis or as mechanical compensatory changes to bone shape with loss in density. However, adult skeletal morphology is the result of a lifetime of genetic, dietary, activity, and biochemical factors. With these influences, it unclear at what age(s) bone geometry shifts to adapt to the physiological and mechanical demands placed on it, or, how these adaptations vary within and between bones.

This research addresses these questions by examining skeletal data obtained from the William M. Bass Donated Skeletal Collection (UT). This collection includes modern individuals with documented age at death, and a digital collection of computed tomography (CT) scans to allow quantification of bone morphology through non-destructive means. The scans of 208 individuals are used to test the hypothesis that bone loss with age is sexually dimorphic, affected by body weight and activity, and varies within and between bones as a result of differential loading environments. A total of 30 cross-sectional images from six skeletal elements (humerus, radius, ulna, femur, tibia, and fibula) are examined from each individual. Fifteen geometric properties quantifying bone mass, shape, strength, and rigidity are compared from each cross-section.

Results indicate that geometry is sexually dimorphic and varies across the skeleton. The relationship of geometric properties to age is not linear; skeletal response to aging is more complex than previously understood. Loading environments in the limbs significantly affect bone geometry. In the upper limb, the radius and ulna appear to have complimentary loading-sharing capabilities. Distal limb bones (radius, ulna, and fibula) do not significantly differ in many geometric properties, which has clinical applications for assessment of fracture risk.

Physiological processes associated with senescence are known to decrease bone mass in adults, but the skeletal responses in shape, strength, and rigidity to cumulative effects are rarely studied concomitantly. This study applies conclusions from clinical and anthropological literature to a modern skeletal sample with known demographics, finding that sex, age, and mechanical loading influence the gross morphology of appendicular bone.

TABLE OF CONTENTS

CHAPTER 1 INTRODUCTION 1

Hypotheses and Research Aims 7

Dissertation Layout 11

CHAPTER 2 BONE BIOLOGY AND DEVELOPMENT 13

Limb Bone Development 14
Intramembranous and Endochondral Ossification 14
Heritability of Bone Growth 17
Hormone and Kinetic Signaling 19

Modification of the Limbs 24
Modeling and Remodeling 24
Regulation of Bone Size and Shape 28
Variation in Bone Growth and Mass 32

Chapter Summary 36

CHAPTER 3 STATIC TISSUE MECHANICS 37

Bone Functional Adaptation 38

Engineering Beam Theory 42
Cross-sectional Geometry 47
Scaling 52

Biomechanical Studies in Humans 57
Assessing Mobility 57
Body Mass and Mobility 60

Chapter Summary 61

CHAPTER 4 BONE QUALITY WITH AGE 63

The Aging Skeleton 64
Bone Quality, Mass, and Strength 65
Osteoporosis 67
Hormones and Sex Steroids 70
Structural Compensation for Frailty 74

Modifiable Mechanisms of Bone Loss 75
Nutrition 76
Physical Activity 78
Chronic Disease States 80

Chapter Summary 81

CHAPTER 5 MATERIALS AND METHODS 83

Radiographic Sample 83
Skeletal Collection 83
Selection Criteria 85
Data Collection 89
Segmentation, Alignment, and Slice Selection 89
Diaphyseal Measurements 95
Analytical Methods 96

CHAPTER 6 RESULTS 98

Within Bone Variation 98
Variation by Age Group 116
Variation by BMI, Activity, and Pathology Groups 125
Within Limb Variation 131
Variation in the Upper Limb 132
Variation in the Lower Limb 138
Within Limb Variation Results Summary 144
Between Limb Variation 146
Variation in Proximal Limb Segments 146
Variation in Distal Limb Segments 147
Between Limb Variation Results Summary 149

CHAPTER 7 DISCUSSION AND CONCLUSIONS 151

Synthesis of Within Bone Variation Results 153
Sexual Dimorphism in the Limbs 153
Structural Compensation with Age 155
Mechanical and Physiological Determinants of Bone Geometry 160
Synthesis of Within Limb and Between Limb Variation Results 163
Tapering in the Human Limb 164
Limb Functionality in Bipeds 167
Future Directions and Conclusions 169

LIST OF REFERENCES 173

APPENDICES 193

APPENDIX A ACTIVITY LEVEL ASSIGNMENT CATEGORIES 194

APPENDIX B WITHIN BONE UNIVARIATE COMPARISON RESULTS FOR SLICE AND SEX EFFECTS 195
APPENDIX C WITHIN BONE PAIRWISE RESULTS FOR SLICE AND SEX 198
APPENDIX D WITHIN BONE UNIVARIATE COMPARISON RESULTS FOR SLICE, SEX, AND AGE EFFECTS 214
APPENDIX E WITHIN BONE CORTICAL AREA DISTRIBUTION BY SEX AND AGE 218
APPENDIX F WITHIN BONE LEAST SQUARES MEANS COMPARISONS FOR SEX AND AGE GROUP 234
APPENDIX G WITHIN BONE UNIVARIATE COMPARISON RESULTS FOR SLICE, AGE, SEX, BMI, ACTIVITY, AND PATHOLOGY EFFECTS 264
APPENDIX H WITHIN BONE PAIRWISE COMPARISON RESULTS FOR BMI, ACTIVITY, AND PATHOLOGICAL GROUPS 270
APPENDIX I WITHIN LIMB PAIRWISE COMPARISON RESULTS FOR THE UPPER LIMB 289
APPENDIX J WITHIN LIMB PAIRWISE COMPARISON RESULTS FOR THE LOWER LIMB 297
APPENDIX K BETWEEN LIMB PAIRWISE COMPARISON RESULTS FOR DISTAL LIMB ELEMENTS 305
VITA 313

LIST OF TABLES

Table 1. Cross-sectional properties used to evaluate mechanical performance..... 49

Table 2. Common risk factors associated with osteoporosis in adults 69

Table 3. Final study sample distribution by sex and age for BMI, activity level, and chronic disease condition..... 87

Table 4. BMI categories..... 88

Table 5. Error in maximum length measurement collection..... 91

Table 6. MANOVA results for bone, slice location, sex, and CSG property effects 99

Table 7. MANOVA results for bone, slice location, sex, age group, and CSG property effects 117

Table 8. Geometric trends in the humerus with age 119

Table 9. Geometric trends in the radius with age 120

Table 10. Geometric trends in the ulna with age 121

Table 11. Geometric trends in the femur with age..... 122

Table 12. Geometric trends in the tibia with age..... 123

Table 13. Geometric trends in the fibula with age..... 124

Table 14. MANOVA results for bone, BMI, activity level, pathology group, and CSG property effects..... 126

Table 15. MANOVA results for bone, slice location, and CSG property effects in the upper limb 132

Table 16. Means and standard deviations for CSG properties in the female upper limb 134

Table 17. Means and standard deviations for CSG properties in the male upper limb 136

..... 137

Table 18. MANOVA results for bone, slice location, and CSG property effects in the lower limb 138

Table 19. Means and standard deviations for CSG properties in the female lower limb 140

Table 20. Means and standard deviations for CSG properties in the male lower limb 142

Table 21. MANOVA results for bone, slice location, and CSG property effects between proximal limb segments 147

Table 22. MANOVA results for bone, slice location, and CSG property effects in distal limb segments..... 148

Table A.1. Examples of activities, hobbies, and occupations in the final sample by activity level category..... 194

Table B.1. Results of ANOVA type III models for slice location and sex in the humerus..... 195

Table B.2. Results of ANOVA type III models for slice location and sex in the radius..... 195

Table B.3. Results of ANOVA type III models for slice location and sex in the humerus..... 196

Table B.4. Results of ANOVA type III models for slice location and sex in the femur 196

Table B.5. Results of ANOVA type III models for slice location and sex in the tibia..... 197

Table B.6. Results of ANOVA type III models for slice location and sex in the fibula 197

Table D.1. Results of ANOVA type III models for slice location, sex, and age group in the humerus..... 214

Table D.2. Results of ANOVA type III models for slice location, sex, and age group in the radius 215

Table D.3. Results of ANOVA type III models for slice location, sex, and age group in the ulna 215

Table D.4. Results of ANOVA type III models for slice location, sex, and age group in the femur 216

Table D.5. Results of ANOVA type III models for slice location, sex, and age group in the tibia 216

Table D.6. Results of ANOVA type III models for slice location, sex, and age group in the fibula 217

Table F.1. Cortical area LS means in the upper limb by sex and age..... 234

Table F.2. Cortical area LS means in the lower limb by sex and age..... 235

Table F.3. Total area LS means in the upper limb by sex and age 236

Table F.4. Total area LS means in the lower limb by sex and age group 237

Table F.5. Medullary area LS means in the upper limb by sex and age 238

Table F.6. Medullary area LS means in the lower limb by sex and age group 239

Table F.7. Percent cortical area LS means in the upper limb by sex and age 240

Table F.8. Percent cortical area LS means in the lower limb by sex and age 241

Table F.9. I_x LS means in the upper limb by sex and age 242

Table F.10. I_x LS means in the lower limb by sex and age group 243

Table F.11. I_y LS means in the upper limb by sex and age 244

Table F.12. I_y LS means in the lower limb by sex and age group 245

Table F.13. Polar section modulus (J) LS means in the upper limb by sex and age 246

Table F.14. Polar section modulus (J) LS means in the lower limb by sex and age 247

Table F.15. I_{max} LS means in the upper limb by sex and age 248

Table F.16. I_{max} LS means in the lower limb by sex and age 249

Table F.17. I_{min} LS means in the upper limb by sex and age 250

Table F.18. I_{min} LS means in the lower limb by sex and age 251

Table F.19. Shape (I_{max}/I_{min}) LS means in the upper limb by sex and age 252

Table F.20. Shape (I_{max}/I_{min}) LS means in the lower limb by sex and age 253

Table F.21. Z_x LS means in the upper limb by sex and age 254

Table F.22. Z_x LS means in the lower limb by sex and age group 255

Table F.23. Z_y LS means in the upper limb by sex and age 256

Table F.24. Z_y LS means in the lower limb by sex and age group 257

Table F.25. Z_p LS means in the upper limb by sex and age 258

Table F.26. Z_p LS means in the lower limb by sex and age group 259

Table F.27. Z_{max} LS means in the upper limb by sex and age 260

Table F.28. Z_{max} LS means in the lower limb by sex and age 261

Table F.29. Z_{min} LS means in the upper limb by sex and age 262

Table F.30. Z_{min} LS means in the lower limb by sex and age 263

Table G.1. Results of ANOVA type III models for slice location, age, sex, BMI, activity, and pathology group in the humerus 264

Table G.2. Results of ANOVA type III models for slice location, age, sex, BMI, activity, and pathology group in the radius 265

Table G.3. Results of ANOVA type III models for slice location, age, sex, BMI, activity, and pathology group in the ulna 266

Table G.4. Results of ANOVA type III models for slice location, age, sex, BMI, activity, and pathology group in the femur 267

Table G.5. Results of ANOVA type III models for slice location, age, sex, BMI, activity, and pathology group in the tibia 268

Table G.6. Results of ANOVA type III models for slice location, age, sex, BMI, activity, and pathology group in the fibula 269

Table H.1. Within bone pairwise comparisons for BMI category for the humerus 271

Table H.2. Within bone pairwise comparisons for BMI category for the radius 272

Table H.3. Within bone pairwise comparisons for BMI category for the ulna 273

Table H.4. Within bone pairwise comparisons for BMI category for the femur 274

Table H.5. Within bone pairwise comparisons for BMI category for the tibia 275

Table H.6. Within bone pairwise comparisons for BMI category for the fibula 276

Table H.7. Within bone pairwise comparisons for activity level in the humerus 277

Table H.8. Within bone pairwise comparisons for activity level in the radius 278

Table H.9. Within bone pairwise comparisons for activity level in the ulna 279

Table H.10. Within bone pairwise comparisons for activity level in the femur 280

Table H.11. Within bone pairwise comparisons for activity level in the tibia 281

Table H.12. Within bone pairwise comparisons for activity level in the fibula 282

Table H.13. Within bone pairwise comparisons for activity level in the humerus 283

Table H.14. Within bone pairwise comparisons for activity level in the radius..... 284

Table H.15. Within bone pairwise comparisons for activity level in the ulna..... 285

Table H.16. Within bone pairwise comparisons for activity level in the femur..... 286

Table H.17. Within bone pairwise comparisons for activity level in the tibia 287

Table H.18. Within bone pairwise comparisons for activity level in the fibula 288

Table I.1. Cortical Area (CA) pairwise comparisons by slice location in the upper limb..... 289

Table I.2. Total Area (TA) pairwise comparisons by slice location in the upper limb 289

Table I.3. Medullary Area (MA) pairwise comparisons by slice location in the upper limb 290

Table I.4. Percent Cortical Area ((CA/TA) x 100) pairwise comparisons by slice location in the upper limb 290

Table I.5. Second moment area about ML axis (I_x) pairwise comparisons by slice location in the upper limb 291

Table I.6. Second moment area about AP axis (I_y) pairwise comparisons by slice location in the upper limb 291

Table I.7. Polar section moment of area (J) pairwise comparisons by slice location in the upper limb 292

Table I.8. Maximum second moment area (I_{max}) pairwise comparisons by slice location in the upper limb 292

Table I.9. Minimum second moment area (I_{min}) pairwise comparisons by slice location in the upper limb 293

Table I.10. Shape index (I_{max}/ I_{min}) pairwise comparisons by slice location in the upper limb .. 293

Table I.11. Section modulus about ML axis (Z_x) pairwise comparisons by slice location in the upper limb 294

Table I.12. Section modulus about AP axis (Z_y) pairwise comparisons by slice location in the upper limb 294

Table I.13. Polar section modulus (Z_p) pairwise comparisons by slice location in the upper limb 295

Table I.14. Maximum section modulus (Z_{max}) pairwise comparisons by slice location in the upper limb 295

Table I.15. Maximum section modulus (Z_{min}) pairwise comparisons by slice location in the upper limb 296

Table J.1. Cortical Area (CA) pairwise comparisons by slice location in the lower limb..... 297

Table J.2. Total Area (TA) pairwise comparisons by slice location in the lower limb 297

Table J.3. Medullary Area (MA) pairwise comparisons by slice location in the lower limb..... 298

Table J.4. Percent Cortical Area ((CA/TA) x 100) pairwise comparisons by slice location in the lower limb 298

Table J.5. Second moment area about ML axis (I_x) pairwise comparisons by slice location in the lower limb 299

Table J.6. Second moment area about AP axis (I_y) pairwise comparisons by slice location in the lower limb 299

Table J.7. Polar section moment of area (J) pairwise comparisons by slice location in the lower limb 300

Table J.8. Maximum second moment area (I_{max}) pairwise comparisons by slice location in the lower limb 300

Table J.9. Minimum second moment area (I_{min}) pairwise comparisons by slice location in the lower limb 301

Table J.10. Shape index (I_{max}/ I_{min}) pairwise comparisons by slice location in the lower limb .. 301

Table J.11. Section modulus about ML axis (Z_x) pairwise comparisons by slice location in the lower limb 302

Table J.12. Section modulus about AP axis (Z_y) pairwise comparisons by slice location in the lower limb 302

Table J.13. Polar section modulus (Z_p) pairwise comparisons by slice location in the lower limb 303

Table J.14. Maximum section modulus (Z_{max}) pairwise comparisons by slice location in the lower limb 303

Table J.15. Maximum section modulus (Z_{min}) pairwise comparisons by slice location in the lower limb 304

Table K.1. Cortical Area (CA) pairwise comparisons by slice location in distal limb elements 305

Table K.2. Total Area (TA) pairwise comparisons by slice location in distal limb elements 305

Table K.3. Medullary Area (MA) pairwise comparisons by slice location in distal limb elements 306

Table K.4. Percent Cortical Area ((CA/TA) x 100) pairwise comparisons by slice location in distal limb elements 306

Table K.5. Second moment area about ML axis (I_x) pairwise comparisons by slice location in distal limb elements 307

Table K.6. Second moment area about AP axis (I_y) pairwise comparisons by slice location in distal limb elements 307

Table K.7. Polar section moment of area (J) pairwise comparisons by slice location in distal limb elements 308

Table K.8. Maximum second moment area (I_{max}) pairwise comparisons by slice location in distal limb elements 308

Table K.9. Minimum second moment area (I_{min}) pairwise comparisons by slice location in distal limb elements 309

Table K.10. Shape index (I_{max}/ I_{min}) pairwise comparisons by slice location in distal limb elements 309

Table K.11. Section modulus about ML axis (Z_x) pairwise comparisons by slice location in distal limb elements 310

Table K.12. Section modulus about AP axis (Z_y) pairwise comparisons by slice location in distal limb elements 310

Table K.13. Polar section modulus (Z_p) pairwise comparisons by slice location in distal limb elements 311

Table K.14. Maximum section modulus (Z_{max}) pairwise comparisons by slice location in distal limb elements 311

Table K.15. Maximum section modulus (Z_{min}) pairwise comparisons by slice location in distal limb elements 312

LIST OF FIGURES

Figure 1. Modeling and remodeling to achieve the adult form 26

Figure 2. Periosteal expansion with age 29

Figure 3. Summary ranks for health factors in Tennessee counties 35

Figure 4. Bone remodeling equilibrium 40

Figure 5. Basic loading conditions experienced by a beam (long bone) 44

Figure 6. Generalized stress-strain curve for cortical bone 46

Figure 7. Typical class 3 lever in the human body 55

Figure 8. Age-related declines in hormones ultimately result in a decrease in bone mass 71

Figure 9. Trends in adult obesity and diabetes in the United States 82

Figure 10. Bone segmentation from CT scan image stack 90

Figure 11. Surface model construction and alignment 93

Figure 12. Slice locations with example cross-sections 94

Figure 13. Cortical area (CA) by bone and sex within each element 101

Figure 14. Total area (TA) by bone and sex within each element 102

Figure 15. Medullary area (MA) by bone and sex within each element 103

Figure 16. Percent Cortical Area (%CA) by bone and sex within each element 104

Figure 17. Second moment of area about the mediolateral (ML) axis (I_x) by bone and sex within each element 105

Figure 18. Second moment of area about the anteroposterior (AP) axis (I_y) by bone and sex within each element 106

Figure 19. Polar second moment of area (J) by bone and sex within each element 107

Figure 20. Maximum second moment of area (I_{max}) by bone and sex location within each element 108

Figure 21. Minimum second moment of area (I_{min}) by bone and sex within each element 109

Figure 22. Shape index by bone and sex within each element 110

Figure 23. Section modulus about the mediolateral (ML) axis (Z_x) by bone and sex within each element 111

Figure 24. Section modulus about the anteroposterior (AP) axis (Z_y) by bone and sex within each element 112

Figure 25. Polar section modulus (Z_p) by bone and sex within each element 113

Figure 26. Maximum section modulus (Z_{max}) by bone and sex within each element 114

Figure 27. Minimum section modulus (Z_{min}) by bone and sex within each element 115

Figure 28. Summary age changes to bone properties of bone mass, shape, strength, and rigidity in females 129

Figure 29. Summary age changes to bone properties of bone mass, shape, strength, and rigidity in males 130

Figure 30. Summary differences in bone mass, strength, and rigidity in the upper and lower limbs 145

Figure 31. Summary differences in bone mass, shape, strength, and rigidity in proximal and distal elements 150

Figure C.1. Cortical area (CA) by sex and slice location within each element 199

Figure C.2. Total area (TA) by sex and slice location within each element 200

Figure C.3. Medullary area (MA) by sex and slice location within each element 201

Figure C.4. Percent Cortical Area (%CA) by sex and slice location within each element 202

Figure C.5. Second moment of area about the mediolateral (ML) axis (I_x) by sex and slice location within each element 203

Figure C.6. Second moment of area about the anteroposterior (AP) axis (I_u) by sex and slice location within each element 204

Figure C.7. Polar second moment of area (J) by sex and slice location within each element 205

Figure C.8. Maximum second moment of area (I_{max}) by sex and slice location within each element 206

Figure C.9. Minimum second moment of area (I_{min}) by sex and slice location within each element 207

Figure C.10. Shape index by sex and slice location within each element 208

Figure C.11. Section modulus about the mediolateral (ML) axis (Z_x) by sex and slice location within each element 209

Figure C.12. Section modulus about the anteroposterior (AP) axis (Z_y) by sex and slice location within each element 210

Figure C.13. Polar section modulus (Z_p) by sex and slice location within each element 211

Figure C.14. Maximum section modulus (Z_{max}) by sex and slice location within each element 212

Figure C.15. Minimum section modulus (Z_{min}) by sex and slice location within each element. 213

Figure E.1. Cortical area (CA) by sex and age group within each element..... 219

Figure E.2. Total area (TA) by sex and age group within each element 220

Figure E.3. Medullary area (MA) by sex and age group within each element 221

Figure E.4. Percent Cortical Area (%CA) by sex and age group within each element 222

Figure E.5. Second moment of area about the mediolateral (ML) axis (I_x) by sex and age group within each element 223

Figure E.6. Second moment of area about the anteroposterior (AP) axis (I_y) by sex and age group within each element 224

Figure E.7. Polar second moment of area (J) by sex and age group within each element..... 225

Figure E.8. Maximum second moment of area (I_{max}) by sex and age group within each element 226

Figure E.9. Minimum second moment of area (I_{min}) by sex and age group within each element 227

Figure E.10. Shape index (I_{max}/I_{min}) by sex and age group within each element..... 228

Figure E.11. Section modulus about the mediolateral (ML) axis (Z_x) by sex and age group within each element..... 229

Figure E.12. Section modulus about the anteroposterior (AP) axis (Z_y) by sex and age group within each element 230

Figure E.13. Polar section modulus (Z_p) by sex and age group within each element..... 231

Figure E.14. Maximum section modulus (Z_{max}) by sex and age group within each element 232

Figure E.15. Minimum section modulus (Z_{min}) by sex and age group within each element 233

Figure F.1. Results of cortical area LS means comparisons in the upper limb by sex and age.. 234

Figure F.2. Results of cortical area LS means comparisons in the lower limb by sex and age.. 235

Figure F.3. Results of total area LS means comparisons in the upper limb by sex and age..... 236

Figure F.4. Results of total area LS means comparisons in the lower limb by sex and age..... 237

Figure F.5. Results of MA LS means comparisons in the upper limb by sex and age 238

Figure F.6. Results of MA LS means comparisons in the lower limb by sex and age 239

Figure F.7. Results of percent CA LS means comparisons in the upper limb by sex and age ... 240

Figure F.8. Results of percent CA LS means comparisons in the lower limb by sex and age ... 241

Figure F.9. Results of I_x LS means comparisons in the upper limb by sex and age group..... 242

Figure F.10. Results of I_x LS means comparisons in the lower limb by sex and age group..... 243

Figure F.11. Results of I_y LS means comparisons in the upper limb by sex and age group..... 244

Figure F.12. Results of I_y LS means comparisons in the lower limb by sex and age group..... 245

Figure F.13. Results of J LS means comparisons in the upper limb by sex and age 246

Figure F.14. Results of J LS means comparisons in the lower limb by sex and age 247

Figure F.15. Results of I_{max} LS means comparisons in the upper limb by sex and age..... 248

Figure F.16. Results of I_{max} LS means comparisons in the lower limb by sex and age group ... 249

Figure F.17. Results of I_{min} LS means comparisons in the upper limb by sex and age 250

Figure F.18. Results of I_{min} LS means comparisons in the lower limb by sex and age 251

Figure F.19. Results of shape index LS means comparisons in the upper limb by sex and age. 252

Figure F.20. Results of shape index LS means comparisons in the lower limb by sex and age. 253

Figure F.21. Results of Z_x LS means comparisons in the upper limb by sex and age..... 254

Figure F.22. Results of Z_x LS means comparisons in the lower limb by sex and age group 255

Figure F.23. Results of Z_y LS means comparisons in the upper limb by sex and age 256

Figure F.24. Results of Z_y LS means comparisons in the lower limb by sex and age 257

Figure F.25. Results of Z_p LS means comparisons in the upper limb by sex and age 258

Figure F.26. Results of Z_p LS means comparisons in the lower limb by sex and age 259

Figure F.27. Results of Z_{max} LS means comparisons in the upper limb by sex and age 260

Figure F.28. Results of Z_{max} LS means comparisons in the lower limb by sex and age 261

Figure F.29. Results of Z_{min} LS means comparisons in the upper limb by sex and age 262

Figure F.30. Results of Z_{min} LS means comparisons in the lower limb by sex and age 263

CHAPTER 1

INTRODUCTION

This dissertation examines the relationship between aging and senescence with biomechanical properties in the diaphyses of the long bones of the appendicular skeleton among adult humans. Understanding the changes in bone material and mechanical properties with adult senescence is important for a variety of applications, from clinical treatment to interpretations of activity in archaeological and paleontological skeletal remains. Yet, while bone mineral properties and histologic variation among old-age adults have been subjects of intense study (reviewed below and in further detail in Chapter 4), few researchers have also examined the geometric distribution of cortical bone within cross-sections of diaphyses (cross-sectional geometric properties) as a measure of changes in mechanical properties with agedness among the limbs.

Bone loss in human adulthood is nearly universal (Garn 1971; Nelson and Weiss 1999; Pfeiffer and Lazenby 1994). Changes in metabolism, the emergence of endocrine and disease processes, genetic variations, and decline in activity are among the factors that affect bone mass and the macroscopic geometry of cortical bone in cross-section in adulthood. However, researchers have not established the broad patterns of age-related change within and between limb elements in cortical bone cross-sectional geometric properties for humans aged more than 40 years. While age-related bone mineral loss is well established (Agarwal 2007; Agarwal and Grynpas 1996; Grynpas 2003; Martin 1993; Martin 2003), we do not know whether there is an age at which bone geometry changes to adapt to age-related bone loss. Because of restrictions inherent in collecting longitudinal clinical data, no such studies have been conducted. We must

rely on cross-sectional data taken from the skeletal remains of individuals with documented demographic and anthropometric data. Age-related patterns in cross-sectional morphology measured at death reflect the cumulative effects of environmental and genetic factors within individuals (Agarwal 2016). Their documentation establishes a baseline currently missing from the literature necessary for future studies of senescence and bone mechanics, measured herein using cross-sectional geometric properties.

Researchers have established the relationship between senescence and changes in bone mineral properties. These investigations use bone mineral content (BMC) or bone mineral density (BMD) as values for assessing bone strength (Forwood and Burr 1993; Turner 2002). The vast majority of these previous examinations of bone loss and decrease in bone strength were conducted with clinical studies of living individuals, focusing on the relationships between bone mass and fracture risk as a result of hormonal changes (Anderson et al. 1963; Riggs et al. 2002) and the effectiveness of exercise intervention at preventing or rescuing bone from lost mass (Smith et al. 2010; Smith and Walker 1964; Vincent et al. 2012; Wallace and Cumming 2000). Others examine kinematic changes in gait as a result of age-related osteoarthritis (Aspden 2008; Paquette et al. 2015; Rasnick et al. 2016). While these and other studies have established a model for bone material properties, they cannot describe how elements will respond to loading alone. A more robust evaluation of bone rigidity and resilience includes diachronic changes, targeted resorption and deposition, and geometric distribution of bone.

A small number of studies of diaphyseal cross-sectional geometry have identified age-related patterns in cortical bone distribution, primarily by augmentation in medullary and total bone area. In adult males and females, long bone diaphyses demonstrate a pattern of subperiosteal apposition and endosteal resorption as age increases (Biver et al. 2016; Martin and

Atkinson 1977; Mays 2001; Ruff and Hayes 1982). Medullary area and subperiosteal area both increase with age along the diaphyses of the second metacarpal (Garn et al. 1992; Mays 2001), the femur (Ruff and Hayes 1982; Smith and Walker 1964) and tibia (Ruff and Hayes 1982), and the humerus and radius (Biver et al. 2016). Across studies, females consistently show greater rates of endosteal resorption, particularly after menopause. In both sexes, this relationship between age and resorption is linear and results in a decrease in cortical bone (but not necessarily bone bending rigidity). These findings corroborate clinical observations of decreasing BMD and BMC with age, especially in females after age 50 and men after 60 (Karlsson et al. 2000). A major shortcoming to these studies, however, is that most only include individuals with a minimum age of fifty, and older ages above 70, which are common in industrialized populations. This range does not adequately capture the scope of skeletal variation with age; little is known about how bone cross-sectional properties change in sexagenarians, septuagenarians, and older age groups. Further, these studies do not look at the distribution of cortical bone, which reflects directional loading despite changes in bone at a histological scale (Eleazer and Jankauskas 2016) and instead only consider changes in total area.

Only two studies have examined measures of bone's mechanical strength (section moduli) and rigidity (second moments of area (SMAs)). Ruff and Hayes (1982) examined eleven locations across the diaphyses of the femur and tibia to find that maximum, minimum, and polar SMAs increased with age in the Pecos Pueblo archaeological collection. As ages were estimated using skeletal markers for Pecos Pueblo, and therefore were prone to age estimation errors as outlined by Boldsen and others (2002), the applicability of their finding to other studies with documented ages-at-death and sex is limited (e.g., Garn et al. 1992; Mays 2001). Although the individuals from Pecos Pueblo displayed the pattern of net bone loss as expected, an increase in

SMAs meant that more bone was located farther from the centroid of the cross-section, increasing its rigidity. These results were sex and location-specific within each bone, likely as a result of differential loading conditions from sex-specific work roles within the culture. Martin and Atkinson (1977) found similar results in a modern autopsy collection, but only in males, possibly reflecting a difference in activity patterns between Pecos Pueblo and modern individuals.

In other analyses, the upper limb, the humerus, radius, and second metacarpal have demonstrated similar, but more limited, patterns. Biver and colleagues (2016) studied a combination of documented twentieth century male skeletons and living males, finding that humeral and radial bending strength and radial torsional strength were greater among individuals occupationally engaged in "heavy-loading activity" from a young age. Heavy loading during early adulthood results in increased bone strength and slows the expected pattern of subperiosteal expansion and medullary resorption of later adulthood. Their study combined individuals across a range of ages, whereby, they could not distinguish at what age the changes occurred (other than after 45 years). Their sample also did not permit an investigation into sex effects on diachronic change in bone cortical geometry.

These studies are limited in a number of ways addressed in this dissertation. First, as noted, most studies do not include a large age range of individuals or rely on broad age categories (Biver et al. 2016), or rely on estimated age of skeletal material (Ruff and Hayes 1982). As a result, no specific age range has been identified for the transitional shift to net bone loss or specifically when shape changes may occur to mechanically compensate for increasing frailty of the material. That the differences in these patterns between the sexes remain unresolved is a consequence of sampling to date. Second, the effects of age on diaphyseal

geometry have not been compared between the upper and lower limbs within the same sample. Regardless of occupation or habitual activity, the upper and lower extremities are functionally designed to adapt to different loading requirements (e.g. walking versus manipulation). Comparisons of differences between elements from the upper and lower limbs within individuals presents one method for determining whether shifts in cortical bone properties are systemic or localized (e.g. Reeves, 2014). Finally, there is no documentation of morphological changes within the ulnar or fibular diaphyses with age, likely based on an assumption that they contribute little to sharing the load experienced by the limb segment. It is remiss to leave them unexamined, though, precisely because these bones experience loads differently than their paired counterparts (Auerbach et al. 2017), and so may exhibit different sensitivities to the effects of aging than their paired elements. They serve as a further test of systemic versus local effects of age-related changes in cortical bone geometric properties.

This dissertation contributes to previous research and addresses gaps in knowledge by testing the relationship between age and diaphyseal cortical bone distribution across an adult age range that captures mid-life and senescence in a modern sample. A cross-sectional (as opposed to longitudinal) sample (n = 208) of modern adult males and females over a large age range (40-99 years) is used to compare cross-sectional (CSG) properties of the long bones of the upper and lower limbs (humerus, radius, ulna, femur, tibia, and fibula). Cross-sectional geometric properties are collected at five locations along the length of the diaphyses (20%, 35%, 50%, 65%, and 80% of bone length) to address three aims:

1) The primary goal is to document the relationship between age and diaphyseal cortical bone distribution within each bone. That is, do the long bones of the limb follow the precedent patterns of net periosteal expansion and endosteal resorption as age

increases? Prior studies suggest that this pattern is linear with age, but it is uncertain if this will be the case in individuals older than 60 years. Do differences in these patterns exist between the sexes? Does variation exist With BMI, activity level, or chronic pathology? Assuming the anisotropic nature of long bones, do differences exist in distribution of cortical bone among the five sites within each bone?

2) A second aim of this research is to assess variation in cortical bone distribution within each limb. These comparisons test the relationship within human (and all tetrapod) limbs between one proximal bone followed by two paired distal bones. Does tapering of the limb have an effect on properties of bone mass, shape, bending strength, and rigidity?
3) The final aim of this dissertation is to compare variation between the limbs. These comparisons test whether relationships exist between proximal elements and between distal elements, despite vastly different loading environments, namely from locomotion and body weight. How are differences in distribution of bone at the sites or between the bones reflective of differences in the mitigation of mechanical loads? Is there evidence for systemic as well as localized effects of bone loss?

These three objectives are accomplished using computed tomography (CT) scans of modern individuals from the William M. Bass Donated Skeletal Collection. As opposed to CT studies focusing primarily on the midshaft, results from this study provide a "whole bone" and "whole limb" perspective (Cristofolini et al. 2010; Gosman et al. 2013; Hubbell et al. 2011) on variation in cortical bone distribution across the limbs. As these data were previously collected, this study is retrospective in nature.

Hypotheses and Research Aims

As noted, the aim of this research is to test the relationships between age and cortical bone apposition and resorption in the human limbs, particularly in the later years of the modern human life span. To address this aim, the cross-sectional diaphyseal geometry of three bones of the upper limb (humerus, radius, ulna) and three bones of the lower limb (femur, tibia, fibula) are compared. Each limb, and the bones within, experience and mitigate biomechanical forces differently as a result of differential distribution of body mass and locomotor repertoires *in vivo*. The first set of hypotheses outlined below establishes the existence of an average shift in geometry with age and the relationship between cortical bone distribution and sex within elements. This has yet to be documented in a modern sample of individuals with known age and sex. The second set of hypotheses addresses intra-limb variation and whether selection for limb tapering in humans has resulted in varying abilities of the bone to resist deformation and failure under loading. While the geometric effects of limb constraint have been studied in various hominin species and young adult humans, they have not been tested in older adults. The final set of hypotheses examines inter-limb variation. Precisely because the human limbs have vastly different roles related to locomotion and carrying of body mass, diaphyseal variation should be evident.

Mid-life to elderly adults are an appropriate population in which to assess the changing biomechanics of the limb bones after skeletal maturity. Previous research has examined many of these relationships, but with discrete comparisons. The hypotheses outlined below were developed from what is currently known about cortical bone distribution in the limbs and changes to that distribution as a result of bone functional adaptation (see Chapter 3 for full discussion). Bone mass has been shown to systemically decrease with age (Garn 1970; Nelson

and Weiss 1999; Pfeiffer and Lazenby 1994) as a result of normal physiological processes of aging, while other structural changes, such as an increase in medullary and total subperiosteal areas (Ruff and Hayes 1982; Smith and Walker 1964) also occur as mechanical compensation for the increase in strain from low bone mass. These relationships, along with comparison of all properties quantifying diaphyseal geometry, have not yet been examined across all of the long bones. Hypotheses used to test for the existence of functional adaption in the adult years, and throughout the adult skeleton, are grouped into three main sets based on the aims of this study.

Hypothesis Set 1- Within Bone Variation

a. When comparing the sexes, males are expected to have greater bone mass, shape, strength, and rigidity than females in all bones. Sexual dimorphism in adult human cortical bone distribution has been established by a number of studies both clinical (Ahlborg et al. 2003, Meakin et al. 2014) and anthropological (Burr 1997, Peck and Stout 2007), as the result of hormonal changes throughout life. However, the magnitude of difference between the sexes, particularly, in older age groups and across multiple elements is unknown.

b. When comparing age groups within each sex, older age groups are expected to have decreased cross-sectional property values of cortical bone, but increased measures of medullary and total area. This increase has been argued by Ruff and Hayes (1982) and others (Biver et al. 2016; Martin and Atkinson 1977; Mays 2001) to serve as a compensation for lower bone mass, and thus should result in similar measures of bending strength and rigidity throughout the adult years. This compensatory model has yet to be

documented in the upper limb, and at multiple sites along the diaphyses of all six limb bones.

c. Other determinants of cortical bone distribution- body mass, habitual activity level, and chronic disease states- are expected to have an effect on diaphyseal geometry. Individuals with higher body mass indexes (BMIs) will corroborate previous studies (Moore 2013, Reeves 2014) by demonstrating greater properties of bone mass and bending strength and rigidity. Similarly, because of increased force from activity, individuals with higher reported levels of activity will show greater values of mass, strength, and rigidity. Because many chronic disease states contribute to lower bone mass (Imel 2014, Stout 1989, Wong et al. 2007), it is expected that mass and all other CSG properties will be reduced in individuals whose cause of death fell into the pathological category. Although prior studies have examined these effects, none have done so with older adults and across the limbs.

Hypothesis Set 2- Within Limb Variation

a. When comparing measures of cortical bone distribution in the upper limb, the humerus is expected to show greater CSG properties at all diaphyseal locations than the two paired bones- the radius and ulna. Because of their shared loading environment, the radius and ulna will not differ significantly in measures of bending strength and rigidity. The precise load-sharing relationship between these two distal bones is still unclear and their geometric properties have not been compared in older adults.

b. In the lower limb, the femur is expected to show greater CSG properties at all diaphyseal locations than the two paired bones- the tibia and fibula. Although the tibia and fibula share a loading environment, the vast difference in muscle action (i.e. force) on the tibia will result in greater values of all CSG properties than in the fibula.

Hypothesis Set 3- Between Limb Variation

a. The bones of the proximal limb segments- the humerus and femur- will differ significantly in all CSG properties. While they share a similar position in their respective limbs, the femur is responsible for mitigating forces associated with body mass and locomotion. As such, the femur will demonstrate greater properties of bone mass, shape, and bending strength and rigidity than the humerus. This has yet to be studies in older adults, in which a decrease in loading (both from body mass and activity) are common.

b. When comparing the bones of the distal limb segments- the radius, ulna, tibia, and fibula- the tibia is expected to exhibit greater values of CSG properties than the other three bones at all diaphyseal locations. Because the radius and ulna share a relatively equal load of forces across the lower arm, they are expected to have greater bone mass, strength, and rigidity properties than the fibula, which takes on a much smaller proportion of loads in the leg with its paired bone, the tibia (Auerbach et al. 2017; Goh et al. 1992; Takebe et al. 1984).

Dissertation Layout

The expectations outline above aim to identify 1) whether an average shift in diaphyseal geometry exists at a particular age within bones, 2) how cortical bone distribution differs within limb segments, and 3) whether any relationship exists between limb bone distribution despite differences in loading environments. Given the anisotropic nature of bone as a material, support of these expectations suggests that not only does each bone experience mechanical loads differently, but that loads are mitigated differently even within a single element. Furthermore, a relationship exists between skeletal senescence, cortical bone remodeling, and diaphyseal dimensions. Support of expectations also suggests that adult patterns in cortical bone loss and a decrease in strength are sex and bone-specific.

An understanding of bone development and aging is fundamental before presenting the analyses of this dissertation. Chapter 2 summarizes the physical and biochemical processes of human limb bone development and maintenance. I review the mechanisms behind bone growth before skeletal maturation and modification of bone throughout life, which produces the variation in adult form. Genetic and hormone signaling of bone growth are covered, as well cell kinetics of the growth plate. The chapter concludes by reviewing modeling and remodeling, the regulatory processes of bone size and shape. Variation in these processes as a result of environmental stressors is also highlighted.

The third chapter describes bone functional adaptation and its use in the assessment of bone morphology, namely through the estimation of static bone mechanical properties. Bone functional adaptation provides the theoretical model for understanding the adaptive responses of bone to forces exerted on it, so it may withstand them without failing. To measure these effects, engineering beam theory is applied for quantifying the cross-sectional geometry of long bone

diaphyses. As a key method for studying bone properties in previous research as well as this dissertation, these concepts are reviewed in detail with respect to bone functional adaptation.

The fourth chapter illustrates the scope and application of these perspectives and methods to understanding aging of the human skeleton. Clinical and anthropological studies of declining bone mass and osteoporosis are then reviewed with particular attention to the trend of decreasing bone strength correlated with loss in bone mass. With bone loss also comes patterns of apposition, which may serve as a compensatory measure for the loss of mechanical strength. Understanding what is currently known about patterns of cortical bone gain and loss throughout life is vital to testing the existence of similar patterns in this sample.

Chapter 5 outlines the sample and methodologies used to collect and analyze the data for this dissertation. The nature and composition of the radiographic sample and selection criteria are provided. Then, methods are reviewed, including the creation of 3-dimensional computer models for each bone, extraction of diaphyseal cross-sectional slice, and calculation of CSG properties from each slice. The chapter concludes by summarizes the statistical analyses used in this research.

The sixth chapter provides the results of the statistical analyses. These are organized by the three aims and hypothesis sets of the study- within bone variation, within limb variation, and between limb variation. Chapter 7 discusses these results in the same organizational structure. Potential explanations are offered while limitations inherent with the sample and methods are highlighted throughout.

CHAPTER 2

BONE BIOLOGY AND DEVELOPMENT

As this dissertation investigates changes in cortical bone apposition and loss with senescence, it is essential to document the biological processes that underlie the modification of cortical bone. Osteogenesis and the regulation of bone size and shape throughout life are modulated by intrinsic (e.g. genetic, age, sex, diet, and biochemical) and extrinsic (e.g. body mass, activity or locomotor patterns) factors. Variation in these factors likely results in shifts in diaphyseal geometry and failure to preserve bone with increasing age. Normal physiological aging determinants, changes in mobility, and pathological processes associated with adulthood alter how the genome and environment interact to affect bone. This chapter reviews these intrinsic and extrinsic factors, relating them to the growth and maintenance of bone. These concepts are fundamental for the review of the response of bone to a changing environment, either due to mechanical loads (reviewed in Chapter 3) or the biological changes associated with aging (considered in Chapter 4).

To this end, it is critical to understand the developmental underpinnings of bone morphology and cell turnover that ultimately result in the adult form. Thus, I begin with a review of the formation of bone and limb development, including factors influencing these, before examining some of the sex, age, mechanical, and environmental regulators of bone size and shape. Because the skeletal system is multi-functional, it should be noted that these processes are not aimed solely at the modification of bone geometry, but many physiological functions (e.g. hematopoiesis) that are beyond the scope of this study.

Limb Bone Development

Long bone growth requires the orchestration of a number of different processes to achieve adult form, which is the focus of this dissertation. Achievement of the adult form occurs through the processes of modeling and remodeling. These processes occur inside the context of complex interactions within and between the genome, biochemical signaling, and mechanical environments, which together initiate and regulate skeletal development. The effects of these interactions are cumulative and vary with age, sex, bone, and even within bones, ultimately resulting in the variation seen at any one point in time.

To understand the processes of bone modification through modeling and remodeling, one first must appreciate the development bone, and the factors that guide those events. Bone development commences in utero during the third trimester and continues until early adulthood, and thus adult bone morphology reflects aspects of this long period of growth and development. Growth of the long bones of the limbs occurs in three dimensions, though through different processes. Increases in length are primarily the result of endochondral activity, wherein a cartilage model (anlage) of bone is replaced by bone. Changes in diameter (both anteroposterior and mediolateral) are largely the result of intramembranous growth, wherein bone is deposited without the anlage (Currey and Butler 1975). These processes are not discrete, but interrelated through genetic, biochemical, and mechanical factors. A number of these processes and their influence on skeletal growth and adult variation are discussed in this chapter and in Chapters 3 and 4.

Intramembranous and Endochondral Ossification

Endochondral ossification occurs during primary bone growth and development, especially in the long bones of the limbs, as well as the basicranium and portions of the axial

skeleton. Intramembranous ossification is the first process of bone formation in utero and continues to play a role in bone apposition into adult years, primarily in the bones of the cranial vault, the viscerocranium, and the flat bones of the postcrania (e.g. the scapula) (Erlebacher et al. 1995; O'Connor et al. 2010; Scheuer and Black 2000). Both processes are generally finished by adulthood, though, as reviewed below, apposition of bone to the periosteum of limb bone diaphyses with age has similarities to intramembranous growth. By adulthood, most bone growth occurs through processes other than these. Nevertheless, to understand the appearance of the adult skeleton, the processes that were active both in its origination and in its maintenance, it is useful to review the factors that contribute to these methods of bone formation.

Before ossification can commence, mesenchymal tissue is condensed into the earliest precursor of the bone- the skeletal blastema. Within this condensation mesenchyme cells differentiate into osteoblasts, regulated by transcription factors Sox9 and RUNX2 (O'Connor et al. 2010) and the oxytocin gene and receptor (Colaianni et al. 2014). Mineralization begins with the formation of hydroxyapatite crystals from calcium and phosphates, regulated by proteoglycans (Allen and Burr 2014; Burr and Akkus 2013). Mature crystals are deposited within collagen fibrils of early osteoid (Bruder and Caplan 1989) where they continue to grow, resulting in the formation of bone nodules. When a large density of nodules is reached, the matrix becomes vascularized and woven bone forms. This early bone is comprised of small trabeculae bridging mesenchymal cells, eventually growing into a network of boney spicules known as the primary spongiosa. As the primary spongiosa grows by way of increased osteoid deposition on the trabeculae, the structure becomes the primary center of ossification (Scheuer and Black 2000). From this center, the trabeculae increase in length (Ogden 1979) while secondary trabeculae are laid down in a perpendicular fashion. The mineralized structure is still covered

with mesenchyme, which then converts into the periosteum. The trabecular structure will continue to expand until it reaches the periosteum, which then develops a thin layer of cortical bone to enclose and protect the internal bone. This process continues as the bone matures and begins to take its adult form. Any later changes to the bone's structure will be the result of remodeling (discussed below) (Scheuer and Black 2000).

The nature of endochondral ossification starts as intramembranous (Scheuer and Black 2000), but ultimately forms bone based on a cartilaginous template or "target". The process begins when the external cells of the blastema form a perichondrium, under which chrondoblasts reside in preparation for division (Purves et al. 2004). Formation of the perichondrium is initiated by the transcription factor Sox9 (Allen and Burr 2014; O'Connor et al. 2010). Chondroblast division and subsequent secretion of type II collagen result in the formation of the cartilage model.

Ossification begins with the thickening of the perichondrium in the center (midshaft) of the diaphysis model and differentiation of osteoblasts from osteoprogenitor cells. This process results in a periosteal collar around the midshaft of the cartilage template (Allen and Burr 2014; Purves et al. 2004). As the individual matures, the collar is remodeled into the compact bone of the adult diaphysis. Because this bone is largely periosteal and continues to be osteogenic throughout life, this portion of a long bone forms via intramembranous ossification (Scheuer and Black 2000).

The epiphyses (or secondary and tertiary centers of ossification) also form via endochondral ossification. Isogenic cells in the center of the cartilage model of the epiphysis begin to hypertrophy while matrix vesicles begin the process of crystal formation. Vascularization occurs through cartilage canals at many different sites on the non-articular

surface of the epiphysis (Brookes 1963). As in the diaphysis, osteoid is laid down and then remodeled into the mature trabecular structure. The cartilaginous border of the ossification center serves as the growth plate of the epiphysis. As the center grows, chrondrocytes proliferate in the growth plate and are later replaced by trabecular bone (Scheuer and Black 2000).

Increase in bone length- and width to some degree- is the result of the cellular processes at a separate growth plate between the new diaphysis and epiphysis (O'Connor et al. 2010; Rang 1969). The physiology of this plate can be understood as a series of five cellular zones, each serving a function in the growth of the bone. Chondrocytes undergo mitosis, regulated by bone morphogenic proteins (BMPs), Indian hedgehog protein (IHH), and somatropin among others (Allen and Burr 2014). After hypertrophy, the chondrocytes begin to degenerate (Felber et al. 2011), modulated by homeobox genes Dlx5 and Dlx6 (O'Connor et al. 2010; Tadic et al. 2002). The replacement of chondrocytes by hydroxyapatite causes the diaphyseal growth plate to unite with the epiphysis. At this point, the epiphyseal trabeculae convert to a terminal plate, which serves as a separation of the epiphyseal and diaphyseal marrow spaces (Martin et al. 1998; Scheuer and Black 2000; Weinmann and Sicher 1974). Ultimately the rate of chondrogenesis will be surpassed by osteogenesis, initiating the process of epiphyseal union (Rang 1969).

Heritability of Bone Growth

As shown above, the formation of the adult skeletal morphology requires internal (i.e. genetic) controls to regulate cell division rate and size of the physeal plate and thereby changes in bone length (Frost and Jee 1994; Villemure and Stokes 2009). Bone growth and development are clearly the product of gene by environment interactions, whereby environmental factors, such as nutrition and metabolism, affect gene expression. The influence of the environment and the timing that these occur during growth and development have only recently been examined. These

interactions likely explain a portion of the variation documented in this study, although to what degree cannot be known.

A few studies have investigated the relationship between genes and environment when examining the timing in which environmental variance contributes to bone length variance on a bone-specific level. In a large sample of modern Americans of European ancestry with known familial relationships, obtained from the Fels Study, Duren and colleagues (2013) found that through two years of age, phenotypic trait variance matches variance due to genetic relatedness; the environment has minimal effect on variation in bone lengths (barring possible effects due to shared environments between siblings). Between three to six years of age, the variance in length still remains similar to genetic variance, which remains the case until late adolescence. The length of the second metacarpal is sexually dimorphic by age 14, which corroborates the results of other longitudinal studies using smaller samples sizes (Nguyen et al. 2001; Ruff 2003a). The oxytocin receptor gene may be responsible for bone gain throughout this time as it readily binds with estrogen in both sexes (Duren et al. 2011; Duren et al. 2013).

Research in the amount of variation in diaphyseal dimensions that is reflected in genetic variance (as measured through relatedness) has largely focused on changes in diameter and distribution or thickness of cortical bone. In the same study as the examination of length variance reviewed above, Duren and colleagues (2013) demonstrated that second metacarpal (MC2) diameter is sexually dimorphic by two years of age. Differences in MC2 diameter between the sexes remain constant until 14 years of age, when they increase. However, more relevant to the mechanics of the metacarpals, cortical thickness distribution is roughly equal between males and females until about 10 years. At this point, females display thicker dimensions until 15 years when male dimensions rapidly surpass those of females. Duren also found that cortical index is

sexually dimorphic (females are higher) by two years, continuing through 35 years. Overall, these authors report that only 50% of variance in cortical bone diameters by an age of two years is attributable to shared genes between siblings, though this increases after that age to 74% of the variance, decreasing again to approximately 50% into adulthood. In a mouse model, Wallace and colleagues (2012) corroborated these patterns finding that genetic contribution had a large effect on femoral cross-sectional indices.

It is clear from these studies that factors that distinguish the sexes are active early in ontogeny in shaping both bone length and cortical bone properties. Moreover, these distinctions are only in part explained through direct genetic control; gene by environment interactions are increasingly responsible for individual variation with age. Hormones and signals from movement (kinetic signaling) are two factors that distinguish between the sexes and are essential factors for understanding bone growth and development and bone maintenance (or lack of) in adults.

Hormone and Kinetic Signaling

In addition to a genetic component, bone growth requires biochemical and mechanical stimuli to regulate division rate in the physeal plate, size of the proliferation zone, rate of expansion and size of hypertrophic cells, and the rate of division of the stem cell at the top of each cell column (Frost and Jee 1994; Villemure and Stokes 2009). These controls can be classified as temporal (short or long term) or spatial (Armstrong 1988). Differentiation of cells may be explained by diffusion gradients of substances that are either produced in the growth plate or brought in by vascularization. At a set point of concentration, they change cell activity from proliferation to expansion.

Of particular interest to this dissertation are hormonal substances—notably estrogen and testosterone—that place a vital role in bone development (O'Connor et al. 2010; Syed and

Khosla 2005) and bone maintenance with age. Their particular effects on the adult skeleton are discussed in Chapter 4. Although historically attributed only to their sex-specific effects (i.e. estrogen in females, testosterone in males), these sex steroids are now understood to be integral to bone growth and maintenance in both sexes (Orwoll 2003; Syed and Khosla 2005; Vanderschueren et al. 2004). Much of this research is experimental in nature using genetically modified mice, which leaves some components of hormonal influences unclear.

Estrogens play a vital role in building peak bone mass. Premenarcheal females can gain up to 83% of adult bone mass density (BMD), but the associated exposure of estrogen at puberty can increase bone mass up through the 30s (Lloyd et al. 1992; Warren 1999). The hormone is known to have an "osteoprotective" effect in females (O'Connor et al. 2010; Syed and Khosla 2005), as estrogen is thought to regulate osteoblasts during differentiation. In female knockout mice in which estrogen receptors are blocked, bone turnover is reduced, specifically that which increases trabecular bone density. Male mice with the same receptors knocked out demonstrated a reduction in bone resorption, resulting in the opposite effect as female mice (Sims et al. 2002).

The relationship between androgens, such as testosterone, and achievement of peak BMD is less understood (LeBoff and Glowacki 1999; Warren 1999). Some studies suggest that testosterone can alter the lifespan of mature osteoblasts and osteocytes (Manolagas 2000; Syed and Khosla 2005). The influence of androgens in the growth of the female skeleton is even less understood (O'Connor et al. 2010). Female mice with androgen receptors knocked out have shown no skeletal abnormalities, but more studies are needed to investigate other possible causes of these results (Syed and Khosla 2005). The role of estrogens and androgens in surface-specific remodeling are discussed in a later section and their role in bone senescence is reviewed further in Chapter 4.

Despite healthy hormone levels, stem cells contain only a limited amount of biochemical signals necessary for division. When that concentration is too low, proliferation stops. Somatomedin levels are the most likely biochemical factor and closure of the growth plate is largely explained by adrenogenic hormone levels. In immature lab animals given these hormones, an acceleration of growth is seen, followed by a premature cessation of growth and closure of the plate. Also possible is that the stem cell is capable of only a certain number of divisions (Armstrong 1988; Robling and Turner 2009; Villemure and Stokes 2009).

The degree of influence of hormones on skeletal growth and adult variation is also likely related to the local mechanical loading environment. Understanding how bone adaptation to mechanical forces during growth and throughout life requires a review of kinetic signaling. A decrease in the rate or efficiency of cell kinetic signaling may be one mechanism for the loss of bone in adulthood. The developmental relationship between the epiphysis and metaphysis is also a function of kinetic activity of the growth plate. Two hypotheses exist about the kinetic system of division and hypertrophy of physeal chondrocytes. The first suggests that within a single growth plate, the rate of cell proliferation and the determination of the size of the cells are independently controlled. Alternatively, within a single organism, cell proliferation rate is the same across all growth plates, but the sizes of the proliferative zones are specific to each plate. The rate of longitudinal growth has been shown to be equal to the rate of new cell production multiplied by the average height of the hypertrophic cells (Martin et al. 2015; Sissons 1955). Cell production is dependent on the division rate and number of dividing cells in the proliferation zone. Histological studies have shown there is only 30% variation in size of hypertrophic cells, which limits the variability in division rate as well (Armstrong 1988).

Further investigation into cell kinetics has revealed mechanical mechanisms underlying modulation of physeal activity. Villemure and Stokes (2009) demonstrate that the zone of hypertrophy is the most flexible region in the growth plate, and as such, experiences the greatest amount of loading during growth. Following this reasoning, this zone is important in providing mechanical stimuli for reducing chondrocyte volume. Tanck and colleagues (2006) found that in growing pig tibiae, trabecular structure at the diaphyseal end of the growth plate filled with bone as a response to increased loading. They conclude that the process of metaphyseal ossification is due to the large number of osteocytes in this region, which are believed to be mechanically sensitive (Cowin et al. 1991; Robling and Turner 2009). Similar results were demonstrated in computational modeling by Cox et al. (2011), which indicated that osteocytes under mechanical stimulation are responsible for the turnover of physeal cartilage into bone. Collectively these results provide much needed evidence for the mechanical processes that induce bone growth and regulate its homeostasis (Robling and Turner 2009).

Loading stress as a result of muscle contractions is required for the development of cartilage and bone at the growth plate and will later be required for maintenance of adult bone tissue (Chen et al. 2010; Cowgill 2010; Hall and Herring 1990; Lieberman and Pearson 2001; Tardieu et al. 2006). In utero, paralysis of major muscle groups can lead to slowed growth velocity in the limbs (Hall and Herring 1990). *In vivo*, the Hueter-Volkmann Principle (Braun et al. 2006; Hueter 1862; Stokes 2002) suggests that growth velocity at the epiphyseal plate is decelerated by compressive loading along the axes and increased by reduced loading. Although seemingly contradictory, muscle contractions generally produce tensile forces across bone, whereas body mass and associated ground force reaction compressively load long bones along their axes. Clinical studies document tall vertebrae in paralytic patients where reduced loading

resulted in a decrease in mechanical regulation of growth in length (Gooding and Neuhauser 1965; McCall et al. 1981). Both in rat tail vertebrae and human patients with scoliosis, unbalanced force distribution was attributed to differential growth between compression and tensile sides (Stokes et al. 1996). Because this imbalance occurred during growth, these asymmetries were corrected when load distribution was reversed (Mente et al. 1999). When growth is finished, bone apposition is stimulated by both muscle contractions and ground reaction force, although muscle contraction appears to have a greater effect with age (Kerr et al. 1996a). Additional relationships between mechanical loading and apposition with advanced age are discussed in Chapter 4.

A more macroscopic perspective of the interplay of the genome and mechanical influences is of use to the current study, in which many of the influences during growth and development cannot be measured. Rauch and Schoenau (2001) suggest that bone development is the cumulative effect of mechanically-induced growth determinants and regulators. There are two functional phases of bone development: 1) skeletal patterning (based on a genetic plan) and 2) the mineralization process where information about where bone needs to be added and removed is provided by mechanical strain. Early theoretical models argued that the entire blueprint of a bone is contained in the genes of the bone model. Although there is strong evidence this is true during embryonic patterning, the fault in this approach is the assumption that the genome contains information on the adult structure, placement of trabeculae and osteons, and how each bone cell assembles the final product. The storage of this amount of information in the genome seems improbable and ignores other physiologic and environmental (mechanical) influences on the development of bone shape and size. Further, as an individual ages, environmental factors (e.g. activity level) change considerably, which may contribute to

variation in cortical bone regardless of genomic determinants. A number of these environmental influences and their morphological impacts are discussed later in this chapter and in Chapters 3 and 4.

Modification of the Limbs

Bone growth and maintenance, especially in the limbs, requires the orchestration of a number of different processes to achieve the adult form. As reviewed above, growth in length is primarily the result of endochondral activity, while growth in diameter is largely the result of intramembranous activity (Scheuer and Black 2000). The shape and integrity of the bone are modified by two additional processes, modeling and remodeling. Through these mechanisms, bone is able to dynamically resist the mechanical stresses and strains that result from growth and changes in loading (largely due to locomotor activity), and a reservoir is created for bone mass while maintaining a functionally light structure. In the adult skeleton, it is these processes of modeling and remodeling that are responsible for the preservation of bone density and modification of bone shape to compensate for loss in that density with age. This dissertation tests for the existence of some of these modifications through the quantification of diaphyseal geometry in the mature skeleton.

Modeling and Remodeling

Though primary ossification of tissue establishes bone shape and size, it does not result in a geometry of the bone that is best suited to the mechanical demands placed on the limbs and skeletal elements within. Bones must be modified throughout growth to maximize their function. Changes to bone shape, and size after ossification, from modeling, or the independent actions of

bone formation (osteoblasts) and bone resorption (osteoclasts) initiated by tissue strain (O'Connor et al. 2010; Olsen et al. 2000). Modeling is usually continuous at a site, though the rate of modeling reduces with advancing skeletal maturity, and is generally thought to cease in adulthood (with potentially important exceptions, noted below). In the long bones, metaphyseal modeling reduces bone diameter but results in an increase in bone mass systemically. As the bone grows, new metaphyseal bone must be constricted to create the diaphysis via osteoclastic activity on the periosteal surface of the metaphysis. This pattern is evidenced most prominently in bones that require flaring metaphyses (e.g. proximal tibia) to properly manage mechanical loads (Gosman et al. 2013) (Figure 1). Modeling in long bones can also occur on the endosteal and periosteal surfaces of the diaphyses. Resorption on the endosteal surface and addition of bone to the periosteal surface result in enlargement of the shaft. Site-specific changes and periosteal expansion in adults as a result of modeling are discussed later sections. Unidirectional resorption and deposition on these surfaces will result in diaphyseal drift or a change in the curvature of the bone. Similarly, modeling alters the curvature of the cranial bones to accommodate continued growth throughout childhood (Allen and Burr 2014; Martin et al. 1998).

As opposed to modeling, remodeling occurs throughout life, though its rate does slow after skeletal maturity (Allen and Burr 2014; Martin et al. 1998; Pivonka et al. 2008). Remodeling is the paired action of osteoblastic and osteoclastic activity at one site to replace previously formed bone. It can be classified as targeted remodeling or stochastic remodeling. Targeted remodeling is believed to be initiated by microdamage and osteocyte apoptosis at sites that have been mechanically compromised. Alternatively, stochastic remodeling is more likely responsible for calcium homeostasis with no site-specific signal. Maintenance of somatic

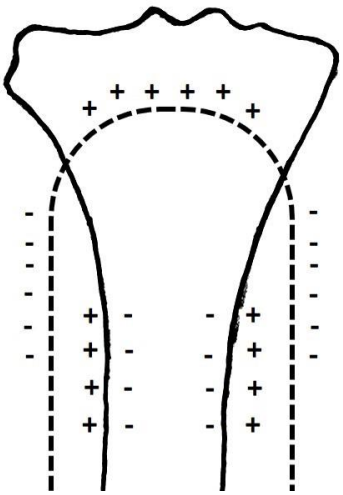

Figure 1. Modeling and remodeling to achieve the adult form
The cartilaginous bone model (dashed outline) will be modified through apposition (+) and resorption (-) of none to narrow the metaphysis, and expand the diaphysis and medullary cavity. This process achieves the most mechanically stable size and shape for the demands experienced by adult bone.

calcium levels becomes more difficult in older adults, which contributions to the increase in stochastic remodeling with age. Remodeling does not usually affect the macroscopic shape of the bone, but contributes greatly to its structural integrity by repairing fatigue cracks and other trauma (Burr et al. 1998), as well as becoming the cause of bone porosity with age. This process, then, results in the maintenance of or slight decrease in bone mass. Because of its role in the repair process, it tends to occur in shorter, more defined, episodes.

Basic multicellular units (BMUs), comprised of a small number of osteoclasts and often hundreds of osteoblasts, perform the work of modeling and remodeling. Osteoclasts, a specialized type of macrophage cell, remove bone, while osteoblasts produce the organic matrix

of bone, into which they incorporate the mineral matrix of bone. In modeling, these two cell types work on different surfaces of the bone (e.g., the endosteal and periosteal surfaces of a long bone). The cells work in concert to remove and replace bone in remodeling. A BMU operates in six basic stages to remodel a primary osteon and create a secondary one. The first stage, activation, happens when monocytes fuse together to form osteoclasts and osteoblasts are recruited to form the BMU. Next, a resorption phase begins. The osteoclasts tunnel longitudinally through the bone, secreting acids that demineralize the bone and enzymes to dissolve the collagen component at approximately 40 μm per day. A capillary bud that provides nutrients and a supply of progenitor cells for the BMU leads this 'cutting zone'. The reversal stage signals the end of the cutting zone and the beginning of osteoblastic activity. In the formation stage, osteoblasts then line the border of the cutting zone and lay down concentric lamellae, leaving a Haversian canal for a nutrient artery. After osteoid is laid down, the site will enter the mineralization stage in which mineral crystals will form within the network of collagen fibers. This process can continue for six months (but can vary with the age and health of the individual) and is followed by the quiescence phase. Here, the osteoblasts are taken away or turned into osteocytes and the secondary osteon has reached full maturity. This entire process happens in a similar fashion in trabecular bone although BMUs create and refill trenches of trabeculae. Remodeling of trabecular bone also happens at a much faster rate- approximately 25% faster per year- than cortical bone (Martin et al. 1998; Scheuer and Black 2000).

Understanding factors influencing rates of modeling and remodeling is key to the interpretation of variation in the amount and distribution of bone between the sexes and throughout the lifespan. Cumulative rates of modeling and remodeling ultimately determine the size and shape of a bone at any particular point in time. In a longitudinal study, rates of

remodeling and modeling within an individual can be empirically tested across time. However, in the case of a cross-sectional study such as the one herein, it is useful to review the site-specific locations on which these processes occur and some of the regulatory factors that may determine the morphology of the bone throughout life.

Regulation of Bone Size and Shape

The evidence presented above demonstrates that the shape and architecture of bones are the result of genetic control and interaction with the environment, which mediate some factors that modify bone (e.g. hormones) or directly affect bone maintenance (e.g., mechanical loading and BMUs; see Chapter 3). Not only do the effects of these interactions vary with age and sex, with also vary within a single skeletal element. Clinically, mechanical influences on adult bone maintenance are presented in a more limited and systemic fashion, primarily as intervention strategies (e.g. lifting weight to increase or maintain BMD) (Smith et al., 2010; Smith and Walker, 1964; Vincent et al., 2012; Wallace and Cumming, 2000). These relationships require further investigation, particularly in regards to the interaction between genotypes and environmental influences and their effects on the fully mature skeleton at different locations. To understand some of these possible interactions, it is useful to review how and where bone size and shape is regulated during growth.

Modeling occurs on four surfaces (periosteal, trabecular, intracortical, and endosteal) of the growing bone. Periosteal expansion increases with age, particularly in older adults (Biver et al., 2016; Martin and Atkinson, 1977; Mays, 2001; Ruff and Hayes, 1982) (Figure 2). This is the function of site-specific mechanical loading (see Chapters 3 and 4) and biochemical regulators of apposition (Gosman et al. 2011). Biochemical influences on periosteal bone formation include periostin, parathyroid hormone (PTH), insulin-like growth factor (IGF-I) and growth hormone

(GH), and sex steroids. The sex steroids have been identified as having age-related influences including estrogen which prohibits periosteal apposition and androgens that enhance periosteal apposition (Daly et al. 2004; Frisancho et al. 1970; Gosman et al. 2011; Parfitt 2002a; Salle et al. 2002; Schoenau et al. 2000; Venken et al. 2008).

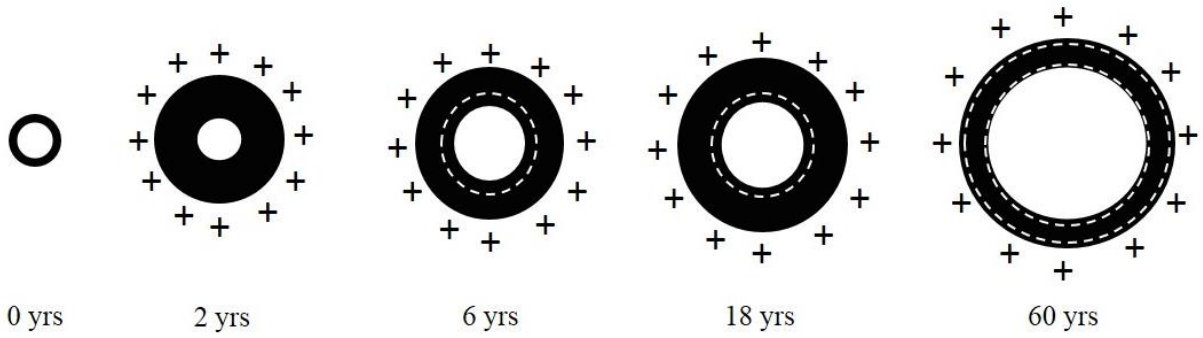

Figure 2. Periosteal expansion with age
Idealized model of a human long bone cross-section across the lifespan. Plus marks (+) indicate patterns of periosteal modeling, which increases with age and results in a net increase in total cross-sectional area. Dashes (-) indicate endosteal and intracortical resorption, causing expansion of the medullary cavity throughout life and a decrease in total cortical area in adulthood. This figure is adapted from Martin et al. (1998), Riggs et al. (2004), and van der Meulen and Carter (1999).

Conversely, modeling of the microstructure of trabecular bone is likely initiated by maternal-fetal perturbations (Salle et al. 2002). These early influences may affect peak bone mass in adolescence, which is a primary factor in the variation observed in adult bone mass. First, intrauterine environmental influences may interact with the genome to establish neonatal bone mass (Cooper et al. 2002). This interaction is referred to as “fetal programming” theory (Duren et al. 2013) and may serve in part to increase or decrease cell numbers in the growth plate (Gosman et al. 2011). Trabecular architecture in young children can be attributed to changes in joint kinematics during locomotor ontogeny. Particularly, the increased flexion in the hip and

knee in infants decreases and reaches adult status around seven years of age. Loading patterns during this time generate higher ground reaction forces (Beck et al. 1981), which create and increase the valgus angle (Tardieu et al. 2006) after heel strike is established around 18 months (Gosman et al. 2011; Ruff 2003c). After the transition to walking is completed, ground reaction forces decrease in magnitude and change in direction, causing slight accommodations in trabecular structure through adolescence (Frost and Jee 1994; Gosman et al. 2011). Although trabecular architecture approaches adult patterning by late childhood, changes in cortical bone structure and shape continue into adulthood.

Modeling of the remaining two surfaces—intra- and endocortical—is characterized by the progressive and methodical process of shape readjustment, primarily in length and diameter (Gosman et al. 2011). During years of peak growth longitudinal and appositional growth of the metaphysis is due to compaction of trabecular bone at the edge of the growth plate as a result of the inductive effects of the periosteum and mechanical stimuli (Armstrong 1988). Population variance in density and cross-sectional area of cortical bone have been established as early as two years of age (Duren et al. 2013). Adult cross-sectional shape is a result of body mass loads and periosteal loads from muscle activity, all of which increase with age (Schoenau and Frost 2002). Longitudinal studies have shown that the increase in cortical strength slows during the period of peak growth velocity (PGV) in height in adolescents of both sexes. Additionally, cortical thinning during adolescence may be associated with secondary hypothyroidism as a result of a strong demand for calcium (Parfitt 2002a). Sex hormones produced during this time make cortical surfaces more sensitive to mechanical loading (Rauch and Schoenau 2001). Ultimately, bone formation processes are related to age-dependent gene expression (Duren et al. 2013; Gosman et al. 2011) modulated by biochemical and mechanical influence. Continued

documentation of age and bone surface-specific modifications is needed to further validate these claims.

While overall patterning is controlled by genes, certain dimensions of shape may be more plastically sensitive to mechanical strain (Godfrey et al. 1995; Pearson and Lieberman 2004). That is, constraint of bone size and shape is not uniform throughout each element. As previously mentioned, fetal movements in utero and the transition to walking are thought to modify articular surface shape at the joints and create the femoral bicondylar angle particular to bipedal movement (Cowgill et al. 2010; Lieberman et al. 2001; Pearson and Lieberman 2004; Ruff 2003c; Tardieu et al. 2006). In the small body of literature existing, two components of the epiphyses in the lower limbs have been assessed for potential for mechanically-induced changes in phenotype- articular surface area and the trochlear lip (Wanner 1977). Lieberman and colleagues (2001) were unable to identify any relationship between articular surface size and mechanical loading in juvenile sheep. Their findings suggest this component is only related to locomotor patterns at the species level, meaning that is very highly genetically constrained. Tardieu et al. (2006) investigated this same relationship in the human femoral trochlear lip as related to the transition to walking. The lip protects against lateral displacement of the patella during extension, and thus has been assumed to be related to the mechanically induced creation of the bicondylar angle. The authors found that in their sample of juvenile femora, the lip was not correlated with bicondylar angle. As such, it is likely a trait that has been selected for in humans to aid in bipedal walking, although it develops independently of walking behaviors.

Tardieu and colleagues (2006) also hypothesized that during the transition to walking, the rapid formation of diaphysis to attain the bicondylar angle may cause the expansion of the lateral condyle. Results of their study indicate that the lateral side of the metaphysis (lateral pillar)

increases in length in an anteroposterior direction significantly more than the medial side with age. Moreover, the growth of the both pillars is significantly (lateral pillar significantly more than the medial) correlated with bicondylar angle. Between the two components associated with bicondylar angle, the profile of the lateral condyle appears to be more developmentally plastic and epigenetic in growth. The authors surmise that processes occurring at the lateral condyle may be compensation for those happening to the medial pillar to provide stability during increased full knee extension. This extension during learning to walk promotes anteroposterior expansion of the lateral pillar, making the load distribution more efficient. What is unclear, however, is exactly how efficiency of load distribution is modulated in adolescence, and then later into adulthood, when genetic determinants of bone shape presumably have been expressed to their fullest capability and environmental conditions remain the principal factors in bone maintenance.

Variation in Bone Growth and Mass

Although genotype has the greatest impact on the rate of and total bone growth, additional environmental conditions such as nutrition and socioeconomic status (SES) experienced before adulthood are known to impact growth and the achievement of peak bone mass (PBM). These conditions are rarely considered in the investigation of adult bone architecture, which is inappropriate given the fact that the achievement of PBM is a primary factor in adult bone health. Assessment of SES can aid in the identification of causative factors of variation in growth and adult height of a population. SES factors include level of education, local crime rates, household income, access to health care, and the physical environment where individuals live (Stinson et al. 2012). Trends over time and across regions consistently demonstrate a positive trend between height and SES. That is, low-SES children are shorter than

their high-SES counterparts. Although SES levels differ between countries, particularly in well-off versus developing regions, the same trends are evident world-wide (Fredriks et al. 2000a; Padez et al. 2009; Stinson et al. 2012)

Variation in bone growth as a result of SES may also be affected by the degree of inequality between high and low-SES groups (Wilkinson and Pickett 2006). Levels of malnutrition have been found to increase in populations with greater disparity between household incomes (Larrea and Kawachi 2005; Stinson et al. 2012). This may be because the influence of low-SES on growth is greater than that of high-SES, or because of psychological stress that could negatively affect overall health (Wilkinson and Pickett 2006). In well-off countries like the United States, SES is negatively correlated with body fatness. Because of the low cost of nutritionally-poor foods, sedentary jobs, and lack of time for exercise, low-SES groups in these countries tend to have higher rates of obesity (Monteiro et al. 2004; Ulijaszek and Lofink 2006).

While bone is growing in length, it is also accruing mass. Peak bone mass is measured by bone mineral density (BMD) and is typically reached immediately following fusion of the epiphyses (Weaver and Fuchs 2014). Although PBM differs across skeletal sites (Baxter-Jones et al. 2011), females reach their highest BMD sooner than men. Rates of bone accrual usually reach their maximum at 12.5 and 14.1 years of age in females and males, respectively (Bailey et al. 1999). Males however, gain higher peak BMD than females as a result of a greater efficiency in calcium retention during childhood. Almost half of PBM is obtained during adolescence and failure to reach high levels of bone mass during this time is positively correlated with lower BMD in later adulthood. Understanding the relationship between peak bone mass and adult

patterns of bone mass is critical to clinical diagnosis of osteoporosis, fracture risk, and assessment of bone strength in adults. These concepts are discussed further in Chapter 4.

Adequate nutrition is generally agreed upon to have the greatest impact on achievement of PBM and regulating bone turnover in later life (Lloyd and Cusatis 1999; Stinson et al. 2012; Weaver and Gallant 2014b). Specifically, calcium, zinc, and protein-calorie deficiencies can slow growth and bone mass accrual during childhood and increase the rate of bone loss associated with lactation and aging. Other SES-related interruptions to bone growth, such as undernutrition, chronic disease, or a sedentary lifestyle can decrease rates of skeletal accretion (Stinson et al. 2012; Weaver and Fuchs 2014; Weaver and Gallant 2014b). Obese children have been found to have higher absolute bone mass than age-matched peers, often attributed to the increased loading from higher body mass. However, when this value is standardized by bone length, they actually have lower BMD and are less likely to reach PBM of normal weight peers (Weaver and Fuchs 2014). It is increasingly clear, particularly in the clinical literature (Bonjour and Chevalley 2007; Bonjour et al. 2009; Johnston and Slemenda 1994), that adult bone mass and risk of osteoporosis and fracture are directly correlated with achievement of PBM in adolescence.

Disparity in SES, including dietary and lifestyle factors that ultimately influence adult morphology, may be inherent in the sample used in this study. A majority of individuals in the sample lived in Tennessee and other states in the southeastern United States at the time of death (DW Steadman, personal communication). Figure 3 shows summary ranks for factors related to SES and general health across the state of Tennessee. County SES ranks vary from the highest (1) to the lowest (95) with a higher overall average of adult smokers, obese adults, and percentage of adults reporting poor health than the national average. It is not known if or how the

inconsistency in these ranks may affect bone accrual and it is beyond the scope of this study to collect data on childhood nutrition and lifestyle. Selection criteria (see Chapter 5) for individuals in the current study were designed to limit the inadvertent selection of those in which a SES-related condition (e.g. malnutrition) may be present, but these criteria do not account for other environmental factors (e.g. chronic poverty) that may affect variation in cortical bone mass or distribution. Pathological conditions in the final sample, including chronic addictions and infectious diseases were included to test for their effects on bone architecture, but it is beyond the scope of this study to determine whether these were related to SES conditions for each individual. Some of these factors and their effects on bone health in later adulthood are discussed in Chapter 4.

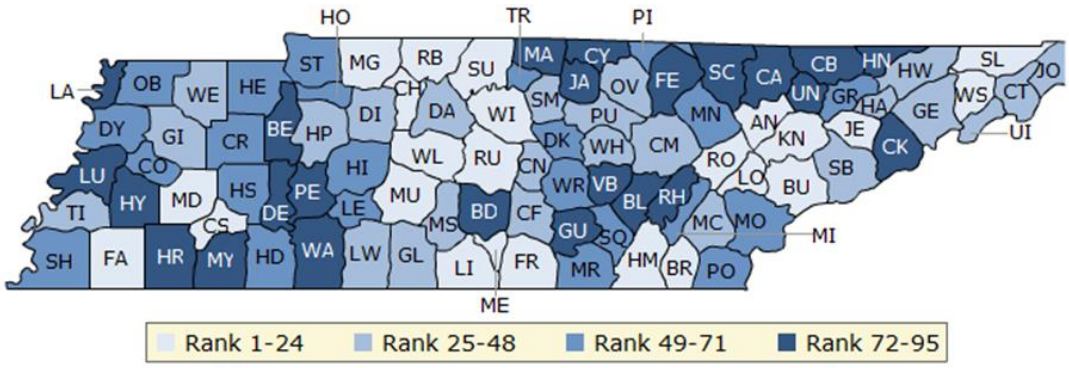

Figure 3. Summary ranks for health factors in Tennessee counties
Ranks are based on weighted scores for health behaviors (e.g. smoking, obesity, alcohol consumption), clinical care (e.g. uninsured, access to dental care, diabetic monitoring), social and economic factors (e.g. high school graduation, children in poverty, violent crime), and the physical environment (e.g. air pollution, drinking water quality, commute time). Smaller rank numbers are indicative of better performance in these areas. This figure is reproduced from the University of Wisconsin Population Health Institute 2016 County Health Rankings Report (www.countyhealthrankings.org).

Chapter Summary

The growth and maintenance of the human skeleton requires a complex set of interactions between the individual's genotype and environmental forces. Timing of some interactions (e.g., genetic and biochemical signaling) and degree of exposure to others (e.g., hormonal influences, mechanical forces) result in the variation observed in adult skeletal morphology. An understanding of these mechanisms during growth is crucial to interpreting how their decline, or even absence, can account for why adults fail to preserve bone as they age. Further, sex differences in skeletal apposition during growth will be exacerbated in adulthood. The mechanical compensation for this loss can be quantified using engineering beam theory, detailed in the next chapter. Chapters 3 and 4 will examine applications of this mechanical approach to investigating the etiologies of patterned (e.g., across populations) and pathological (e.g., osteoporosis) bone loss in both skeletal and clinical populations.

CHAPTER 3

STATIC TISSUE MECHANICS

To examine the relationships between age and cortical bone distribution within the limbs, it is necessary to test whether these relationships are systemic, or a function of mechanical loading. Loading regimes change over the course of the human lifespan (e.g., crawling in infancy, walking in childhood, and decreasing range of motion with age). Further, loading environments differ between the upper and lower limbs, and even within limbs. This dissertation examines the effects of these different environments with age, and with two additional factors that can change loading regimes: habitual activity patterns and body mass. It is useful then, to review theoretical models of bone adaption to loading and how this adaptation can be quantified and compared within and between groups.

As reviewed in Chapter 2, through the processes of modeling and remodeling, bone is maintained to meet homeostatic, metabolic, and mechanical responses to diet, body mass, and activities, as well as genetic and hormonal effects (Allen and Burr 2014; Bogin 1999; Burr and Akkus 2013; Frisancho et al. 1980; Frost 2001; Ruff et al. 2006). The distribution of bone in limb diaphyses is sensitive to these factors and adapts to maintain homeostasis, a phenomenon referred to as *bone functional adaptation* (Cowin 2001; Pearson and Lieberman 2004; Ruff et al. 2006). The shape and strength of the bone are morphological reflections of adaptation in bone in response to these factors. Furthermore, because these factors change over the course of an individual's life, understanding the relationship between adult aging and bone mechanical properties can shed light on the effect that such changes have on cortical bone.

Biomechanics is the study of energy resistance, or how energy is modulated and operationalized by an organism and its tissues. Examination of a material's properties and its ability to function in a loaded environment is common across many fields, including functional anatomy, clinical medicine, and kinesiology. In biological anthropology, skeletal tissue properties are used to test the mechanical responses of human (Cowgill 2010; Davies and Stock 2014; Wescott 2006) and non-human primate bone (Polk et al. 2000; Ruff and Runestad 1992; Sarringhaus et al. 2016; Schaffler et al. 1985). These analyses provide a static "snapshot" of the cumulative osseous response to mechanical loading up to the time of data collection, which, in the case of skeletal remains, is death. Response to mechanical loading can be measured experimentally as strain, or bone's deformation in response to forces (and, conversely, its resistance to force; see page 45 below for further explanation), or retrospectively as cortical bone geometry in cross-section. Comparing these responses within the skeleton, a population, or even across populations, can shed light on genetic and environmental influences on bone morphology and function. In this dissertation, the static tissue mechanics of the limbs are examined under the theoretical framework of bone functional adaptation using a methodology adapted from engineering beam theory.

Bone Functional Adaptation

Bone size and shape can be understood under the framework of bone functional adaptation (BFA) and subsequent models developed within it (Carter and Orr 1992; Pearson and Lieberman 2004). Initiation and control of remodeling processes to achieve mechanically efficient long bone morphology was first defined by Wolff's Law (Wolff 1892), which ascribed the directional strutting in femoral trabecular bone as a product of loading stress in life. More

specifically, Wolff devised a mathematical explanation for the structure of trabecular bone in the femoral neck. His work demonstrated how the architecture of bone reflected engineering principles, which later works would expand upon to include cortical bone. Wolff's Law, however, does not describe the specific mechanisms of strain and its influence on changes in bone shape. As a principle that supplants Wolff's Law, BFA also expands on Frost's mechanostat principle (also referred to as the Utah paradigm) (Frost 1987; Frost 2001; Frost and Jee 1994), which suggests that bone has an inherent threshold for strain. When this threshold is exceeded, bone will adapt its architecture to decrease strain back to normal levels. Similarly, when the threshold is not regularly met, material is removed to lower the threshold (Frost 2003). As described by Ruff (2006), BFA widens the scope of the mechanostat to understand the variety of ontogenetic, environmental, and mechanical factors that regulate bone cell response to mechanical strain during life. This theoretical framework can help guide the study of biochemical and mechanical interactions in bone, reflected by changes in size and shape, particularly in developing bone where sensitivities to these influences may be quite high (Eleazer and Jankauskas 2016; Gosman and Ketcham 2009; Lieberman et al. 2001; Lieberman et al. 2003).

The effects of mechanical loading on bone turnover and deposition vary throughout life and can best be understood as components of a strain feedback loop (Figure 4) (Lanyon 1984; Rauch and Schoenau 2001; Ruff 2008). This model predicts that the bone organ will continually attempt to reach an optimum customary strain level, or general homeostasis (Pearson and Lieberman 2004). Homeostasis can be disrupted by increased strain from strenuous activity (e.g. hunter/gathering subsistence strategies, athletic competition, etc.) (Bridges et al. 2000; Ruff and Hayes 1983b; Ruff and Larsen 1990) or decreased strain from inactivity (e.g. agricultural or

other sedentary lifestyle, space flight, etc.) (Ruff and Larsen 1990). Further examples of these relationships are provided below. Early descriptive models of the relationship between mechanical loading and bone turnover were supported by a large body of observational data that correlated pre-agricultural subsistence strategies with thick cortical bone and increased bending strength as compared with more sedentary populations and modern humans (Ruff et al. 1993; Trinkaus 1976; Trinkaus and Ruff 1989). Similarly, in growing bone of highly active individuals, it has been noted that the rate of endosteal resorption is decreased, while subperiosteal bone is added (Daly et al. 2004; Ducher et al. 2011; Frisancho et al. 1970; Garn 1972; Ruff et al. 1994).

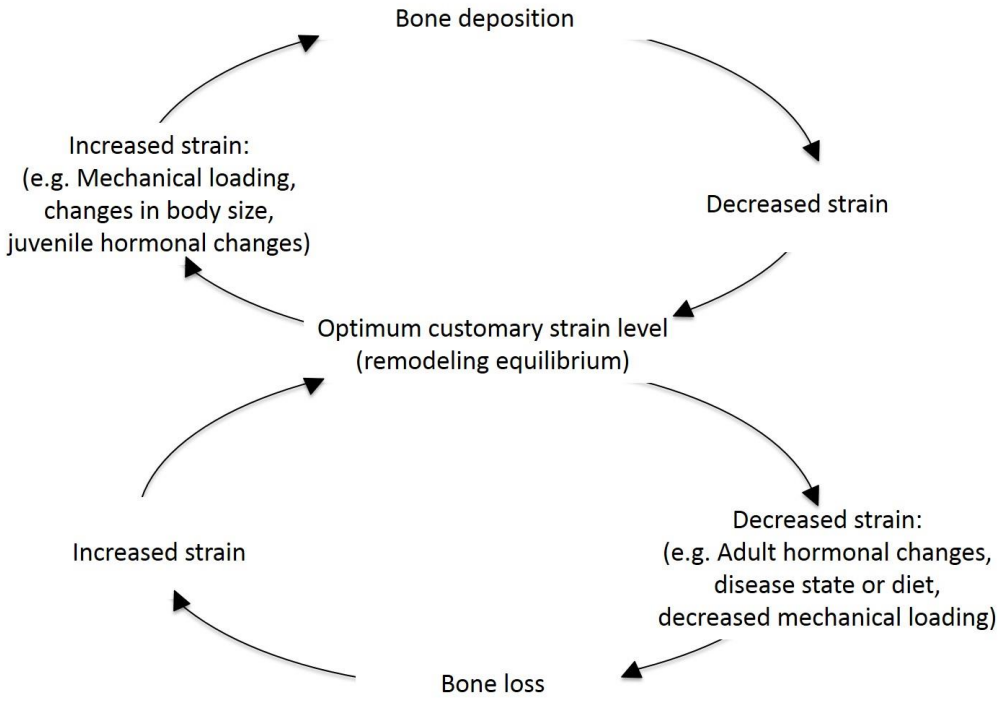

Figure 4. Bone remodeling equilibrium
A feedback loop demonstrating the equilibrium of bone strength achieved through the phenomenon described as bone functional adaptation. This figure is adapted from Ruff (2008) and Lanyon (1982).

Later equilibrium models (e.g. Frost's mechanostat) propose that the relationships observed in skeletal populations are due to modifications of bone geometry during growth to diminish dynamic strain while keeping it below the threshold for turnover (Biewener et al. 1986; Frost 2003; Rubin and Lanyon 1984). During ontogeny, diaphyseal dimensions develop in a manner such that the directionality of strain magnitude can be maintained during strenuous activity while avoiding failure (Biewener et al. 1986). For these models, the initiation of bone turnover is the result of a mechanical disruption to the equilibrium of a customary (or "lazy zone") strain level (Beaupre et al. 1990; Pearson and Lieberman 2004; Rubin and Lanyon 1984). The equilibrium represents a static state of no net bone deposition or resorption. A mechanical stimulus is required to disrupt the equilibrium and the minimum effective strain (MES) for this perturbation is approximately 0.0008-0.002 (Frost 1983). Strains below this threshold do not violate the equilibrium and thus do not signal a remodeling response. These perspectives, however, have been criticized as being phenomenological (Chen et al. 2010); that is, they are descriptive in nature and do not specify the mechanisms behind Haversian remodeling or account for differential response to loading across the skeleton (Carter and Beaupre 2001; Pearson and Lieberman 2004; Turner et al. 2002). As an amendment, mechanotransduction theory provide for the mechanics of these processes (Donahue et al. 2003; Jacobs et al. 1998), but is less developed and does not concretely establish a relationship between hydrostatic shear stress at the cellular level and modeling and remodeling (Chen et al. 2010) as reviewed in the prior chapter.

Optimization models use the equilibrium principle but expand upon it to include a cost-benefit analysis. Proponents of these models suggest that the ratio between bone modeling and Haversian remodeling, both as a response to loading, will differ between elements of the skeleton and chronological age (Drapeau and Streeter 2006; Lieberman et al. 2001; Lieberman et al. 2003;

Pearson and Lieberman 2004). Concerning age-related changes to functional modeling and remodeling, optimization models predict that the cost of slowed response to mechanical stimuli by osteoprogenitors as age increases is balanced by an increased response in Haverisan remodeling, especially in older individuals (Lieberman et al. 2003). A "benefit" to modeling is an increase in bone strength in the direction of loading. However, the "cost" of this activity will vary across the skeleton, particularly in locations where increased mass results in an inefficient use of energy during movement or other physiological functions. For example, the energetic cost of additional bone mass in the lower limb, and to a greater degree in the distal portion (Lieberman et al. 2003), is exponentially higher than in the upper limb. This is because the cost of limb acceleration during locomotion is proportional to **m** (mass of the limb) x **R** (distance of the center of mass for that limb to the hip or shoulder joint)^2 (Marsh et al. 2004; Winter 1990). This has great implications for the proportional changes in limb length mass through senescence, especially as individuals lose muscle mass and changes to body weight occur after approximately 40 years of age (cite). This study will quantify some these "costs"—macroscopic effects of age, activity, and body mass—to the skeleton using engineering beam theory, discussed below.

Engineering Beam Theory

Whether using an *in vivo* experimental sample or skeletonized remains, BFA can be tested quantitatively using engineering beam theory. Beam theory is especially useful in modeling the responses of long bone diaphyses to mechanical stimuli. Under externally loaded forces, diaphyses perform in a similar manner to I-beams used for structural support in buildings. In a beam, material placed farther away from the center of a beam's cross-section makes for a stronger structure than material placed closer to the center (Ruff 2000a; Ruff 2000b; Ruff and

Larsen 1990). Following this principle, the distance of material away from the center can indicate the strength of the beam and its resistance to bending. Thus a hollow beam, such as a long bone diaphysis, can withstand greater bending resistance depending on the distribution of material, than a solid beam (Chen et al. 2010). In bone, the largest amount of material is concentrated in the direction of greatest loading stress (Carter 1984; Rubin and Lanyon 1984). The size and shape of the diaphysis is continually modified to maintain a balance between strength and efficiency. Too great an amount of material results in poor tissue economy during locomotion, while too little bone mass increases the risk of failure.

Beams experience five basic loading conditions: compression, tension, shear, bending, and torsion (Figure 5). Compression, and its opposite force, tension, act parallel to the longitudinal axis of the beam. Compressive forces shorten and widen the beam along the axis, while tensile forces stretch the material, causing it to elongate. Conversely, a shearing force acts on a perpendicular plane to the axis of the beam. The opposing combination of shear forces causes lateral deformation of the beam. Compression, tension, and shearing are rarely experienced in isolation in living bone. Instead, a combination of these three, either as a bending or torsional force, is more common. Bending occurs when tension is applied to one side of the beam, while compression is applied to the other. In bending, the external opposing surfaces of the beam experience maximum compression and tension. These forces dissipate towards the central axis of the beam until a neutral zone (axis) is reached in which no tension or compression is experienced. During human locomotion, bending occurs in multiple planes and is accompanied by some torsion, or fixed shearing in a circular motion. Some of the forces producing these loads result from the loading of body mass or the reaction of the substrate (e.g. ground reaction forces),

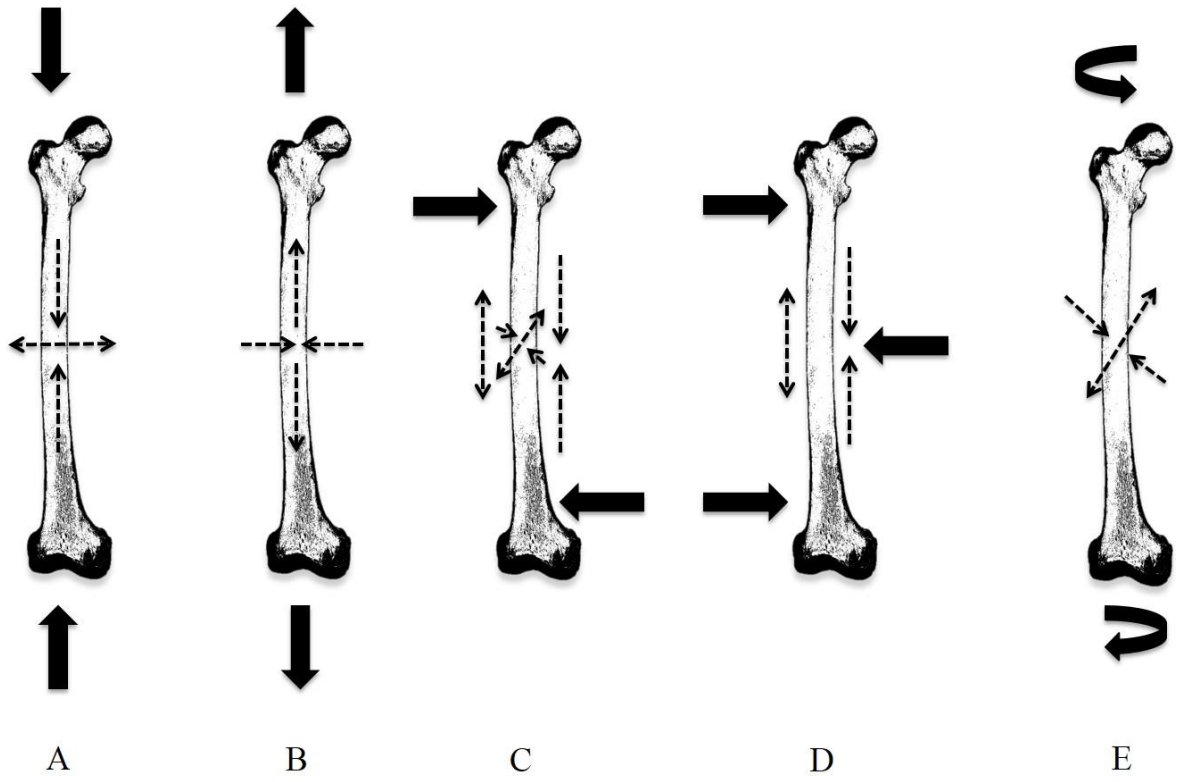

Figure 5. Basic loading conditions experienced by a beam (long bone)
Bone are loaded under A) compression, B) tension, C) shearing, D) bending, or E) torsion; usually in combination *in vivo*. Dark arrows indicate the direction(s) of force applied to the bone during the loading condition. The dashed arrows indicate the directionality of strain from these forces.

while other forces are produced internally by joint reaction forces or the strains of muscle tendons on bone.

Under these five loading conditions, bone experiences both stress and strain (Figure 5). Mechanical stress is the amount of force applied to a region, while strain is the amount of deformation of the material as a result of the force. Tensile stress results in a positive strain, or an elongation of the material. Compressive stress results in a negative strain, or a shortening. Shearing forces represent a combination of modalities and thus result in both positive and negative strain. These forces both add and subtract bone length. For any material, the ratio between stress and strain independent of geometry can be calculated as a stress-strain curve (Figure 6). The slope of the curve, called Young's (or elastic) modulus, represents the material's stiffness (Burr and Turner 1999). Young's modulus reflects the strength of the bone to resist stress before strain results in failure. This relationship differs depending on the loading condition and is specific to the composition of the material.

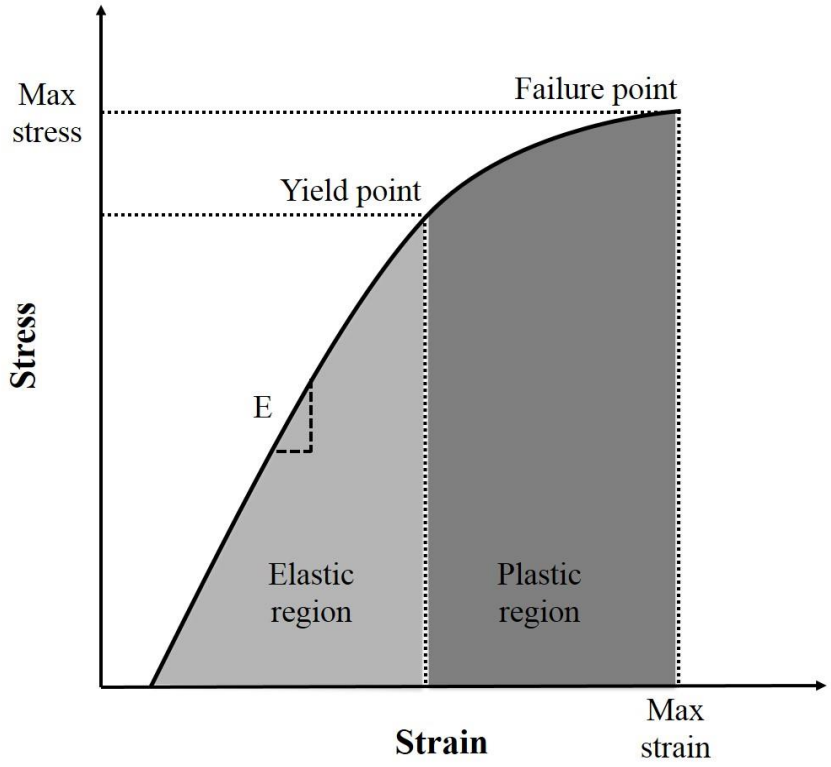

Figure 6. Generalized stress-strain curve for cortical bone
Under loading, bone is able to resist deformation until it reaches a yield point, or the end of the material's ability to return to its original shape (elastic deformation). Deformation past this point is considered to be plastic, or unable to return to its original form. When maximum strain and stress levels are reached, the material will fail. Young's modulus (E) is the slope of the curve. It represents the bone's ability to resist stress before strain results in failure. Figure adapted from Martin et al. (2015).

The material composition of bone is inherently anisotropic. That is, a single long bone will respond to stresses dissimilarly because collagen fibers within it are not oriented the same in all directions (Currey 2006; Lieberman et al. 2003). The diaphysis, most often used in mechanical analyses, is also not uniformly shaped along its length, further complicating the application of strict engineering principles (Pearson and Lieberman 2004; Ruff 2008; Ruff et al. 2006). The condition of the bone can also affect its mechanical properties. The strength of bone against failure can be dependent on its moisture content, whether it is in isolation or *in situ* in the limb, or age and health of the individual (Currey et al. 2009). In any condition, experimental testing of bone strength to the point of mechanical failure is destructive in nature and is not easily replicated using human elements.

Cross-sectional Geometry

As an alternative to experimentally testing bone strength, bony response to externally loaded forces can estimated by analyzing the geometry of the cross-section of the element's diaphysis. Cross-sections can be obtained non-destructively through cast methods in which a molded contour of the external bone surface is used to calculate the shape and spatial relationship of the medullary cavity (O'neill and Ruff 2004). A more precise method of imaging cross-sections is through the use of computed tomography (CT) scans (Mak et al. 2016; O'neill and Ruff 2004; Shaw 2010). This study utilizes CT images of the diaphysis in the transverse plane as a way of measuring its geometry using cross-sectional geometric (CSG) properties.

Cross-sectional properties (Table 1) are static measurements that reflect habitual kinematics, or how an object reacts to motion. Variation in the amount of material in the shape and its distribution along the diaphysis can be tested using these calculated properties. However, CSG properties are fairly meaningless when examined individually. They have no units of

measure and thus their utility exists in comparison of individual variation present along the diaphysis, between bones or limb segments, or collectively between populations. Because the response of bone to a loading environment is most obvious in the adaptive geometry rather than its material properties (Robling et al. 2002; Ruff 2008; Woo et al. 1981), stress and strain are proportional and can be used to relate CSG properties to the strain stimulus for adaptation (Ruff 2008). It should be noted that CSG properties provide only a static picture of bone geometry at one time. That geometry is the result of compounded loading and intrinsic factors (discussed in Chapter 2) experienced over a lifetime that often cannot be identified. However, when CSG properties are analyzed in relation to one another, their values reflect the rigidity and strength of the bone in that location. These can be informative if understood in the context of their limitations (Lieberman et al. 2004; Ruff 2008).

Table 1. Cross-sectional properties used to evaluate mechanical performance
Table adapted from Ruff (2008), page 185.

	Property	Definition	Standardization
Measurements of bone mass	Cortical area (CA)	Compressive and tensile strength	Body mass[1]
	Total subperiosteal area (TA)	Total area within outer boundary	
	Medullary area (MA)	Area within medullary cavity	
Measurements of bone shape	Percent cortical area (%CA)	(CA/TA) x 100	NA
	Shape index (I_{max}/I_{min})	Positive values indicate AP elongation; negative values indicate ML elongation; values approaching 0 indicate a circular shape	
Measurements of bone strength	Section modulus about ML (x) axis (Z_x)	AP bending strength	The product of body mass and moment arm length.
	Section modulus about AP (y) axis (Z_y)	ML bending strength	
	Maximum section modulus (Z_{max})	Maximum bending strength	
	Minimum section modulus (Z_{min})	Minimum bending strength	
	Polar section modulus (Z_p)	Torsional and twice average bending strength (J/moment arm)	
Measurements of bone rigidity	Second moment of area about ML axis (I_x)	AP bending rigidity	The product of body mass and moment arm length.[2]
	Second moment of area about AP axis (I_y)	ML bending rigidity	
	Maximum second moment of area (I_{max})	Maximum bending rigidity	
	Minimum second moment of area (I_{min})	Minimum bending rigidity	
	Polar second moment of area (J)	Torsional and twice average bending rigidity	

[1]Standarization following Ruff (2000b).
[2]Standarization following Ruff (2008).

Properties of bone rigidity indicate the element's ability to resist deformation, particularly under bending and torsional stress (Burr and Turner 1999). These properties are referred to as second moments of area (SMAs) and are represented by *I* (Ruff 1987; Ruff and Hayes 1983a). Bending rigidity is calculated about the anteroposterior (AP) (I_y) and mediolateral (ML) (I_x) anatomical axes of the bone, as well as in maximum (I_{max}) and minimum (I_{min}) directions. Bone is strongest in the direction of I_{max}. I_{min} is set perpendicular to I_{max} to isolate rigidity to bending, rather than conflating bending with torsional rigidity. These calculations provide a value for the amount of material in the extremes of the cross-section without the requirement for orientation in an anatomical direction. This can be a useful assessment when the nature of the sample does not allow for an exact anatomical alignment, such as samples derived from clinical settings (Shaw and Stock 2009a; Shaw and Stock 2009b). The degree of displacement of the region of maximum bending rigidity relative to the anatomical axes can also be calculated, and is designated as theta (θ). Twice bending rigidity, the polar second moment of area (represented by *J*), is calculated about the centroid of the cross-section, where the AP and ML axes intersect. It should be noted that this centroid is a matter of computational convenience, and not the true neutral axis of the bone; the neutral axis shifts under dynamic loads (Lieberman et al. 2004). *J* is considered a good overall indicator of bone rigidity and is the best reflection of SMA when loading patterns are unknown or estimated (Lieberman et al. 2004). Larger *J* values indicate less material farther away from the centroid, and thus greater resistance to torsional forces.

Cross-sectional geometric properties indicate the capability of bone to resist failure under bending and torsional forces (Burr and Turner 1999). These properties are referred to as section moduli and are represented by *Z*. They are calculated by dividing SMAs by the distance from the external edge of the cross-section to the relevant axis or the centroid. The external surface of the

bone experiences the maximum stress during torsion and bending (Figure 5, D and E). A section modulus about the ML axis (Z_x) is indicative of bending strength in the AP plane, while the same about the AP axis (Z_y) is indicative of ML bending strength. Similarly, maximum (Z_{max}) and minimum (Z_{min}) bending strength can be calculated using the I_{max} or I_{min} axes. Torsional or twice average bending strength (polar section modulus, Z_p) is computed by dividing J by the moment arm, or distance between the centroid and the external surface of the cross-section.

Bone mass and shape can also be calculated using geometric analysis. The total area within the external boundary of the cross-section is referred to as total subperiosteal area (TA). Subtracting the area within the medullary cavity (MA) from TA results in a measurement of cortical area (CA), which reflects cortical thickness. Cortical thickness is correlated with compressive and tensile strength of the bone, although bone rarely experiences these loads in isolation of bending and torsion. Cortical area can also be used to calculate percent cortical area (%CA) by (CA/TA) x 100 to give a better indication of cortical thickness. However, Ruff (2008) suggests that cortical area provides no information about bony response to habitual locomotion. This is because increase in cortical area is a response to compressive forces, which are rarely experienced in isolation of other forces during life. Rather, these measures are more informative of morphology than direct biomechanical adaptation.

Conversely, the shape of a diaphyseal cross-section can be very informative of growth patterns or habitual patterns of movement. Shape index is calculated as I_{max}/I_{min}. Positive values indicate elongation in the AP plane, while negative values indicate ML elongation (Shaw and Stock 2009a; Shaw and Stock 2009b). Following beam theory, movement repertoires in which the bone is loaded more heavily in one direction over the other can result in corresponding modification of shape in that direction. Values approaching zero suggest a more circular shape,

or a limb that has experienced relatively equal loading in all directions. These relationships are fairly consistent in adult populations (see review in Ruff and Larsen 2014), but less so in older adults and etiology is unknown. These concepts are further explored in the next chapter.

Scaling

Although diaphyseal cross-sectional geometry is calculated using beam theory, bones of the limbs do not exist, nor are loaded, in isolation like traditional beams. A number of factors must be accounted for to avoid extraneous conclusions about geometric relationships to loading patterns. If non-scaled CSG properties are used, interpretations regarding the effect of occupation, habitual activity patterns, or locomotion on cortical bone distribution can be conflated with the effects of bone length and body mass. By scaling measurements of bone geometry, meaningful patterns of loading can be distinguished more readily from the effects of body size and shape.

Body mass is a suitable proxy for body size[1] when examining diaphyseal geometry (Ruff 2007; Ruff 2008; Vogel 2013). For skeletal samples, femoral head diameter or bi-iliac breadth can be used to estimate body mass (Auerbach and Ruff 2004; Pearson et al. 2014; Ruff 2007), as they have been shown to be significantly correlated with body mass in living individuals. However, these measurements suggest genetically-determined mass and cannot speak to actual living mass in the case that *in vivo* lifestyle choices led to a low or high body mass index (BMI). In older adults, these relationships are even less clear, especially in modern samples where sedentary lifestyles and/or poor nutrition can alter a "pre-determined" weight. Further, illness associated with the end of life can lead to a dramatic decrease in weight. In prehistoric or

[1] Body size is comprised of body mass and stature (Ruff 2007). Stature on its own, however, does not have mechanical relevance to the manner in which bones experience loading.

unidentified skeletal samples, reliable body mass prediction for population demographics is further confounded by the estimation of chronological age from morphological changes associated with senescence. Ideally, body size is obtained from medical records in which height and weight are taken by a medical professional and BMI calculated according to adult-specific standards (CDC). For the sample used in this study, body mass was self-reported. Potential issues associated with self-reporting of anthropometrics are discussed in Chapter 5.

Cross-sectional geometric measures of bone mass, strength, and rigidity are all scaled by body mass, regardless of skeletal location (Table 1). An argument can be made that bones of the upper limb do not experience loads directly as an effect of body mass, however recent research (Reeves 2014; Stock and Shaw 2007) suggests that effects of increased body mass can be systemic. Dimensions of cross-sectional area and bone mass (CA and TA) are scaled by body mass. In addition to body mass, measurements reflecting bone strength and rigidity are scaled by bone length (discussed below). This methodology is relatively new. Earlier anthropological investigations (Churchill 1994 Bridges et al. 2000 Ruff et al. 1993) standardized measurements of bone strength by bone length alone. This was a sufficient method for more homogenous populations, however, body size differs greatly in modern groups, and without scaling to it, variation across populations is not comparable. Body mass also varies considerably among individuals, particularly in modern samples.

As mentioned above, CSG properties related to bone strength and rigidity are also scaled by bone length, or moment arm. In a lever system, the moment arm is the distance between the axis of movement and the force or effort used to move against the resistance. In the human body, joints serve as axes of movement, while muscles produce force across the joint (Figure 7). The length of the moment arm determines the amount of torque produced at the joint, and thus the

amount of loading experienced by the bone. Thus, to account for the length of the beam under loading, bone length must be used to scale CSG measurements reflecting the bone's ability to resist that loading (Vogel 2013). In some elements, a difference exists between total bone length and a mechanically meaningful moment arm length. In the ulna, for example, physiological length (distance from the deepest point on the coronoid process to the distal articular surface) more closely approximates the moment arm rather than the maximum length. The procedures for measurement of bone length for this study and any potential issues related to the current sample are discussed further in Chapter 5.

For bones that stand alone within a limb segment (e.g. the humerus and femur), a single bone length as a proxy for lever arm is appropriate. However, paired bones within a segment share a loading environment and a portion of the segment's load (Auerbach et al. 2017; Markolf et al. 1998); up to 9- 43% for the ulna (Ekenstam et al. 1984; Shepard et al. 2001) and 7- 10% for the fibula (Goh et al. 1992; Marchi and Shaw 2011; Rantalainen et al. 2010). Although the lever arm length for these paired bones is relatively similar, scaling paired bones by the segment length, rather than individual bone length, may be more appropriate. In samples of living individuals, limb segment length is routinely used (Shaw and Stock 2009a; Shaw and Stock 2009b) because of the difficulty in obtaining individual bone length. The sample utilized in this study is skeletal, which does not allow for the measurement of limb segment length. Although not idea results of this study are still comparable to others in which skeletal samples were also used.

Difficulties in measurement of bone length also complicate the location(s) at which CSG properties are collected (Sladek et al. 2010). However, measures are taken in this study to avoid

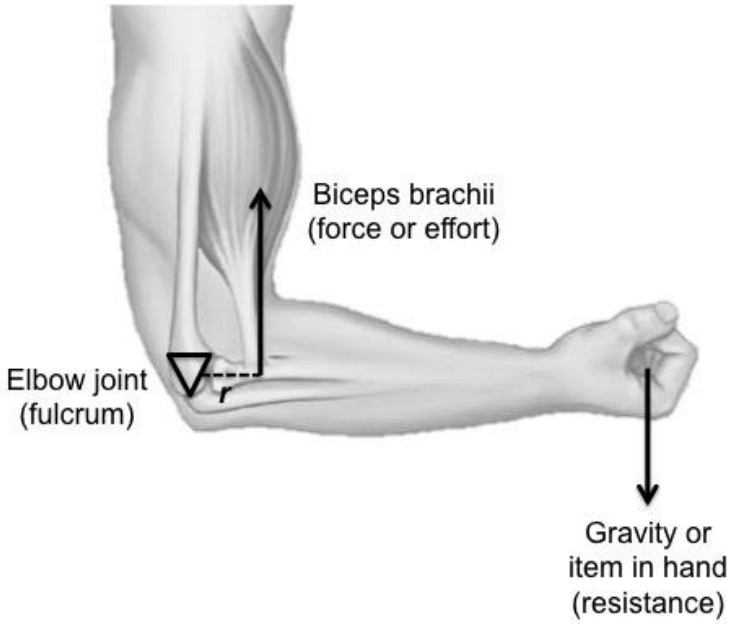

Figure 7. Typical class 3 lever in the human body
The elbow joint is an example of a class 3 lever in which the force or effort is situated between the axis (fulcrum) and the resistance. The moment arm (*r*) is the distance between the fulcrum (the joint) and the muscle (biceps brachii). The limb segment size of an individual is correlated with this distance, as longer bones increase the moment arm. The length of the moment arm affects the amount of muscle force placed on the bone, and as such, properties of bone geometry reflecting bone adaptation to loading must be scaled by bone length. Background image reproduced from Scheff et al. (2014).

these complications and capture the greatest scope of diaphyseal variation possible. Traditionally, cross-sections of adult long bones are assessed at the most mechanically relevant point, 50% of bone length (Ruff 2003b; Ruff 2008). As a beam, the midshaft location represents the region in which the greatest bending and torsional forces are experienced, and thus, where targeted remodeling results in a greater rate of bone deposition (Drapeau and Streeter 2006). However, as discussed previously, the anisotropic nature of bone morphology means that loads are mitigated differently along the shaft resulting in varied properties of size and shape (Lieberman et al. 2003). For example, in the proximal femur the maximum distribution of bone is in the ML direction due to strengthening against bowing from the forces associated with body mass (Ruff et al. 1993). At the midshaft, however, this distribution is more heavily anteroposteriorly dominant due to loading from basic locomotion (Ruff 2000a; Ruff 2003c; Shaw and Stock 2009b; Shaw and Stock 2013). With this knowledge, contemporary studies calculate CSG properties at 20%, 35%, 50%, 65%, and 80% of bone length to obtain a comparative dataset of loading across the diaphysis. This study utilizes these five locations on all six elements examined in the appendicular skeleton. This approach may be modified depending on the anatomy of the specific element (e.g. humeral 50% is often taken at 40% to avoid the deltoid tuberosity) (Ruff 2002). In this study, though, slice location was not modified so that comparison would be possible between elements. In the case of paired bones in which there is a discrepancy between lever arm lengths, collection of CSG properties at percentage of segment length, rather than bone length, would be ideal. However, use of bone length to calculate slice location does not significantly limit the results of this study.

Biomechanical Studies in Humans

Analysis of diaphyseal cross-sectional geometry cannot be used to assess general variation, but specific effects of loading environments from habitual movement and body mass. Their effects on the human skeleton can be examined on three broad levels. Idiosyncratic activities are those done by the individual and are particular to that skeleton. Analysis of idiosyncratic activities requires that a relationship between the activity and diaphyseal geometry be previously established with similarly aged and sexed individuals. Variation in activity can also be assessed through mobility, or how an individual or group moves through their environment. This requires an understanding that locomotor repertoires produce different diaphyseal geometries depending on the landscape in which they are performed. On a larger scale, populational patterns of behavior can be assessed at the group level. These investigations are particularly useful when drawing conclusions about age or sex-specific activities. This dissertation examines a modern population of adults, drawing conclusions about osteological response to activity and body mass. Before proceeding, the analysis of bone geometry to ascertain *in vivo* locomotion repertoires requires a more nuanced discussion of the mechanical inputs that comprise a group's mobility.

Assessing Mobility

One aim of the current study is to test the relationship between activity and older adult bone geometry. Claims regarding the direct link between CSG properties and activity repertoires rely on the premise that in response to mechanical strain, the bone organ lays down material in the direction needed to support increased bending and return strain levels to normal (Rauch and Schoenau 2001). This has been tested numerous times in both archaeological (Davies and Stock

2014; Ruff and Hayes 1983a; Ruff and Hayes 1983b; Ruff et al. 2015; Shackelford 2014) and living populations (Auerbach et al. 2017; Shaw and Stock 2009a; Shaw and Stock 2009b; Shaw and Stock 2013). Questions surrounding mobility in archaeological or paleontological populations are generally aimed at getting a sense of how humans traversed the landscape to access resources, particularly in regards to hunting practices. The interpretation of mobility, however, actually connotes two different components of habitual movement (see discussion in Carlson and Marchi (2014) and Sparacello et al. (2014)). The first is the amount or level of movement. How often did traveling take place? What was the average distance traveled? The second component of mobility is the type of movement. What was the terrain or landscape like? What subsistence strategies were employed?

While specific answers to these questions may not be possible without written accounts, the amount of traveling can be assessed by examining AP-oriented loads on the lower limbs. Walking and running, the most typical ways of traversing a landscape, produce AP-oriented loading along the diaphyses of the femur, tibia, and fibula. Mediolateral-oriented forces are produced relative to the type of movement, rather than the amount. For instance, walking across uneven topography, ascending, or descending causes ML stabilization across the lower limb. Specific movement types, like cross-cutting, load the limb in a similar fashion, even on a level surface. As such, the cross-sectional geometry of lower limb diaphyses is a function of both the amount and type of movement performed. These measures are not without fault, as they rely on beam theory, which does not account for the often inconsistent material and responsive properties of bone (Currey 2006; Vogel 2013).

Stock (2006) tested some of these relationships throughout the postcranial skeleton in a geographically diverse group of hunter-gathers. Strength properties were negatively correlated

with climate but positively correlated with water or terrestrial movement patterns. Additionally, results demonstrated that distal elements tend to be more responsive to the effects of these loading patterns than are more proximal elements. Similar results have been demonstrated in experimental testing with sheep (Lieberman et al. 2001). Bone shape was significantly altered by an exercise regime, and effects were more pronounced in younger sheep. From these results, the authors conclude that both age and activity type have a positive relationship with the strength properties of limb bones.

Shaw and Stock produced two works in 2009 detailing a similar examination in the upper and lower limbs of living collegiate athletes. Here, the authors were able to identify specific patterns associated with each sport. In the lower limb, the cross-sectional shape of the midshaft of the tibia was most indicative of sport type; a rounder shape in field-hockey players was the result of greater patterns of multi-directional movement, while more AP elongation was found in cross-country runners as a result of consistent unidirectional running patterns. In the upper limb, humeral torsional strength was higher in the dominant arm of cricket players due to throwing movements. Swimmers, on the other hand, demonstrated bilateral changes to ulnar and humeral rigidity. The upper limb can thus produce great amounts of asymmetry in strength properties depending on the functional requirements of the activity repertoire (Shaw and Stock 2009a; Shaw and Stock 2009b; Shaw and Stock 2013).

Recent investigation into the reflection of locomotor patterns in the skeleton has revealed a more complicated picture. When comparing bones of the lower limb, research suggests that the femur, tibia, and fibula reflect the level of mobility and directionality of loading (type of mobility) differently (Sparacello et al. 2014). Femoral cross-sectional shape appears to be one the strongest correlates of mobility across the three bones (Holt 2003; Stock 2006).

Alternatively, tibial cross-sectional geometry less consistently correlates with mobility. Level of activity corresponds best with tibial robusticity, whereas directionality of loading (type of activity) has a stronger correlation with the cross-sectional shape of the bone (Higgins 2014; Shaw and Stock 2009b; Sparacello et al. 2014). In the fibula, robusticity relative to that of the tibia may better reflect ML movement (eversion and inversion) as the result of mobility type or perhaps an uneven terrain (Marchi 2007; Marchi and Shaw 2011; Rantalainen et al. 2010). Auerbach et al. (2017) corroborate findings that the fibula and tibia experience different mechanical environments despite sharing the load of the shank[2].

These studies collectively demonstrate the need for comparison of geometric properties across bones and along the diaphysis of each. In an experimental or longitudinal study, concomitant effects of amount and type of activity could potentially be identified. This study relies on self-reported information regarding activity, which of course, may not be reflective of activity patterns at the time of death. Although assessment of mobility in the case of this dissertation is less clear than in experimental studies, it is worth examining any possible effects across the bones of the upper and lower limbs.

Body Mass and Mobility

An additional aim of this dissertation is test whether body mass has any mechanical effects with age on cortical bone distribution. With all CSG properties scaled for body mass, body mass index (BMI), a function of height and weight (see Chapter 5), can then be used to compare those scaled properties across sex and age groups. As discussed earlier, both body mass and habitual activity patterns increase the load on bones, resulting in increased cortical areas.

[2] The term "shank" is commonly used in the biomechanical literature to refer to the lower leg segment, which allows its dynamics to be easily comparable across bipedal and quadrupedal species.

The direction of cortex thickening can differentiate the two, as elongation is expected in the primary direction of loading for active individuals (Shaw and Stock 2009a; Shaw and Stock 2009b), and more generalized for obese individuals (Moore 2008; Moore 2013; Reeves 2014).

However, an individual's mass also creates different loading environments in the upper and lower limbs. Because skeletal loading is the result of stress from muscle contraction, it follows that increased forces are required to move those with greater BMI values. Therefore, while cortical area is greater across the limbs in obese individuals versus their non-obese counterparts, the magnitude of this difference is far greater in the lower limbs (Reeves 2014). Further, because the lower limbs are responsible for mobility in humans (with the exception of crawling during infancy), the bones of the lower limbs also demonstrate greater measures of strength and rigidity with increased BMI. The relationships between body mass and older adult bone health are discussed further in Chapter 4.

Chapter Summary

Bone adapts throughout the life of an individual to meet the mechanical demands of body mass and movement. Periods of increased loading disrupt skeletal homeostasis and result in localized apposition, while a decrease in strain can signal resorption after an extended period. Bone functional adaptation (BFA) provides a theoretical model for understanding these processes in adults, particularly as co-varying physiological processes (see Chapter 5) may also serve to disrupt homeostasis with age. Engineering beam theory allows for quantification of this variation and diaphyseal cross-sectional geometric properties can be compared across populations with appropriate scaling. This has been achieved in samples of modern athletes and archaeological populations in relation to mobility. However, none of the studies have

satisfactorily resolved whether these relationships remain consistent in older adults. The next chapter explores how bone tissue mechanics may be affected by natural processes of senescence and a number of etiologies behind these changes, including hormones, nutrition, and activity.

CHAPTER 4

BONE QUALITY WITH AGE

The prior chapters have discussed the how bone size and shape are developed and modified through skeletal maturity with respect to a variety of biochemical, genetic, metabolic, and mechanical influences. Also discussed were some of the ways in which skeletal adaptation to these factors can be quantified and compared between groups. However, a dearth of knowledge still remains as to how variation in these factors affects adult bone maintenance after mid-life. Hormone deficiencies, a decrease in activity levels, and loss of muscle mass are a few of many age-related shifts that take place in the later years of human life. Because this dissertation is primarily concerned with these years, it is useful to finish by reviewing how normal mechanisms of aging can vary and what is known about their relationship to bone loss in adults.

Modern humans in industrialized societies are living longer than any previous hominin population. Longevity has its drawbacks, however, as at least some degree of bone loss occurs after mid-life in humans (Garn 1971; Nelson and Weiss 1999) as well as non-human primates (Burr 1980; Summer et al. 1989). Past populations of anatomically modern humans generally do not demonstrate the same degree of bone loss, and those that do still appear to have had higher bone quality and lower fracture incidences than their age-matched industrialized counterparts (Agarwal and Grynpas 1996). Whether this is the result of differences in longevity, subsistence patterns, other environmental factors, or a combination of all of these is still unclear. Further, the morbidity and mortality associated with advanced bone loss and its co-morbidities seem

maladaptive. While a longer life may be an adaptation to other biocultural needs[3], the increased frequency of osteoporosis and related bone diseases cannot be explained through conventional evolutionary models (Nelson and Weiss 1999).

This chapter examines processes of senescence as related to the maintenance of the adult human skeleton. Human aging is a complex and highly variable set of interactions between genetics, the endocrine system, body composition, and a variety of environmental factors (Karasik et al. 2005; Sehl and Yates 2001; Sherman 1999). The difficulty lies in determining which changes with age are the result of normal processes or the interaction between these processes and a disease state (Rowe and Kahn 1987). Earlier quantification of aging in the human skeleton has primarily come from a clinical perspective. This includes measures of trabecular bone mass and density at key sites (e.g., femoral neck and lumbar vertebrae) known for high risk of fracture. Little is known about cortical bone density with age, and even less is known about structural changes along the diaphysis of the long bones. To establish what the current state of research has revealed, I first discuss normal processes of aging, including differing concepts of bone health. Next, some of the environmental and modifiable lifestyle factors contributing to bone loss that may be inherent in this study's sample.

The Aging Skeleton

In the adult skeleton, remodeling (see Chapter 2) is the principal mechanism for replacing bone that has lost mechanical integrity with age (Parfitt 2003). This dissertation is primarily concerned with the remodeling of structural bone, and specifically, cortical bone in the

[3] One such theory is the "grandmother hypothesis," which suggests that that the selection for a longer life span after the reproductive period ends increases alloparenting and efficiency of resource management for a kin group (see discussion in Pavard et al. (2008)).

extremities. Structural bone is remodeled in the adult skeleton to replace damaged bone through targeted remodeling (Burr et al. 1997), and to prevent bone senescence through stochastic or non-targeted remodeling (Parfitt 2002b; Parfitt 2003). Regardless of the tempo or location of remodeling, a net loss of bone with time is inevitable and agreed upon to be nearly universal across human groups (Nelson and Weiss 1999; Parfitt 2003). In an effort to capture the scope of this decline, this dissertation examines a sample of adults aged 40-99 years at the time of death. It is useful then, to review what is currently known regarding bone quality through adulthood.

Bone Quality, Mass, and Strength

The definition of "bone quality" is murky, as it has been used across clinical and anthropological literature to denote amount of bone mass, mineral density of the skeleton, and bone strength. As a primary descriptor of skeletal health in both past and modern populations, a more robust use of the term includes *all* measureable factors that help resist bone failure. Although the definition of bone quality is not necessary universal, a more comprehensive evaluation of bone rigidity and resilience includes diachronic changes, targeted resorption and deposition, and geometric distribution of bone (Hernandez and Meulen 2017).

Clinically, "bone quality" is most commonly assessed by two measures of bone mass, bone mineral density (BMD) and bone mineral content (BMC), which are often used as proxies for "bone strength." Measured with a dual-energy absorptiometry (DEXA) scanner, BMC is the sum of density across the skeleton, while BMD is the amount of mineral content in a location of interest. In adults, clinical concern over these measures of bone strength is contextualized by risk of fracture (Anderson et al. 1963; Grynpas 2003; Riggs et al. 2002). However, BMD can be a problematic indicator of risk. Values of density or mass can be affected by the amount of adipose

tissue over the site of collection and reference samples are not available for all populations. Bone density differs between ancestral groups, which is understood to be a major determinant of peak bone mass (Key and Norman 1999; Nelson and Villa 2003). Further, some parts of the skeleton experience fracture more commonly from a single overload (e.g., wrist), while others from many cycles of small loads (e.g., hip) (Hernandez and Meulen 2017).

Experimentally, bone strength has also been tested using basic properties of geometry and material properties, including some of those described in Chapter 3. Multiple studies show mechanical strength and stiffness of cortical bone decline after 35 years (Burstein et al. 1976; McCalden et al. 1993; Zioupos and Currey 1998), continuing to reduce thereafter by two to five percent per decade. Bone mineralization increases with age, causing older bone to be weaker. This fact, along with increased porosity and slower bone turnover, contribute to a decrease in work to fracture, or a decrease in tensile plastic deformation (Burr and Turner 1999; Currey 1990; Currey et al. 1996). Even slight loss in density is correlated with a larger decrease in strength (Carter and Hayes 1977; Schaffler and Burr 1988). That is, over the span of a few adult years, bone mass may stay relatively the same but fracture risk increases exponentially due to decreasing density (Hui et al. 1988). This fact further evidences the incongruent relationship between BMD and bone strength. The scant anthropological literature concerning changes in geometry with age (summarized in Chapter 1) establishes a generalized pattern of increased cross-sectional area alongside decreased cortical area, particularly after the fifth decade (Ruff and Hayes 1982). However, no specific age range has been identified for the transitional shift to net bone loss or specifically when and in what location(s) shape changes may occur to mechanically compensate for increasing frailty of the material. This is discussed further in a section below.

Without the use of technology designed for living bodies, assessment of bone health in past populations necessitates a different set of parameters. Here, the utility of BMD is reduced, and instead, measures of mineralization, microarchitecture, and mechanical properties are used to evaluate bone quality (Grynpas 2003). Histological analyses demonstrate the number of remodeled osteons, which increase with age, as well as intra-osteonal modeling (Maggiano et al. 2008; Peck and Stout 2007; Trotter and Hixon 1974). Intra-osteonal modeling results in a type II osteon, also referred to as a double osteon. Double osteons have been found to increase with age, while single osteons decrease after the third decade of life by 2.5% per decade. A number of corroborating studies have also suggested that after 30 years, normal aging results in net bone loss (Atkinson 1969; Grynpas 2003; Riggs et al. 1982; Riggs et al. 2004). A decrease in muscle mass in both sexes starting in the third and fourth decades is likely correlated with this remodeling pattern in older adults.

Osteoporosis

An examination of bone health with age would be remiss without inclusion of the most common systemic skeletal condition in humans, osteoporosis (Imel et al. 2014). Although the incidence of the disease in the study sample is unknown, it is likely that a large number of both males and females were affected during life. Osteoporosis, and its precursor osteopenia, is marked by low bone density, degradation of the bone tissue, and ultimately an increase in fracture risk (National Institutes of Health 2001). Type I osteoporosis occurs in females after menopause. It is differentiated by increased bone turnover and a high rate of loss of trabecular bone, particularly in the vertebrae. The etiology of Type I is estrogen deficiency. Type II occurs in older adults of both sexes. Unlike post-menopausal osteoporosis, Type II is not associated

with increased bone turnover, but leads to fractures of the hip and is correlated with greater mortality and morbidity (Grynpas 2003, Kanis 1994, World Health Organization 2003). Type II is attributed to a reduction in bone formation rates and decreased ability of the kidneys to produced vitamin D with age. Because females may experience both types, it can be difficult to discern the root cause of bone loss, even in otherwise healthy patients. Table 2 summarizes established factors that increase the risk of osteoporosis. In addition to measures of bone mass used in this study (e.g., cortical area), some of these factors may influence measures of bone geometry as well, and as such, are discussed further below.

Osteoporosis is clinically diagnosed by proxy, using BMD of the spine, hip, and wrist, to calculate a T-score. T-scores represent the range of standard deviations an individual's BMD occurs from the mean of healthy 30 year-old individual of the same sex and race. Osteopenic patients have a T-score between -1 and -2.5, while a score of less than -2.5 is considered osteoporotic. A second measure, the Z-score, is the number of standard deviations an individual's BMD is from an age, sex, weight, and ethnic cohort (Allen and Krohn 2014; Imel et al. 2014). Two or more standard deviations away from the mean suggests that advanced bone loss may be the result of a factor, in addition to normal aging (Mayo Clinic 2016; World Health Organization 2003). In osteoporotic patients, additional factors have been identified to increase fracture risk, including prior fracture, alcohol and tobacco use, low or high BMI, and the use of glucocorticoids (Kanis et al. 2000; Kanis et al. 2010). Generally, as discussed previously, most cases of osteoporosis are considered a normal correlate of aging, and so bone density loss occurs in conjunction with changes in bone distribution through remodeling with age.

Table 2. Common risk factors associated with osteoporosis in adults
Risk factors are categorized as fixed (genetically or otherwise canalized) and modifiable (related to lifestyle habits, may be able to be changed). Table adapted from Imel et al. (2008).

	Risk Factor Examples
Fixed	
Race/ethnicity/ancestry	White, Asian
Sex	Female
Age	40 years and above
Menopausal state	Postmenopausal
Body size	Small body and bone size
Inherited conditions and disorders	Predisposition to low bone mass Osteogenesis imperfecta Cystic fibrosis Muscular dystrophy Marfan syndrome
Modifiable	
Nutrition	Anorexia nervosa Calcium and vitamin D deficiencies General malnutrition
Activity	Low level or lack of physical activity
Drug Use	Smoking Ethanolism
Medication	Anticonvulsants Glucocorticoids Blood thinners
Systemic conditions and disorders	Cancers Hyperparathyroidism Hyperthyroidism Inflammatory diseases Liver disease Kidney disease

Hormones and Sex Steroids

The influence of hormones on the adult skeleton is vast, and complicated by the general decline in the production of hormones and sex steroids with age. Because of the age range of the sample used in this study ($\geq$ 40 years), decline in hormone production can be assured. Homeostasis of bone minerals requires coordination between organ systems, particularly the intestines and kidneys, and the skeleton. Among others, their interactions are controlled by parathyroid hormone (PTH), phosphate regulating hormones, fibroblast growth factor 23 (FGF-23), and vitamin D metabolites (Bergwitz and Juppner 2010; Dimeglio and Imel 2014). The adult skeleton stores approximately 99 percent of the body's calcium (Ca) and 85 percent of the phosphorus (PO) as hydroxyapatite ($[(Ca)_{10}(PO)_4(OH)_2]$). PTH is largely responsible for regulating the concentration of calcium in the blood. This is accomplished by stimulating resorption of the bone matrix by osteoclasts and then increasing calcium absorption by the kidneys. Phosphate regulating hormones and FGF-23 contribute to phosphate absorption in the intestines and excretion by the kidneys (Dimeglio and Imel 2014; Quarles 2008). Lower or higher than necessary blood concentrations of these minerals signal an increase or decrease in secretion of hormones, which slows with age and results in net bone loss (Bellido and Gallant 2014). See Chapter 3 for hypotheses concerning signaling and maintenance of bone mineral homeostasis as related to structural functionality.

Net loss of bone in both males and females is also the result of changing levels of estrogen (menopause), testosterone (andropause), and adrenal androgens (adrenopause) (Leboff and Glowacki 1999). The relationship of these processes to bone mass is illustrated in Figure 8 and merits review. Together, these processes can result in losses of 0.7 to one percent of bone mass per year in both sexes, although pre-menopausal women can lose up to one to three percent

per year (Greenspan et al. 1994; Mazess 1982; Mazess et al. 1987). Males and females both demonstrate a significant increase in the rate of loss in the eighth and ninth decades of life (Ensrud et al. 1995; Riggs et al. 1981). Between young adulthood and death, females can lose an average of 42 percent of bone mass in the vertebrae and 58 percent in the femoral neck. Conversely, approximately ten percent of bone mass in the vertebrae and 38 percent in the femoral neck is lost in males during the same period (Riggs et al. 1982). As discussed earlier, little data exists on the effects of these processes across the skeleton, rather than just at clinical collection sites (e.g., spine, hip, wrist). Further, it is unclear whether and how these processes affect diaphyseal geometry.

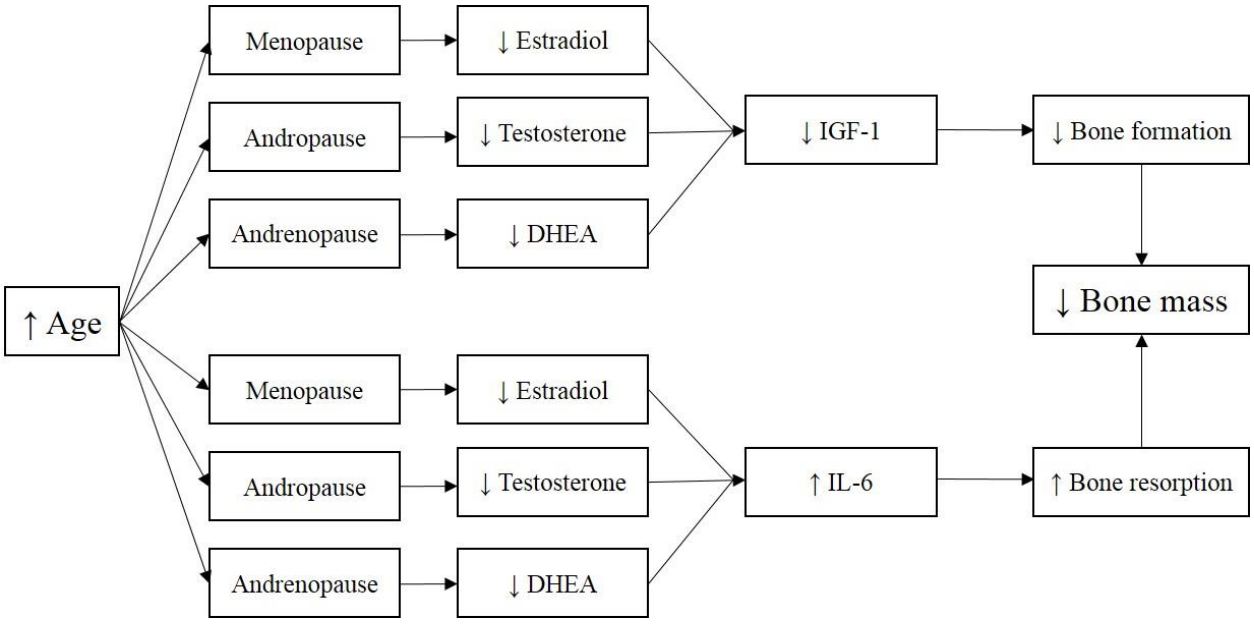

Figure 8. Age-related declines in hormones ultimately result in a decrease in bone mass
The decline in sex steroid production with age leads to a decrease in serum levels of estradiol (estrogen), testosterone, and dehydroepiandrosterone (DHEA). These lower levels are believed to cause a decrease in insulin-like growth factors (IGF-1) while simultaneously resulting in an increase in Interleukin-6 (IL-6). The former is responsible for osteoblast production and bone formation (Rosen et al. 1998), while the latter plays a role in osteoclast formation and bone resorption (Bellido et al. 1995). Figure adapted from Leboff and Glowacki (1999).

Menopause, or the age at the final menstrual period, marks a time when circulating levels of estrogen are drastically reduced. Estrogen works to increase endosteal formation (see Chapter 2), which is outpaced by resorption in older adults (Martin 2003; Turner et al. 1989; Turner et al. 1990). Although generally agreed upon to increase the rate of bone loss, studies provide conflicting results as to minimum levels required for bone maintenance after menopause (LeBoff and Glowacki 1999). Estrogen deficiency increases bone turnover, largely due to an imbalance in site-specific remodeling. During this time, osteoblasts and osteoclasts are produced in greater numbers, however, the lifespan of the former increases while that of the latter decreases. The result is deeper resorption pits and a delay in BMU activity (Bellido and Gallant 2014). In men, declining levels of estrogen have been identically correlated with bone loss. Further, estrogen therapy has been shown to increase bone density in osteoporotic men (Greendale et al. 1997; LeBoff and Glowacki 1999; Slemenda et al. 1997). The timing at which menopause occurs in women (and a marked estrogen-level drop in men) is associated with life expectancy, rate of bone loss, total bone loss, and risk of certain cancers and cardiovascular disease. The age of onset for these changes is dependent on socioeconomic status, racial/ethnic differences, body mass, genetic and familial factors, environmental exposures, diet, physical activity, and reproductive history (Cooper and Sandler 1998; Gold 2011; Ossewaarde et al. 2005; Snowdon et al. 1989; Wise et al. 1996). Although these factors and the age of onset of menopause cannot be accounted for in this study, it is assumed they have some degree of covarying influence on measures of bone mass collected.

Andropause is the generally accepted term for the gradual decline in androgen, particularly testosterone, levels in aging men (Vermeulen et al. 1989). Testosterone works to increase periosteal formation (see Chapter 2) during growth and is the leading stimulant of

periosteal expansion in older adults (Martin 2003; Turner et al. 1989; Turner et al. 1990). Between the fourth and the seventh decade of life, however, circulating levels of testosterone can decrease by approximately one percent per year (Gray et al. 1991). Low levels can inhibit calcium absorption and like estrogen, increases fracture risk (Bellido and Gallant 2014; Boonen et al. 1997; LeBoff and Glowacki 1999). However, most of the mechanisms for steady bone loss in men are related to estrogen deficiency and it is unclear the full scope of estrogen-independent effects androgens may have on the skeleton (Bellido et al. 2014). Much like the onset and net effects of menopause on bone density, body mass, smoking, and alcohol abuse decrease site-specific mass and increase fracture risk during andropause (Nyquist et al. 1998).

Adrenopause is the ageing of the adrenal gland, which is responsible for secretion of dehydroepiandrosterone (DHEA) and other androgens, including cortisol. DHEA is the only of these that declines significantly with age in both sexes; approximately twenty percent is lost by the seventh decade of life (Orentreich et al. 1984). In anorexic (Zumoff et al. 1983) and postmenopausal women (Raisz et al. 1996), DHEA replacement therapy has been shown to reduce bone resorption. The addition of estrogen therapy not only decreases markers of turnover in these patients, but also stimulates bone formation (Leboff and Glawocki 1999; Raisz et al. 1996).

While the individual effects of these processes on the skeletons used in this study cannot be identified, some degree of bone loss with age will exist throughout the sample. With net loss, bone must compensate structurally to maintain resistance against failure. This compensation may be able to be quantified using cross-sectional geometric properties, but little precedent exists. What is currently known about that mechanical compensation is reviewed next.

Structural Compensation for Frailty

As the skeleton ages through many of the processes outlined above, it becomes increasingly lighter. Following the premise of the mechanostat model (see Chapter 3), a lighter skeleton can be mechanically and physiologically advantageous. The skeleton also has a built-in system for balancing strain levels against bone mass. However, when frailty reaches the point of fragility, the geometry of the bone diaphysis must change to resist failure (Burr and Turner 1999; Frost 1997; Martin 2003; Parfitt 2003). A small number of studies of diaphyseal cross-sectional geometry identify specific age-related patterns of augmentation in medullary and total cross-sectional areas, with a decrease in cortical bone area. In both adult males and females, long bone diaphyses demonstrate a pattern of subperiosteal apposition and endosteal resorption as age increases (Biver et al. 2016; Martin and Atkinson 1977; Mays 2001; Ruff and Hayes 1982). However, no specific age range has been identified when shape changes may occur to mechanically compensate for increasing frailty of the material.

As discussed above, mineralization of bone increases with age, which makes older bone weaker than younger or less mineralized bone, regardless of density (Burstein et al. 1976; Currey 1979; Dickenson et al. 1981; Turner 2002). Increased porosity at this time amplifies the effects of mineralization on mechanical properties and the ability of the bone to absorb and resist energy upon impact (Burr and Turner 1999; Courtney et al. 1996). That energy is most commonly due to bending and torsional loads (Martin 1993), which can be better resisted by moving bone tissue further from the center axis. This then explains the compensatory pattern of increased medullary and cross-sectional, or subperiosteal, areas to make up for a decrease in cortical area.

Structural compensation in this way does appear to be sexually dimorphic in modern humans. Although many studies report that both sexes undergo periosteal expansion alongside

endosteal resorption (Bouxsein et al. 1994; Garn et al. 1967; Smith and Walker 1964), others have found that females experience geometric changes resulting in decreased bone strength (Burr and Martin 1983; Martin and Atkinson 1977). Ruff and Hayes (1988) report that the diaphyses of male femora and tibiae retain most of their cortical area with age and moments of inertia increase slightly. Both variables decrease with age in females. In the femoral neck, however, moments of inertia have been found to decline by five percent, per decade, in females over 50 years of age (Beck et al. 1993). That is, although both men and women lose bone mass at an increased rate in older years, females are less likely to make mechanically effective compensatory changes. However, these findings are still controversial (Bouxsein 1999), as variation in geometry with age may also be the result of many modifiable mechanisms, in addition to sexual differences and normal processes of aging.

Modifiable Mechanisms of Bone Loss

Lifestyle choices in adulthood can affect the maintenance of bone mass after peak bone mass is reached in adolescence. Factors identified to have the greatest affect alongside the above reviewed processes of aging are nutrition, body weight, physical activity, and some chronic conditions. Some of these exacerbate the rate of bone loss already in effect as a result of hormonal changes, while others are associated with the increased likelihood of maintenance, or even an increase, in mass. While it is not possible to know the exact medical history or lifestyle choices of individuals in this study, it is important to recognize some factors discussed below that are likely to have affected bone quality.

Nutrition

Like any other organ system, bone requires a variety of nutrients to maintain homeostasis and repair damage. In addition to macronutrients such as protein and fat, essential micronutrients are required for bone health. These include calcium, phosphorus, zinc, copper, and iron minerals, and vitamins D, K, C, and A (Weaver and Gallant 2014a). While all of these nutrients are readily available in animal foods, fruits, and vegetables, modification of the food supply in the United States in the last fifty years is correlated with in an increase in bone health issues. As the sample for this study was derived from a large pool of individuals from the southern United States, it is worthwhile to review some of the major issues regarding dietary intake effects on adult bone maintenance. Intimately related to diet are the broader effects of socioeconomic status on the skeleton, which are reviewed in Chapter 2.

Highly processed foods are often fortified with nutrients at the expense of fiber, but have increased salt and phosphate content (Anderson 1999). Fast and snack foods generally have a very high sodium content, which weakens the body's ability to conserve calcium and long term intake of high sodium foods can increase bone loss (Massey and Whiting 1996). Soft drinks and other processed foods are also high in phosphate additives. Phosphorus makes up approximately 15-20 percent of bone ash (Mitchell et al. 1945; Weaver and Gallant 2014a) and is part of an essential acid-base buffer system that helps to maintain pH. Increased intake of phosphate additives can cause an imbalance in the calcium-to-phosphate ratio. At healthy levels, this ration helps maintain hormone levels through the system. The imbalance in phosphates can lead to deleterious effects on hormone concentrations (e.g., FGF-23) that are essential to bone health (Dimeglio and Imel 2014).

A final point of concern regarding adult nutrition is excessive animal protein consumption. Although animal foods can provide macronutrients fat and protein, high levels of animal proteins cause calcium loss through urinary excretion (Lutz 1984; Schuette and Linkswiler 1982). Some studies have even found that animal protein intake in excess of recommended levels is attributed to higher rates of osteoporosis in industrial nations (Abelow et al. 1992; Anderson 1999; Sellmeyer et al. 2001). A vegetarian diet, on the other hand, produces relatively neutral urinary pH values and is recommended by some to protect bone health (Lemann et al. 1993).

Obesity and Weight Loss

Related to nutrition in many Western countries is an increase in mean body masses within the population. Approximately forty percent of the sample used in this study had a body mass index (BMI) categorized as overweight or obese in life (see Chapter 5, Table 4). Adults with higher BMI demonstrate greater BMD than lower BMI categories, which as discussed in Chapter 3, is likely a function of increased mechanical loading. These effects may be amplified by the higher levels of adipokines, cell-signaling proteins secreted by fat tissue in overweight individuals (Weaver and Gallant 2014). Adipokines like leptin have dual effects on bone; they increase remodeling in trabecular bone and stimulate bone formation in cortical bone (Bellido and Gallant 2014). Serum estrogen levels are forty percent higher in obese women because fat tissue also supplies the body with estrogen (Cauley et al. 1989; Frisch 1990). Despite higher BMD values, obese individuals have a greater risk of fracture as a result of other co-morbidities.

On the other side of the mechanostat model, weight loss in adulthood reduces mechanical strain and triggers bone loss to return strain levels to normal. However, the picture may be

slightly more complicated in obese and overweight individuals, as a decrease in total body fat is more tightly correlated with decreased BMD than is weight loss. Changes in bone turnover with weight loss are generally not regained with weight gain (Weaver and Gallant 2014), and extreme weight loss can result in increased fracture risk (Nagata et al. 2017). Clinically, it is recommended that weight loss be achieved through weight-lifting exercise to help counteract any deficit in bone mass as a result of decreased strain from body weight (Kerr et al. 1996a; Leichter et al. 1989; Syed and Ng 2010; Turner and Robling 2003), which is discussed further below. Of importance to this study is the use of extreme or "yo-yo" dieting techniques, in which weight is lost and regained quickly and inconsistently, that may produce concomitant results with normal processes of bone loss with aging.

Physical Activity

From an anthropological perspective, the advent of industrialization was marked by a gradual decrease in physical activity, muscle strength, and skeletal robusticity from that of prior subsistence strategies. That is, as modern humans age, strain on skeleton is reduced at an earlier age and to a greater degree than present preindustrial populations (Agarwal and Grynpas 1996; Frost 1996; Frost 2003; Garn 1971; Nelson and Weiss 1999; Parfitt 2003). If the mechanostat premise is accepted, loss of bone mass with age returns strains to homeostatic levels, and the risk of failure is decreased. However, fracture risk increases in modern humans as they get older. Frost (1997) and Parfitt (1996; 2003) suggest that perhaps the mechanostat is "blind" to the greater chance of falls and accidents of populations living longer. That is, individuals are living past the mechanostat's limit for compensating for age-related bone loss. As a result, the skeleton of elderly individuals can absorb and resist low, everyday levels of loading from minimal

locomotion and body weight, but cannot support high levels of force incurred during a fall, as younger adults can.

Clinically, exercise therapies are still recommended to counteract bone loss and increase geometric properties related to strength. Physical activity interventions in weight-bearing bones have been shown to result in maintenance or increase of bone geometric properties (Nilsson et al. 2016). The evidence for effectiveness of exercise intervention at preventing or rescuing bone lost in with aging throughout the skeleton is unresolved (Hughes et al. 2016; Smith et al. 2010; Smith and Walker 1964; Vincent et al. 2012; Wallace and Cumming 2000). Although no one exercise program has universally proved to increase bone mass, there is general acceptance that resistance training produces greater gains (1- 2%) than walking (Robling et al. 2014). Walking is still recommended as preventative exercise and models show stress on the femoral neck during walking to be effective (Qian et al. 2014). In perimenopausal women, studies of 18 months of endurance exercise (Heinonen et al. 1998) and 6 months of resistance exercise (Dornemann et al. 1997) have been shown to maintain BMD in the femoral neck and vertebrae. The lumbar spine of early menopausal women appears to respond in the same way (Pruitt et al. 1992), but effects on the rest of the skeleton remain unclear. After menopause, multiple skeletal sites (Nilsson et al. 2017), including the radius (Kerr et al. 1996b; Krolner et al. 1983) and calcaneus (Williams et al. 1984) show maintained, and even increased, BMD in some women after long term endurance exercise and resistance training. In men, step and jumping exercise studies have shown to increase femoral neck BMD in individuals aged 50-70 years (Welsh and Rutherford 1996).

The threshold of exercise loading for adult bone maintenance is still relatively unclear (Bergmann et al. 2011) and its effects on individuals in the current study cannot be definitively known. What is clear is that structural changes as a result of physical activity still need to be

established (Hughes et al. 2016; Robling et al. 2014; Turner and Robling 2003) from multiple skeletal sites particularly in cortical bone (e.g., periosteal expansion in the diaphysis).

Chronic Disease States

The World Health Organization (2003) and others (Imel et al. 2014; Kanis et al. 2005; Wong et al. 2007) have identified several chronic diseases and conditions, also present in the current study sample, that affect bone mass in adults. These include alcohol and drug abuse, cancer, and diabetes. Chronic alcoholism reduces osteoblastic activity, and affects osteon remodeling and the number of osteons in a region (Frost 1985; Michael and Bengtson 2016; Stout 1989). As a result, chronic alcoholics have lower bone mass than age-matched healthy cohorts. Similarly, loss of bone mass of three to fifteen percent has been demonstrated in both male and female smokers in the femoral neck and spine (Jones and Scott 1999; Kiel et al. 1996). The exact mechanisms behind bone loss in smokers are unclear (Wong et al. 2007), but lower body fat levels (Jones and Scott 1999) and decreased appetite may play a role (Kanis et al. 2005; Rasmussen 1998).

Conversely, adult onset diabetes, or type 2 diabetes mellitus (T2DM), demonstrates the incongruent relationship between bone mass and bone health. Figure 9 reflects the changing trends in obesity and diabetes in adults in the United States (Centers for Disease Control and Prevention 2015), which is highly relevant to the sample used in this dissertation. T2DM patients generally have higher bone mass than in healthy cohorts, likely as a result of higher body mass. However, individuals with T2DM are almost twice as likely to incur a fracture as a result of poor bone quality (Liefde et al. 2005; Vestergaard 2007). Although not entirely understood, the collagen matrix in diabetics may be impaired as a result of chronically high blood glucose,

leading to more brittle bones (Weaver and Gallant 2014). This cannot be empirically tested in the current sample, but should be considered when comparing the results of this study to other samples in which mean obesity rates, socioeconomic status, and dietary trends differ.

Chapter Summary

This chapter reviewed many of the processes contributing to senescence of the adult human skeleton. Most of what is known is from a clinical perspective and concerns measures of bone mass, which is not a good substitute for actual bone strength. Skeletal aging differs in many ways between males and females, which will be tested in the current sample. Although the evolutionary reasons for the high incidence of osteoporosis and non-pathological bone loss in industrialized groups have not been established, it appears that an interaction between normal biological aging and environmental factors plays a large role. It is clear that there is a need for a more comprehensive picture of how bone changes with age. This dissertation seeks to fulfill that need by examining the variation present in diaphyseal geometry and measures of bone mass in middle age through the elderly years. Chapter 5 outlines the study sample, data collection, and methods of analysis used.

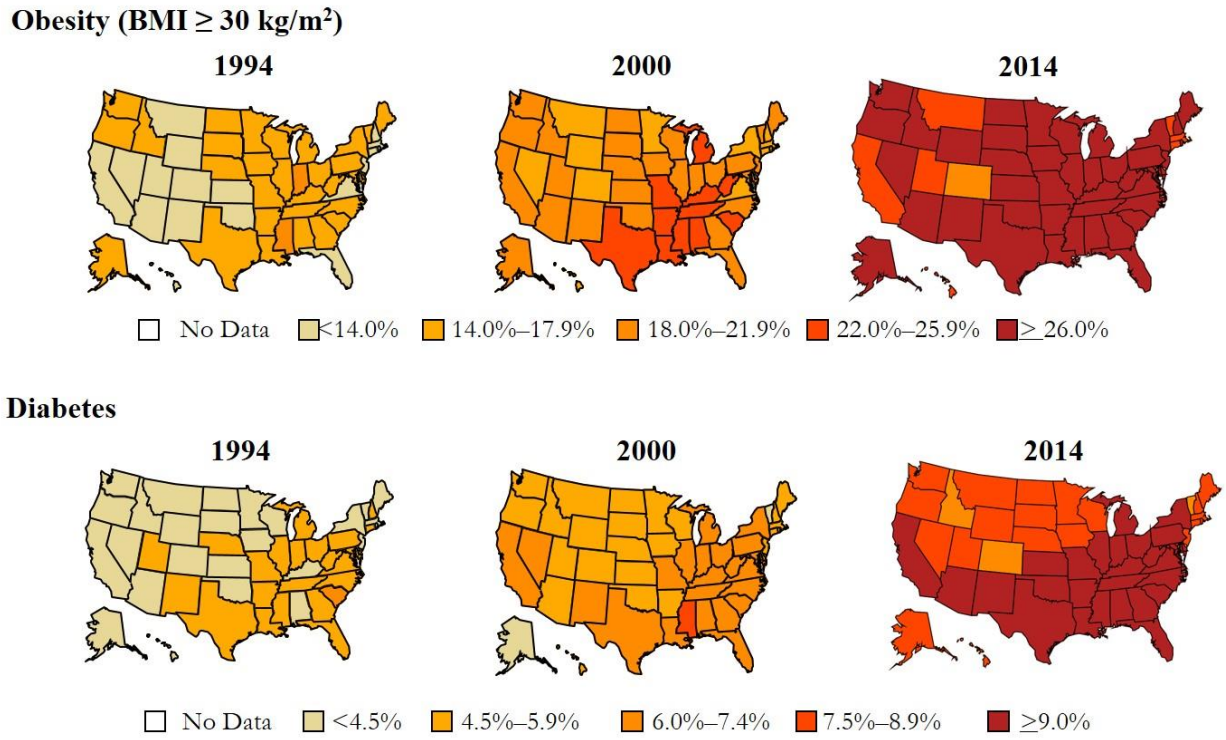

Figure 9. Trends in adult obesity and diabetes in the United States
A clear trend in increased incidences of obesity and diabetes (considered to be a co-morbidity of obesity) exists over the last twenty years. The sample used in this study is derived largely from individuals who lived in the southern region of the United States, particularly in Tennessee. With an incidence rate of greater than or equal to nine percent of the population, it can be assumed that the bone health of a number of individuals used in this study may have been affected by diabetes. This figure is reproduced from the Centers for Disease Control and Prevention 2014 Diabetes Report Card (www.cdc.gov/diabetes/data).

CHAPTER 5

MATERIALS AND METHODS

This chapter details the study sample and methods used to test the hypotheses outlined in Chapter 1. The radiographic sample is described first, including the selection criteria for the final sample used in the study. The variables examined in this study are listed and additional factors that cannot be accounted for in this sample are highlighted. Methods for data collection are then provided: detailing the protocol for CT scan segmentation of each bone and extraction of CSG properties (described in Chapter 3) from selected bone locations, the bone sections chosen, and the measurements taken. This chapter ends with a description of the analytical methods chosen. Limitations of the methodologies used in this study are defined throughout.

Radiographic Sample

Skeletal Collection

This study utilized X-ray computed tomography (CT) scans of skeletal remains from the William M. Bass Donated Skeletal Collection. The scans originate from a series of projects undertaken at the University of Tennessee, Knoxville (UT) since 2005. Over 900 individuals have been scanned through a collaboration between the Center for Musculoskeletal Research and the UT Department of Biomedical Engineering. The scans were obtained using a high-resolution GE Lightspeed 16 slice computed tomography scanner. The procedures used for positioning the bones for scanning been described in previous studies (Moore 2008; Moore 2013; Reeves 2014). CT scans are advantageous over traditional two-dimensional (2D) radiographs for quantifying

the morphology of bone because of the quality of the resultant image. Each CT image is comprised of voxels (volume elements), as opposed to pixels in 2D imaging. The voxel size of the available scans was either 0.625 or 0.703 mm/pixel, depending on the original scanning project. All data was scaled to the same resolution of 0.703 mm/pixel before analysis. CT scans contain many image files, which are stored as a stack of image slices. The stacks for this sample were loaned from the WM Bass Collection to the researcher as Digital Imaging Communications in Medicine (DICOM) files on a secured data storage device.

Donors to the Bass Collection have died within the last forty years and are asked to complete biological questionnaires before death. These questionnaires cover a wide variety of demographic (e.g., sex, age, "race," height, weight) and lifestyle (e.g., occupational and medical history) information. Because this information is self-reported or provided by next of kin after death, it is possible that a degree of error exists. It is likely that individuals may not have reported accurate or complete information. Of particular relevance to this dissertation are unreported conditions that may affect bone mass or mobility. Much of the reported information is also incomplete. As the questionnaires have expanded with time, more information is generally available for the most recently deceased. Potential issues associated with self-reported data are discussed below. It is noted that an experimental sample of living humans with a more robust questionnaire or access to medical histories, as opposed to a skeletal one, would be ideal in testing the aims of this study. In this case, however, the skeletal sample used avoids radiation concerns associated with living participants as well any difficulties in obtaining data from a large, fairly homogenous population.

Selection Criteria

A final sample of individuals (N = 208) was selected from the total scanned population based on several criteria. Scans were obtained from males and females between the ages of 40 and 99 years at the time of the death. This age range captures the reported chronological age at which decline in bone density and muscle mass commences in both sexes (Biver at al. 2016) and the oldest age present in the available scans.

Individuals need to minimally have the following data: a record containing known age-at-death, known sex and body weight, and a CT scan containing intact left humeri, radii, ulnae, and bones of either lower limb. Only left limbs were used to avoid issues associated with asymmetry. However, in the cases in which the left lower limb was unavailable or presented with a pathology that may impact diaphyseal shape, right femora, tibiae, and fibulae were substituted. The degree of asymmetry in the lower limb is generally considered negligible in comparison with the upper limb (Auerbach and Ruff 2006; Reeves et al. 2016). Finally, CT images that indicated the presence of trauma, including fracture, healing callus, orthopedic devices or implants, advanced periostitis, or active infection were not included.

Demographic data was also collected from the record of each individual, if available: height, occupation/hobbies, and cause of death (COD). Although known differences exist in bone density and propensity for osteoporosis among ancestral/racial groups (Key and Norman 1999), ancestry was not used as a variable for comparison in this study. Moreover, populations other than “white” (i.e. European American ancestry) are poorly represented in the Bass Collection; current (September, 2016) statistics for the collection report that 89 percent of donated adult individuals are white (DW Steadman, personal communication).

In addition to age and sex, the first set of hypotheses (outlined in Chapter 1) tests whether body mass index (BMI), activity level, and chronic disease state have any effects on the distribution of diaphyseal cortical bone. A breakdown of individuals in the final sample by sex and age, then by BMI, activity level, and disease state is provided in Table 3. BMI, a measure of body mass relative to height, is the first of these secondary variables. An individual's BMI was calculated by dividing weight (kg) by height (m^2). The categories for adults as defined by the Centers for Disease Control and Prevention (2015) are provided in Table 4. BMI is used clinically for diagnostic purposes and experimentally as a proxy for body fat content. However, as reviewed previously, BMI can be a problematic method of categorization of body mass. While it is strongly correlated with body fatness, it is not a direct measure of body fat. That is, two individuals may differ in body adiposity, but have the same BMI value. BMI values can be particularly misleading in instances of individuals of very high or very low body fat percentage. Implications of the incongruence between BMI and body fat content on bone mass are discussed in Chapter 4.

Table 3. Final study sample distribution by sex and age for BMI, activity level, and chronic disease condition

Sex	Age	*N*	BMI category[1] (*N*)				Activity level[2] (*N*)			Disease state[3] (*N*)	
			underweight	normal	overweight	obese	light	moderate	heavy	healthy	pathological
Female	40 - 49	6	0	2	1	2	5	1	0	1	2
	50 - 59	27	2	8	3	11	21	5	0	16	8
	60 - 69	21	1	4	5	5	9	6	2	10	7
	70 - 79	19	2	5	6	6	8	9	2	13	3
	80 - 99	17	3	8	3	2	10	6	1	14	2
Total		90	8	27	18	26	53	27	5	54	22
Male	40 - 49	21	0	5	2	7	4	6	7	7	8
	50 - 59	30	0	9	2	10	8	10	6	19	5
	60 - 69	24	2	9	4	7	11	4	6	11	4
	70 - 79	26	4	12	3	3	4	8	10	14	6
	80 - 99	17	2	6	3	3	4	4	7	10	2
Total		118	8	41	14	30	31	32	36	61	25
Grand Total		208	16	68	32	56	84	59	41	115	47

[1] BMI for each individual was based on reported height and body weight and categorized by CDC standards. *n* = 37 individuals in the final sample did not report height, and thus, BMI could not be calculated.
[2] Activity levels were determined by declared occupation or notation of habitual hobby activity. *n* = 23 individuals in the final sample did not report occupation or hobbies.
[3] Disease state refers to the COD and other reported medical conditions. Individuals are classified as "healthy" (i.e. no chronic condition was noted that would interfere with the regions of interest) or "pathological" (i.e. chronic condition noted that may affect bone density or shape). *n* = 45 individuals in the final sample have no record of COD.

Table 4. BMI categories
This table is adapted from the Centers of Disease Control and Prevention (2015).

Weight Category	Body Mass Index (BMI)
Underweight	< 18.5
Normal weight	18.5 - 24.9
Overweight	25.0 - 29.9
Obese	> 30.0

Activity level was assigned as one of three categories: light, moderate, or heavy. These categories are commonly used in fitness and other clinical assessments (Biver et al. 2016, Suurnäkki et al. 1991, Vingård 1996) and in this case, assignment was based on declared occupation and/or hobby. Each category represents an assumed level of skeletal loading from habitual locomotor or activity repertoires. Light activities include occupations requiring a great degree of sitting (e.g. accountant) and hobbies in which mobility is limited (e.g. fishing). Moderate activities utilize an increased amount of locomotion or light lifting (e.g. retail sales or teaching assistant). Heavily-loaded activities are those in which locomotion or lifting is habitual and substantial (e.g. brick layer or wrestler). Appendix A (Table A.1) provides examples of self-reported activities in this sample and the category to which they were each assigned.

Bias is inherent in these activity level categories for a number of reasons. First, the reported occupation or hobby may not have been done as frequently or with as much vigor towards the end of life. This may be especially true for older age groups (70+ years) and also for those whose occupation or hobby was classified as heavy loading. Second, sexual bias may exist. From the final sample distribution (Table 3), it is clear that males reported participation in heavy loading activities far more often than females. Finally, some individuals who reported an

occupation or hobby, may not have reported their height. Without height, BMI could not be calculated, and any interaction between BMI and habitual loading from activity cannot be assessed.

Chronic diseases such as alcohol or drug abuse, cancers, and diabetes are known to affect bone mass in adults (see review in Chapter 4). Based on questionnaire data, COD and any other medical condition noted were used to categorize individuals as "healthy" or "pathological". "Healthy" individuals had a declared COD that does not alone clinically compromise bone mass or mechanical strength (e.g., cardiac arrest, natural death), however, it is likely that many of these individuals may have had undeclared or undiagnosed conditions that affect bone integrity. Individuals were categorized as "pathological" if their COD or other conditions (e.g. ethanolism, metastasized cancers) are known to directly affect bone composition. Again, it is entirely possible that there is error in reporting of COD, and these conditions cannot be directly identified as lone causative factors for bone loss in this particular sample.

Data Collection

Segmentation, Alignment, and Slice Selection

Segmentation protocol of the full-body DICOM stacks was developed by Adam Sylvester (personal communication) (Figure 10). DICOM stacks from the final study sample were uploaded in Avizo 3D software (FEI 2017). Each bone of interest (left humerus, radius, ulna, femur, tibia, fibula) was segmented by creating an isosurface of the entire stack and thresholding the model to render the bone in the CT scan visible (Figure 10a.). All models were thresholded at -500. Once visible, the six left long bones were identified and viewed in the transverse plane using Avizo's orthoslice mode (Figure 10b). This view is equivalent to the cross-section of the

bone perpendicular to the long axis of the diaphysis. Stacks were then manually cropped (Figure 10b) one slice beyond the minimum and maximum slices containing the bone of interest. Proximal and distal ends of bones were identified visually; however, it is not expected that this introduced any meaningful error into the data collection. Individual bone image stacks were saved as tiff files.

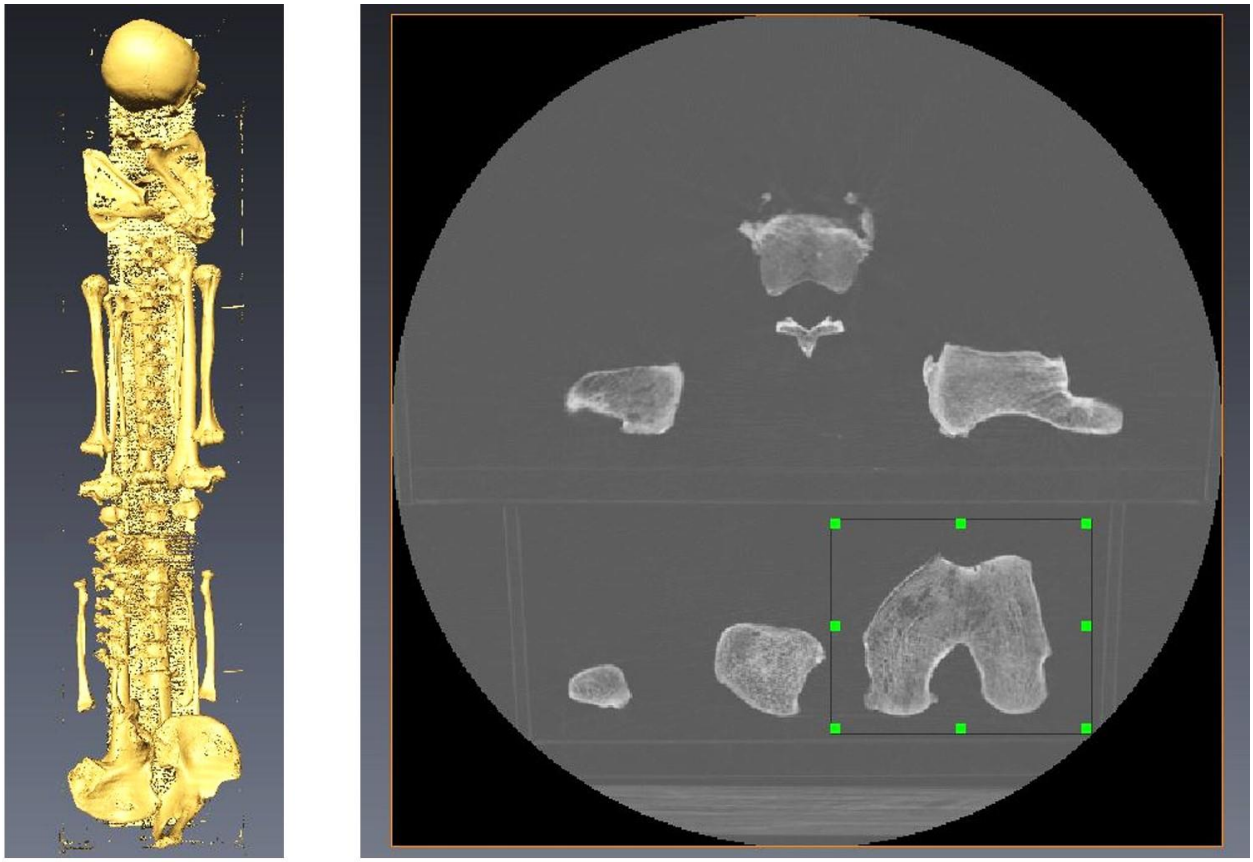

Figure 10. Bone segmentation from CT scan image stack
(a.) An isosurface in Avizo 3D allows the viewer to visualize the bone material in the entire DICOM stack of images and identify the bones of interest. **(b.)** In Avizo's orthoslice mode, the bone of interest (in this case, a left femur) can be segmented from the entire stack.

Segmented bone image stacks were then uploaded in Avizo. A surface model was created from the stack (Figure 10) and maximum bone length was measured. Maximum length was taken from the most proximal point to the most distal point on each bone. Although this method of measurement is not necessarily mechanically relevant in all bones (e.g., ulna and tibia), capturing length from more conventional locations (see those for the ulna and tibia in Buikstra and Ubelaker 1994, Langley et al. 2016) produced inconsistent measurements. Error in maximum length measurement was tested using a sub-sample $n = 30$ individuals ($n = 30$ of each of the six elements examined in the study) (Table 5). After the initial data collection for the entire sample was complete, maximum length was re-measured for these thirty individuals and compared to the original measurements using a repeated measures analysis of variance (ANOVA) for each bone ($\alpha = 0.05$). There was no significant difference between rounds of measurement for any element.

Table 5. Error in maximum length measurement collection

Bone	**df**	**F**	*p*
Humerus	29	1.33	0.22
Radius	29	1.09	0.41
Ulna	29	1.86	0.09
Femur	29	1.62	0.10
Tibia	29	1.69	0.08
Fibula	29	1.71	0.08

The surface models were then aligned along the principle axes of the bone using the alignment function in Avizo. Alignment along the neutral axis of the diaphysis allows bones of different shapes and sizes to be compared. That is, slice locations collected perpendicular

(transverse plane) to the neutral plane of the diaphysis will be homologous regardless of variation among individuals. If slices were collected on a non-perpendicular plane, geometric values would be skewed (Ruff and Hayes 1983). Most models could be aligned as they were, however, femora provided a unique exception. As a result of femoral bowing, alignment using the entire bone caused the long axis of the bone to veer towards the neck and medical condyle, rather than in the middle of the diaphysis as it would be in the other five bones, which are naturally oriented straighter. To correct for this, the proximal and distal epiphyses of the model were removed before aligning the bone (Figure 11). For all bones, the alignment was copy and pasted to the original stack and then resampled.

A central aim of this study was to examine variation in cortical bone distribution using a "whole bone" perspective (Cristofolini et al. 2010; Gosman et al. 2013; Hubbell et al. 2011). As discussed in Chapter 3, many early studies only examined cross-section geometry at midshaft, or 50 percent of bone length, as this is the most mechanically sensitive location of a beam. However, the anisotropic nature of bone diaphyseal morphology means that loading forces are mitigated differently along the entire length of the bone. For this reason, cross-sectional properties were taken at five locations along the diaphysis: 20, 35, 50, 65, and 80 percent of bone length from the distal end (Figure 12). This required identification of the appropriate locations within each segmented bone. Once the aligned model was saved, percentage of bone length was calculated using the total number of bone slices. The corresponding slice files were pulled from the stack and saved separately for measurement of diaphyseal properties.

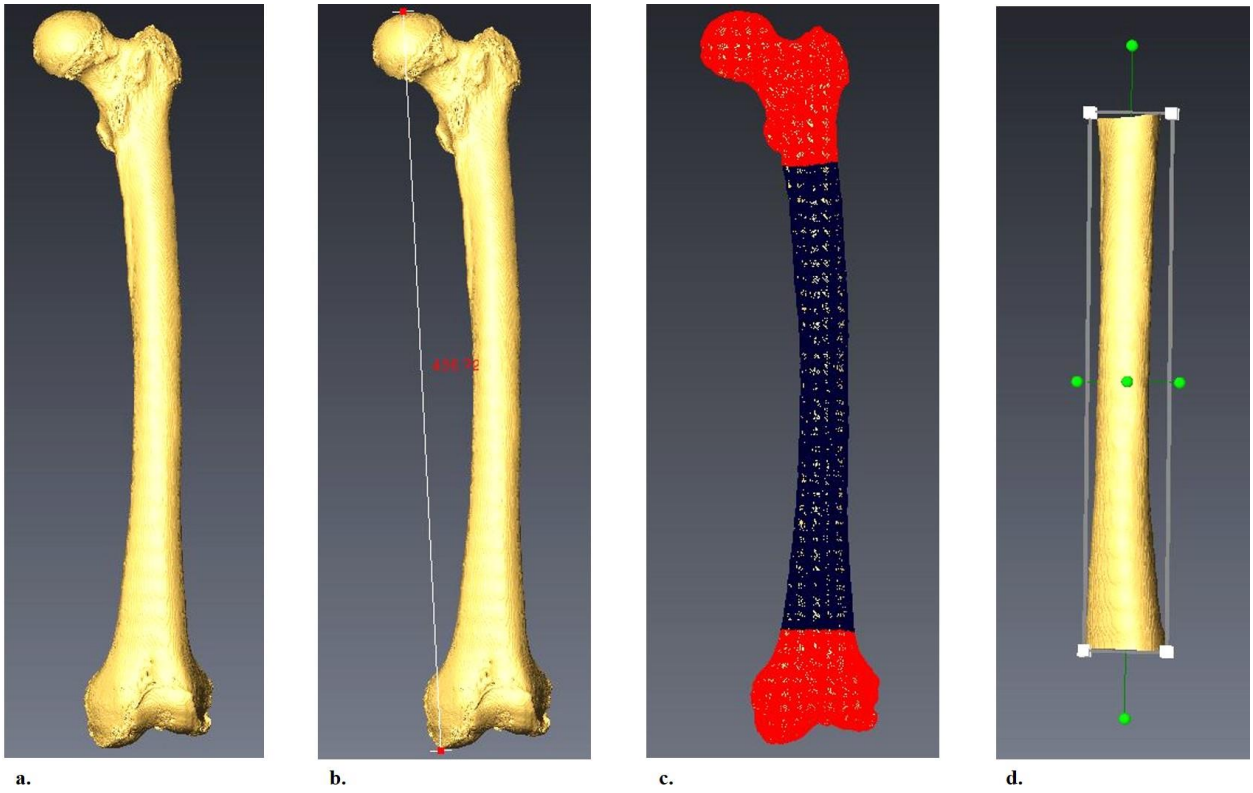

Figure 11. Surface model construction and alignment
(a.) An example of a surface model of a left femur. **(b.)** Maximum length was taken from the most proximal point to the most distal on each bone. **(c.)** Alignment for femora was performed after the proximal and distal portions were removed. All other bones were aligned using the entire bone. **(d.)** A properly aligned femur, showing the long axis of the bone through the center of the diaphysis, rather than being skewed by bowing caused by the proximal and distal ends.

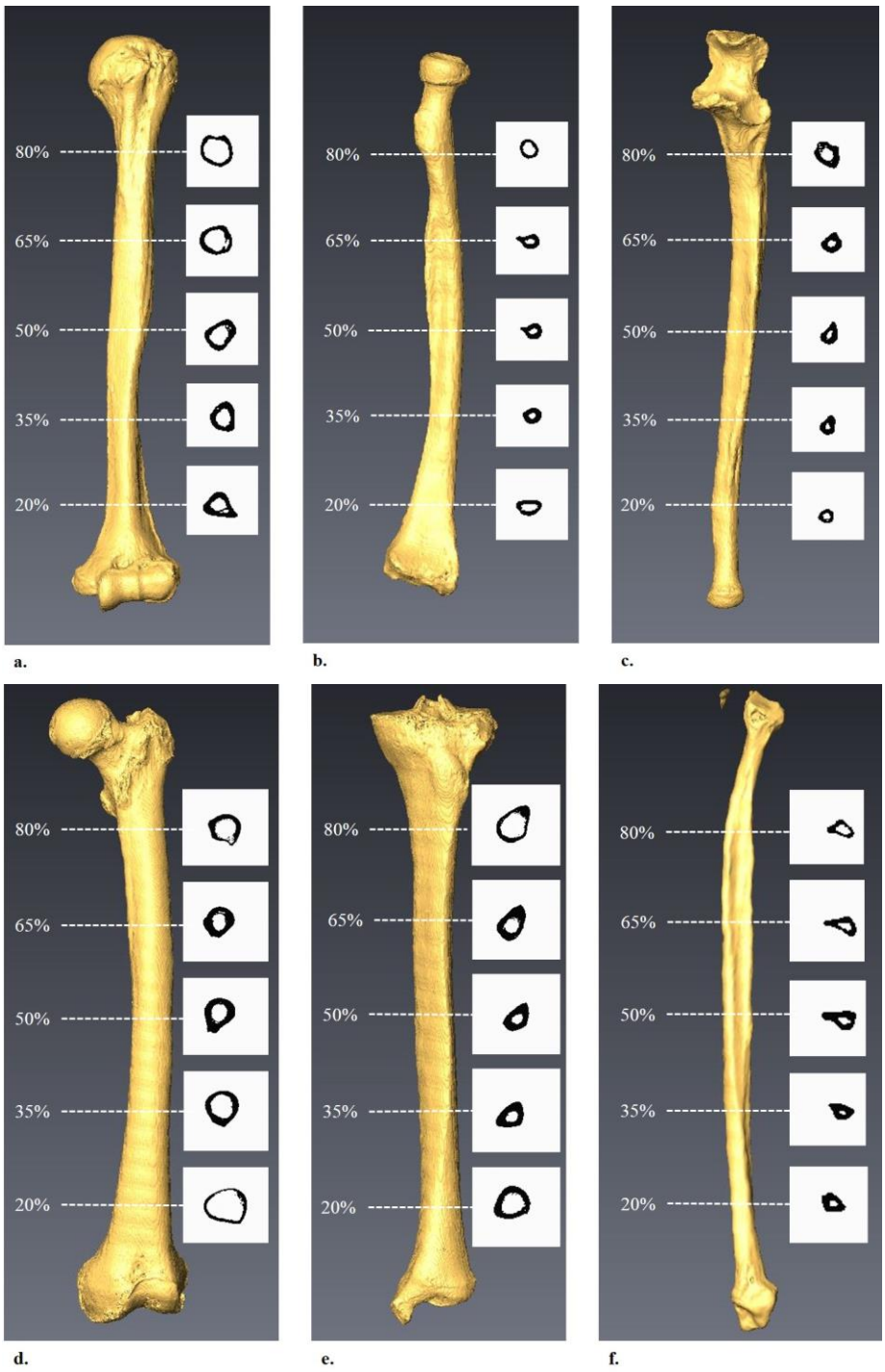

Figure 12. Slice locations with example cross-sections
Slices were collection from five locations on each bone: 20, 35, 50, 65, and 80 percent of bone length as measured from the distal end of the humerus **(a.)**, radius **(b.)**, ulna **(c.)**, femur **(d.)**, tibia **(e.)**, and fibula **(f.)**.

Diaphyseal Measurements

The selected slices were processed for CSG measurements using a MATLAB (Mathworks Inc. 2017) code created by Adam Sylvester (personal communication)[4]. Using this code, MATLAB was used to collect 3D moments and slice geometry of cortical bone distribution, including properties that indicate the bone's mass, shape, and bending strength and rigidity at each site. These measurements were discussed in Chapter 3; Table 1 provides a summary.

It is expected that measurements of the cortical area, total subperiosteal area, and medullary cavity area are sufficient to quantify bone mass. These values were standardized by body mass (Ruff 2000b). To assess shape, percent cortical area was calculated as well as a shape index reflecting the maximum and minimum breadths of the bone. Section moduli were used as a measure of bone strength. These include maximum and minimum bending strength, as well as strength about the anteroposterior (AP) and mediolateral (ML) axes and torsional strength. Measures of strength were standardized by the product of body mass and moment arm (Ruff 2008). Moment arm lengths for all elements were the maximum lengths of the elements, as measured directly from the CT scans using the measure function in Avizo. Lastly, to assess bending rigidity of each cross-section, second moments of area were collected. These properties include AP, ML, maximum, minimum and torsional bending rigidities. Values rigidity were standardized by the product of body mass and bone length^2 (Ruff 2000b; Stock and Shaw 2007).

[4] Adam Sylvester, PhD. Johns Hopkins School of Medicine, Center for Functional Anatomy and Evolution. asylves4@jhmi.edu.

Analytical Methods

General linear model statistics were used to test for variation in cortical bone distribution across the six long bones of the upper and lower limbs. Statistical analyses were performed using SAS version 9.4 software (2017). The critical alpha level for all comparisons was 0.05. This value safeguards against 95% of potential reports of effects where none exist, while allowing potentially meaningful signals through (Bross 1971; Fisher 1956). The large sample size in this study increases statistical power, which leads to an increase in the probability of Type 1 error. To prevent such error, alpha is typically lowered in cases of very large sample sizes. However, power for the comparisons outlined in the next chapter range from 95-99.8% (calculated using G*Power by Faul et al. 2007). Therefore, alpha was preserved at 0.05 because a lowered value would be unable to compensate for the large amount of power. Before proceeding with comparisons between groups, the raw data was first examined for normality of data. To minimize the highly skewed distribution of the total data set, all CSG property values were log-transformed.

The first set of hypotheses concerned variation in cortical bone distribution with sex and age. A series of Type III univariate analysis of variance (ANOVA) tests were run to test for the effects of sex and slice location on cortical bone distribution. Type III ANOVAs are appropriate for mixed models, in which there exist both random (e.g. slice location) and fixed factors (e.g. sex). These comparisons spoke to the existence of sexual dimorphism in the sample. However, a series of ANOVAs increases the probability of incurring Type I error, or the chance of rejecting a null hypothesis when it is true. For this reason, the series ANOVAs were used as an exploratory measure, which was then followed by several multivariate analysis of variance (MANOVA) tests. For within-bone comparisons, MANOVAs were used to test for bone, slice

location, age, and sex effects on CSG properties. Pillai's Trace statistic was used because it is robust against deviations for normality in the distribution of the data and in cases of unequal variance.

Because of the large number of variables in this study, MANOVAs for within-bone comparisons did not provide a complete picture. That is, the variables themselves are not considered independently and thus it is not possible to know which are driving the difference in groups when significance exists. With this in mind, post hoc Least Squares (LS) means tests were performed to compare CSG properties between sexes and age groups at all five locations, within the six bones examined. This allowed for diaphyseal geometry to be compared between age groups of the same sex. LS means are appropriate with an unbalanced data set because they estimate the means based on an equal sample, which allows for testing how any one variable affects the response. This method also allows for a large number of comparisons at once, particularly with the Tukey-Kramer adjustment for multiple comparisons.

After sex and age group differences had been examined, the effects of three demographic variables on CSG values were tested. BMI category, activity level, and pathological group were individually explored using LS means to discern which groups differed within each of the three variables. This same set of procedures was then used for within-limb comparisons, and then again for between-limb comparisons. The secondary (within-limb) and tertiary (between-limb) hypothesis sets were aimed more at questions of loading limb and functionality on the species level, rather than variation between groups. As such, all individuals were pooled for comparisons.

CHAPTER 6

RESULTS

This chapter provides the results of statistical analyses described previously in Chapter 5. General linear model statistics were used to test for variation in cortical bone distribution across the six long bones of the upper and lower limbs. Cortical bone distribution was quantified by fifteen total cross-sectional geometric (CSG) properties reflecting bone mass, shape, bending rigidity, and bending strength (see summary table in Chapter 3, page 51) at five locations along the diaphysis. These sites were 20%, 35%, 50%, 65%, and 80% of length as measured from the distal end of the bone. Results are presented by within bone, within limb, and between limb comparisons. Each of the three sections concludes with a summary in which notable results are highlighted and presented visually. Areas of further study and issues with the current sample in regards to analysis are mentioned throughout.

Within Bone Variation

This section describes the results of cortical bone distribution within the humerus, radius, ulna, femur, tibia, and fibula. These comparisons represent the main aim of this dissertation, which was to generate a dataset encompassing sexual dimorphism and age-related changes across the limbs after the age of 40. Hypotheses related to this aim, outlined in Chapter 1, projected that males would demonstrate greater values of all CSG properties across the limbs than females. Further, it was expected that with an increase in age, all measures would decrease in both sexes. Results are provided first by sex, then by age groups within each sex. Finally, groups are compared by other variables that are known to affect cortical bone distribution: body

mass index (BMI), activity level, and pathological state at death. The section ends with a summary of within bone variation.

Variation by Sex

Before multivariate analyses could take place, it was important to establish whether significant differences in cortical bone distribution existed between males and females. The full data set was first examined for sex and slice location effects on CSG properties within each bone. Sex and slice location produced significant effects ($\alpha = 0.05$) on all fifteen CSG properties in each bone, with only four exceptions. Sex had no effect on the shape index of the humerus ($p = 0.0640$), percent cortical area of the radius ($p = 0.1509$) and ulna ($p = 0.0847$), and medullary area of the fibula ($p = 0.1146$). However, these results indicate that males and females should not be pooled in subsequent analyses. Results of the univariate analyses are presented in Appendix B (Tables B.1-B.6). Distribution figures for CSG properties by sex and slice location within each bone are provided in Appendix C (Figures C.1-C.15).

A set of multivariate analyses was performed to test for bone, slice location, and sex effects on CSG properties. Table 6 displays the results of MANOVAs for each factor. Only the significant highest-order (most number of factors) interactions for each MANOVA are presented herein, as lower-order interactions do not hold statistical significance. All null hypotheses concerning these factors were significant at $p < 0.05$, requiring post-hoc analyses to determine individual differences in sexes by slice location.

Table 6. MANOVA results for bone, slice location, sex, and CSG property effects

Factor	df	F	*p*
Bone*CSG property*slice location	(300, 3220)	47.52	< **0.0001**
Bone*CSG property*sex	(75, 802)	18.70	< **0.0001**

Pillai's Trace statistic, significant values ($p < 0.05$) bolded.

Least Squares (LS) means were used to compare CSG properties between sexes at all five diaphyseal locations within the six bones examined. The Tukey-Kramer method was used to adjust for multiple comparisons. Figures 11-25 provide the distribution of each CSG property by slice location in each bone. Asterisks indicate significant results ($p < 0.05$) of the LS means comparisons between males and females at each location. Males demonstrated greater values for all measurements of bone strength (Z_x, Z_y, Z_{max}, Z_{min}, and Z_p) and rigidity (I_x, I_y, I_{max}, I_{min}, and J) across the length of the diaphyses of all six bones. Measures of bone mass (CA, TA, and MA) and shape (percent CA and shape index) were less consistent. Cortical area proved to be significantly greater in males than females at each of the five sites within each bone. Relationships of total area (TA) between male and female elements were similar to that of CA, however the distal half of the diaphysis (20%, 35%, and 50%) of both the femur ($p = 0.7283$, 0.2840, 0.1749 respectively) and tibia ($p = 0.1448$, 0.0650, 0.0549 respectively) did not differ. Medullary area (MA) was largely similar between the sexes, across the skeleton, with the exception of the distal portions (20% and 35%) of the radius and ulna, and the most proximal locations (80%) on the femur and tibia differing significantly. Properties relating to diaphyseal cross-sectional shape were similarly inconsistent. Both measures of percent cortical area ((CA/TA) x 100) and shape index (I_{max}/I_{min}) were largely similar between the sexes. Differences existed between males and females in percent cortical area in the distal half of the diaphysis (20%, 35%, and 50%) of the humerus and tibia.

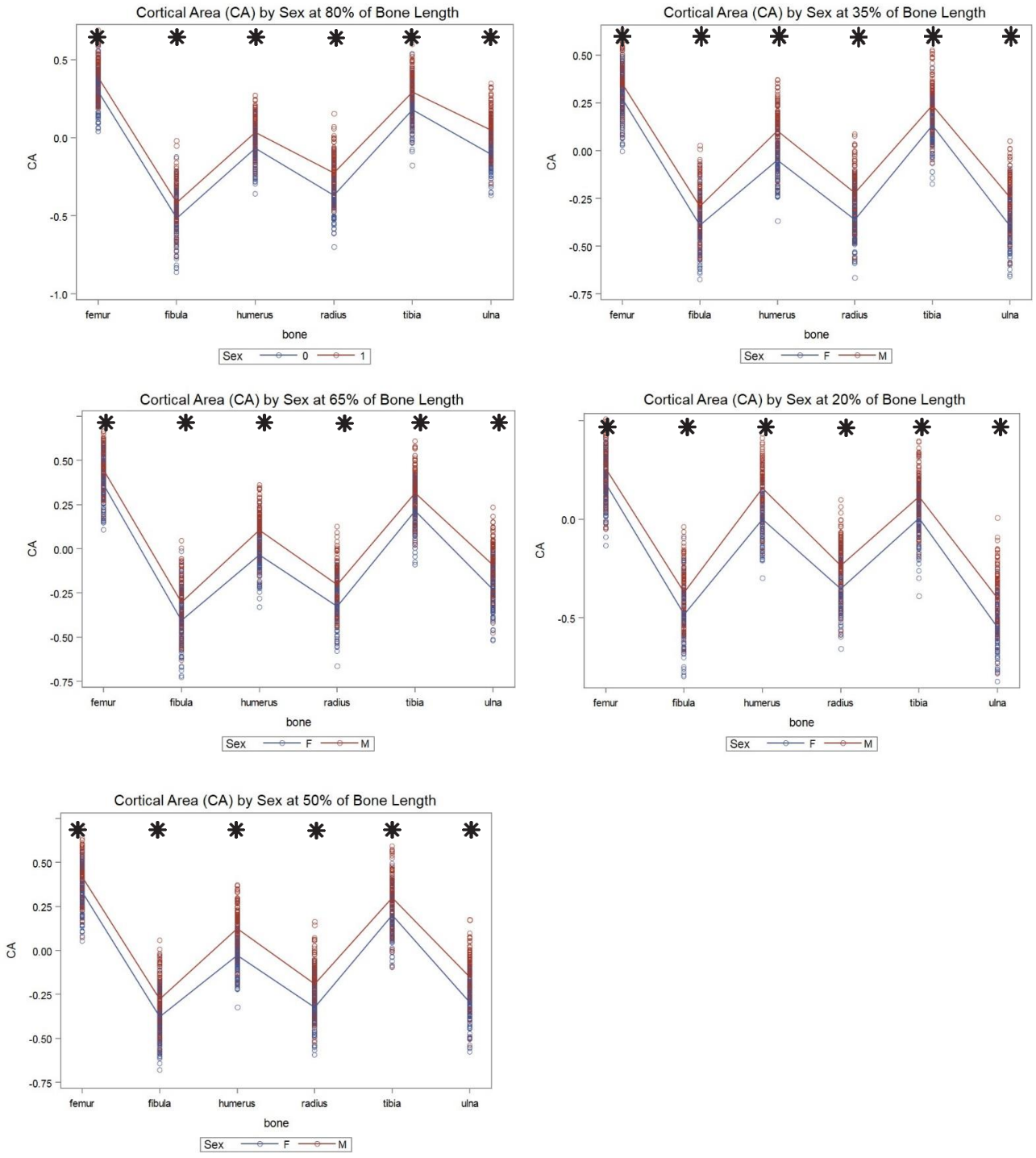

Figure 13. Cortical area (CA) by bone and sex within each element
Asterisks **(*)** indicate significant ($p < 0.05$) results in comparisons of means between sexes from post-hoc Least Squares with Tukey-Kramer adjustment for multiple comparisons.

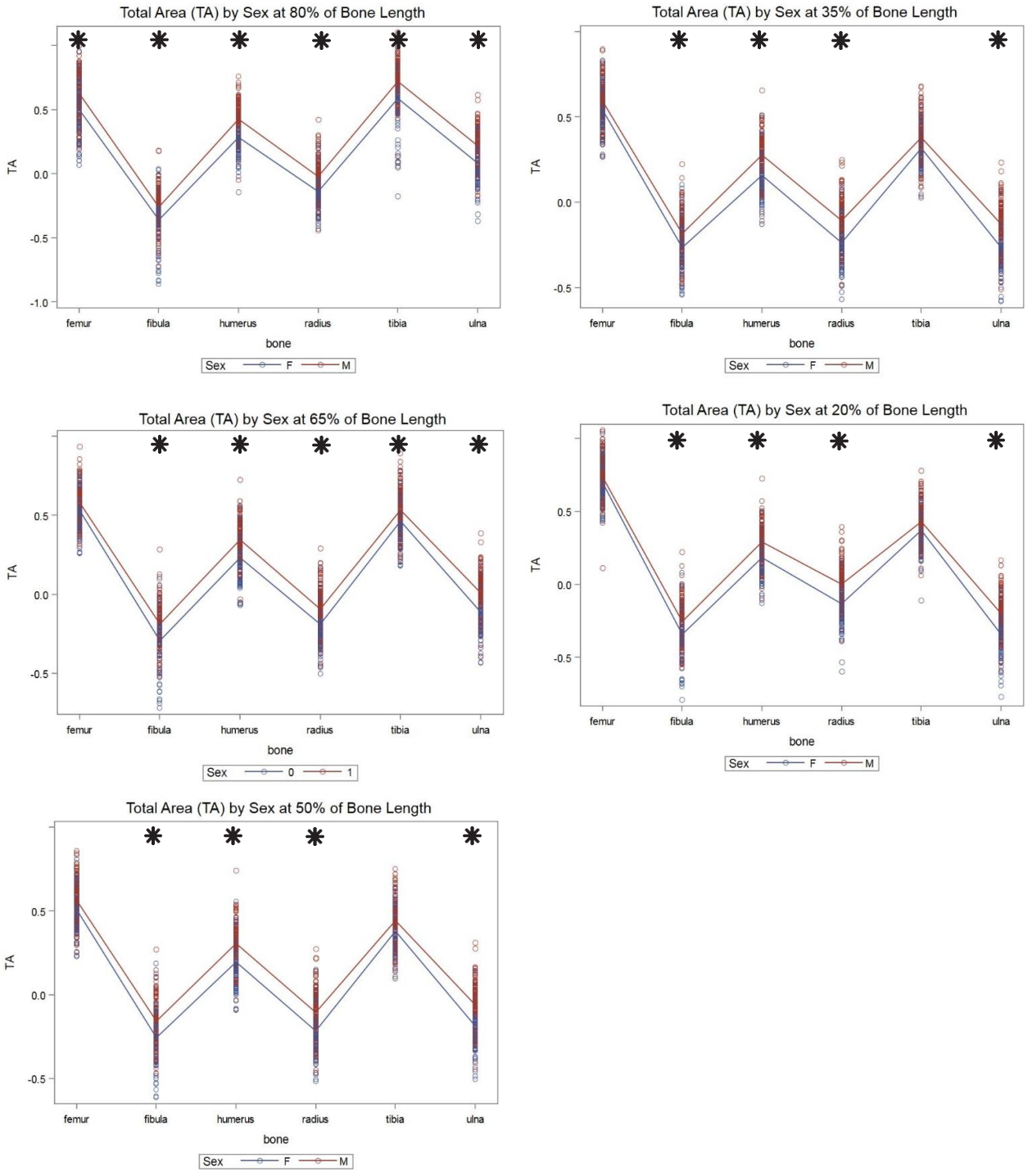

Figure 14. Total area (TA) by bone and sex within each element
Asterisks **(*)** indicate significant ($p < 0.05$) results in comparisons of means between sexes from post-hoc Least Squares with Tukey-Kramer adjustment for multiple comparisons.

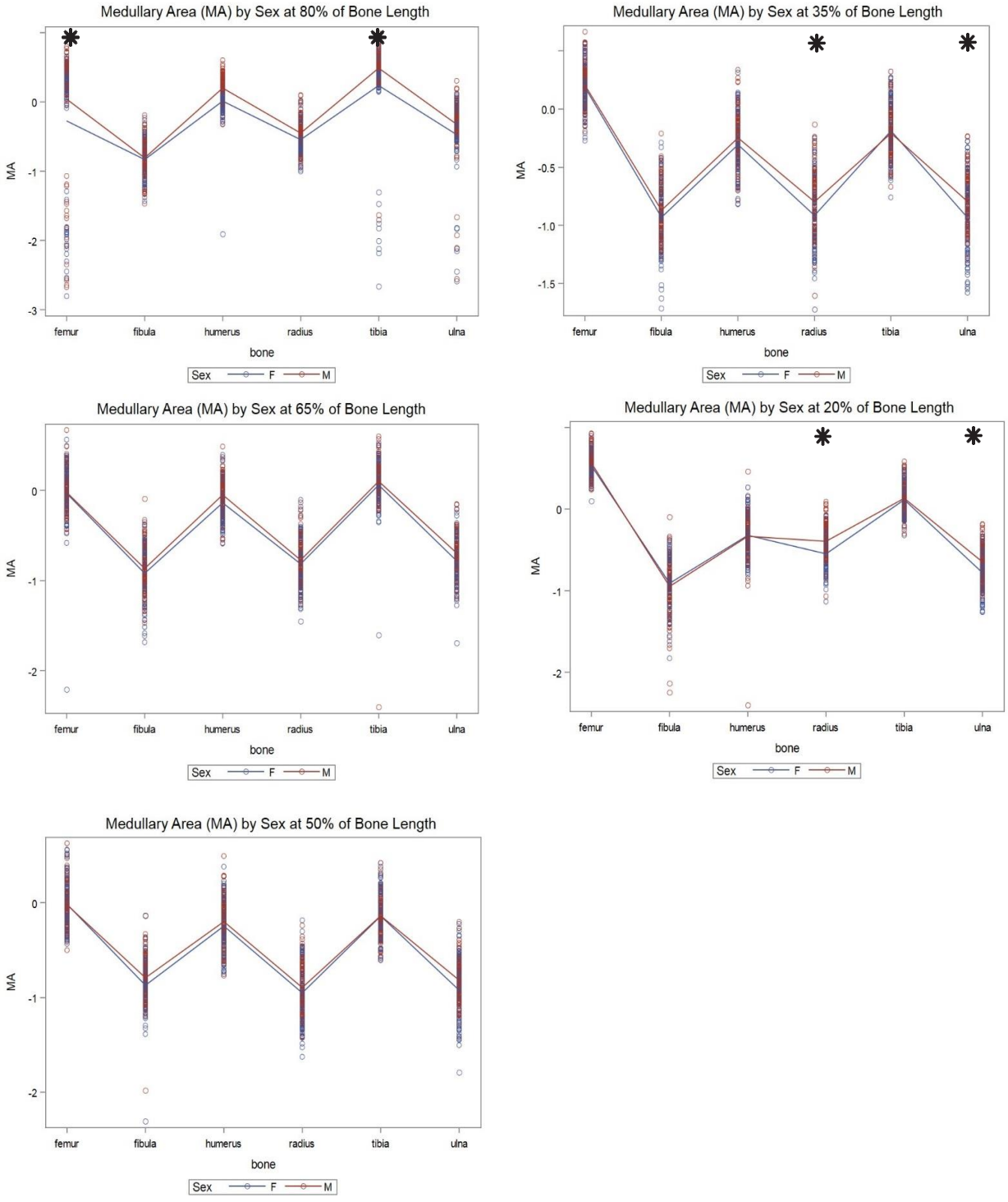

Figure 15. Medullary area (MA) by bone and sex within each element
Asterisks **(*)** indicate significant ($p < 0.05$) results in comparisons of means between sexes from post-hoc Least Squares with Tukey-Kramer adjustment for multiple comparisons.

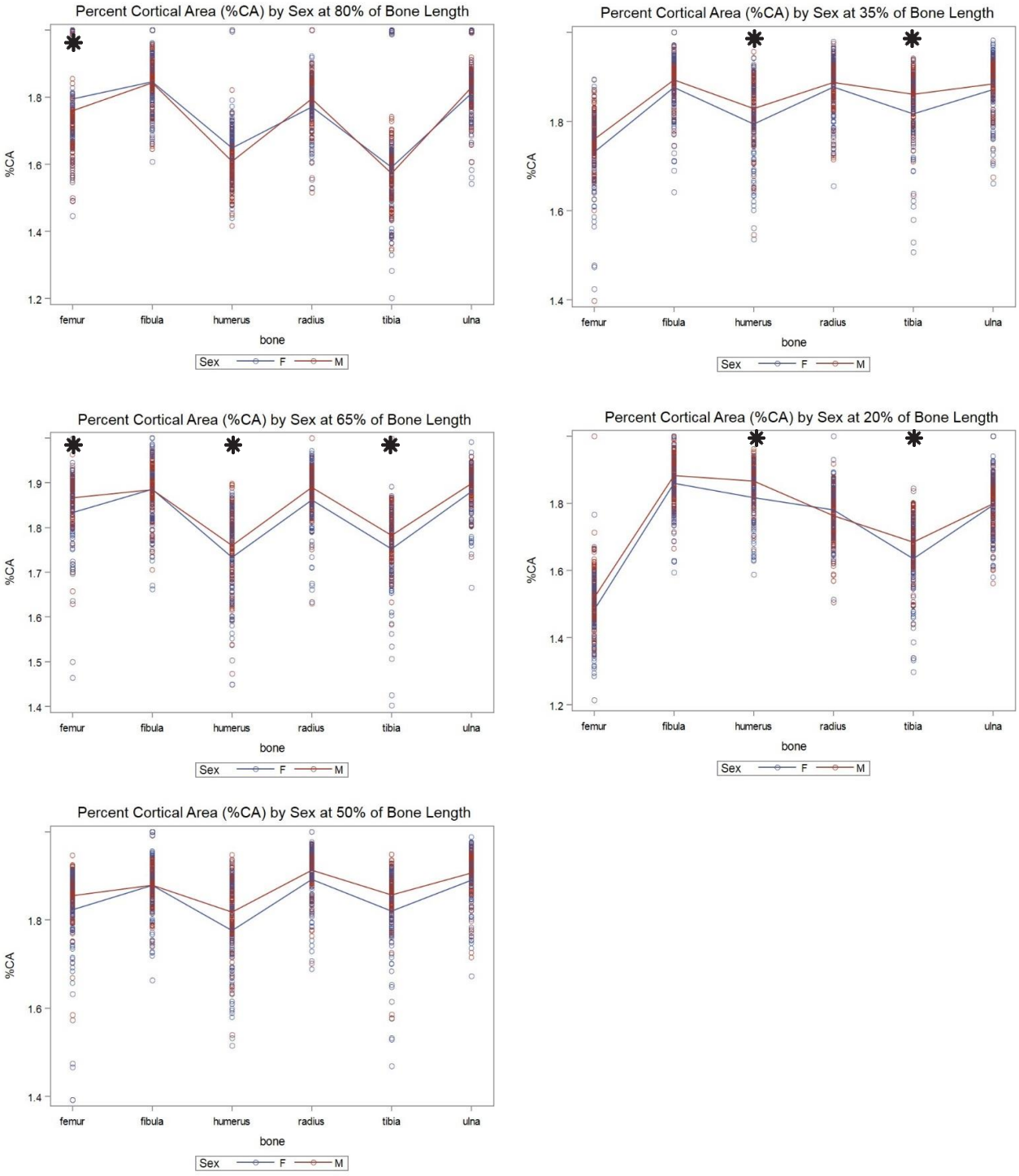

Figure 16. Percent Cortical Area (%CA) by bone and sex within each element
Asterisks **(*)** indicate significant ($p < 0.05$) results in comparisons of means between sexes from post-hoc Least Squares with Tukey-Kramer adjustment for multiple comparisons.

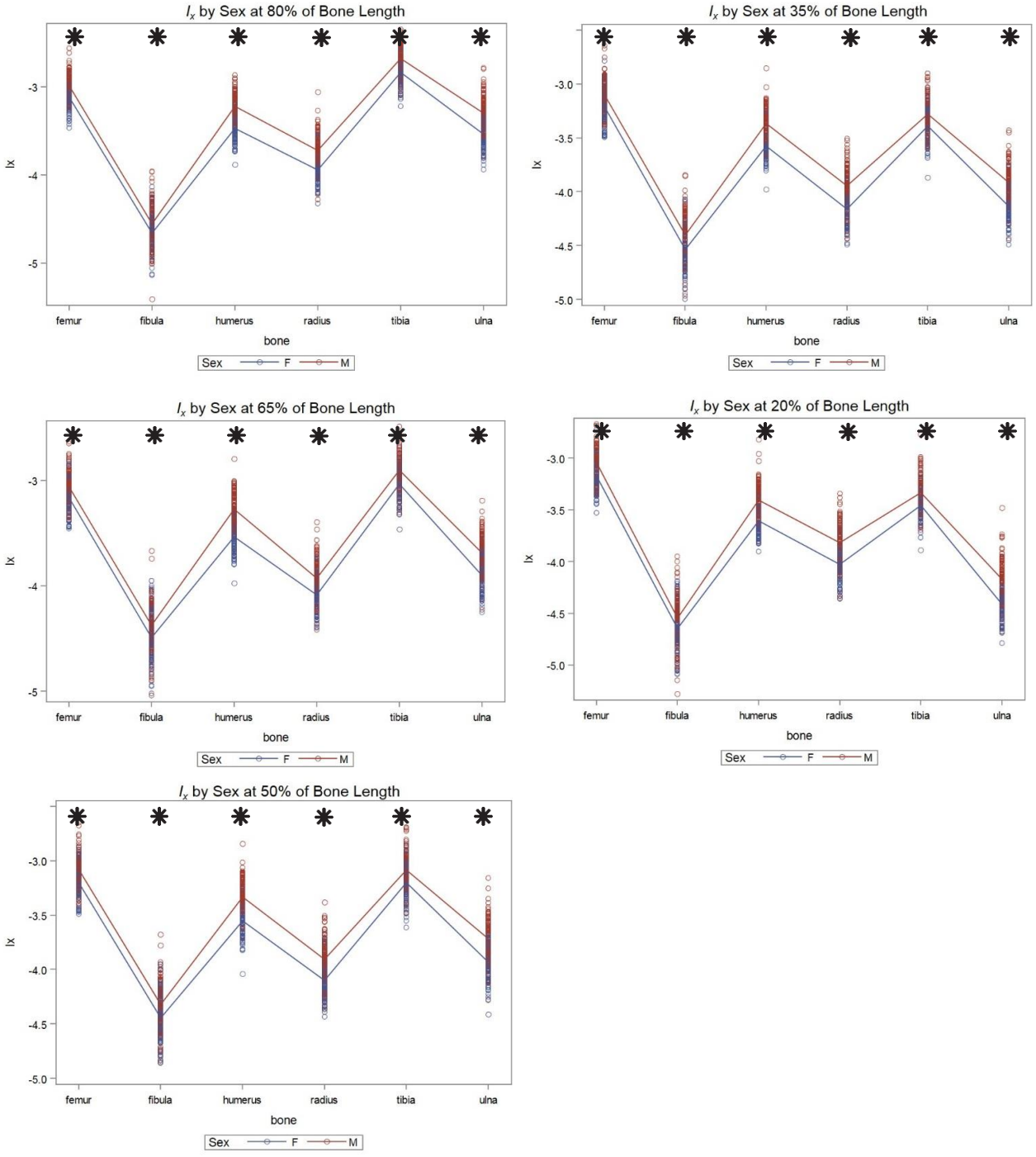

Figure 17. Second moment of area about the mediolateral (ML) axis (I_x) by bone and sex within each element

Asterisks **(*)** indicate significant ($p < 0.05$) results in comparisons of means between sexes from post-hoc Least Squares with Tukey-Kramer adjustment for multiple comparisons.

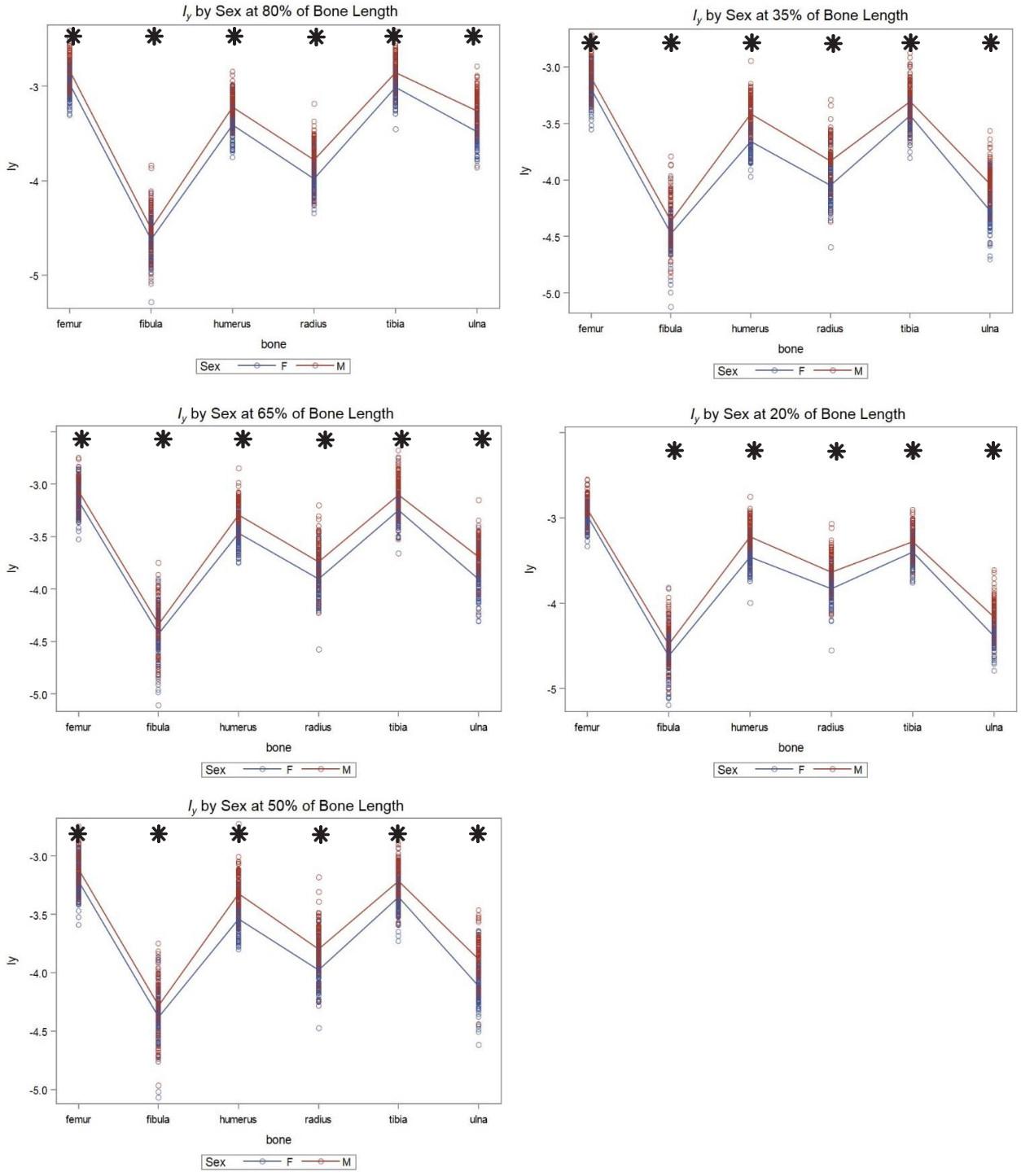

Figure 18. Second moment of area about the anteroposterior (AP) axis (I_y) by bone and sex within each element

Asterisks **(*)** indicate significant ($p < 0.05$) results in comparisons of means between sexes from post-hoc Least Squares with Tukey-Kramer adjustment for multiple comparisons.

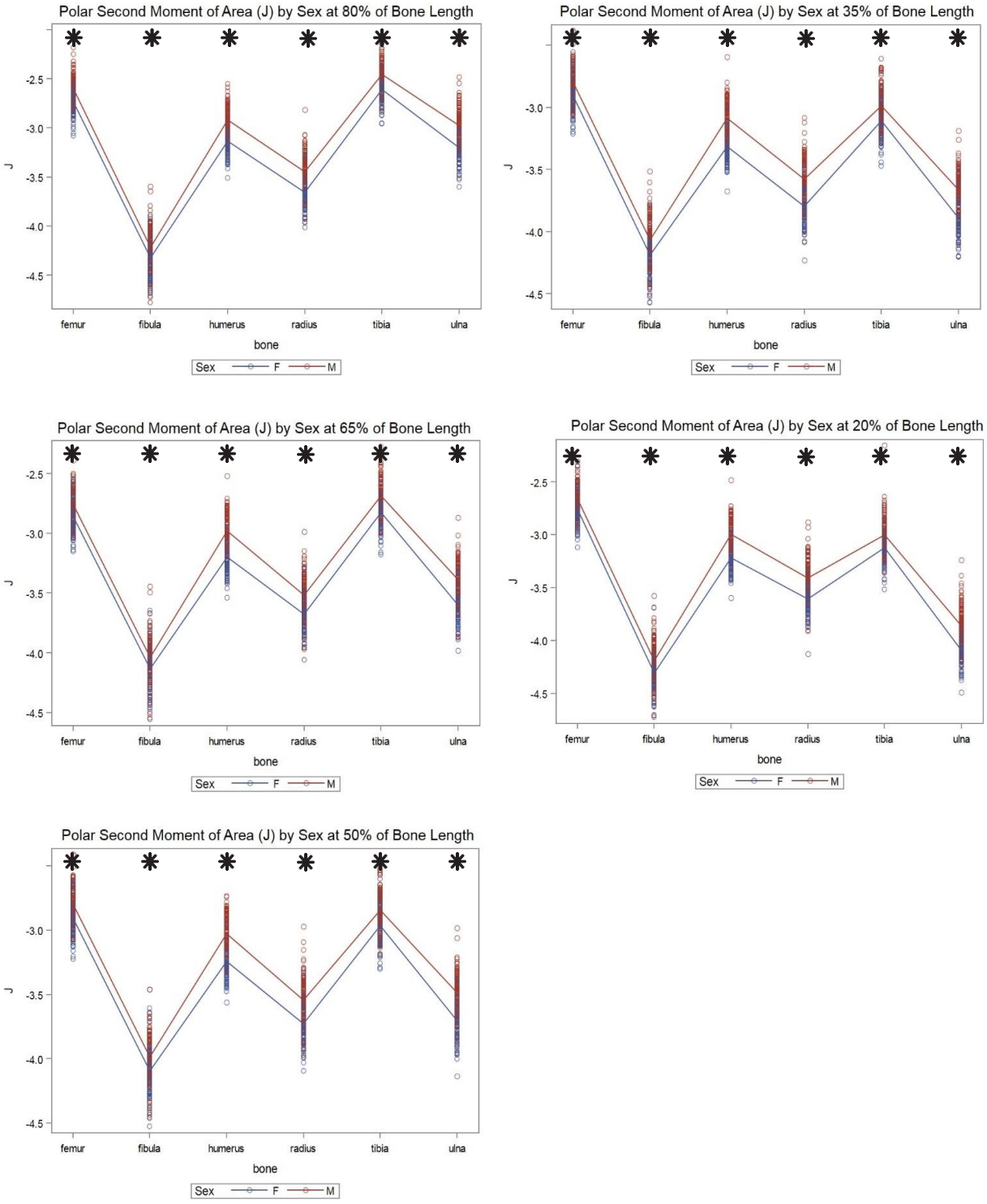

Figure 19. Polar second moment of area (J) by bone and sex within each element
Asterisks **(*)** indicate significant ($p < 0.05$) results in comparisons of means between sexes from post-hoc Least Squares with Tukey-Kramer adjustment for multiple comparisons.

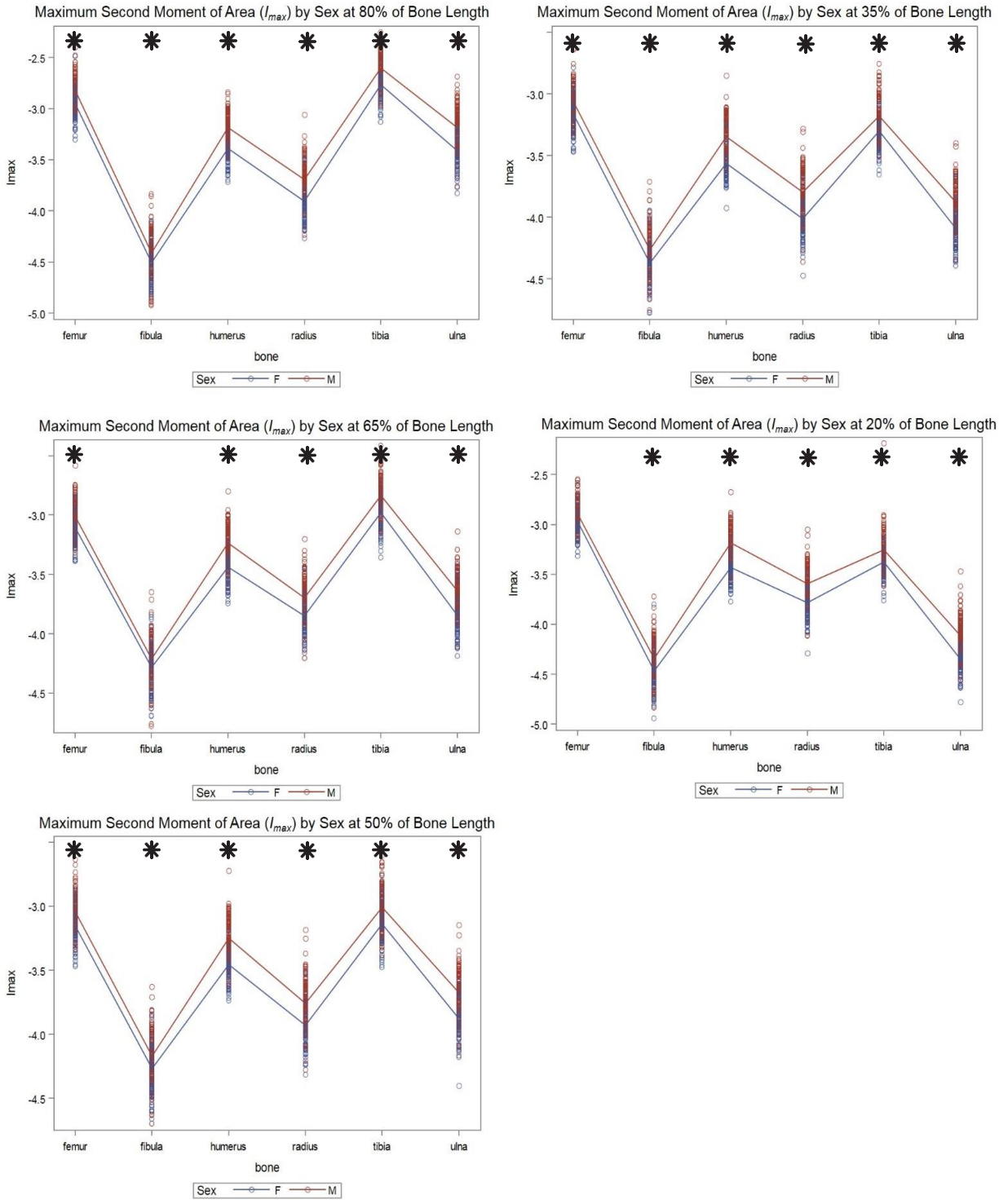

Figure 20. Maximum second moment of area (I_{max}) by bone and sex location within each element

Asterisks **(*)** indicate significant ($p < 0.05$) results in comparisons of means between sexes from post-hoc Least Squares with Tukey-Kramer adjustment for multiple comparisons.

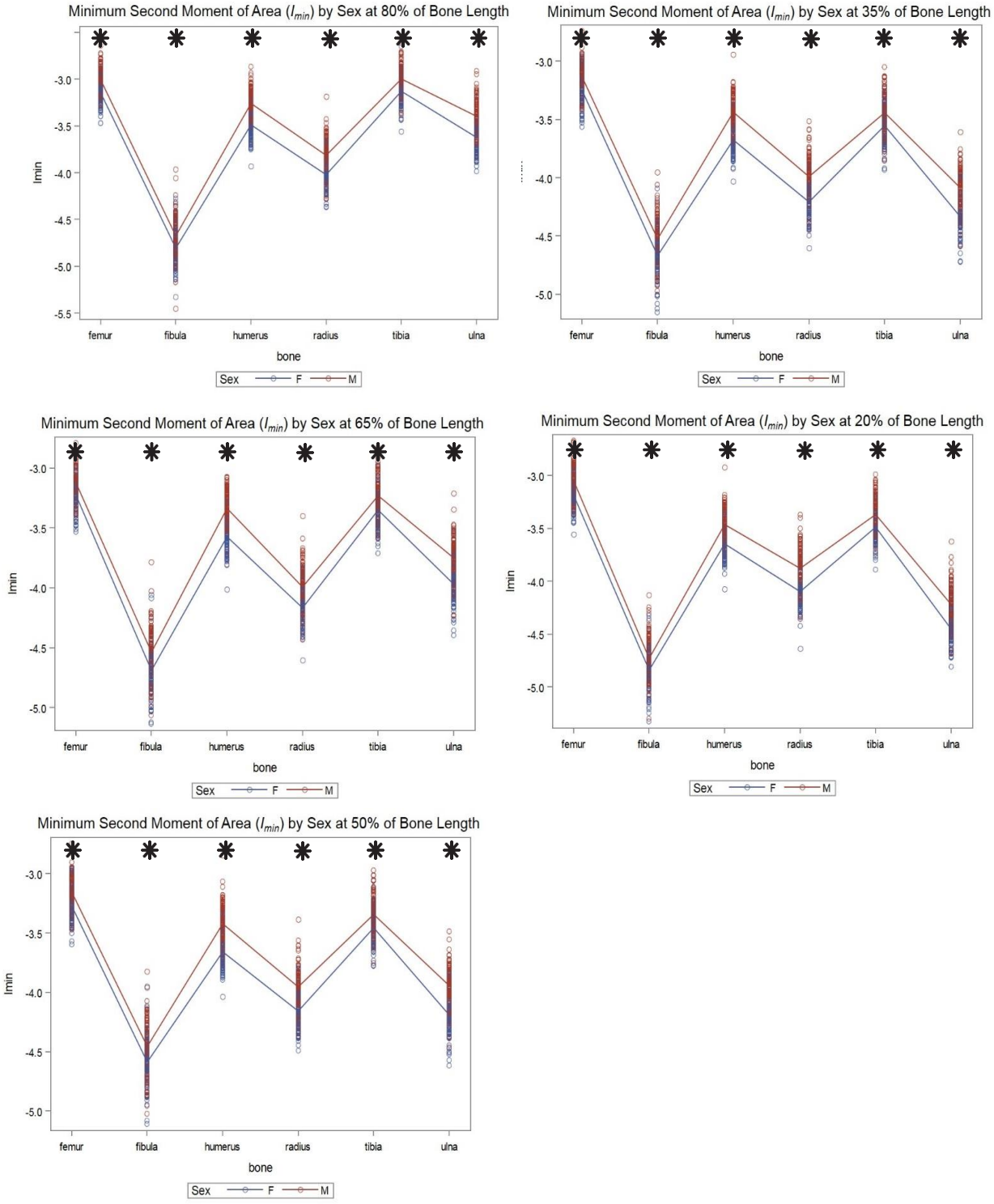

Figure 21. Minimum second moment of area (I_{min}) by bone and sex within each element
Asterisks **(*)** indicate significant ($p < 0.05$) results in comparisons of means between sexes from post-hoc Least Squares with Tukey-Kramer adjustment for multiple comparisons.

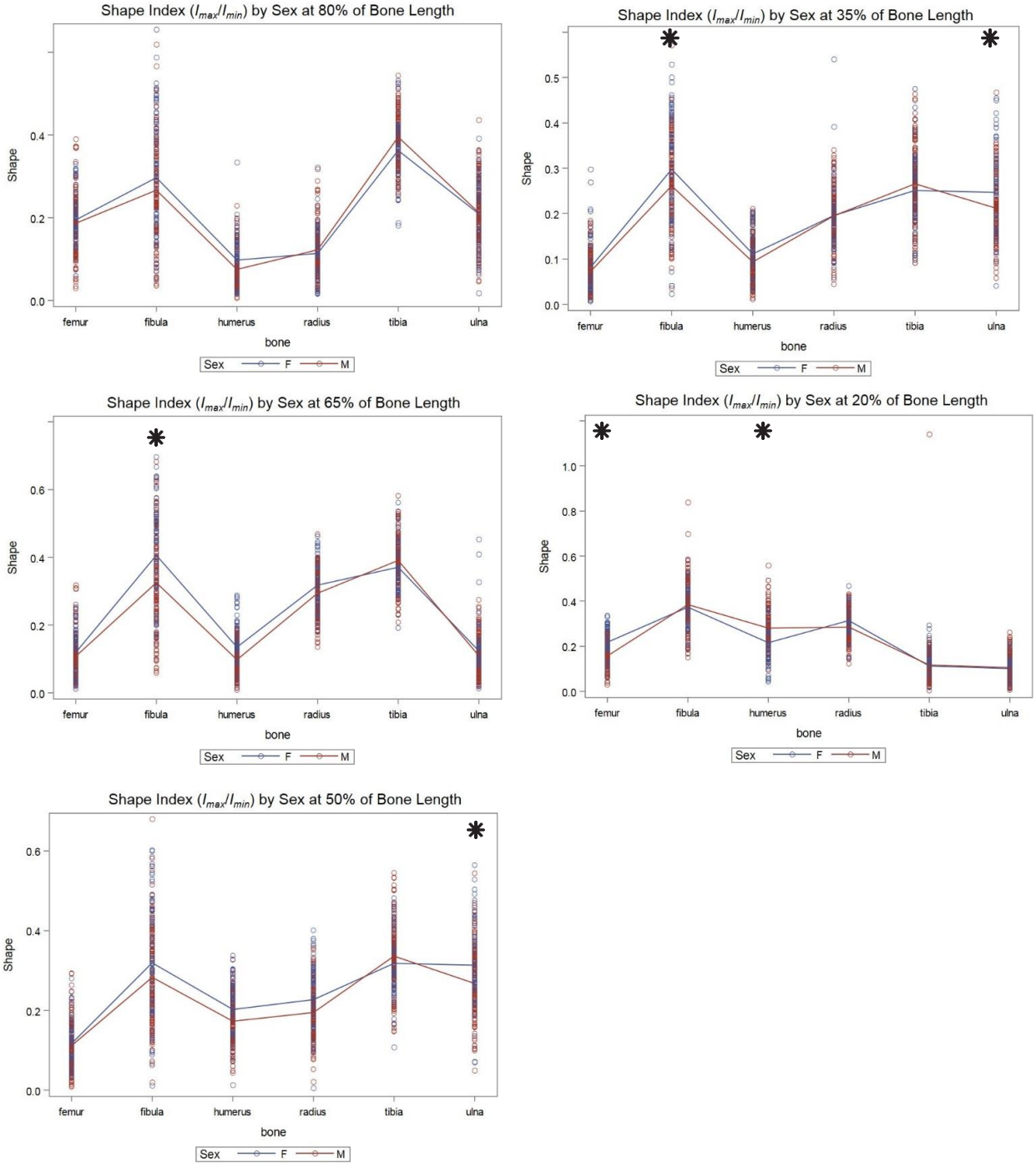

Figure 22. Shape index by bone and sex within each element
Asterisks **(*)** indicate significant ($p < 0.05$) results in comparisons of means between sexes from post-hoc Least Squares with Tukey-Kramer adjustment for multiple comparisons.

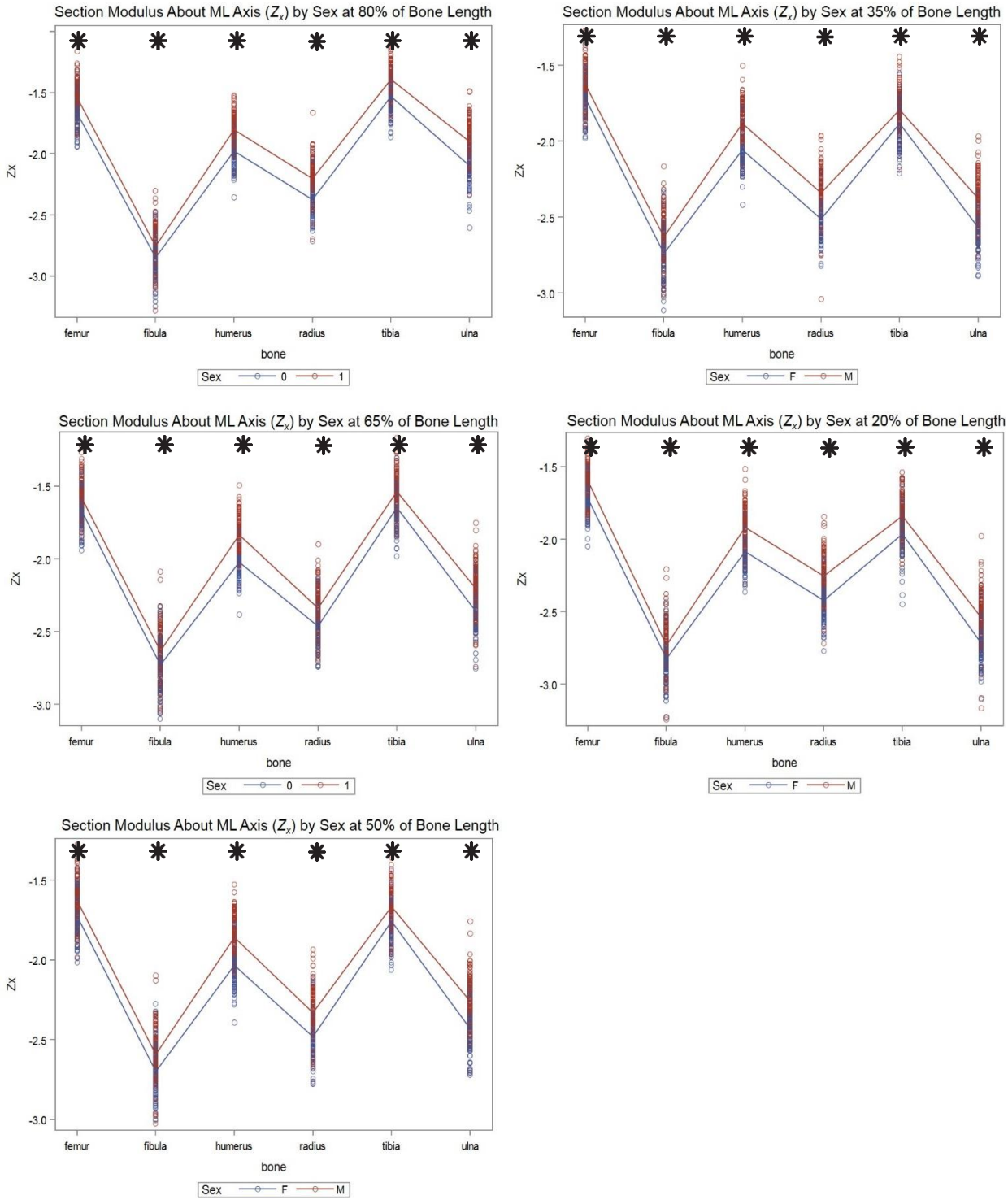

Figure 23. Section modulus about the mediolateral (ML) axis (Z_x) by bone and sex within each element

Asterisks **(*)** indicate significant ($p < 0.05$) results in comparisons of means between sexes from post-hoc Least Squares with Tukey-Kramer adjustment for multiple comparisons.

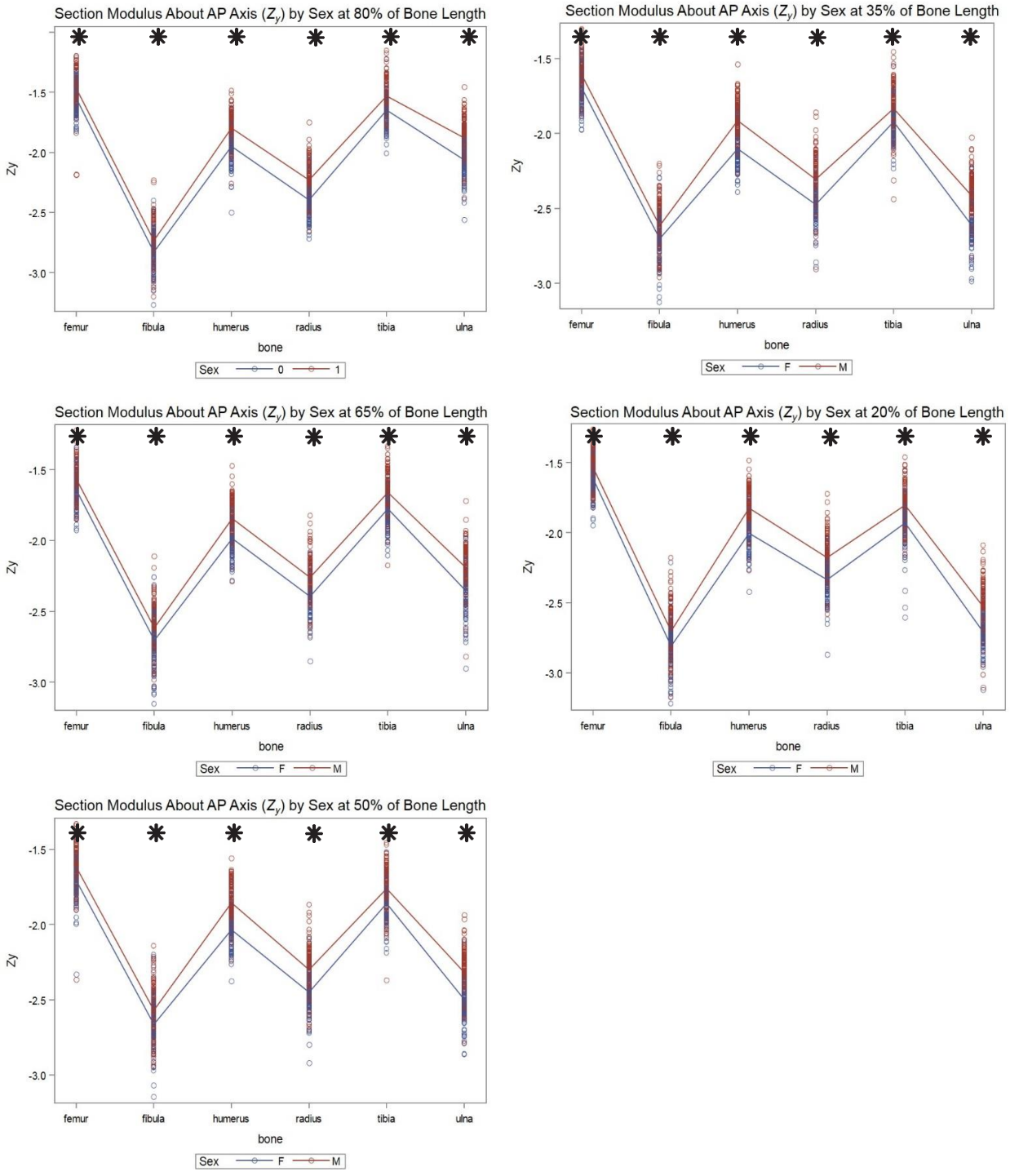

Figure 24. Section modulus about the anteroposterior (AP) axis (Z_y) by bone and sex within each element

Asterisks **(*)** indicate significant ($p < 0.05$) results in comparisons of means between sexes from post-hoc Least Squares with Tukey-Kramer adjustment for multiple comparisons.

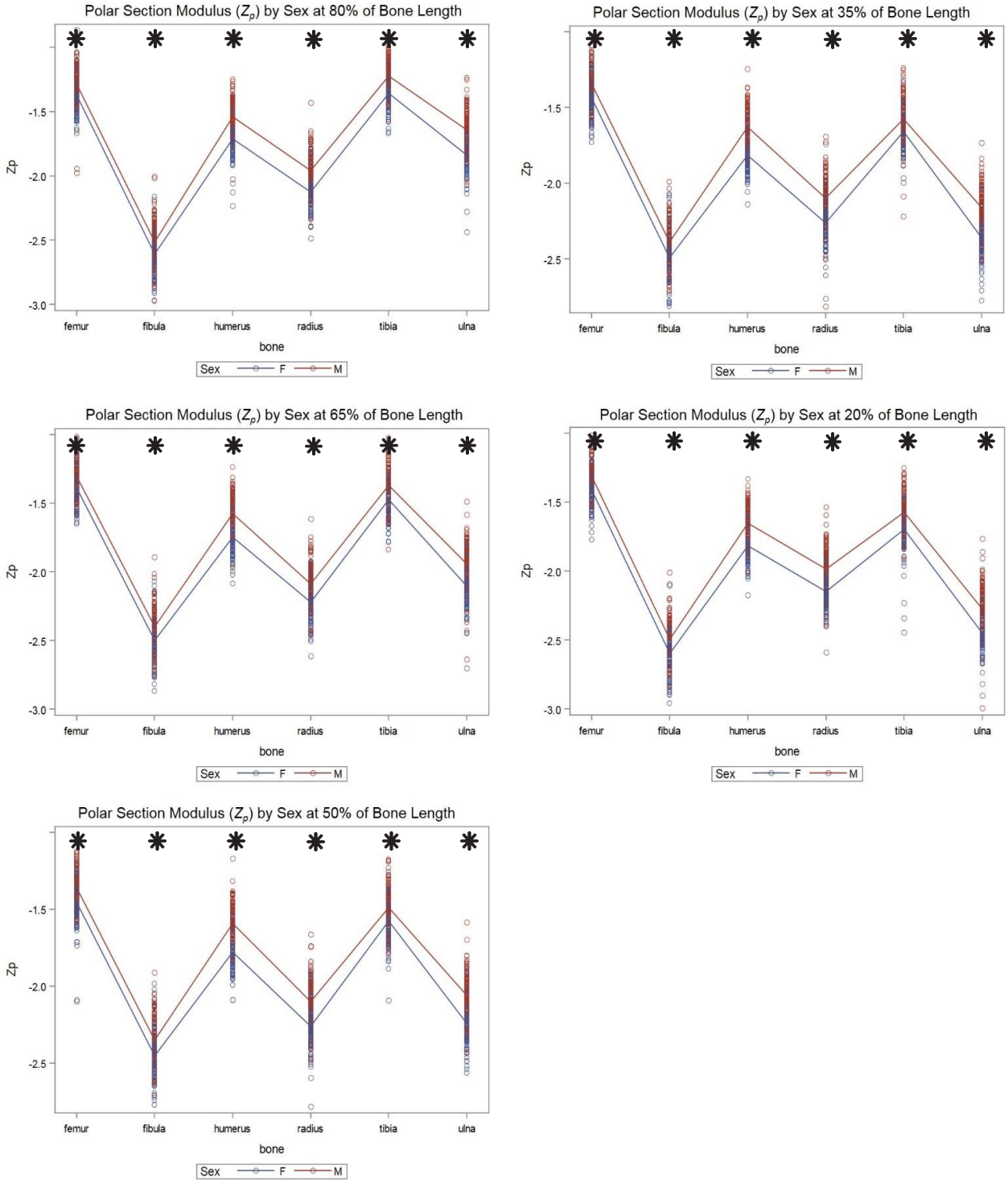

Figure 25. Polar section modulus (Z_p) by bone and sex within each element
Asterisks **(*)** indicate significant ($p < 0.05$) results in comparisons of means between sexes from post-hoc Least Squares with Tukey-Kramer adjustment for multiple comparisons.

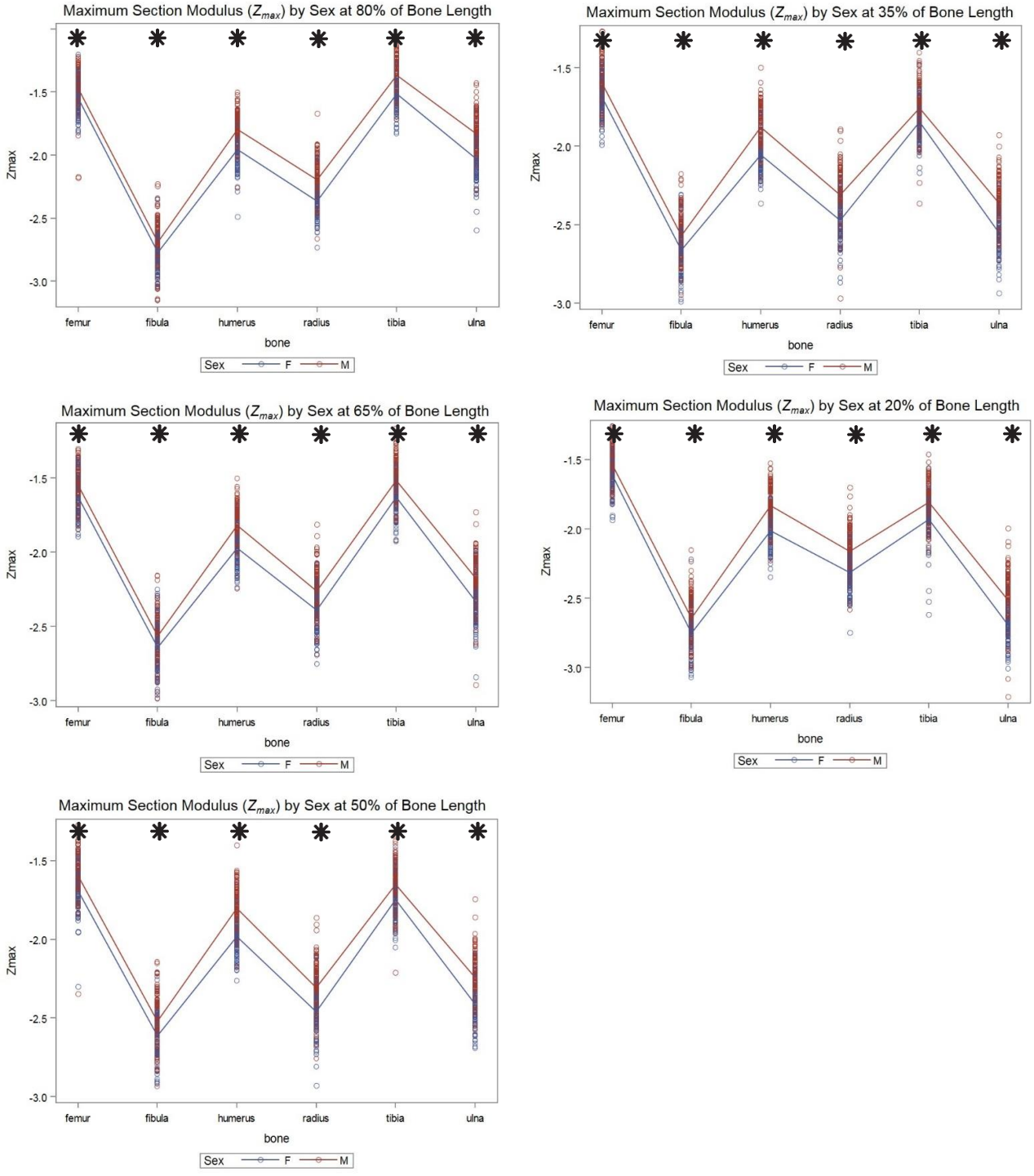

Figure 26. Maximum section modulus (Z_{max}) by bone and sex within each element
Asterisks **(*)** indicate significant ($p < 0.05$) results in comparisons of means between sexes from post-hoc Least Squares with Tukey-Kramer adjustment for multiple comparisons.

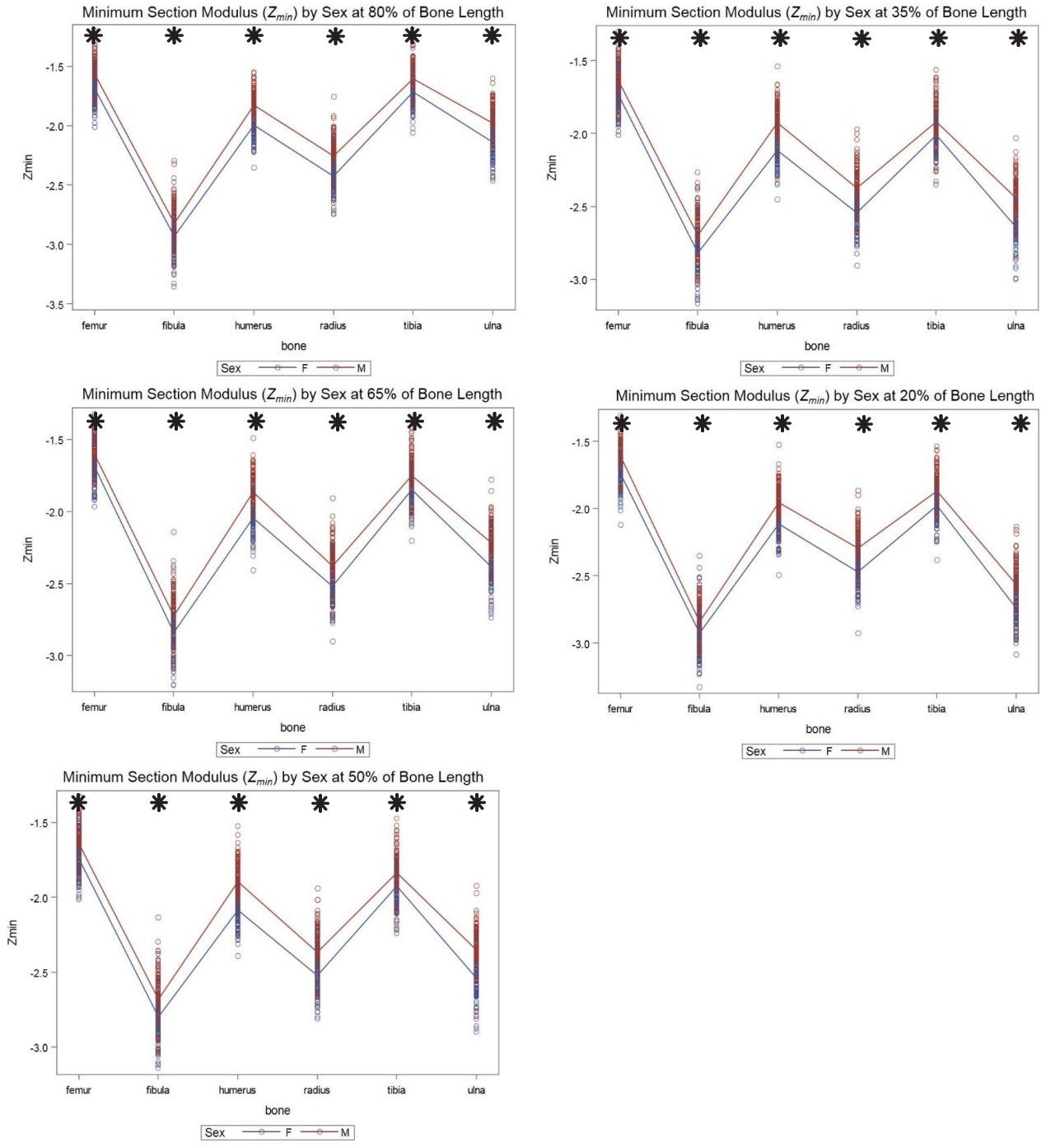

Figure 27. Minimum section modulus (Z_{min}) by bone and sex within each element
Asterisks **(*)** indicate significant ($p < 0.05$) results in comparisons of means between sexes from post-hoc Least Squares with Tukey-Kramer adjustment for multiple comparisons.

Variation by Age Group

The core aim of this dissertation was to test for variation in diaphyseal cross-sectional properties after the age of 40 years. To accomplish this aim, individuals were grouped by decade of age-at-death (40-49, 50-59, 60-69, 70-79, 80-99). Because the tenth decade (90-99) had a small sample size (see summary table in Chapter 5, page 89), it was combined with the ninth decade (80-89) for both sexes. The structure of comparisons here differed slightly from that in the previous section. As opposed to distinguishing between slice locations, average values from the entire length of the diaphysis along each bone for each of the CSG properties were used for comparison. In previous studies (see Moore 2013; Reeves 2014; Sigurdsson et al. 2006), the midshaft (50%) location has been used as a single point of comparison, with the argument being that it is the region of greatest bending and torsion in a beam loaded on its ends (joints). If osseous response to loading exists, it is likely to be evident at this location (Currey 2006; Martin et al. 2015; Ruff 2008)[5]. This idea is valid and is discussed previously in Chapter 3. However, the entirety of the shaft collectively contributes to the ability of the bone to resist force and a vast majority of locations have shown variation as a result of sex, as was shown in the prior section. Using the mean value of CSG properties along the entire shaft provides a "whole bone" perspective (Cristofolini et al. 2010; Gosman et al. 2013; Hubbell et al. 2011) on variation for each measurement within each skeletal element. This perspective was discussed in Chapter 1.

Univariate analyses of variance were first conducted to test for age group, sex, and slice location effects on all CSG properties in each bone. Age groups produced significant effects ($\alpha = 0.05$) on a vast majority of CSG properties in each bone. Age did not, however, have significant effects on the shape index of the humerus, radius, ulna, femur, and fibula. This result is similar to

[5] *cf.* Pearson and Lieberman (2004).

that reported between males and females in the previous section, namely the similarity in shape between the sexes. The fibula also proved to have very little variation, with age not having an effect on I_{min} and most measures of bone strength (Z_x, Z_p, Z_{max}, and Z_{min}). Results of these univariate comparisons are presented in Appendix D (Tables D.1-D.6), and distribution figures for CSG properties by skeletal element for each sex and age group are presented in Appendix E (Figures E.1-E.15).

A set of multivariate analyses was performed to test for bone, slice location, sex, and age group effects. Table 7 displays the results of these MANOVAs. All null hypotheses concerning these factors were significant at $p < 0.05$, requiring post-hoc analyses to determine individual differences in age groups by sex.

Table 7. MANOVA results for bone, slice location, sex, age group, and CSG property effects

Factor	df	F	*p*
Bone*CSG property*slice location	(300, 3204)	47.72	**< 0.0001**
Bone*CSG property*age group	(300, 3204)	2.97	**< 0.0001**
Bone*CSG property*sex	(75, 798)	17.90	**< 0.0001**

Pillai's Trace statistic, significant values ($p < 0.05$) bolded.

As before, CSG properties between sex and age groups for each bone were compared using LS means, and the Tukey-Kramer method was used to adjust for multiple comparisons. In the bones of the upper limb, significant differences ($p < 0.05$) existed between the sexes with all age groups for all CSG properties, except shape index. This further corroborates results from earlier comparisons when ages were pooled. Generally, females aged 40-49 had the fewest differences with all other groups, while females aged 80 and over had the most.

Very few upper limb differences existed between age groups of the same sex. The small amount of age group variation was confined to the humerus and radius. In the humerus, cortical

area was significantly smaller in females 80-99 than the preceding decade. During the fifties, medullary area and percent cortical area in the humerus and radius of females begin to show significant differences with other female age groups. Medullary area increases in both bones during this time period, while percent cortical area starts to decline. The same pattern is evident in males, beginning in the seventh decade. The seventh decade also marks an increased shift in radial I_x in females and I_y in males. By the eighties, these values decrease to similar levels seen in the forties. Additionally, male radial I_{max}, I_{min}, and all properties of bone strength increase in the fifth decade, but also return to fourth-decade values by the 80s.

Bones of the lower limb (femur, tibia, and fibula) have far less age-related variation in cross-sectional geometry than elements of the upper limb. For example, the femur demonstrated no group difference, even between sexes, for total area, medullary area, and percent cortical area. Despite the fact that all other femoral CSG properties varied significantly between sexes, no differences existed in age groups of the same sex. Although male tibial properties remained approximately the same as age increased, a clear pattern existed in the female tibia. The eighth decade marked a significant, unexpected increase in female tibial cortical area, total area, and all measures of bone strength (except Z_{min}) and rigidity from the previous decades. The female fibula showed little variation in CSG properties with age, while the male fibula demonstrated a significant shift in the 40s. This decade represents the highest values of cortical area, total area, and all measures of bone strength and rigidity than any other time period. As in the radius, these fibular strength and rigidity properties return to fourth-decade values by the 80s. CSG property LS means by age group and sex for each bone and figures providing visual representation of significant difference in values between sex and age groups are provided in Appendix F (Figures F.1-F.30).

Table 8. Geometric trends in the humerus with age

CSG Property	Female Age Groups				CSG Property	Male Age Groups			
	40s to 50s	50s to 60s	60s to 70s	70s to 80+		40s to 50s	50s to 60s	60s to 70s	70s to 80+
CA	NS	NS	NS	+	**CA**	NS	NS	NS	NS
TA	NS	NS	NS	NS	**TA**	NS	NS	NS	NS
MA	NS	NS	NS	NS	**MA**	NS	NS	NS	NS
% CA	NS	NS	NS	-	**% CA**	NS	NS	-	NS
I_x	NS	NS	NS	NS	I_x	NS	NS	NS	NS
I_y	NS	NS	NS	NS	I_y	NS	NS	NS	NS
J	NS	NS	NS	NS	**J**	NS	NS	NS	NS
I_{max}	NS	NS	+	NS	I_{max}	NS	NS	NS	NS
I_{min}	NS	NS	NS	NS	I_{min}	NS	NS	NS	NS
Shape index	NS	NS	NS	NS	**Shape index**	NS	NS	NS	NS
Z_x	NS	NS	NS	NS	Z_x	NS	-	NS	NS
Z_y	NS	NS	NS	NS	Z_y	NS	NS	NS	NS
Z_p	NS	NS	NS	NS	Z_p	NS	NS	NS	NS
Z_{max}	NS	NS	NS	NS	Z_{max}	NS	NS	NS	NS
Z_{min}	NS	NS	NS	NS	Z_{min}	NS	-	NS	NS

Orange plus signs (+) indicate significant increases for that CSG property from one decade to the next, blue dashes (-) indicates significant decreases, and NS indicates no significant change.

Table 9. Geometric trends in the radius with age

CSG Property	Female Age Groups				CSG Property	Male Age Groups			
	40s to 50s	50s to 60s	60s to 70s	70s to 80+		40s to 50s	50s to 60s	60s to 70s	70s to 80+
CA	NS	NS	NS	NS	**CA**	NS	NS	NS	NS
TA	NS	NS	NS	NS	**TA**	NS	NS	NS	NS
MA	NS	NS	NS	+	**MA**	NS	NS	NS	NS
% CA	NS	NS	NS	-	**% CA**	NS	NS	NS	-
I_x	NS	NS	-	NS	I_x	NS	NS	NS	NS
I_y	NS	NS	NS	NS	I_y	-	+	NS	NS
J	NS	NS	NS	NS	**J**	NS	+	NS	NS
I_{max}	NS	NS	NS	NS	I_{max}	NS	+	NS	NS
I_{min}	NS	NS	NS	NS	I_{min}	NS	+	NS	NS
Shape index	NS	NS	NS	NS	**Shape index**	NS	NS	NS	NS
Z_x	NS	NS	NS	NS	Z_x	NS	NS	NS	NS
Z_y	NS	NS	NS	NS	Z_y	NS	+	NS	NS
Z_p	NS	NS	NS	NS	Z_p	NS	+	NS	NS
Z_{max}	NS	NS	NS	NS	Z_{max}	NS	+	NS	NS
Z_{min}	NS	NS	NS	NS	Z_{min}	NS	+	-	NS

Orange plus signs (+) indicate significant increases for that CSG property from one decade to the next, blue dashes (-) indicates significant decreases, and NS indicates no significant change.

Table 10. Geometric trends in the ulna with age

CSG Property	Female Age Groups				CSG Property	Male Age Groups			
	40s to 50s	50s to 60s	60s to 70s	70s to 80+		40s to 50s	50s to 60s	60s to 70s	70s to 80+
CA	NS	NS	NS	NS	**CA**	NS	NS	NS	NS
TA	NS	NS	NS	NS	**TA**	NS	NS	NS	NS
MA	NS	NS	NS	NS	**MA**	NS	NS	NS	NS
% CA	NS	NS	NS	-	**% CA**	NS	NS	NS	NS
I_x	NS	NS	NS	NS	I_x	NS	NS	NS	NS
I_y	NS	NS	NS	NS	I_y	NS	NS	NS	NS
J	NS	NS	NS	NS	**J**	NS	NS	NS	NS
I_{max}	NS	NS	NS	NS	I_{max}	NS	NS	NS	NS
I_{min}	NS	NS	NS	NS	I_{min}	NS	NS	NS	NS
Shape index	NS	NS	NS	NS	**Shape index**	NS	NS	NS	NS
Z_x	NS	NS	NS	NS	Z_x	NS	NS	NS	NS
Z_y	NS	NS	NS	NS	Z_y	NS	NS	NS	NS
Z_p	NS	NS	NS	NS	Z_p	NS	NS	NS	NS
Z_{max}	NS	NS	NS	NS	Z_{max}	NS	NS	NS	NS
Z_{min}	NS	NS	NS	NS	Z_{min}	NS	NS	NS	NS

Orange plus signs (+) indicate significant increases for that CSG property from one decade to the next, blue dashes (-) indicates significant decreases, and NS indicates no significant change.

Table 11. Geometric trends in the femur with age

CSG Property	Female Age Groups				CSG Property	Male Age Groups			
	40s to 50s	50s to 60s	60s to 70s	70s to 80+		40s to 50s	50s to 60s	60s to 70s	70s to 80+
CA	NS	NS	NS	NS	**CA**	NS	NS	NS	NS
TA	NS	NS	NS	NS	**TA**	NS	NS	NS	NS
MA	NS	NS	NS	NS	**MA**	NS	NS	NS	NS
% CA	NS	NS	NS	NS	**% CA**	NS	NS	NS	NS
I_x	NS	NS	NS	NS	I_x	NS	NS	NS	NS
I_y	NS	NS	NS	NS	I_y	NS	NS	NS	NS
J	NS	NS	NS	NS	**J**	NS	NS	NS	NS
I_{max}	NS	NS	NS	NS	I_{max}	NS	NS	NS	NS
I_{min}	NS	NS	NS	NS	I_{min}	NS	NS	NS	NS
Shape index	NS	NS	NS	NS	**Shape index**	NS	NS	NS	NS
Z_x	NS	NS	NS	NS	Z_x	NS	NS	NS	NS
Z_y	NS	NS	NS	NS	Z_y	NS	NS	NS	NS
Z_p	NS	NS	NS	NS	Z_p	NS	NS	NS	NS
Z_{max}	NS	NS	NS	NS	Z_{max}	NS	NS	NS	NS
Z_{min}	NS	NS	NS	NS	Z_{min}	NS	NS	NS	NS

Orange plus signs (+) indicate significant increases for that CSG property from one decade to the next, blue dashes (-) indicates significant decreases, and NS indicates no significant change.

Table 12. Geometric trends in the tibia with age

CSG Property	Female Age Groups				CSG Property	Male Age Groups			
	40s to 50s	50s to 60s	60s to 70s	70s to 80+		40s to 50s	50s to 60s	60s to 70s	70s to 80+
CA	NS	NS	NS	+	**CA**	NS	NS	NS	NS
TA	NS	NS	NS	+	**TA**	NS	NS	NS	NS
MA	NS	NS	NS	NS	**MA**	NS	NS	NS	NS
% CA	NS	NS	NS	NS	**% CA**	NS	NS	NS	NS
I_x	NS	NS	NS	+	I_x	NS	NS	NS	NS
I_y	NS	NS	NS	+	I_y	NS	NS	NS	NS
J	NS	NS	NS	+	**J**	NS	NS	NS	NS
I_{max}	NS	NS	NS	+	I_{max}	NS	NS	NS	NS
I_{min}	NS	NS	NS	+	I_{min}	NS	NS	NS	NS
Shape index	NS	NS	NS	NS	**Shape index**	NS	NS	NS	NS
Z_x	NS	NS	NS	+	Z_x	NS	NS	NS	NS
Z_y	NS	NS	NS	+	Z_y	NS	NS	NS	NS
Z_p	NS	NS	NS	+	Z_p	NS	NS	NS	NS
Z_{max}	NS	NS	NS	+	Z_{max}	NS	NS	NS	NS
Z_{min}	NS	NS	NS	+	Z_{min}	NS	NS	NS	NS

Orange plus signs (+) indicate significant increases for that CSG property from one decade to the next, blue dashes (-) indicates significant decreases, and NS indicates no significant change.

Table 13. Geometric trends in the fibula with age

CSG Property	Female Age Groups				CSG Property	Male Age Groups			
	40s to 50s	50s to 60s	60s to 70s	70s to 80+		40s to 50s	50s to 60s	60s to 70s	70s to 80+
CA	NS	-	NS	NS	**CA**	NS	NS	NS	NS
TA	NS	NS	NS	NS	**TA**	-	NS	NS	NS
MA	NS	NS	NS	+	**MA**	NS	NS	NS	NS
% CA	NS	NS	NS	NS	**% CA**	NS	NS	NS	NS
I_x	NS	NS	NS	NS	I_x	NS	NS	NS	NS
I_y	NS	NS	NS	NS	I_y	-	+	NS	NS
J	NS	NS	NS	NS	**J**	NS	NS	NS	NS
I_{max}	NS	NS	NS	NS	I_{max}	-	NS	NS	NS
I_{min}	NS	NS	NS	NS	I_{min}	-	NS	NS	NS
Shape index	NS	NS	NS	NS	**Shape index**	NS	NS	NS	NS
Z_x	NS	NS	NS	NS	Z_x	NS	NS	NS	NS
Z_y	NS	NS	NS	NS	Z_y	-	+	NS	NS
Z_p	NS	NS	NS	NS	Z_p	-	NS	NS	NS
Z_{max}	NS	NS	NS	NS	Z_{max}	-	NS	NS	NS
Z_{min}	NS	NS	NS	NS	Z_{min}	-	NS	NS	NS

Orange plus signs (+) indicate significant increases for that CSG property from one decade to the next, blue dashes (-) indicates significant decreases, and NS indicates no significant change.

Variation by BMI, Activity, and Pathology Groups

A secondary aim of this dissertation was to test for variation in diaphyseal cortical bone distribution in groups based on variables known to mechanically or physiologically affect bone geometry and mass. For this sample, it was possible to compare individuals based on body mass index (BMI) (underweight, normal, overweight, obese), activity level (light, moderate, heavy), and pathological condition at death (pathological, healthy). Chapter 5 describes how individuals were assigned to each group and provides the sample size of each, which are smaller than those of previous analyses, as many of these data were not recorded for many individuals used in this study.

Univariate analyses tested for effects of slice location, age group, sex, BMI, activity level, and pathology group. BMI had a significant ($p < 0.05$) effect on CSG properties in all elements, with the exception of shape index in the humerus, radius, ulna, and femur, and percent cortical area in the radius. Activity level had no effect on diaphyseal properties in the bones of the upper limb, but did significantly affect those in the femur and tibia. These properties included cortical area, and all measures of strength and rigidity (except I_x in the femur and I_y in the tibia). Pathological group had a significant effect on all CSG properties of the humerus and radius, except percent cortical area and shape, and I_y in the humerus and MA in the radius. In the ulna, only cortical area and total area were affected by pathological group. Properties in the femur were unaffected with the exception of total area. Pathological group significantly affected tibial cortical area, total area, I_x, I_{min}, Z_x, and Z_{min}. In the fibula, I_y, I_{min}, shape index, and Z_{min} were significant. All results of univariate comparisons are provided in Appendix G (Tables G.1-G.6).

For multivariate analyses, sex and age were pooled within each BMI, activity, and pathological group due to low power. This method may have produced a false positive in some

later post-hoc analyses, but could be ameliorated with a larger sample in a later study. Similar to earlier comparisons between age groups, mean values for CSG properties among all five diaphyseal locations were used. Table 14 displays the results of the MANOVA for each factor examined. All null hypotheses concerning these factors were significant at $p < 0.05$, requiring post-hoc analyses to determine individual differences in BMI, activity, and pathological groups.

Table 14. MANOVA results for bone, BMI, activity level, pathology group, and CSG property effects

Factor	df	F	*p*
Bone*CSG property*BMI group	(225, 1326)	3.78	**< 0.0001**
Bone*CSG property*activity level	(150, 882)	1.86	**< 0.0001**
Bone*CSG property*pathology group	(75, 440)	2.25	**< 0.0001**

Pillai's Trace statistic, significant values ($p < 0.05$) bolded.

Pairwise comparisons using LS means were used to find significant differences ($p < 0.05$) separately among groups for BMI category, activity level, and pathology. There was a significant increase in all CSG properties with increased BMI in the humerus, radius, and ulna, with the exception of shape (all groups) and percent cortical area (obese individuals differed from all other groups). The femur and fibula followed the same pattern as the upper limb elements, with one exception. Femoral medullary area did not differ between most BMI groups, but values are significantly greater in overweight individuals compared with underweight individuals, and obese individuals compared with underweight and normal weight persons. Fibular medullary area differed between all groups except normal weight and overweight individuals. For a majority of CSG properties in the tibia, a significant increase in values with increased BMI existed between groups, with the exception of overweight and obese individuals.

Activity groups showed similar patterns to BMI groups, in that while most CSG properties significantly increased as activity level increased, percent cortical area and shape index were not different between levels of activity in any of the skeletal elements examined. In the humerus, radius, femur, and fibula, a majority of measures of bone mass and rigidity were not significantly different between light and moderate activity groups, but showed a significant increase in heavy activity groups. In the tibia, the exact opposite pattern existed, with moderate and heavy groups demonstrating relatively similar values, while the light activity group had significantly lower values in measures of bone mass and rigidity.

Pathological and healthy groups showed significant differences in all CSG properties except percent cortical area in the humerus, radius, and tibia, and shape in the humerus, radius, ulna, femur, and tibia. The tibia demonstrated a unique pattern from the rest of the elements. In addition to percent measures of shape, no difference existed in all properties reflecting bone strength (except Z_x) and rigidity. In all cases of significant differences, pathological individuals had higher values than those assigned to the healthy group, contrary to what would be expected if illness had a long-term impact on bone quantity. Complete results of HSD pairwise comparisons for BMI, activity, and pathology groups are provided in Appendix H (Tables H.1-H.18).

Within Bone Variation Results Summary

With the large number of comparisons and mixed results, it is useful to highlight the notable findings of within bone variation. Sexual dimorphism in diaphyseal cortical area distribution was evident. Cortical area and total area, both measures related to bone mass, were greater in males across the skeleton. The distal half of the lower limbs, however, did not differ in

total subperiosteal area between the sexes. Medullary area, another property reflective of bone mass, was largely the same between the sexes in all bones, except for the distal portion of the radius and ulna and the most proximal site on the femur, all of which had greater values in males. Measures of bone shape (percent cortical area and shape index) were largely similar between the sexes in all skeletal elements. However, percent cortical area was greater in males in the distal half of the humerus and tibia. Males also demonstrated greater values in all measurements of bone strength and rigidity across the diaphyses of all six bones.

Differences in cortical area distribution between age groups of the same sex were less consistent. Figures 28 and 29 summarize significant results for measures of bone mass, shape, strength, and rigidity through time in females and males. Broadly, greater variation was observed in CSG properties in the bones of the upper limb than those of the lower. Females demonstrated significant shifts in bone mass and shape in the fifth decade, and in strength and rigidity in the eighth. Males showed mass, strength, and rigidity changes in the fifth decade, mass and shape in the seventh, and mass, strength and rigidity in the eighth.

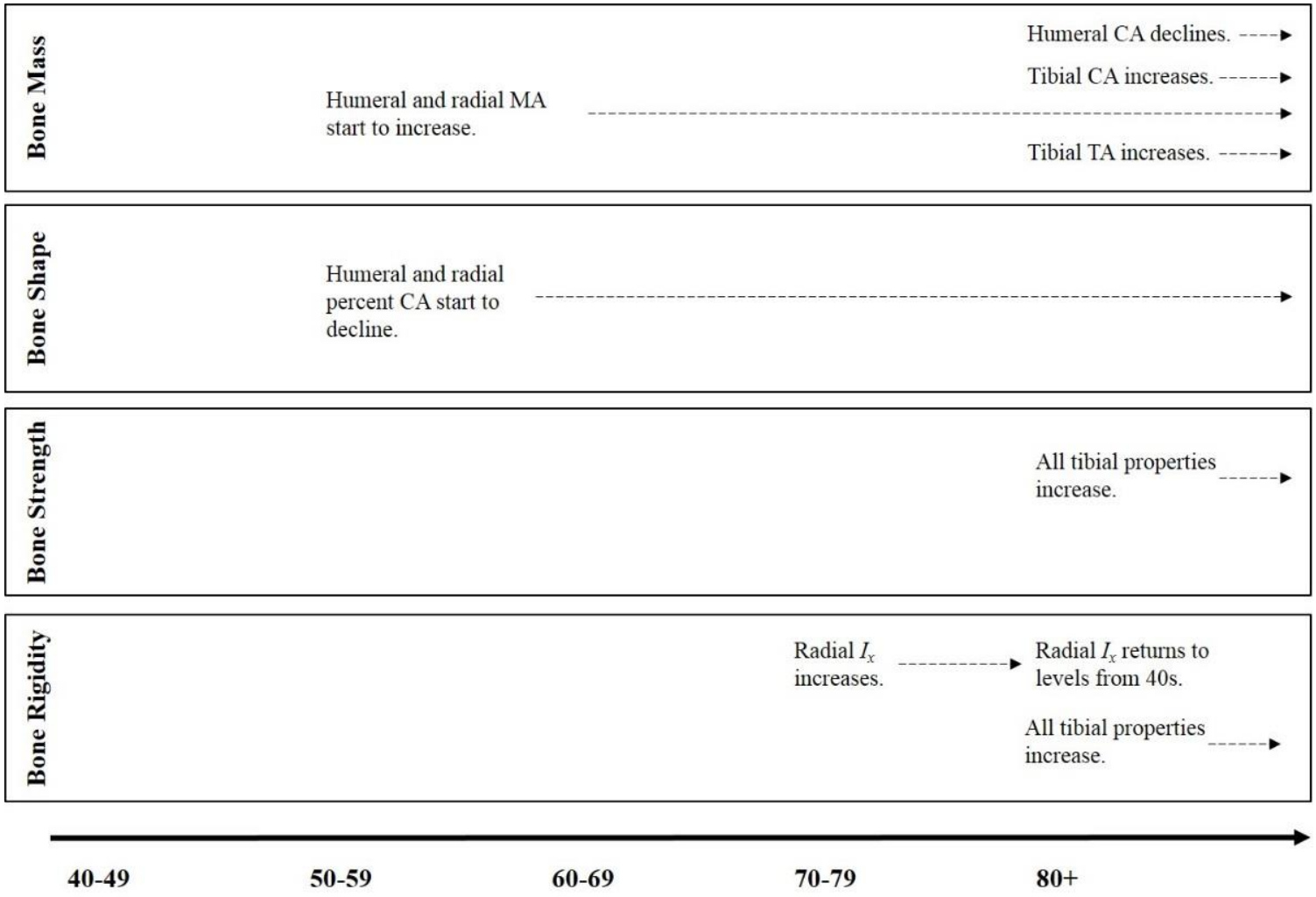

Figure 28. Summary age changes to bone properties of bone mass, shape, strength, and rigidity in females
Females demonstrated significant shifts in bone mass and shape in the fifth decade, and in strength and rigidity in the eighth.

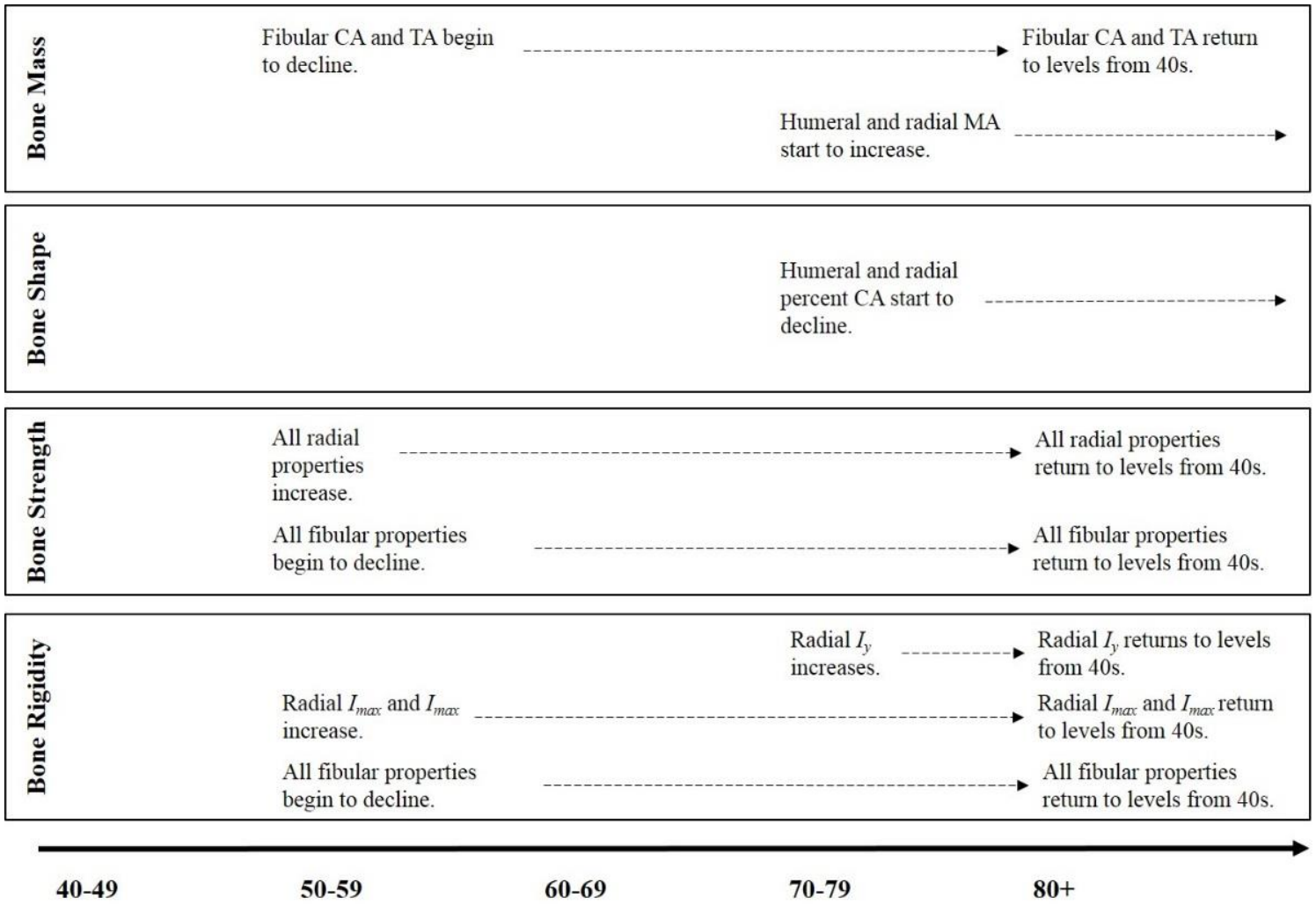

Figure 29. Summary age changes to bone properties of bone mass, shape, strength, and rigidity in males
Males showed mass, strength, and rigidity changes in the fifth decade, mass and shape in the seventh, and mass, strength and rigidity in the eighth.

Finally, variation in cortical bone distribution was tested by BMI, activity level, and pathological condition at time of death. CSG properties of bone mass, strength, and rigidity increased with BMI in the humerus, radius, ulna, femur, and fibula. The tibia showed similar results, but with no meaningful difference between overweight and obese individuals. Activity groups showed similar patterns to BMI groups, in that while most CSG properties significantly increased as activity level increased, measures of bone shape were not different between levels of activity in any of the skeletal elements examined. In the humerus, radius, femur, and fibula, heavy activity groups showed a significant increase in a majority of measures of bone mass and rigidity from light and moderate groups. In the tibia, the exact opposite pattern existed, with moderate and heavy groups demonstrating relatively similar values, while the light activity group had significantly lower values in measures of bone mass and rigidity. The pathological group demonstrated greater values in all CSG properties, except measures of shape, than those of healthy individuals. Here, the tibia showed no difference in any properties reflecting bone strength and rigidity between groups.

Within Limb Variation

This section presents the results of cortical bone distribution within each limb. These comparisons test the relationship within human (and all tetrapod) limbs between one proximal bone followed by two paired bones. This tapering of the limb is hypothesized to have an effect on properties of bone mass, shape, bending strength, and rigidity. Results are provided first by comparison within the upper limb bones (humerus, radius, and ulna) and then by the lower limb bones (femur, tibia, and fibula). The section ends with a summary of within limb variation.

Variation in the Upper Limb

Variation in cortical bone distribution in the humerus, radius, and ulna were tested for sex effects using univariate analyses. Results demonstrated significantly greater values ($p < 0.05$) in males for a vast majority of CSG properties at all locations. However, no differences between the sexes existed in percent cortical area and shape index (both measures of diaphyseal shape) at 80% of bone length in all three bones. A MANOVA was used to test for bone, slice location, and CSG property differences among upper limb bone locations (Table 15). All null hypotheses concerning these factors were significant at $p < 0.05$, requiring post-hoc analyses to determine individual differences in CSG properties by slice location in the three bones. For the purposes of this dissertation, all sexes and ages were pooled for post-hoc comparisons due to small and uneven sample sizes of upper limb CT scans. Sex and age group effects on the upper limb, which are clearly significant, could be tested with a larger sample in a later study.

Table 15. MANOVA results for bone, slice location, and CSG property effects in the upper limb

Factor	df	F	*p*
CSG property* slice location*bone	(104, 1060)	153.86	**< 0.0001**

Pillai's Trace statistic, significant values ($p < 0.05$) bolded.

LS means were compared to find significant differences ($\alpha = 0.05$) among CSG properties at the five diaphyseal locations, between bones. Tables 16 and 17 display means for the bones of the upper limb by sex. The humerus had greater values of all CSG properties at all locations than the radius and ulna, with two exceptions. There was no difference between I_{max} at 80% of bone length ($p = 0.9561$) and shape index at 65% of length ($p = 0.7875$) between the humerus and ulna. The radius and ulna differed significantly in all properties, at all locations, with the exception of I_y ($p = 0.4587$) and I_{max} ($p = 0.1703$) at 65% and I_{min} ($p = 0.8546$) and Z_{min}

(p = 0.9701) at 50%. Interestingly, the proximal half (50%, 65%, and 80% of length) of the ulna demonstrated greater values in a vast majority of properties related to mass, strength, and rigidity. Conversely, the radius exhibited greater values of these same properties in the distal portion (20% and 35% of length). At 50% of length, generally understood as the most mechanically sensitive location, mediolateral (ML) strength and rigidity were greater in the radius, while the ulna showed greater anteroposterior AP, maximum, minimum, and torsional strength and rigidity. Measures related to diaphyseal shape were inconsistent between the two bones. Complete results of pairwise comparisons for CSG properties, slice location, and bones of the upper limb are provided in Appendix I (Tables I.1-I.15).

Table 16. Means and standard deviations for CSG properties in the female upper limb

CSG Property	% of bone length	Humerus		Radius		Ulna	
		Mean	Std	Mean	Std	Mean	Std
CA	20	103.70	29.96	46.09	13.34	29.72	9.53
	35	92.80	26.83	45.29	13.02	42.04	12.45
	50	96.97	27.12	49.31	14.52	52.8	16.04
	65	95.91	27.54	49.05	14.07	61.35	18.84
	80	88.94	25.94	44.60	13.47	81.68	24.92
TA	20	159.68	51.03	77.60	25.54	48.51	17.34
	35	150.62	48.87	60.72	19.87	57.11	18.87
	50	165.07	54.76	63.74	21.02	68.43	22.60
	65	179.30	57.56	68.17	22.51	81.45	27.06
	80	202.60	65.88	76.64	27.10	129.32	47.62
MA	20	55.98	33.72	31.50	16.32	18.78	11.46
	35	57.81	35.03	15.42	11.35	15.06	11.11
	50	68.10	41.96	14.43	11.29	15.63	11.96
	65	83.39	44.67	19.11	13.86	20.10	13.19
	80	113.66	48.52	32.03	18.24	47.64	30.49
% CA	20	6662.36	1168.73	6119.46	1079.46	6375.44	1397.85
	35	6354.65	1247.07	7627.81	1141.69	7543.554	1224.35
	50	6117.93	1316.94	7890.33	1122.83	7856.12	1113.79
	65	5542.22	1194.02	7373.33	1170.36	7653.22	948.57
	80	4548.76	1090.66	6000.32	1130.63	6610.06	1373.81
I_x	20	0.026	0.009	0.010	0.003	0.004	0.001
	35	0.027	0.008	0.007	0.002	0.007	0.003
	50	0.029	0.010	0.008	0.003	0.012	0.005
	65	0.030	0.010	0.008	0.003	0.013	0.005
	80	0.035	0.013	0.012	0.005	0.031	0.013
I_y	20	0.037	0.014	0.015	0.006	0.004	0.001
	35	.023	0.008	0.009	0.004	0.005	0.002
	50	0.030	0.011	0.011	0.004	0.008	0.003
	65	0.011	0.013	0.005	0.004	0.006	0.004
	80	0.041	0.016	0.011	0.004	0.036	0.016
J	20	.063	0.022	0.026	0.009	0.008	0.003
	35	0.016	0.022	0.006	0.009	0.005	0.003
	50	0.060	0.020	0.020	0.007	0.021	0.007
	65	0.066	0.021	0.022	0.007	0.026	0.010
	80	0.077	0.028	0.023	0.009	0.067	0.027
I_{max}	20	0.039	0.014	0.017	0.006	0.004	0.001
	35	0.028	0.009	0.010	0.004	0.008	0.003
	50	0.036	0.012	0.012	0.005	0.014	0.005
	65	0.038	0.012	0.015	0.005	0.015	0.006
	80	0.043	0.016	0.013	0.005	0.041	0.017
I_{min}	20	0.023	0.008	0.008	0.002	0.003	0.001
	35	0.022	0.007	0.006	0.002	0.004	0.001
	50	0.023	0.008	0.007	0.002	0.006	0.002
	65	0.028	0.009	0.007	0.002	0.011	0.004

Table 16. Continued

CSG Property	% of bone length	Humerus		Radius		Ulna	
		Mean	Std	Mean	Std	Mean	Std
	80	0.034	0.012	0.010	0.004	0.025	0.010
Shape	20	166.79	29.44	207.9	29.83	127.0	14.89
	35	129.97	14.16	159.2	30.14	179.8	36.14
	50	160.95	22.67	171.0	29.40	210.6	47.63
	65	137.94	20.03	210.5	33.65	135.2	27.22
	80	126.31	16.92	131.2	18.66	164.6	28.91
Z_x	20	0.859	0.263	0.395	0.012	0.203	0.070
	35	0.915	0.271	0.323	0.104	0.285	0.092
	50	0.965	0.294	0.348	0.126	0.392	0.137
	65	0.989	0.296	0.363	0.123	0.464	0.167
	80	1.09	0.332	0.448	0.165	0.853	0.306
Z_y	20	1.03	0.334	0.486	0.159	0.207	0.071
	35	0.823	0.249	0.354	0.119	0.259	0.095
	50	0.962	0.290	0.374	0.127	0.338	0.131
	65	1.07	0.301	0.424	0.134	0.479	0.194
	80	1.18	0.392	0.424	0.144	0.926	0.350
Z_p	20	1.59	0.503	0.742	0.231	0.372	0.127
	35	1.59	0.485	0.575	0.186	0.460	0.156
	50	1.73	0.513	0.579	0.195	0.606	0.207
	65	1.85	0.542	0.629	0.197	0.843	0.326
	80	2.04	0.677	0.790	0.271	1.55	0.568
Z_{max}	20	1.01	0.328	0.509	0.162	0.214	0.071
	35	0.91	0.271	0.355	0.115	0.296	0.099
	50	1.08	0.321	0.366	0.125	0.410	0.141
	65	1.11	0.326	0.426	0.133	0.497	0.189
	80	1.17	0.393	0.456	0.165	1.00	0.376
Z_{min}	20	0.804	0.250	0.352	0.106	0.191	0.067
	35	0.801	0.246	0.300	0.094	0.241	0.082
	50	0.857	0.254	0.316	0.104	0.306	0.104
	65	0.937	0.274	0.318	0.101	0.440	0.158
	80	1.05	0.330	0.396	0.135	0.773	0.284

All values have been scaled by 100 for better visualization.

Table 17. Means and standard deviations for CSG properties in the male upper limb

CSG Property	% of bone length	Humerus		Radius		Ulna	
		Mean	Std	Mean	Std	Mean	Std
CA	20	149.98	44.08	60.92	18.82	42.04	14.43
	35	132.67	38.66	62.85	19.40	59.47	17.91
	50	138.46	38.84	67.57	21.62	73.97	23.04
	65	132.49	37.18	65.37	20.09	84.39	25.43
	80	111.84	29.23	62.33	19.85	117.16	36.94
TA	20	205.41	66.51	106.42	37.33	67.02	23.06
	35	197.96	61.70	82.12	27.50	78.02	24.51
	50	212.49	68.92	82.67	27.10	91.55	28.67
	65	232.19	71.78	84.90	28.19	107.00	33.20
	80	279.96	87.57	101.35	36.93	175.29	59.33
MA	20	55.43	35.57	45.50	23.31	24.97	12.57
	35	65.28	36.39	19.26	12.66	18.54	10.77
	50	74.03	43.79	15.09	9.72	17.58	10.32
	65	99.70	47.47	19.52	11.95	22.61	11.59
	80	168.12	65.62	39.01	22.37	58.12	31.94
% CA	20	7407.04	939.73	5876.23	973.71	6374.36	1042.06
	35	6829.36	1049.40	7769.13	935.88	7700.85	845.81
	50	6672.29	1086.62	8239.56	833.95	8116.12	784.81
	65	5841.49	1011.97	7797.97	808.14	7929.68	621.53
	80	4133.79	878.94	6331.33	1090.17	6821.18	1053.97
I_x	20	0.042	0.018	0.016	0.007	0.007	0.003
	35	0.046	0.017	0.012	0.005	0.013	0.005
	50	0.049	0.0185	0.013	0.005	0.021	0.009
	65	0.056	0.021	0.013	0.005	0.022	0.009
	80	0.063	0.022	0.020	0.010	0.054	0.025
I_y	20	0.065	0.026	0.025	0.012	0.007	0.003
	35	0.041	0.014	0.016	0.007	0.009	0.003
	50	0.051	0.021	0.017	0.008	0.014	0.005
	65	0.018	0.021	0.009	0.008	0.008	0.005
	80	0.063	0.021	0.018	0.008	0.059	0.026
J	20	0.107	0.041	0.042	0.019	0.015	0.007
	35	0.032	0.041	0.012	0.019	0.009	0.007
	50	0.100	0.038	0.031	0.013	0.035	0.014
	65	0.110	0.039	0.032	0.013	0.043	0.017
	80	0.127	0.043	0.039	0.018	0.114	0.048
I_{max}	20	0.070	0.029	0.027	0.012	0.008	0.004
	35	0.048	0.018	0.017	0.007	0.014	0.005
	50	0.060	0.022	0.019	0.008	0.022	0.009
	65	0.061	0.021	0.021	0.009	0.024	0.009
	80	0.068	0.022	0.022	0.010	0.071	0.031
I_{min}	20	0.036	0.014	0.014	0.006	0.006	0.003
	35	0.038	0.014	0.011	0.004	0.008	0.003
	50	0.040	0.016	0.012	0.005	0.012	0.004
	65	0.049	0.018	0.011	0.004	0.019	0.007
	80	0.058	0.020	0.016	0.007	0.043	0.018

Table 17. Continued

CSG Property	% of bone length	Humerus		Radius		Ulna	
		Mean	Std	Mean	Std	Mean	Std
Shape	20	195.40	42.29	195.68	31.32	128.74	16.58
	35	124.75	13.49	158.43	22.88	165.22	29.05
	50	150.36	19.86	158.39	23.37	189.43	40.57
	65	125.82	13.09	199.15	30.32	129.91	18.42
	80	119.59	12.74	133.90	19.37	165.71	30.16
Z_x	20	1.27	0.431	0.593	0.217	0.314	0.135
	35	1.38	0.449	0.488	0.179	0.444	0.159
	50	1.45	0.452	0.495	0.175	0.589	0.225
	65	1.53	0.485	0.488	0.177	0.669	0.247
	80	1.63	0.489	0.668	0.259	1.343	0.507
Z_y	20	1.57	0.509	0.709	0.273	0.319	0.126
	35	1.28	0.407	0.531	0.203	0.407	0.139
	50	1.46	0.497	0.530	0.194	0.506	0.172
	65	1.49	0.469	0.582	0.215	0.686	0.246
	80	1.66	0.503	0.624	0.229	1.407	0.517
Z_p	20	2.33	0.728	1.10	0.414	0.576	0.240
	35	2.46	0.786	0.851	0.318	0.729	0.253
	50	2.68	0.874	0.840	0.302	0.922	0.329
	65	2.79	0.872	0.869	0.324	1.222	0.434
	80	3.024	0.909	1.175	0.446	2.433	0.873
Z_{max}	20	1.557	0.507	0.736	0.277	0.334	0.143
	35	1.391	0.453	0.524	0.198	0.462	0.167
	50	1.655	0.534	0.522	0.194	0.607	0.227
	65	1.590	0.486	0.582	0.214	0.714	0.256
	80	1.674	0.494	0.679	0.260	1.578	0.583
Z_{min}	20	1.166	0.386	0.542	0.202	0.293	0.115
	35	1.244	0.396	0.449	0.164	0.383	0.131
	50	1.335	0.426	0.456	0.164	0.473	0.164
	65	1.425	0.443	0.444	0.164	0.639	0.218
	80	1.548	0.459	0.589	0.222	1.105	0.371

All values have been scaled by 100 for better visualization.

Variation in the Lower Limb

Variation in cortical bone distribution in the femur, tibia, and fibula were tested for sex effects using univariate analyses. As with the upper limb, results demonstrated significantly greater values ($p < 0.05$) in males for a vast majority of CSG properties at all locations. However, no differences between the sexes existed in medullary area at 20% of bone length, percent cortical area at 80%, and shape index at all sites, in all three bones. A MANOVA was used to test for bone, slice location, and CSG property differences among upper limb bone locations (Table 18). All null hypotheses concerning these factors were significant at $p < 0.05$, requiring post-hoc analyses to determine individual differences in CSG properties by slice location in the three bones. As with the upper limb, all sexes and ages were pooled for post-hoc comparisons due to small and uneven sample sizes of upper limb CT scans. Sex and age groups effects on the lower limb, which are clearly significant, could be tested with a larger sample in a later study.

Table 18. MANOVA results for bone, slice location, and CSG property effects in the lower limb

Factor	df	F	*p*
CSG property* slice location*bone	(104, 1000)	156.35	**< 0.0001**

Pillai's Trace statistic, significant values ($p < 0.05$) bolded.

Pairwise comparisons using LS means were used to find significant differences ($\alpha = 0.05$) among CSG properties at the five diaphyseal locations, between bones. Tables 19 and 20 display means for the bones of the lower limb by sex. Properties related to bone mass (CA, TA, and MA) were greater in the femur, although the proximal portion of the tibia (80%) proved to have greater medullary and total subperiosteal area. Measures of diaphyseal shape produced mixed

results. Both the tibia and fibula had greater shape index values than the femur, but only the fibula demonstrated the significantly greater values at all sites for percent cortical area. Relationships of bone strength and rigidity between bones in the lower limb largely mirrored on another. The femur and tibia had greater strength and rigidity than the fibula at all sites, which was expected. The tibia, however, demonstrated greater maximum, torsional, and AP bending strength and rigidity in the proximal portion of the bone (65% and 80%) than the femur. Further, while the femur proved to have greater values for most strength and rigidity properties at midshaft and distally, there was no difference between femoral and tibial I_y ($p = 0.6622$), I_{min} ($p = 0.5219$), and Z_{min} ($p = 0.0848$) at 80% of length, and I_x ($p = 0.9270$), I_{max} ($p = 0.0524$), and Z_x ($p = 0.1416$), at 50% of length. Complete results of pairwise comparisons for CSG properties, slice location, and bones of the lower limb are provided in Appendix J (Tables J.1-J.15).

Table 19. Means and standard deviations for CSG properties in the female lower limb

CSG Property	% of bone length	Femur		Tibia		Fibula	
		Mean	Std	Mean	Std	Mean	Std
CA	20	157.07	45.77	105.11	30.07	34.91	12.72
	35	194.40	55.35	140.76	38.09	42.96	14.76
	50	223.26	63.88	164.88	46.45	44.44	16.22
	65	240.04	65.99	170.50	47.36	41.91	16.14
	80	205.72	60.60	157.77	48.51	32.51	12.04
TA	20	519.71	163.23	246.35	79.59	49.02	19.33
	35	362.74	109.57	215.91	64.46	57.16	20.05
	50	336.71	101.56	250.61	75.63	59.18	23.32
	65	354.01	102.47	304.60	94.25	54.78	20.84
	80	352.48	160.97	430.17	177.59	47.60	19.70
MA	20	362.64	133.14	141.24	65.64	14.11	10.79
	35	168.33	74.81	75.14	42.86	14.19	10.13
	50	113.45	69.54	85.72	50.49	14.74	11.39
	65	113.97	66.44	134.10	66.95	12.87	10.18
	80	146.75	126.69	272.39	149.09	15.08	11.41
% CA	20	3115.25	695.98	4482.30	1235.32	7393.66	1520.41
	35	5484.12	1005.99	6682.26	1185.59	7629.61	1230.69
	50	6794.25	1206.80	6745.75	1246.21	7678.25	1306.44
	65	6929.76	1184.68	5779.64	1190.50	7831.33	1486.18
	80	6641.19	2419.03	4266.67	2147.85	7189.81	1621.98
I_x	20	0.071	0.024	0.036	0.012	0.002	0.001
	35	0.064	0.022	0.043	0.015	0.003	0.001
	50	0.066	0.022	0.067	0.024	0.004	0.002
	65	0.072	0.025	0.097	0.033	0.003	0.002
	80	0.080	0.024	0.154	0.056	0.002	0.001
I_y	20	0.111	0.037	0.042	0.014	0.002	0.001
	35	0.066	0.020	0.039	0.013	0.003	0.001
	50	0.063	0.021	0.047	0.016	0.004	0.002
	65	0.023	0.021	0.021	0.016	0.002	0.001
	80	0.112	0.040	0.104	0.042	0.002	0.001
J	20	0.182	0.060	0.079	0.026	0.005	0.002
	35	0.041	0.060	0.027	0.026	0.002	0.002
	50	0.129	0.040	0.114	0.038	0.008	0.004
	65	0.144	0.045	0.157	0.051	0.008	0.003
	80	0.192	0.062	0.259	0.093	0.005	0.002
I_{max}	20	0.113	0.038	0.044	0.015	0.003	0.001
	35	0.071	0.023	0.052	0.018	0.004	0.001
	50	0.073	0.023	0.077	0.027	0.005	0.002
	65	0.082	0.026	0.110	0.037	0.005	0.002
	80	0.117	0.039	0.180	0.065	0.003	0.001
I_{min}	20	0.068	0.023	0.034	0.011	0.001	0.000
	35	0.059	0.019	0.029	0.009	0.002	0.001
	50	0.056	0.018	0.036	0.011	0.002	0.001
	65	0.062	0.020	0.046	0.015	0.002	0.001

Table 19. Continued

CSG Property	% of bone length	Femur		Tibia		Fibula	
		Mean	Std	Mean	Std	Mean	Std
	80	0.075	0.024	0.078	0.029	0.001	0.000
Shape	20	166.38	21.02	130.74	18.21	242.51	57.54
	35	121.74	17.12	180.85	31.78	206.21	57.10
	50	131.99	17.15	210.61	35.17	218.83	70.14
	65	132.96	18.58	237.56	38.48	268.39	89.07
	80	158.27	22.51	233.77	38.10	208.60	68.77
Z_x	20	2.00	0.632	1.14	0.354	0.160	0.064
	35	2.00	0.605	1.37	0.430	0.197	0.083
	50	1.96	0.586	1.83	0.591	0.216	0.093
	65	2.23	0.685	2.35	0.718	0.203	0.089
	80	2.23	0.661	3.09	1.040	0.154	0.065
Z_y	20	2.53	0.768	1.25	0.423	0.167	0.075
	35	2.09	0.601	1.24	0.372	0.211	0.079
	50	2.05	0.635	1.44	0.441	0.234	0.100
	65	2.35	0.698	1.75	0.542	0.216	0.094
	80	2.94	0.915	2.36	0.783	0.159	0.065
Z_p	20	4.05	1.255	2.14	0.708	0.269	0.106
	35	3.80	1.109	2.28	0.673	0.343	0.131
	50	3.65	1.072	2.76	0.827	0.377	0.149
	65	4.22	1.226	3.49	1.043	0.339	0.138
	80	4.41	1.325	4.60	1.569	0.266	0.108
Z_{max}	20	2.54	0.775	1.25	0.423	0.190	0.078
	35	2.13	0.611	1.49	0.461	0.231	0.084
	50	2.14	0.638	1.88	0.592	0.260	0.101
	65	2.45	0.719	2.46	0.755	0.244	0.096
	80	2.94	0.880	3.23	1.126	0.181	0.073
Z_{min}	20	1.90	0.595	1.09	0.319	0.126	0.047
	35	1.92	0.560	1.02	0.296	0.162	0.064
	50	1.89	0.574	1.24	0.360	0.171	0.070
	65	2.13	0.645	1.47	0.434	0.156	0.067
	80	2.14	0.655	2.02	0.656	0.126	0.054

All values have been scaled by 100 for better visualization.

Table 20. Means and standard deviations for CSG properties in the male lower limb

CSG Property	% of bone length	Femur		Tibia		Fibula	
		Mean	Std	Mean	Std	Mean	Std
CA	20	187.27	52.01	135.34	38.79	44.68	14.46
	35	232.68	62.88	180.75	54.79	53.44	16.76
	50	270.96	71.86	208.21	62.43	55.34	17.41
	65	288.98	75.94	215.45	62.83	52.13	16.77
	80	251.40	69.19	204.08	59.85	40.61	14.07
TA	20	573.91	182.41	283.41	93.52	59.44	22.58
	35	406.52	119.80	249.89	76.97	68.74	23.00
	50	379.54	108.93	289.33	87.91	73.36	24.51
	65	395.19	113.40	358.13	113.33	68.25	23.17
	80	457.24	179.36	554.94	188.51	58.66	21.31
MA	20	386.64	146.13	148.06	66.58	14.75	11.82
	35	173.84	74.34	69.14	35.07	15.30	8.97
	50	108.58	62.97	81.12	39.84	18.01	10.00
	65	106.20	58.25	142.68	64.92	16.12	10.80
	80	205.83	141.72	350.86	150.24	18.05	11.14
% CA	20	3384.03	861.06	4901.49	813.10	7711.41	1135.54
	35	5819.23	798.97	7297.96	781.24	7845.17	734.68
	50	7249.44	933.26	7247.40	796.66	7614.54	784.98
	65	7393.69	775.62	6112.70	827.87	7725.49	973.30
	80	6058.02	2114.87	3847.76	1064.59	7059.83	1165.78
I_x	20	0.095	0.032	0.049	0.021	0.003	0.001
	35	0.083	0.031	0.056	0.021	0.004	0.002
	50	0.086	0.030	0.087	0.034	0.005	0.002
	65	0.092	0.032	0.132	0.048	0.004	0.002
	80	0.107	0.036	0.220	0.073	0.003	0.001
I_y	20	0.132	0.044	0.059	0.048	0.003	0.002
	35	0.084	0.027	0.053	0.020	0.004	0.002
	50	0.080	0.026	0.065	0.024	0.005	0.002
	65	0.030	0.026	0.032	0.024	0.002	0.002
	80	0.156	0.057	0.150	0.059	0.003	0.002
J	20	0.228	0.075	0.108	0.067	0.007	0.003
	35	0.056	0.075	0.040	0.067	0.004	0.003
	50	0.167	0.053	0.152	0.055	0.011	0.005
	65	0.181	0.059	0.217	0.076	0.009	0.004
	80	0.263	0.089	0.370	0.125	0.006	0.003
I_{max}	20	0.134	0.044	0.063	0.059	0.005	0.002
	35	0.091	0.031	0.071	0.027	0.005	0.002
	50	0.094	0.032	0.104	0.039	0.007	0.003
	65	0.102	0.038	0.154	0.055	0.006	0.002
	80	0.160	0.057	0.263	0.089	0.005	0.002
I_{min}	20	0.093	0.032	0.045	0.017	0.002	0.001
	35	0.077	0.025	0.038	0.014	0.003	0.001
	50	0.072	0.023	0.048	0.017	0.003	0.001
	65	0.079	0.023	0.062	0.023	0.003	0.001

Table 20. Continued

CSG Property	% of bone length	Femur		Tibia		Fibula	
		Mean	Std	Mean	Std	Mean	Std
	80	0.103	0.035	0.106	0.039	0.002	0.001
Shape	20	145.12	18.76	140.15	118.04	251.42	71.74
	35	118.65	10.97	187.71	35.81	187.08	42.90
	50	130.73	19.06	221.07	43.27	200.75	61.18
	65	129.39	19.74	249.86	44.08	224.09	78.15
	80	156.14	28.64	251.11	37.96	192.81	57.97
Z_x	20	2.65	0.781	1.52	0.480	0.200	0.087
	35	2.47	0.764	1.70	0.574	0.249	0.093
	50	2.45	0.740	2.27	0.755	0.274	0.107
	65	2.73	0.831	3.03	0.985	0.250	0.103
	80	2.99	0.912	4.23	1.325	0.190	0.078
Z_y	20	3.02	0.872	1.66	0.604	0.217	0.098
	35	2.55	0.725	1.56	0.542	0.261	0.102
	50	2.51	0.728	1.82	0.602	0.288	0.113
	65	2.79	0.800	2.30	0.779	0.259	0.102
	80	3.57	1.12	3.09	1.06	0.199	0.084
Z_p	20	5.08	1.48	2.81	0.917	0.343	0.137
	35	4.71	1.37	2.81	0.962	0.433	0.157
	50	4.55	1.33	3.41	1.10	0.473	0.176
	65	5.14	1.42	4.49	1.44	0.423	0.161
	80	5.45	1.69	6.28	1.96	0.331	0.139
Z_{max}	20	3.02	0.873	1.65	0.601	0.244	0.098
	35	2.61	0.771	1.85	0.631	0.287	0.105
	50	2.64	0.779	2.35	0.758	0.319	0.116
	65	2.94	0.871	3.20	1.03	0.289	0.104
	80	3.56	1.116	4.52	1.42	0.220	0.090
Z_{min}	20	2.55	0.764	1.41	0.459	0.155	0.063
	35	2.39	0.706	1.27	0.443	0.214	0.080
	50	2.37	0.681	1.53	0.515	0.224	0.092
	65	2.59	0.720	1.86	0.602	0.202	0.084
	80	2.82	0.867	2.58	0.816	1.162	0.069

All values have been scaled by 100 for better visualization.

Within Limb Variation Results Summary

Cortical bone distribution within the limbs was examined in all CSG properties by slice location. The proximal bone of each limb has greater bone mass than the distal bones. In the upper limb, the humerus also has greater values for bending strength and rigidity. The radius and ulna appear to complement one another—the proximal portion of the ulna was stronger and more rigid in some respects, while the distal portion of the radius was stronger and rigid in the remaining properties. Variation in the lower limb is not as clearly patterned as in the upper limb. The fibula is unique with lower values of strength and rigidity at all sites, but greater percent cortical area than the femur and tibia. The femur and tibia have more commonalities in strength and rigidity, particularly at midshaft and 80% of length. The distal portion of the femur, however, is stronger and more rigid than that of the tibia. Figure 30 provides a visual summary of these relationships in the two limbs.

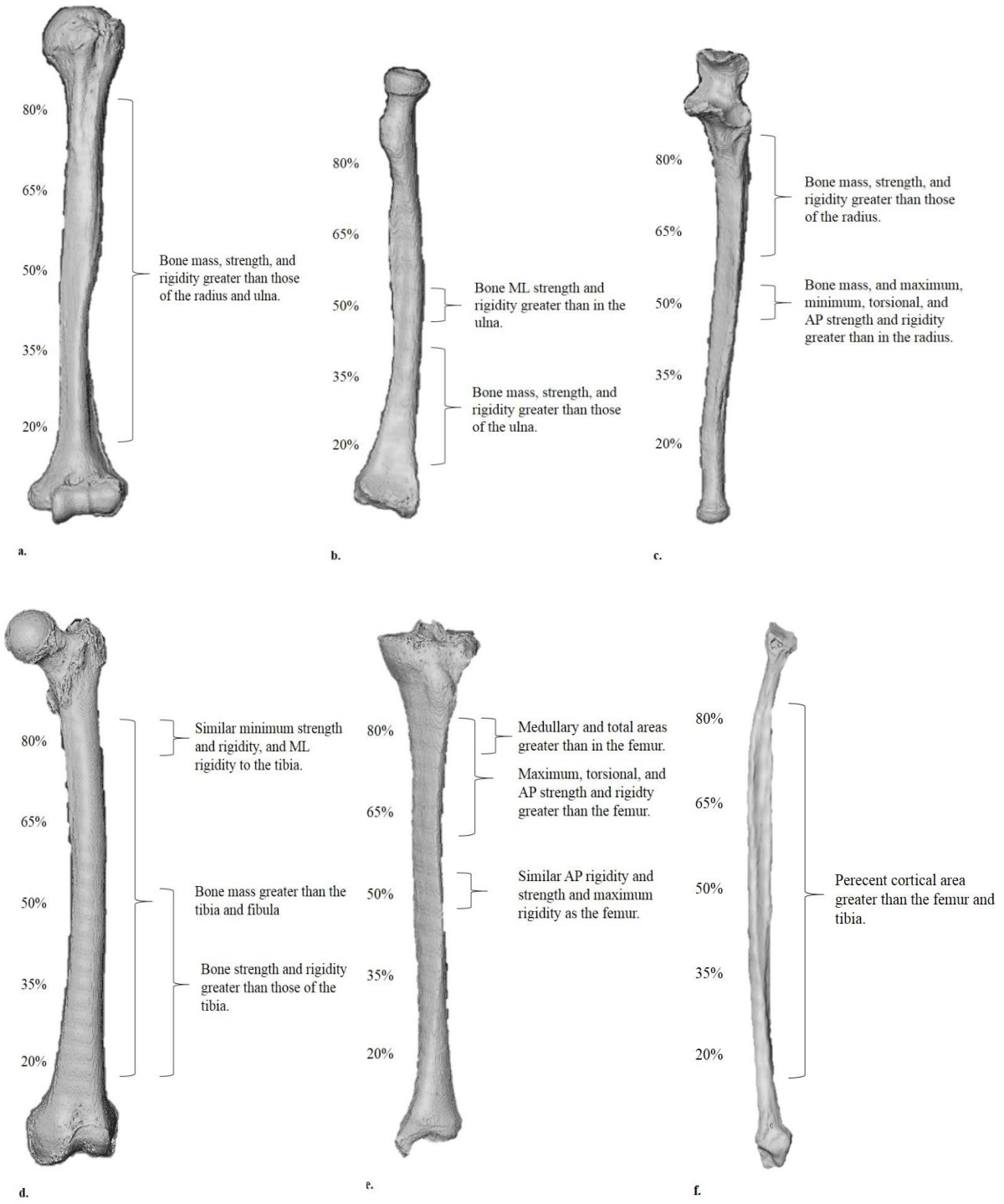

Figure 30. Summary differences in bone mass, strength, and rigidity in the upper and lower limbs

Clear patterns exist within the bones of the upper limb (a. humerus, b. radius, c. ulna), but less so in those of the lower limb (d. femur, e. tibia, f. fibula). Images not to scale.

Between Limb Variation

This section presents the results of cortical bone distribution between the limbs. These comparisons test whether relationships exist between proximal elements and between distal elements, despite vastly different loading environments, namely from locomotion and body weight. Precisely because of these differing exposures to mechanical forces, it was hypothesized that no similarities would exist between the segments of the limbs. Results are provided first by comparison between the proximal limb bones (humerus and femur) and then between the distal limb bones (radius, ulna, tibia, and fibula). The section ends with a summary of between limb variation.

Variation in Proximal Limb Segments

Variation in cortical bone distribution in the humerus and femur was tested for sex effects using univariate analyses. Results demonstrated significantly greater values ($p < 0.05$) in males for a vast majority of CSG properties at all locations. However, no differences between the sexes existed in medullary area at 20% ($p = 0.2348$) and 50% of bone length ($p = 0.2034$) in either bone. Then, MANOVAs were used to test for bone, sex, age, slice location, and age group effects. Table 21 displays the results of multivariate analyses for each factor. All null hypotheses concerning these factors were significant at $p < 0.05$, requiring post-hoc analyses to determine individual differences in CSG properties by slice location in the humerus and femur. As in within limb comparisons, all sexes and ages were pooled for post-hoc comparisons as a result of sample sizes. Ideally, sex and age groups effects on the proximal limb segments, which are significant, should be tested with a larger sample in a later study.

Table 21. MANOVA results for bone, slice location, and CSG property effects between proximal limb segments

Factor	df	F	*p*
CSG property* slice location*bone	(52, 327)	197.70	< **0.0001**

Pillai's Trace statistic, significant values ($p < 0.05$) bolded.

Pairwise comparisons using LS means were used to find significant differences ($\alpha = 0.05$) among CSG properties at the five diaphyseal locations, between the humerus and femur. Not surprisingly, the femur demonstrated greater values in all properties of bending strength and rigidity at all sites along the diaphysis. Measures of bone mass, cortical and total subperiosteal areas, were also greater at all locations in the femur. However, only the distal portion (20%, 35%, and 50%) of the femur proved to have greater medullary area than the humerus. CSG properties relating to diaphyseal shape showed the opposite pattern. The distal portion of the humerus showed greater percent cortical area (20% and 35%) and greater shape index values (20%, 35%, and 50%) than the femur. No difference occurred between the two bones at 65% of bone length for medullary area ($p = 0.0604$) and shape index ($p = 0.9782$).

Variation in Distal Limb Segments

Next, variation in cortical bone distribution in the distal limb bones—radius, ulna, tibia, and fibula—was examined for sex effects using univariate analyses. Results demonstrated significantly greater values ($p < 0.05$) in males for a vast majority of CSG properties at all locations. However, no differences between the sexes existed in percent cortical area at 80% of bone length ($p = 0.1912$), or shape index at 20% ($p = 0.8244$), 35% ($p = 0.0701$), and 80% ($p = 0.6857$). Then, MANOVAs tested for bone, sex, age, slice location, and age group effects. Table 22 displays the results of multivariate analyses for each factor. All null hypotheses concerning

these factors were significant at $p < 0.05$, requiring post-hoc analyses to determine individual differences in CSG properties by slice location in the four bones. Again, all sexes and ages were pooled for post-hoc comparisons as a result of sample sizes. As with prior comparisons, sex and age groups effects on the distal limb segments should be tested with a more robust sample in a later study.

Table 22. MANOVA results for bone, slice location, and CSG property effects in distal limb segments

Factor	**df**	**F**	***p***
CSG property* slice location*bone	(156, 2109)	127.29	< **0.0001**

Pillai's Trace statistic, significant values ($p < 0.05$) bolded.

Pairwise comparisons using LS means were used to find significant differences ($\alpha = 0.05$) among CSG properties at the five diaphyseal locations, between the radius, ulna, tibia, and fibula. As expected, the tibia demonstrated greater values of all properties at all sites, compared with the other three bones. Both upper limb elements also had greater properties of bending strength and rigidity than the fibula. Results of measures of diaphyseal shape and bone mass, however, were particularly interesting because of incidences of non-significance between limbs. Non-significant means in measures of bone mass occurred between the upper elements (radius and ulna) and the fibula in cortical area at 35% of bone length ($p = 0.5287$), total subperiosteal area at 20% ($p = 0.2984$) and 35% ($p = 0.1700$), and medullary area at 35% ($p = 0.1278$) and 50% ($p = 0.3980$). Measures of diaphyseal shape were non-significant in shape index at 50% ($p = 0.9746$), and percent cortical area at 35% ($p = 0.2747$), 65% ($p = 0.4130$), and 80% ($p = 0.113$). Complete results for LS means pairwise comparisons are provided in Appendix K (Tables K.1-K.15).

Between Limb Variation Results Summary

Cortical bone distribution between limbs was examined in all CSG properties by slice location between proximal limb elements (humerus and femur) and between distal limb elements (radius, ulna, tibia, and fibula). Results in the proximal elements were largely expected, with the femur having greater values of bone mass, bending strength, and rigidity at most locations than the humerus. Measures of diaphyseal shape (shape index and percent cortical area), however, were greater in the distal humerus than the femur. In the distal elements, the tibia demonstrated greater values in all properties at all locations than the other three bones. Notable results between the limbs included significantly greater values in measures of strength and rigidity in the radius and ulna than in the fibula. Further, non-significant comparisons between the three bones occurred in measures of bone mass and diaphyseal shape. Figure 31 provides a visual summary of these relationships in the proximal and distal elements.

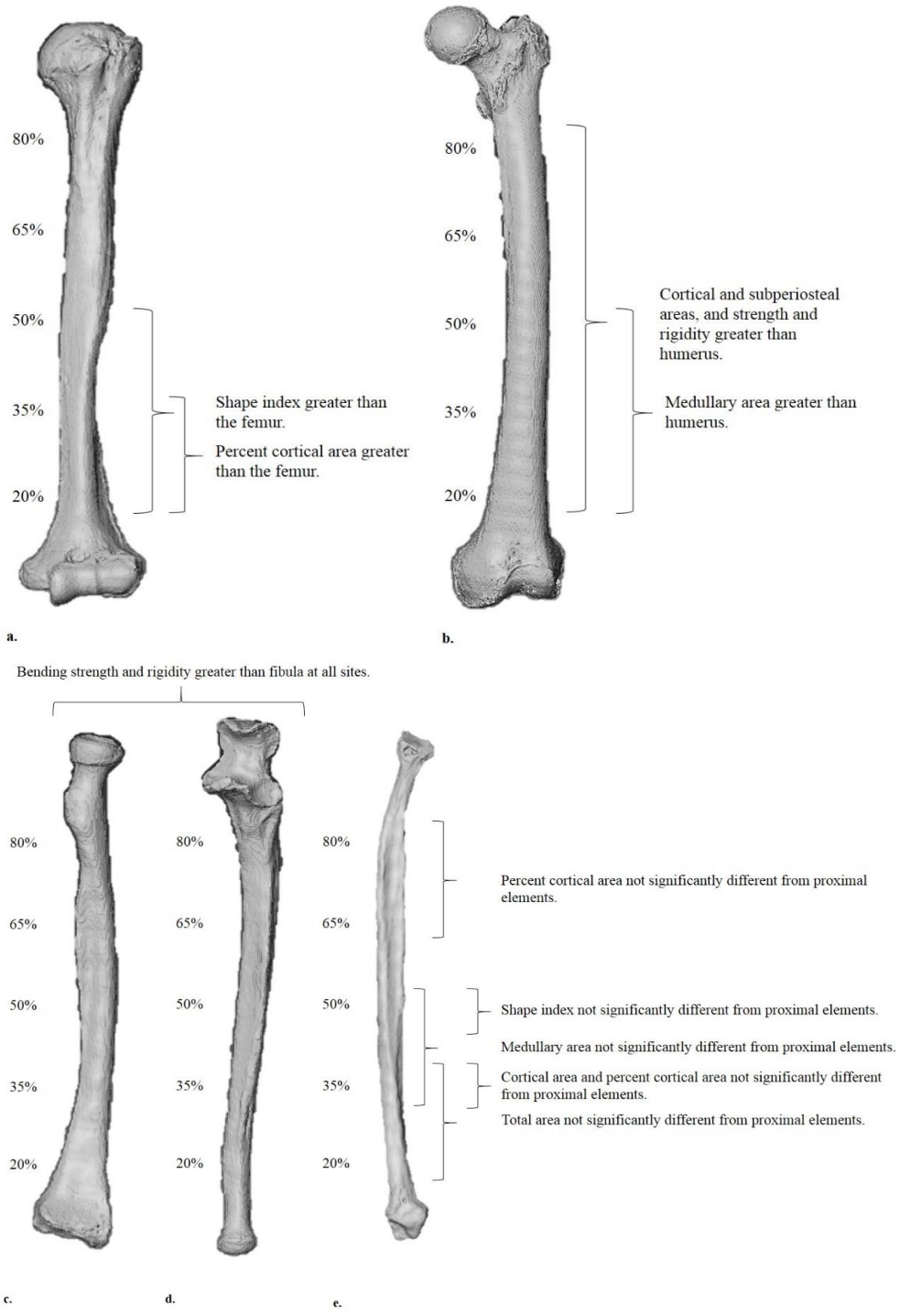

Figure 31. Summary differences in bone mass, shape, strength, and rigidity in proximal and distal elements

Notable results in the proximal elements (a. humerus, b. femur) were differences in measures of shape; in the distal elements (c. radius, d. ulna, e. fibula) were measures that do not differ as expected. Images not to scale.

CHAPTER 7

DISCUSSION AND CONCLUSIONS

This dissertation examines how bone senescence is manifested in cortical bone across all major limb elements. The questions investigated in the prior chapter are predicated on the idea that genetics, environmental factors, biological processes of senescence, and changes in mechanical loading during adulthood affect diaphyseal geometry. As demonstrated in the results of this study, differences exist in cortical bone mass, shape, strength (resistance to failure), and rigidity (resistance to deformation) across the adult appendicular skeleton. Sex, age, environmental factors, diaphyseal location, and skeletal element all served as variables for these differences. Prior to this dissertation, a database comparing adult skeletal morphology across ages and sexes did not exist. While this study does not answer all questions, it provides a solid first step towards quantifying mechanical and biological effects on skeletal senescence. This final chapter synthesizes the results presented in Chapter 6 with the broader concepts concerning bone biology, anatomy, biomechanics, and aging described in Chapters 2-4. It is important to note that causal relationships between bone morphology and variables examined cannot be identified within this study. Discussion of the findings represents only potential explanations for the phenomena observed.

The hypotheses outlined previously in Chapter 1 were developed from what is currently known about cortical bone distribution in the limbs and changes to that distribution as a result of bone functional adaptation (see Chapter 3 for full discussion). Bone mass has been shown to systemically decrease with age (Garn 1970; Nelson and Weiss 1999; Pfeiffer and Lazenby 1994) as a result of normal physiological processes of aging, while other structural changes, such as an

increase in medullary and total subperiosteal areas (Ruff and Hayes 1982; Smith and Walker 1964) also occur as mechanical compensation for the increase in strain from low bone mass.

A consensus about the variation observed in senescence within the skeleton, as reviewed in Chapter 3, tends to reduce its causes to primarily biological, or intrinsic, factors. Bone loss with age continues to be commonly explained by an imbalanced "seesaw" (Parfitt 2003) of osteoclastic activity over osteoblast differentiation and modeling. This representation oversimplifies the complex web of influences on skeletal morphology, whose effects change temporally, but also differ in magnitude across the skeleton (Frost 1993; Pearson and Lieberman 2004; Peck et al. 2007). Even if the timing and location of all bone cell activity was mapped with sex and age, environmental influences (e.g. nutrition and activity) would still remain as major determinants of cortical bone distribution. That is, loss of bone density, decreased strength and rigidity, tissue mineralization, and other patterns associated with skeletal senescence cannot be explained by a simple increase in osteoclastic activity and a corresponding decrease in osteoblastic activity at one point in time. Rather, it is the cumulative effects of a lifetime of factors, both biological and environmental, that result in the amount and distribution of bone at the end of life. As explored in this study, moreover, the effects of aging may not be the same throughout a skeletal element, or between paired elements, let alone across the skeleton. A broader scope of understanding of bone mass and strength in adults is critical to testing hypotheses regarding variation with age. The conclusions provided herein emphasize the complexity of biological and mechanical determinants of adult bone morphology and stress the continued need for "whole bone" and "whole limb" perspectives in future studies.

The following sections discuss the results of this study in light of broader concepts presented in Chapters 2-4. Possible causative factors are suggested and arguments for their

implications are provided throughout. First, within bone variation is reviewed, followed by variation within each limb, and then finally that between limbs.

Synthesis of Within Bone Variation Results

This section discusses the results in light of the first set of hypotheses. These hypotheses anticipated significant associations between sex, age, and environmental factors and measures of cortical bone distribution within each bone.

Sexual Dimorphism in the Limbs

Sexual dimorphism in adult human cortical bone distribution has been established by a number of studies, both clinical (Ahlborg et al. 2003, Meakin et al. 2014) and anthropological (Burr 1997, Peck and Stout 2007, Ruff and Hayes 1982 and 1988), as the result of hormonal changes throughout life. Male skeletal elements tend to be larger than those of females, with more robust sites of muscle attachment. It was hypothesized that in this sample, males would have greater properties of bone mass, shape, strength, and rigidity than females in all elements. Males demonstrated a greater cross-sectional measure of bone mass, cortical area, and all measures of bending strength and rigidity. This was the case across all five sites of the diaphyses of the six skeletal elements studied.

As discussed in Chapters 2 and 4, these results can likely be attributed to hormonal differences between the sexes that begin at puberty and continue through senescence. Traditionally, both clinical and anthropological examinations of bone loss with age operate on an a priori assumption that the female menopause is the primary cause of bone loss and skeletal fragility (Agarwal and Beauchesne 2011). However, this assumption can be too reductionist

because it minimizes the effects of hormonal influences prior to this time, while also excluding the fact that males experience similar changes (e.g. andropause) with age. It is true that estrogens play a vital role in building peak bone mass (PBM), the amount of which is a major factor in retention of mass later in life. The hormone is known to have an "osteoprotective" effect in females (O'Connor et al. 2010; Syed and Khosla 2005), as estrogen is thought to regulate osteoblasts during differentiation. In males, estrogen is believed to increase bone turnover (Sims et al. 2002). Although it is beyond the scope of this dissertation to account for the cumulative effects of a lifetime of sex steroids and other hormones on the skeleton, it is important to recognize the amount of cortical bone at any given age is the result of these processes.

However, biochemical factors cannot explain all of sex-based differences in cortical bone distribution observed in this sample. Total subperiosteal area differed between males and females throughout the limbs. Research has demonstrated that there must be a genetic component contributing to these results. Sexual dimorphism in diaphyseal diameter (highly correlated with total cross-sectional area) is evident by two years of age. Further, the rates of diaphyseal expansion continue to differ between the sexes throughout adolescence and adulthood. Diameter is also the result of direct heredity. In an adult population such as the one used for this study, up to half of the variation in diaphyseal diameter can be attributed to shared genes between siblings (Wallace 2012; Duren et al. 2013). Of particular interest would be an investigation into any hormonal influences on the expression of the genome.

It is clear that factors distinguishing the sexes are active early in ontogeny in shaping both bone length and cortical bone distribution. Moreover, these distinctions are in part explained through direct genetic control, which cannot be known in this sample. Gene by

environment interactions, however, are increasingly responsible for individual variation with age and are discussed next.

Structural Compensation with Age

With sexual differences established in this sample, it was next appropriate to explore whether any relationship existed between age groups within sex in distribution of cortical bone. It was hypothesized that when comparing age groups within each sex, older age groups would demonstrate decreased amounts of cortical bone, but greater measures of medullary (MA) and total area (TA). This increase has been argued by Ruff and Hayes (1982) and others (Biver et al. 2016; Martin and Atkinson 1977; Mays 2001) to serve as a compensation for lower bone mass, and thus, should result in relatively similar measures of bending strength and rigidity throughout the adult years.

It is prudent to question why, outside of a mechanical need, bone must structurally compensate for a loss in density. Our species appears to have reached an evolutionary mismatch, or disequilibrium, in which osteoporosis has become the most common systemic skeletal condition associated with increasing age (Imel et al. 2004; Nelson and Weiss 2003). Two related factors have been attributed to the problem. First, with modern advances in healthcare, humans are expressing trade-offs previously less frequently encountered simply as a result of average increased lifespans. Because significant bone loss with age has been documented in non-human primates (Burr 1980; Summer et al. 1989), it has been suggested (Nelson and Weiss 1999) that bone loss may have affected early humans if they had lived longer lives. However, in early hominin species, including archaic *Homo sapiens*, activity levels were much higher during adolescence and early adulthood than those encountered in post-industrial groups. Theoretically,

this would have established a greater reservoir of bone tissue (i.e. PBM) for later in life (Lieberman 2013). An increasingly sedentary lifestyle only serves to compound the issue of a potential mismatch between skeletal health and longevity. While age-related bone mineral loss is well established in modern populations, it is not known whether there is an age at which bone geometry changes to mechanically adapt to age-related loss. As life spans continue to increase in Western societies, there may be a limit to the amount or degree of compensation possible.

As expected in this sample of modern individuals, female humeral and radial TA is at its greatest by the ninth decade. This result supports the hypothesis that with age, resorption of bone on the endosteal surface is compensated for by periosteal apposition, with a net result of a larger total cross-sectional area. Because this result was not demonstrated in males, it is possible that even though the same process may be happening, slower rates of surface-level apposition and resorption result in non-significant differences. At the cellular level, the decreased efficiency of cell kinetic signaling for turnover could explain these differences. The exact mechanisms of signaling are still unclear, but androgens and other hormones may help maintain turnover in males, while failing to do so in females (Syed and Khosla 2005; Warren 1999). As argued in Chapter 3, a decrease in loading activity will also result in decreased turnover (Frost 2003; Rubin and Lanyon 1984; Ruff et al. 1993), which would exacerbate hormonal effects if older males were more mobile than their female age-matched counterparts.

Both sexes exhibit age-related changes in AP and ML bending rigidity in the upper limb. Rigidity in the humerus and radius is increased in the 70s for both males and females, but in the following decade, drops to the levels present in the 40s. Following the mechanostat model (Frost 1987; Frost 2001; Frost and Jee 1994), higher resistance to deformation from bending and torsional forces in the 70s is necessitated by an increase in total area, but because the decrease in

bone mass outpaces structural compensation, rigidity is decreased starting in the 80s. This corroborates a previous study (Burr and Turner 1999), which suggest that there is not a linear relationship between bone density and strength. That is, slight reductions in density (or mass) result in larger reductions in strength. Clinically, these findings are important for assessing fracture risk in older adults from falls (Riggs et al. 2004). During a fall, the arms are generally placed in front of the body, resulting in high frequencies of distal radial and ulnar fractures. As fracture risk is primarily determined by BMD in the radius and other sites, these results suggest that additional caution should be taken with making a direct link between BMD and strength.

Interestingly, the elements of the lower limb displayed very different trends. The femur did not demonstrate significant age-related changes in cortical bone distribution in either sex. The same is true for male tibiae. Following the compensatory model proposed by Ruff and Hayes (1982), the lack of change in measures of bone mass did not signal a need for any significant change in TA or MA. This theory explains why no change was observed in femoral and tibial strength and rigidity with age in males. While these findings do not directly support those of Ruff and Hayes' examination of the Pecos Pueblos archaeological collection, they cannot refute it. That is, non-significant changes in cortical bone distribution between age groups may suggest that compensatory skeletal adaptation is keeping these bones in a mechanical equilibrium (see Chapter 3 for review). The individuals from Pecos Pueblo displayed the pattern of net bone loss as expected, and an increase in SMAs meant that more bone was located farther from the centroid of the cross-section, increasing its rigidity. An increase in strength and rigidity was not found in males in this sample. This discrepancy may be the result of populational or subsistence (i.e. activity) effects, as well as bias incurred from the age estimation of archaeological skeletal remains.

These findings have implications for archaeological investigations of morphological change with age, as femora especially are more likely to be recovered than many other skeletal elements. In this case, caution should be applied when models of bone senescence based on modern male femora and tibiae are used to interpret skeletal changes with age in archaeological populations. The exception is cortical area, which both this study and those of Ruff and Hayes (1982; 1988) found to remain approximately the same with age in male femora and tibiae.

Female tibiae, however, show a very different pattern than males. By the 80s, CSG measures of bone mass, shape, strength, and rigidity significantly increase. If the logic outlined above is to be followed, the female tibia does not reach a ceiling of mechanical compensation for bone loss with age. This may be the case because of continued need for mitigation of forces associated with body mass and locomotion that are experienced by the lower limb. These age-related patterns help resist bending and torsional loads, which the appendicular skeleton experiences more than other skeletal elements. Similar results may not be seen if other bones of the postcranial skeleton were examined.

These sex-specific findings with age both corroborate and contrast previous studies. Ruff and Hayes (1988) also reported that the diaphyses of female femora and tibiae lose much of their cortical area with age and moments of inertia decrease. They, with others (Burr and Martin 1983; Martin and Atkinson 1977; Bouxsein et al. 1994; Garn et al. 1967; Smith and Walker 1964) posit that although both men and women lose bone mass at an increased rate in older years, females are less likely to make mechanically effective compensatory changes. Female tibiae in this sample defy this pattern, supporting an argument that variation in geometry with age may more likely be the result of many modifiable mechanisms (e.g. diet and activity), than solely sexual differences and normal processes of aging (Bouxsein 1999). In particular, these mechanisms

could explain differential results in modern individuals versus archaeological populations, where females had a vastly different diet and activity repertoire than their modern counterparts.

Although the expected model of compensatory structural changes described by Ruff and Hayes (1982, 1988) was not evident across all skeletal elements in this sample, the findings of this study introduce important questions regarding the complex nature of functional adaption as the body ages. Non-significant changes in cortical bone distribution with age may be evidence for the efficacy of compensatory skeletal adaptation. Results are further complicated by the fact that not all changes in cortical bone with age are actually the result of chronological age. A recent study by Mays (2015) found that approximately sixty percent of bony indicators of age in the adult skeleton are associated with metabolic, dietary, reproductive, and genetic factors. As discussed in Chapter 2, environmental factors related to socioeconomic status (SES) affect bone health (Stinson et al. 2012). Individuals in this sample lived in a region of the United States in which the rates of reported poor health in adults are higher than the national average (see Figure 3, page 37). As such, the cumulative effects of SES over a lifetime may be amplified as age increases, and could have produced some concomitant effects in these individuals.

Bioarchaeological and forensic studies often utilize skeletal samples with chronological ages inferred from bony indicators. In these cases, it is vital to consider confounding factors, such as SES, when drawing conclusions about age-related changes to bone geometry. Regardless of etiology, these findings demonstrate first, that changes to cortical bone distribution are not always linear with age. That is, caution should be applied when associating bone quality, weight, and density with specific age groups. Second, the variation present in a modern sample may not serve as a suitable proxy in all cases for interpretation of bone geometry in the past. Further investigations should examine populational discrepancies in diaphyseal geometry with age. The

use of latent transitional analysis may help identify groups when considering multiple geometric, subsistence, nutritional, and age-related effects.

Mechanical and Physiological Determinants of Bone Geometry

Although many studies of age effects on the adult skeleton examine environmental factors, a vast majority return to the idea that the biological processes of hormone decline and senescence are the principal determinants of changes in cortical bone distribution (Agarwal and Beauchesne 2011). This study went beyond reliance on hormonal effects as a source of changes in the skeleton by examining three common examples of extrinsic factors that affect bone health: body mass, activity, and chronic disease. The results collectively demonstrate that attention must be paid to environmental factors that affect cortical bone loss and gain when examining older adult groups.

As argued previously (see Reeves 2014 and Eleazer 2013; Eleazer and Jankauskas 2016), the effects of body mass on the skeleton are the results of metabolic and endocrine changes, but also a change in the physical load demanded of the skeleton. The discrete effects of these chemical and mechanical influences are not easily identified. However, trends have been observed relating cortical bone distribution to body mass in adults. In the most direct relationship, an individual's mass creates different loading environments in the upper and lower limbs. Because skeletal loading is the result of stress from muscle contraction, it follows that increased forces are required to move those with greater BMI values. Therefore, while cortical area is greater across the limbs in obese individuals versus their non-obese counterparts, the magnitude of this difference is far greater in the lower limbs (Reeves 2014). Further, because the lower limbs are responsible for mobility in humans (with the exception of crawling during

infancy), the bones of the lower limbs also demonstrate greater measures of strength and rigidity with increased BMI.

Adults with higher BMI demonstrate greater BMD than lower BMI categories because of this loading. These effects are amplified by the higher levels of adipokines, cell-signaling proteins secreted by adipose tissue in overweight individuals (Weaver and Gallant 2014). Adipokines, like leptin, stimulate bone formation in cortical bone (Bellido and Gallant 2014). Additionally, serum estrogen levels are forty percent higher in obese women because fat tissue also supplies the body with estrogen (Cauley et al. 1989; Frisch 1990). Based on this knowledge, it was expected that individuals in this study with higher BMIs would demonstrate greater properties of bone mass and bending strength and rigidity.

As hypothesized, BMI groups were significantly associated with measures of bone mass, shape, strength, and rigidity for all six skeletal elements. Findings from this study corroborate previous work, demonstrating that higher BMI groups have greater CSG values than lower BMI groups. The tibia is an exception. Here, overweight and obese individuals did not differ in CSG geometry. As others (Reeves 2014) have suggested, the tibia may have a limit for functional adaptation to body mass. That is, once an individual's BMI reaches the overweight category (25.0- 29.9), maximal tissue efficiency is reached in the tibia. Because fractures to the tibia in obese individuals are not necessarily more common than in those of overweight individuals, it can be argued that the tibia's most efficient geometry for force mitigation and resistance to deformation is effective for a greater range of BMI values than those of other bones.

Activity level, both in studies of past mobility and clinical intervention therapies, is an important mechanical factor to consider with age. Activity frequency, range of motion, stability, and muscle strength all generally decrease in older adults, resulting in changes to the loads

placed on the skeleton. Comparison of activity levels in this sample corroborate expectations that increased loading—whether from body mass or habitual activity—results in increased cross-sectional measures of bone mass, shape, strength, and rigidity. The humerus, radius, femur, and fibula of individuals engaged in heavy-level activity demonstrated significantly greater CSG properties than moderate and light-level activity groups. This finding supports that of Biver et al. (2016) in which individuals engaged in "heavy loading" activity over the age of 45 displayed similar trends. These results indicate that effects of the skeleton as a result of activity are non-linear. Although it is not clear why this may be the case, it should be noted that the relationship between age and diaphyseal geometry was also non-linear in this study (see Tables 8-13 and Appendix F). It is certainly possible that age is affecting the magnitude of how skeletal response to loading.

As with body mass comparisons, the geometry of the tibia proved unique. While heavy and moderate level groups had greater values of all CSG properties than light activity groups, they did not differ from one another in the tibia. This is not entirely surprising, given the results of studies that address both the amount and type of mobility. The cross-sectional geometry of the tibia is known to better correlate with the type of activity (Higgins 2014; Shaw and Stock 2009b; Sparacello et al. 2014), rather than the frequency of activity performed, as does the femur (Holt 2003; Stock 2006). Bending and torsional forces from both moderate body mass and activity levels are clearly enough to illicit a bony response in the tibia that is mechanically adequate to resist deformation and failure, even as forces continue to increase.

A final contributing factor, chronic disease state, was examined with respect to cortical bone distribution. Individuals with causes of death associated with bone loss (labeled "pathological") were compared with individuals whose cause of death is not known to contribute

to changes in bone mass ("healthy"). Because many chronic disease states (e.g. smoking, alcohol abuse, cancer) contribute to lower bone mass (Imel 2014, Stout 1989, Wong et al. 2007), it was expected that mass and all other CSG properties would be reduced in individuals whose cause of death fell into the pathological category. The hypothesis was not confirmed. Pathological individuals had greater values of properties relating to bone mass, strength, and rigidity than the healthy group in the humerus, radius, ulna, femur, and fibula. Once more, results for the tibia appeared to be less sensitive over other elements. Measures of bone mass were significantly higher in pathological group tibiae, but no difference was found in measures of shape, strength, or rigidity between pathological and healthy groups. It would be inappropriate here to suggest a causative factor for these results, as they defy what is currently understood regarding chronic diseases and bone mass.

Undoubtedly, the variation diaphyseal cortical bone distribution in adulthood is the result of a number of cumulative factors, both intrinsic and extrinsic. The results of this study attest to the complicated nature of their interactions and the need for continued study in older human age groups.

Synthesis of Within Limb and Between Limb Variation Results

This section discusses the results of testing the second and third sets of hypotheses. The second set of hypotheses expected a significant association to exist between the pattern of human limb bones and measures of cortical bone distribution within each limb. A significant association between loading environments as a result of bipedal locomotion and measures of cortical bone distribution between the upper and lower limbs was projected by the third set of hypotheses. The previous section examining within bone variation was focused solely on somatic adaptation. Some of the questions posed in this second set of hypotheses address evolutionary trends in our

species in addition to individual variation. The results of within bone variation in this study suggest that the major limb elements follow a more deterministic model (Nowlan and Prendergast 2005) than a purely purposeful pathway of adaptation. The fact that some elements did not follow expected compensatory patterns with age provides evidence for the competing demands of the skeleton from mechanical loads, immune function, and mineral homeostasis (Martin et al. 2015). However, skeletal tissue may approach an "optimal" geometry as it attempts to meet the demands placed on it. The quantification of this approach is synthesized below, first in relation to taper and tissue economy within each limb. Then, the effects differential loading environments between the limbs as the result of bipedal locomotion are discussed.

Tapering in the Human Limb

Limb tapering, or the variation in robusticity of elements within a limb, was expected to have a significant effect on properties of bone mass, shape, strength, and rigidity in this sample. Argued to be a selection for tissue economy (Lieberman and Crompton 1998; Nadell and Shaw 2016; Shaw et al. 2014), proximal limb elements have greater mass, while distal, paired elements are more constrained in terms of weight and size. The reasoning is lighter and more gracile bone are more energetically efficient during movement. Further, because they experience greater loads than proximal elements within the same limb, they have increased rates of bone turnover and less variation. This is a prime example of cost-benefit models (see full discussion in Chapter 3) of skeletal adaptation. A benefit to modeling is an increase in bone strength in the direction of loading. However, the cost of this activity will vary across the skeleton, particularly in locations where increased mass results in an inefficient use of energy during movement or other biological functions. Relevant here is the energetic cost of additional bone mass in the lower limb, and to a

greater degree in the distal portion (Lieberman et al. 2003), which is exponentially higher than in the upper limb.

When comparing measures of cortical bone distribution in the upper limb, the humerus was expected to show greater CSG properties at all diaphyseal locations than the radius and ulna. Precisely because of their shared loading environment, the radius and ulna were not hypothesized to differ significantly in measures of bending strength and rigidity. This pattern was demonstrated in the upper limb elements of this sample. Greater CSG properties at all diaphyseal locations in the humerus reflect selection for greater mass. The radius and ulna showed constraint (i.e. lack of variation) in measures of bone mass. Notably, however, properties relating to strength and rigidity varied in a complementary way between the two bones. Traditionally, kinematic research has presented a single loading pathway for force transmission across the forearm (Marklof et al. 2008). A compressive load to the hand travels primarily through the distal radius, then up through the interosseous membrane, and across the elbow to the upper arm through the ulnotrochlear joint. The core assumption here is that the radius takes the majority of the load, leading many studies to exclude the ulna in analyses. However, load sharing by the ulna has been shown to range from approximately ten to 40 percent (Ekenstam et al. 1984; Halls and Travill 1964; Hotchkiss et al. 1989), depending on the position of the forearm (e.g. in varus alignment).

Greater values of strength in rigidity in the proximal portion of the ulna and distal portion of the radius may suggest that the loading environment in the forearm is shared more equally between the two bones than previously thought. Muscles that serve to extend the forearm (triceps brachii and anconeous) insert on the proximal portion of the ulna, while major flexors (biceps brachii and brachialis) insert on the proximal portion of the radius. The radius is also the

insertion point for a majority of muscles responsible for supination and pronation. The antagonistic nature of these muscle actions in the forearm may also be responsible for the complementary directional strength and rigidity results at midshaft of the ulna (greater AP strength and rigidity) and radius (greater ML strength and rigidity). These results have clinical implications for cases of Colles fracture (fracture of the distal radius, usually as the result of a fall) and Kienbock disease (avascular necrosis of the lunate), both of which are more common in elderly individuals (Markolf et al. 1998). Treatment of these conditions can include excision of the radius or ulna to change the distribution of force born by the wrist or elbow. Further investigation into the kinematics of these paired bones and their role in load bearing in the forearm is critical to advancing orthopedic interventions.

In the lower limb, the femur was expected to show greater CSG properties at all diaphyseal locations than the tibia and fibula. Although the tibia and fibula share a loading environment, the vast difference in muscle action (i.e. force) on the tibia was hypothesized to result in greater values of all CSG properties than in the fibula. The lower limb did not follow the hypothesis regarding selection for tissue economy as clearly as in the upper limb. Measures of bone mass were greater throughout the diaphysis of the femur, which is consistent with the findings of Shaw et al. (2014) in mid- to late-Holocene Native American agriculturists and foragers. The proximal tibia, however, demonstrated greater values of maximum, torsional, and AP strength and rigidity than the femur. This is not entirely unsurprising, as the largest group of muscles (quadriceps femoris) in the lower limb, which extend the knee, insert on the anteroproximal portion of the tibia. Greater torsional strength and rigidity at this location can be explained as the tibia is also the insertion site for lateral rotators of the hip, stabilizers and medial rotators of the hip, and lateral and medial rotators of the knee. In a geographically diverse group

of hunter-gathers, Stock (2006) showed that the tibia is more responsive to different loading patterns, or types of mobility, than the other lower limb elements. Even with decreased mobility in older age, these muscles are still activated during isometric stabilization of the body with use of supportive equipment, such as canes and walkers. The fibula demonstrated lower values of all CSG properties at all sites along the diaphysis. The potential implications of fibular results are discussed below in comparison to the distal elements of the upper limb.

Limb Functionality in Bipeds

Comparison of cortical bone distribution between limbs is less common in habitual bipeds because of obvious differences in limb functionality with locomotion. However, until very recently in human evolutionary history, the fore- and hind limbs shared the burden of transporting the body across the landscape. Tapering of bone size and mass in the limbs, as discussed above, would have increased efficiency. It is still unclear, though, what amount of arboreal versus terrestrial locomotion was utilized by early hominin species (Marchi 2015; Stern 2000; Ward 2013). Although serving different functions now, it was worthwhile to test whether meaning relationships in bone geometry exist between analogous limb elements.

The bones of the proximal limb segments—the humerus and femur—were expected to differ significantly in all CSG properties. While they share a similar position in their respective limbs, the femur is responsible for mitigating forces associated with both body mass and locomotion. As such, the femur should demonstrate greater properties of bone mass, shape, strength, and rigidity than the humerus. True to form, the femur demonstrated greater cortical area, total area, and all measure of strength and rigidity than the humerus. These results are consistent with the shortening of and decrease in robusticity of the upper limb and extension and increase of robusticity of the lower limb as our species transitioned to habitual bipedalism

(Larsen 2016). These results are further supported by the earlier argument that although both limbs carry increased loads with increased body mass, the magnitude of difference is far greater in the lower limb (Lieberman et al. 2003; Moore 2008; Reeves 2014). Yet, no difference existed in medullary area between the proximal portions of each of the two bones. It would be unprecedented and mechanically unsubstantiated to suggest that the effects of body mass and locomotion on the femur only affect medullary cavity area in the distal portion, but this idea could be explored further in a later study.

The distal limb elements were expected to differ greatly between limbs. When comparing the bones of the distal limb segments—the radius, ulna, tibia, and fibula—the tibia was hypothesized to exhibit greater values of CSG properties than the other three bones at all diaphyseal locations. Because the radius and ulna share more of the load across the lower arm, they are expected to have greater bone mass, strength, and rigidity properties than the fibula, which takes on a much smaller proportion of loads in the leg with its paired bone, the tibia. During quadrupedal locomotion, all distal elements have closer contact with the substrate, and thus receive greater ground reaction forces. In humans, the radius and ulna no longer contribute to transport, but cause of the slower pace of evolutionary adaptation (versus that of somatic), hypothetically, they could still share evidence of use in locomotion with the distal lower limb elements. It is not known whether CSG properties are in part driven by covariances among analogous limb segments.

As the largest bone, it was unsurprising that the tibia demonstrated greater values of all CSG properties at all diaphyseal locations than the radius, ulna, and fibula. As discussed at various points in this chapter, the distal portion of the lower limb is more mechanically sensitive because of its proximity to the ground. The tibia then, experiences a much greater amount of

ground reaction force at heel strike, which travels upward through the tibiotarsal joint complex (Hennig et al. 1993; Shelburne et al. 2006; Vogel 2013). Also unsurprisingly, the radius and ulna had greater values of strength and rigidity than the fibula. As argued above, this is likely the result of the number of muscle attachments (and thus, increased force) across the two bones. The fibula, on the other hand shares approximately ten percent of the load across the shank (Auerbach et al. 2017; Goh et al. 1992; Takebe et al. 1984), which is less than forces shared by the forearm elements (see discussion above).

What is notable among these findings however, is that the distal portions of the radius, ulna, and fibula did not differ significantly in measures of bone mass or shape. This has direct clinical significance for older adults. Assessment of bone density in a clinical setting is often achieved by collecting data from the lower arm and wrist (Mayo Clinic 2016). These findings suggest that levels of bone mass could also be assessed in the distal fibula in the case that the arm is obstructed. Fibular resection for reconstruction of the radius or ulna after trauma is also common (Innocenti et al. 2005; Jupiter et al. 1997; Pho 1981). The efficacy of these operations corroborates the similarities found here in the morphology of the three bones. The direct causative factor(s) behind this apparent similarity between the two limbs, with very different loading environments, is unclear. However, continued investigation of these bones in conjunction with one another may lead to a more complete picture of locomotion in early hominins (Marchi 2015) and advancement in clinical applications.

Future Directions and Conclusions

This study found that distribution in diaphyseal cortical bone varies with sex, age, environmental factors, location, and bone within the human limbs. It accomplishes an initial step

in documenting the full range of skeletal variation as humans age. Specifically, it was able to establish significant associations between variable groups and measures of cortical bone distribution in the diaphysis. These groups represent broad physiological and mechanical factors that influence the adaptation of bone to an efficient geometry for individual loading environments. This research also examines these geometric measures along the entire diaphysis of six skeletal elements, which provides a much more complete picture of diaphyseal morphology that what was previously known.

Although a great number of comparisons were made, the notable patterns discovered actually lead to more questions rather than concretely answering the central questions of this dissertation. An experimental or longitudinal sample would be ideal for further investigation of the variables used to assess changes in diaphyseal geometry. Principally, it is recommended that future studies gather greater detail of demographic parameters and health histories. This would allow researchers to tease out some of the concomitant effects of the many complex biological and environmental factors that cumulatively impact bone geometry later in life. It was noted in Chapters 4 and 5, that ancestral differences in bone mass are well documented. It would then be prudent to assess a more diverse ample to see if patterns identified here hold true in non-White individuals. Finally, because of some levels of CSG properties appear to increase at the end life to levels seen in the 40s, a secondary study should include individuals in the 30s. A broadening of what this study classifies as the "later" adult years would also potentially capture peak bone mass levels, a known determinant of later bone density.

When the entire study is examined, it is clear that biological processes of aging and mechanical loading have a complex relationship with bone maintenance and loss. As suggested

earlier, causes of the significant results cannot be gleaned from this work, but useful conclusions can be drawn:

1. Mechanical loading environments and processes of senescence are sexually dimorphic in the human limbs and do vary with age. The bones of the upper limb demonstrate a compensatory structural change, likely as a general result of bone mass with age. Cortical bone distribution in the femur is almost entirely unaffected by age.

2. The tibia, over the other five elements, has a unique association with sex, age, BMI, activity level, and chronic disease state. Results suggest that it may reach an optimal geometry for differential loading at a lower threshold than other bones.

3. Although the midshaft is regarded as the most mechanically sensitive diaphyseal site in each long bone, this research suggests that reliance on the midshaft does not provide a complete picture of bone mass, strength, or rigidity and should not be used as a proxy for the structural functionality of the entire bone. Rather, examination of at least one site above and below the midshaft may illuminate complimentary or antagonistic relationships between bones within and between limbs.

As modern humans, particularly in Western nations, continue to live longer, it is critical to continue the investigation of skeletal senescence. This study and other future examinations have a direct benefit to clinicians in the assessment of bone density in living patients and biomedical researchers in the testing of therapies to modify rates and locations of bone

maintenance and loss. In the process of developing advanced joint replacement options, biomedical engineers also require a full understanding of skeletal aging, as US and European adults are most likely to receive knee and hip replacements during ages 50-80 (Krucik 2015) and 60-80 years of age (Crawford and Murray 1997), respectively.

This study also has a significant impact in the fields of anthropology, evolutionary biology and medicine, and functional anatomy. Bioarchaeological investigations of bone loss in past societies are common, but still lack modern models for known demographic and environmental variables. These, along with all biological anthropological studies of skeletal morphology must avoid the tendency to reduce the causes of variation to primarily biological, or intrinsic, factors. A broader scope of understanding of bone mass and strength in adults is also critical to testing hypotheses regarding the evolutionary transition to a fully erect bipedal locomotor pattern. The conclusions provided here emphasize the complexity of mechanical and biological determinants of adult bone morphology and emphasize the continued need for "whole bone" and "whole limb" perspectives in future studies.

LIST OF REFERENCES

Abelow B, Holford T, and Insogna K. 1992. Cross-cultural association between dietary animal protein and hip fracture: A hypothesis Calcified Tissue International(150):14-19.
Agarwal SC. 2007. Light and Broken Bones: Examining and Interpreting Bone Loss and Osteoporosis in Past Populations. Biological Anthropology of the Human Skeleton: John Wiley & Sons, Inc. p 387-410.
Agarwal SC. 2016. Bone morphologies and histories: Life course approaches in bioarchaeology. Yearbook of Physical Anthopology 159:S130-S149.
Agarwal SC, and Grynpas MD. 1996. Bone quantity and quality in past populations. The Anatomical Record 246(4):423-432.
Allen M, and Krohn K. 2014. Skeletal imaging. In: Burr D, and Allen M, editors. Basic and Applied Bone Biology. New York: Elsevier. p 93-114.
Allen MR, and Burr DB. 2014. Bone modeling and remodeling. In: Burr DB, and Allen MR, editors. Basic and Applied Bone Biology. London: Elsevier. p 75-92.
Anderson J. 1999. Nutritional mechanisms of age-related bone loss. In: Rosen C, Glowacki J, and Bilezikian J, editors. The Aging Skeleton. San Diego: Academic Press. p 229-236.
Anderson M, Green W, and Messner M. 1963. Growth and pedictions of growth in the lower extremeties. Journal of Bone & Joint Surgery 45A:1-14.
Armstrong PF. 1988. Cell Kinetics and Control of Physeal Growth. In: Uhtoff HK, and Wiley JJ, editors. Behavior of the Growth Plate. New York: Raven Press. p 233-236.
Aspden RM. 2008. Osteoarthritis: A problem of growth not decay? Rheumatology 47:1452-1460.
Atkinson PJ. 1969. Structural Aspects of Ageing Bone. Gerontology 15(2-3):171-173.
Auerbach BM, Gooding AF, Shaw CN, and Sylvester AD. 2017. The relative position of the human fibula to the tibia influences cross-sectional properties of the tibia. American Journal of Physical Anthropology.
Auerbach BM, and Ruff CB. 2004. Human body mass estimation: a comparison of "morphometric" and "mechanical" methods. American Journal of Physical Anthropology 125:331-342.
Auerbach BM, and Ruff CB. 2006. Limb bone bilateral asymmetry: Variability and commonality among modern humans. Journal of Human Evolution 50(203-218).
Bailey DA, McKay HA, Mirwald RL, Crocker PRE, and Faulkner RA. 1999. A six-year longitudinal study of the relationship of physical activity to bone mineral accrual in growing children: The University of Saskatchewan bone mineral accrual study. Journal of Bone and Mineral Research 14(10):16-72-1679.
Baxter-Jones A, Faulkner RA, Forwood MR, Mirwald RL, and Bailey DA. 2011. Bone mineral accrual from 8 to 30 years of age: An estimation of peak bone mass. Journal of Bone and Mineral Research 26(8):1729-1739.
Beaupre G, Orr T, and Carter D. 1990. Approach for time-dependent bone modeling and remodeling- theoretical development. Journal of Orthopedic Research 8(5):651-661.
Beck R, Andriacchi T, Kuo K, Fermier R, and Galante J. 1981. Changes in the gait patterns of growing children. The Journal of Bone and Joint Surgery American volume 63(9):1452-1457.
Beck T, Ruff C, and Bissessur K. 1993. Age-related changes in female femoral neck geometry: Implications for bone strength. Calcified Tissue International(53(Suppl. 1)):S41-S46.
Bellido T, and Gallant K. 2014. Hormonal Effects on Bone Cells. In: Burr D, and Allen M, editors. Basic and Applied Bone Biology. Amsterdam: Academic Press. p 299-313.

Bergmann P, Body J, Boonen S, Boutsen Y, Devogelaer J, Goemaere S, Kaufman J, Reginster J, and Rozenberg S. 2011. Loading and Skeletal Development and Maintenance. Journal of Osteoporosis 2011.

Bergwitz C, and Juppner H. 2010. Regulation of phosphate homeostasis by PTH, vitamin D, and FGF23. Annual Review of Medicine(61):91-104.

Biewener AA, S.M. S, and J.E.A. B. 1986. Bone modeling during growth: dynamic strain equilibrium in the chick tibiotarsus. Calcified Tissue International 39:390-395.

Biver E, Perreard Lopreno G, Hars M, van Rietbergen B, Vallee JP, Ferrari S, Besse M, and Rizzoli R. 2016. Occupation-dependent loading increases bone strength in men. Osteoporosis International 27:1169-1179.

Bogin B. 1999. Environmental factors influencing growth. Patterns of Human Growth. 2nd ed. Cambridge: Cambridge University Press. p 268-328.

Boldsen JL, Milner GR, Konigsberg LW, and Wood JW. 2002. Transition analyes: A new method for estimating age from skeletons. In: Hoppa RD, and Vaupel JW, editors. Paleodemography: Age Distributions from Skeletal Samples. Cambridge, NY: Cambridge University Press. p 73-106.

Bonjour J, and Chevalley T. 2007. Pubertal timing, peak bone mass and fragility fracture risk. BoneKey-Osteovision 4:30-48.

Bonjour J, Chevalley T, Ferrari S, and Rizzoli R. 2009. The importance of peak bone mass in the prevalence of osteoporosis. Salud Publica de Mexico 51(Supplement 1):S5-17.

Boonen S, Vanderschueren D, Cheng X, Verbeke G, Dequeker J, Geusens P, Broos P, and Bouillon R. 1997. Agerelated (Type II) femoral neck osteoporosis in men: biochemical evidence for both hypovitaminosis D and androgen deficiency induced bone resorption. Journal of Bone Mineral Research(12):2119-2126.

Bouxsein M, Myburgh K, Meulen Mvd, Lindenberger E, and Marcus R. 1994. Age-related differences in cross-sectional geometry of the forearm bones in healthy women. Calcified Tissue International(54):113-118.

Bouxsein ML. 1999. Application of biomechanics to the aging human skeleton. In: Rosen CJ, Glowacki J, and Bilezikian JP, editors. The Aging Skeleton. San Diego: Academic Press. p 315-332.

Braun JT, Hines JL, Akyuz E, Vallera C, and Ogilvie JW. 2006. Relative versus absolute modulation of growth in the fusionless treatment of experimental scoliosis. Spine 31(16):1776-1782.

Bridges P, Blitz J, and Solano M. 2000. Changes in long bone diaphyseal strength with horticultural intesification in west-central Illinois. American Journal of Physical Anthropology 112:217-238.

Brookes M. 1963. Cortical vascularisation and growth in foetal tubular bones. Journal of Anatomy 97:597-609.

Bross I. 1971. Critical Levels, Statistical Language and Scientific Inference. In: Godambe V, and Sprott, editors. Foundations of Statistical Inference. Toronto: Holt, Rinehart & Winston of Canada, Ltd.

Bruder SP, and Caplan AI. 1989. Cellular and molecular events during embryonic bone development Connective Tissue Research 20:65-71.

Burr D. 1980. The relationships among physical, geometrical and mechanical properties of bone, with a note on the properties of nonhuman primate bone. Yearbook of Physical Anthopology 1980(23):109.

Burr D, Forwood M, Fyhrie D, Martin R, Schaffler M, and Turner C. 1997. Bone microdamage and skeletal fragility in osteoporotic and stress fractures. Journal of Bone Mineral Research(12):6-15.
Burr D, and Martin R. 1983. The effects of composition, structure adnn age on the torsional properties of the human radius. Journal of biomechanics(16):603-608.
Burr DB, and Akkus O. 2013. Bone morphology and organization. In: Burr DB, and Allen MR, editors. Basic and Applied Bone Biology. London: Elsevier. p 3-26.
Burr DB, and Turner CH. 1999. Biomechanical measurements in age-related bone loss. In: Rosen CJ, Glowacki J, and Bilezikian JP, editors. The Aging Skeleton. San Diego: Academic Press. p 301-314.
Burr DB, Turner CH, Naick P, Forwood MR, Ambrosius W, Sayeed HM, and Pidaparti R. 1998. Does microdamage accumulation affect the mechanical properties of bone? Journal of biomechanics 31(4):337-345.
Burstein A, Reilly D, and Martens M. 1976. Aging of bone tissue: Mechanical properties. Journal of Bone & Joint Surgery(58A):82-86.
Carlson K, and Marchi D. 2014. Introduction: Towards refining the concept of mobility. In: Carlson K, and Marchi D, editors. Reconstructing mobility: Environemental, behavioral, and morphological determinants. New York: Springer. p 1-12.
Carter D. 1984. Mechanical loading histories and cortical bone remodeling. Calcified Tissue International 36:19-24.
Carter D, and Hayes W. 1977. The compressive behavior of bone as a two phase porous structure. Journal of Bone & Joint Surgery(59A):954-962.
Carter D, and Orr T. 1992. Skeletal development and bone fuctional adaptation. Journal of Bone and Mineral Research 7(Supplement 2):S389-S395.
Carter DR, and Beaupre GS. 2001. Skeletal function and form: mechanobiology of skeletal development, aging, and regineration. New York: Cambridge University Press.
Cauley J, Gutai J, Kuller L, LeDonne D, and Powell J. 1989. The epidemiology of serum sex hormones in post-menopausal women. American Journal of Epidemiol(129):1120-1131.
Chen G, Schuetz M, and Pearcy M. 2010. Mechanobiology of bone development and computational simulations. In: Bronner F, Farach-Carson MC, and Roach HI, editors. Bone and development: Topics in bone biology. London: Springer-Verlag. p 279-295.
Clinic M. 2016. Test and procedures: Bone density test.
Colaianni G, Tamma R, Benedetto AD, Yuen T, Sun L, Zaidi M, and Zallone A. 2014. The oxytocin-bone axis. Journal of Neuroendocrinology 26(2):53-57.
Cooper C, Javaid M, Taylor P, Walker-Bone K, Dennison E, and Arden N. 2002. The fetal origins of osteoporotic fracture. Calcif Tissue International 70(5):391-394.
Cooper G, and Sandler D. 1998. Age at natural menopause and mortality. Ann Epidemiol(8):229-235.
Courtney A, Hayes W, and Gibson L. 1996. Age-related differences in post-yield damage in human cortical bone. Experiment and model. Journal of biomechanics(29):1463-1471.
Cowgill LW. 2010. The ontogeny of Holocene and Late Pleistocene human postcranial strength. American Journal of Physical Anthropology 141:16-37.
Cowgill LW, Warrener A, Pontzer H, and Ocobock C. 2010. Waddling and toddling: The biomechanical effects of an immature gait. American Journal of Physical Anthropology 143:52-61.

Cowin S, Moss-Salentijn L, and Moss M. 1991. Candidates for the mechanosensory system in bone. Journal of biomechanical engineering 113(2):191-197.
Cowin SC. 2001. The False Premise in Wolff's Law. In: Cowin SC, editor. Bone Mechanics Handbook. 2nd ed. New York: CRC Press LLC. p 30-31- 30-15.
Cox L, Rietbergen Bv, Donkelaar Cv, and Ito K. 2011. The turnover of mineralized growth plate cartilage into bone may be regulated by osteocytes. Journal of biomechanics 44(9):1765-1770.
Cristofolini L, Conti G, Juszczyk V, Cremonini S, Van Sint Jan S, and Viceconti M. 2010. Structural behaviour and strain distribution of the long bones of the human lower limbs. Journal of biomechanics 43(5):826-835.
Currey J. 1979. Changes in impact energy absorption of bone with age. Journal of biomechanics(12):459-469.
Currey J. 1990. Physical characteristics affecting the tensile failure properties of compact bone. Journal of biomechanics(23):837-844.
Currey J, Brear K, and Zioupos P. 1996. The effects of ageing and changes in mineral content in degrading the toughness of human femora. Journal of biomechanics(29):257-260.
Currey J, and Butler G. 1975. The mechanical properties of bone tissue in children. Journal of Bone & Joint Surgery 57-A:810-814.
Currey JD. 2006. Bones: Structure and Mechanics. Princeton, NJ: Princeton University Press.
Currey JD, Landete-Castillejos T, Estevez JA, Oligiun A, Garcia AJ, and Gallega L. 2009. The young's modulus and impact energy absorption of wet and dry deer cortical bone The Open Bone Journal 1:38-45.
Daly RM, Saxon L, Turner CH, Robling AG, and Bass SL. 2004. The relationship between muscle size and bone geometry during growth and in response to exercise. Bone 34(2):281-287.
Davies T, and Stock J. 2014. Human variation in the periosteal geometry of the lower limb: Signatures of behaviour among human Holocene populations. In: Carlson K, and Marchi D, editors. Reconstructing Mobility: Environmental , Behavioral, and Morphological Determinants. New York: Springer. p 67-90.
Dickenson R, Hutton W, and Stott J. 1981. The mechanical properties of bone in osteoporosis. Journal of Bone & Joint Surgery(63B):233-238.
Dimeglio L, and Imel E. 2014. Calcium and Phosphate: Hormonal Regulation and Metabolism. In: Burr D, and Allen M, editors. Basic and Applied Bone Biology. Amsterdam: Academic Press. p 261-282.
Donahue T, Haut T, Yellowley C, Donahue H, and Jacobs C. 2003. Mechanosensitivity of bone cells to oscillating fluid flow induced shear stress may be modulated by chemotransport. Journal of biomechanics 36(9):1363-1371.
Dornemann T, McMurray R, Renner J, and Anderson J. 1997. Effects of high intensity resistence exercise on bone mineral density and muscle strength of 40-50 year old women. Journal of Sports Medicine and Physical Fitness(37):246-251.
Drapeau MSM, and Streeter MA. 2006. Modeling and remodeling responses to normal loading in the human lower limb. American Journal of Physical Anthropology 129(3):403-409.
Ducher G, Bass SL, Saxon L, and Daly RM. 2011. Effects of repetitive loading on the growth-induced changes in bone mass and cortical bone geometry: A 12-month study in pre/peri- and postmenarcheal tennis players. Journal of Bone and Mineral Research 26(6):1321-1329.

Duren DL, Blangero J, Sherwood RJ, Seselj M, Dyer T, Cole SA, Lee M, Choh AC, Chumlea WC, Siervogel RM et al. . 2011. Cortical bone health shows significant linkage to chromosomes 2p, 3p, and 17q in 10-year-old children. Bone 49(6):1213-1218.

Duren DL, Seselj M, Froehle AW, Nahhas RW, and Sherwood RJ. 2013. Skeletal growth and the changing genetic landscape during childhood and adulthood. American Journal of Physical Anthropology 150(1):48-57.

Ekenstam Fa, Palmer A, and Glisson R. 1984. The load on the radius and ulna in different positions of the wrist and forearm: A cadver study. Acta orthopaedica Scandinavica 55:363-365.

Eleazer CD, and Jankauskas R. 2016. Mechanical and metabolic interactions in cortical bone development. American Journal of Physical Anthropology 160:317-333.

Ensrud K, Palermo L, Black D, Cauley J, Jergas M, Orwoll E, Nevitt M, and Fox K. 1995. Hip and calcaneal bone loss increase with advancing age: Longitudinal results from the study of osteoporotic fractures. Journal of Bone and Mineral Research(10):1778-1787.

Erlebacher A, Filvaroff E, Gitelman S, and Derynck R. 1995. Toward a molecular understanding of skeletal development. Cell 80:371-378.

Felber K, Croucher P, and Roehl HH. 2011. Hedgehog signalling is required for perichondral osteoblast differentiation in zebrafish. Mechanisms of development 128(1-2):141-152.

Fisher R. 1956. Statistical Methods and Scientific Inference. New York: Hafner.

Fredriks A, Buuren Sv, Burgmeijer R, Meulmeester J, Beuker R, Brugman E, Roede M, Verloove-Vanhorick S, and Wit J-M. 2000a. Continuing positive secular growth changes in the Netherlands 1955-1997. Pediatric research 47:316-323.

Frisancho AR, Garn SM, and Ascoli W. 1970. Subperiosteal and endosteal bone apposition during adolescence. Human biology 42(4):639-664.

Frisancho AR, Guire K, Babler W, Borkan G, and Way A. 1980. Nutritional influence on childhood development and genetic control of adolescent growth of Quechuas and Mestizos from the Peruvian lowlands. American Journal of Physical Anthropology 52(3):367-375.

Frisch R. 1990. Body fat, menarche fitness and fertility Proggressive Reproductive Biological Medicine(14):1-26.

Frost H. 1983. Determinant of bone architecture: the minimum effective strain. Clinical Orthopaedic and Related Research (175):286-292.

Frost H. 1985. The new bone: some anthropological potentials. Yearbook of Physical Anthopology(28):211-226.

Frost H. 1996. Perspectives: A proposed general model of the "mechanostat.". Anatomical Record (244):139-147.

Frost H. 1997. On our age-related bone loss: Insights from a new paradigm. Journal of Bone Mineral Research(12):1539-1546.

Frost HM. 1987. Bone "Mass" and the "Mechanostat": A Proposal. The Anatomical Record 219:1-9.

Frost HM. 2001. From Wolff's law to the Utah paradigm: insights about bone physiology and its clinical applications. The Anatomical Record 262(4):398-419.

Frost HM. 2003. Bone's mechanostat: a 2003 update. Anatomical Record Part A Discoveries in Molecular Cellular and Evolutionary Biology 275(2):1081-1101.

Frost HM, and Jee WS. 1994. Perspectives: a vital biomechanical model of the endochondral ossification mechanism. The Anatomical Record 240(4):435-446.

Garn S. 1972. The earlier gain and later loss of cortical bone. Springfield, IL: Charles C. Thomas.
Garn S, Rohmann C, Wagner B, and Ascoli W. 1967. Continuing bone growth throughout life: a general phenomenon. American Journal of Physical Anthropology(26):313-318.
Garn S, Sullivan T, Decker S, Larkin F, and Hawthorne V. 1992. Continuing bone expansion and increasing bone loss over a two-decade period in men and women from a total community sample. American Journal of Human Biology 4:57-67.
Garn SM. 1971. The earlier gain and the later loss of cortical bone in nutritional perspective. Springfield: Charles C. Thomas.
Godfrey L, Sutherland M, Paine R, Williams F, Boy D, and Vuillaume-Randriamanantena M. 1995. Limb joint surface areas and their ratios in Malagasy lemurs and other mammals. American Journal of Physical Anthropology
97:11-36.
Goh JC, Mech AM, Lee EH, Ang EJ, Bayon P, and Pho RW. 1992. Biomechanical study on the load-bearing characteristics of the fibula and the effects of fibular resection. Clin Orthop Relat Res(279):223-228.
Gold E. 2011. The timing of the age at which natural menopause occurs. Obstet Gynecol Clin North Am 38(3):425-440.
Gooding CA, and Neuhauser EB. 1965. Growth and development of the vertebral body in the presence and absence of normal stress. American Journal Roentgenol Radium Ther Nucl Med 93:388-394.
Gosman JH, Hubbell ZR, Shaw CN, and Ryan TM. 2013. Development of cortical bone geometry in the human femoral and tibia diaphysis. The Anatomical Record 296:774-787.
Gosman JH, and Ketcham R. 2009. Patterns in ontogeny of human trabecular bone from SunWatch village in the prehistoric Ohio Valley: general features of microarchitectural change American Journal of Physical Anthropology 138:318-332.
Gosman JH, Stout SD, and Larsen CS. 2011. Skeletal biology over the life span: A view from the surfaces. American Journal of Physical Anthropology 146(S53):86-98.
Gray A, Feldman H, McKinlay J, and Longcope C. 1991. Age, disease, and changing sex hormone levels in middle-aged men: results of the Massachusetts Aging Study. Journal of Clinical Enducrinol Metabolism(73):1016-1025.
Greendale G, Edelstein S, and Barrett-Connor E. 1997. Endogenous sex steroids and bone mineral density in older women and men: The Rancho Bernardo Study. Journal of Bone and MIneral Research(12):1833-1843.
Greenspan S, Maitland L, Myers E, Krasnow M, and Kido T. 1994. Femoral bone loss progresses with age: A longitudinal study in women over age 65. Journal of Bone and Mineral Research(9):1959-1965.
Grynpas M. 2003. The role of bone quality on bone loss and fragility. In: Agarwal S, and Stout S, editors. Bone Loss and Osteoporosis: An Anthropological Perspective. New York: Kluwer Academic/Plenum Publishers. p 33-46.
Hall BK, and Herring SW. 1990. Paralysis and growth of the musculoskeletal system in the embryonic chick. journal of Morphology 206(1):45-56.
Halls A, and Travill A. 1964. Transmission of pressures across the elbow joint. Anat Rec 150:243-247.

Heinonen A, Oja P, Sievanen H, Pasanen M, and Vuori I. 1998. Effect of two training regimens on bone mineral density in healthy perimenopausal women: A randomized controlled trial. Journal of Bone Mineral Research(13):483-490.
Hennig EM, Milani TL, and Lafortune MA. 1993. Use of Ground Reaction Force Parameters in Predicting Peak Tibial Accelerations in Running. Journal of Applied Biomechanics 9(4):306-314.
Hernandez C, and Meulen Mvd. 2017. Understanding bone strength is not enough. Journal of Bone and Mineral Research:1-6.
Higgins RW. 2014. The Effects of Terrain on Long Bone Robusticity and Cross-Sectional Shape in Lower Limb Bones of Bovids, Neandertals, and Upper Paleolithic Modern Humans. In: Carlson KJ, and Marchi D, editors. Reconstructing Mobility: Environmental, Behaviorla, and Morphological Determinants. New York: Springer. p 227-252.
Holt BM. 2003. Mobility in Upper Paleolithic and Mesolithic Europe: Evidence From the Lower Limb. American Journal of Physical Anthropology 122:200-215.
Hotchkiss R, An K, Sowa D, Basta S, and Weiland A. 1989. An anatomic and mechanical study of the interosseous membrane of the forarm: Pathomechanics of proximal migration of the radius. Journal of Hand Surgery 14A(256-261).
Hubbell Z, Gosmas J, Shaw C, and Ryan T. 2011. Age-related changes in cortical bone geometry in the human tibial diaphysis: a whole-bone perspective. Journal of Bone Mineral Research 26:S389.
Hueter C. 1862. Anatomische studien an den extremitatengeleken neugeborener unde erwachsener (Anatomic studies on the joints of the extremities in newbords and adults. Virchow Arch 26:484-519.
Hughes JM, Charkoudian N, Barnes JN, and Morgan BJ. 2016. Revisiting the Debate: Does Exercise Build Strong Bones in the Mature and Senescent Skeleton? Frontiers in Physiology 7.
Hui S, Slemenda C, and Johnston C. 1988. Age and bone mass as predictors of fracture in a prospective study. Journal of Clinical Investigation(81):1804-1809.
Imel E, Dimeglio L, and Burr D. 2014. Skeletal Disease and Treatment. In: Burr D, and Allen M, editors. Basic and Applied Bone Biology. Amsertdam: Academic Press. p 317-344.
Inc. SI. 2017. SAS. 9.4 ed. Cary, NC, USA.
Innocenti M, Delcroix L, Manfrini M, Ceruso M, and Capanna R. 2005. Vascularized proximal fibular epiphyseal transfer for distal radial reconstruction. The Journal of bone and joint surgery American volume 87 Suppl 1(Pt 2):237-246.
Jacobs C, Yellowley C, Davis B, Zhou Z, Cimbala J, and Donahue H. 1998. Differential effect of steady versus oscillating flow on bone cells. Journal of biomechanics 31(11):969-976.
Johnston C, and Slemenda C. 1994. Peak bone mass, bone loss and risk of fracture. Osteoporosis international : a journal established as result of cooperation between the European Foundation for Osteoporosis and the National Osteoporosis Foundation of the USA 4(Supplement 1):43-45.
Jones G, and Scott F. 1999. A cross-sectional study of smoking and bone mineral density in premenopausal parous women: effect of body mass index, breastfeeding, and sports participation. Journal of Bone Mineral Research(14):1628-1633.
Jupiter JB, Gerhard HJ, Guerrero J, Nunley JA, and Levin LS. 1997. Treatment of segmental defects of the radius with use of the vascularized osteoseptocutaneous fibular autogenous graft. The Journal of bone and joint surgery American volume 79(4):542-550.

Kanis J, Johnell O, and Oden A. 2005. Smoking and fracture risk: a meta-analysis. Osteoporosis international : a journal established as result of cooperation between the European Foundation for Osteoporosis and the National Osteoporosis Foundation of the USA(16):155-162.

Kanis J, Johnell O, Oden A, Jonsson B, Laet CD, and Dawson A. 2000. Risk of hip fracture according to World Health Organization criteria for osteoporosis and osteopenia. Bone(27):585-590.

Kanis J, McCloskey E, Johansson H, Oden A, and Strom O. 2010. Development and use of FRAX in osteoporosis Ostoeporosis International(21 Suppl 2):S407-413.

Karasik D, Demissie S, Cupples LA, and Kiel DP. 2005. Disentangling the Genetic Determinants of Human Aging: Biological Age as an Alternative to the Use of Survival Measures. The journals of gerontology Series A, Biological sciences and medical sciences 60(5):574-587.

Karlsson M, Linden C, Karlsson C, Johnell O, Obrant K, and Seeman E. 2000. Exercise during rowth and bone mineral density and fractures in old age. Lancet 355:469-470.

Kerr D, Morton A, Dick I, and Prince R. 1996a. Exercise effects on bone mass in postmenopausal women are site-specific and load-dependent. Journal of Bone and Mineral Research 11(2):218-225.

Kerr D, Morton D, Dick I, and Prince R. 1996b. Exercise effects on bone mass in postmenoausal women are site-specific and load-dependent. Journal of Bone Mineral Research(11):218-225.

Key LL, and Norman HB. 1999. Racial Determinants of Peak Bone Mass. In: Rosen CJ, Glowacki J, and Bilezikian JP, editors. The Aging Skeleton. San Diego: Academic Press. p 127-136.

Kiel D, Zhang Y, Hannan M, Anderson J, Baron J, and Felson D. 1996. The effect of smoking at different life stages on bone mineral density in elderly men and women. Ostoeporosis International(6):240-248.

Krolner B, Toft B, Nielsen S, and Tondevold E. 1983. Physical exercise as prophylaxis against involutional vertebral bone loss: a controlled trial. Clinical Science(1983):544-546.

Lanyon LE. 1984. Static versus dynamic loads as an influence on bone remodeling. Journal of biomechanics 17:897-905.

Larrea C, and Kawachi K. 2005. Does economic inequality affect child malnutrition? The case of Ecuador. Social Science & Medicine 60:165-178.

LeBoff MS, and Glowacki J. 1999. Sex steroids, bone, and aging. In: Rosen CJ, Glowacki J, and Bilezikian JP, editors. The Aging Skeleton. San Diego: Academic Press. p 159-174.

Leichter I, Simkin A, and Margulies J. 1989. Gain in mass density of bone following strenuous physical activity. Journal of Orthopedic Research(7):86-90.

Lemann JJ, Pleuss J, and Gray R. 1993. Potassium causes calcium retention in healthy adults. Journal of Nutrition(123):1623-1626.

Lieberman D. 2013. The Story of the Human Body: Evolution, Health, and Disease. New York: Patheon Books.

Lieberman D, and Crompton A. 1998. Response to stress: Constrainst on symmorphosis. In: Weibel E, Taylor C, and Bolis L, editors. Principles of Animal Design: The Optimization and Symmorphosis Debate. Cambridge: University of Cambridge. p 78-86.

Lieberman DE, Devlin MJ, and Pearson OM. 2001. Articular area responses to mechanical loading: effects of exercise, age, and skeletal location. American Journal of Physical Anthropology 116(4):266-277.
Lieberman DE, and Pearson OM. 2001. Trade-off between modeling and remodeling responses to loading in the mammilian limb. Bulletin of the Museum of Comparative Zoology 156:269-282.
Lieberman DE, Pearson OM, Polk JD, Demes B, and Crompton AW. 2003. Optimization of bone-growth and remodeling in response to loading in tapered mammalian limbs. Journal of Experimental Biology 206:3125-3138.
Lieberman DE, Polk J, and Demes B. 2004. Predicting long bone loading from cross-sectional geometry American Journal of Physical Anthropology 123:156-171.
Liefde Id, Klift Mvd, Laet Cd, Daele Pv, Hofman A, and Pols H. 2005. Bone mineral density and fracture risk in type-2 diabetes mellitus: the Rotterdam Study. Osteoporos International 16(12):1713-1720.
Lloyd T, and Cusatis DC. 1999. Nutritional determinants of peak bone mass. The Aging Skeleton. San Diego: Academic Press. p 95-104.
Lloyd T, Rollings N, Andon M, Demers L, Egglie D, Keiselhorst K, Kulin H, Landis J, Martel J, and Orr G. 1992. Determinants of bone density in young women. I. Relationships among pubertal development, total body bone mass, and total body bone density in premenarchal females. Journal of Clinical Endocrinology and Metabolism 75:383-387.
Lutz J. 1984. Calcium balance and acid-based status of women as affected by increased protein intake and by sodium bicarbonate ingestion. Journal of Nutrition(39):281-288.
Maggiano IS, Schultz M, Kierdorf H, Sosa TS, Maggiano CM, and Blos VT. 2008. Cross-sectional analysis of long bones, occupational activities and long-distance trade of the classic maya from Xcambo - Archaeological and osteological evidence. American Journal of Physical Anthropology 136:470-477.
Mak IL, DeGuire JR, Lavery P, Agellon S, and Weiler HA. 2016. Dual-energy x-ray absorptiometry, peripheral quanititative computed tomography, and micro-computed tomography techniques are discordant for bone density and geometry measurements in the guinea pig. Journal of Bone and Mineral Metabolism 34:266-276.
Manolagas SC. 2000. Birth and death of bone cells: basic regulatory mechanisms and implications for the pathogenesis and treatment of osteoporosis. Endocrine reviews 21:115-137.
Marchi D. 2007. Relative strength of the tibia and fibula and locomotor behavior in hominoids. J Hum Evol 53(6):647-655.
Marchi D. 2015. Using the morphology of the hominoid distal fibula to interpret arboreality in Australopithecus afarensis. J Hum Evol 85:136-148.
Marchi D, and Shaw CN. 2011. Variation in fibular robusticity reflects variation in mobility patterns. J Hum Evol 61(5):609-616.
Markolf K, Lamey D, Yang S, Meals R, and Hotchkiss R. 1998. Radioulnar load-sharing in the forearm: A study in cadavera. Journal of Bone & Joint Surgery 80(6):879-888.
Marsh RL, Ellerby DJ, Carr JA, Henry HT, and Buchanan CI. 2004. Partitioning the energetics of walking and running; swinging the limbs is expensive. Science 303:80-83.
Martin R. 1993. Aging and strength of bone as a structural material. Calcified Tissue International(53 (Suppl. 1)):S34-S40.

Martin R. 2003. Functional adaptation and fragility of the skeleton. In: Agarwal S, and Stout S, editors. Bone Loss and Osteoporosis: An Anthropological Perspective. New York: Kluwer Academic/Plenum Publishers. p 121-138.
Martin R, Burr D, Sharkey N, and Fyhrie D. 2015. Skeleta tissue mechanics. New York: Springer.
Martin RB, and Atkinson PJ. 1977. Age and sex-related changes in the structure and strength of the human femoral shaft Journal of biomechanics 10:223-231.
Martin RB, Burr DB, and Sharkey NA. 1998. Skeletal Tissue Mechanics. New York, NY: Springer.
Massey L, and Whiting S. 1996. Dietary salt, urinary calcium, and bone loss. Journal of Bone Mineral Research(11):731-736.
Mays S. 2001. Effects of age and occupation on cortical bone in a group of 18th-19th century British men. American Journal of Physical Anthropology 116:34-44.
Mazess R. 1982. On aging bone loss. Clinical Orthopaedic and Related Research(165):239-252.
Mazess R, Barden H, Ettinger M, Johnston C, Dawson-Hughes B, Baran D, Powell M, and Notelovitz M. 1987. Spine and femur density using dual-photon absorptiometry in U.S. white women. Journal of Bone Mineral Research(2):211-219.
McCalden R, McGeough J, Barker M, and Court-Brown C. 1993. Age-related changes in the tensile properties of cortical bone. Journal of Bone & Joint Surgery(75A):1193-1205.
McCall IW, Galvin E, O'Brien JP, and Park WM. 1981. Alterations in vertebral growth following prolonged plaster immobilisation Acta Orthopaedica 52(3):327-330.
Mente PL, Aronsson DD, Stokes IAF, and Iatridis JC. 1999. Mechanical modulation of growth for the correction of vertebral wedge deformities. Journal of Orthopedic Research 17(4):518-524.
Michael A, and Bengtson J. 2016. Cronic alcoholism and bone remodeling processes: Caveats and considerations for the forensic anthropologist. Journal of Forensic and Legal Medicine(38):87-92.
Mitchell H, Hamilton T, Steggerda F, and Bean H. 1945. The chemical composition of the adult human body and its bearing on the biochemistry of growth. Journal of Biological Chemistry(158):625-637.
Monteiro CA, Moura EC, Conde WL, and Popkin BM. 2004. Socioeconomic status and obesity in adult populations of developing countries: a review. The Bulletin of the World Health Organization 82:940-946.
Moore MK. 2008. Body mass estimation from the human skeleton University of Tennessee.
Moore MK. 2013. Functional morphology and medical imaging. Reserch Methods in Human Skeletal Biology: Academic Press. p 397-424.
Nadell JA, and Shaw CN. 2016. Phenotypic plasticity and constraint along the upper and lower limb diaphyses of *Homo sapiens*. American Journal of Physical Anthropology 159:410-422.
Nagata J, Golden N, Leonard M, Copelovitch L, and Denburg M. 2017. Assessment of sex differences in fracture risk among patients with anorexia nervosa: A population-based cohort study using the health improvement network. Journal of Bone and Mineral Research 32(5):1082-1089.
Nelson D, and Villa M. 2003. Ethnic differences in bone mass and architechture. In: Agarwal S, and Stout S, editors. Bone Loss and Osteoporosis: An Anthropological Perspective. New York: Kluwer Academic/Plenum Publishers. p 47-62.

Nelson DA, and Weiss ML. 1999. Aging through the ages. In: Rosen CJ, Glowacki J, and Bilezikian JP, editors. The Aging Skeleton. San Diego: Academic Press. p 3-8.
Nguyen TV, Maynard LM, Towne B, Roche AF, Wisemandle W, Li J, Guo SS, Chumlea WC, and Siervogel RM. 2001. Sex differences in bone mass acquisition during growth: the Fels Longitudinal Study. Journal of Clinical Densitometry 4(2):147-157.
Nilsson M, Sundh D, Mellstrom D, and Lorentzon M. 2017. Current physical activity is independently associated with cortical bone size and bone strength in elderly swedish women. Journal of Bone and Mineral Research 32(3):473-485.
Nowlan NC, and Prendergast PJ. 2005. Evolution of mechanoregulation of bone growth will lead to non-optimal bone phenotypes. Journal of theoretical biology 235(3):408-418.
Nyquist F, Gardsell P, Sernbo I, Jeppson J, and Johnell O. 1998. Assessment of sex hormones and bone mineral density in relation to occurrence of fracture in men: A propective population-based study. Bone(22):147-151.
O'Connor RD, Farach-Carson MC, and Schanen NC. 2010. Genetic and Epigenetic Aspects of Bone Development. In: Bronner F, Farach-Carson MC, and Roach HL, editors. Bone and Development, Topics in Bone Biology: Springer-Verlag London Limited.
O'neill MC, and Ruff CB. 2004. Estimating human long bone cross-sectional geometric properties: a comparison of noninvasive methods. Journal of Human Evolution 47:221-235.
Ogden JA. 1979. The development and growth of the musculo-skeletal system. In: Albright JA, and Brands R, editors. Scientific Basis of Orthopaedics. New York: Appleton-Century-Crofts. p 41-103.
Olsen BR, Reginato AM, and Wang W. 2000. Bone development. Annual Review of Cell Developmental Biology 16:191-220.
Orentreich N, Brind J, Rizer R, and Vogelman J. 1984. Age changes and sex differences in serum dehydroepiandrosterone sulfate concentrations throughout adulthood. Journal of Clinical Endocrinol Metabolism(59):551-555.
Organization WH. 2003. Prevention and management of osteoporosis. Geneva.
Orwoll ES. 2003. Men, bone and estrogen: unresolved issues. Osteoporosis international : a journal established as result of cooperation between the European Foundation for Osteoporosis and the National Osteoporosis Foundation of the USA 14:93-98.
Ossewaarde M, Bots M, and Verbeek A. 2005. Age at menopause, cause-specific mortality and total life expectancy. Epidemiology(16):556-562.
Padez C, Varela-Silva M, and Bogin B. 2009. Height and relative leg length as indicators of quality of the environment among Mozambican juveniles and adolescents. American Journal of Human Biology 21:200-209.
Paquette MR, Klipple G, and Zhang S. 2015. Greater Step Widths Reduce Internal Knee Abduction Moments in Medial Compartment Knee Osteoarthritis Patients During Stair Ascent. Journal of Applied Biomechanics 31(4):229-236.
Parfitt A. 1996. Skeletal heterogeneity and the purposes of bone remodeling: Implications for the understanding of osteoporosis. San Diego: Academic Press.
Parfitt A. 2002a. Misconceptions (1): Epiphyseal fusion causes cessation of growth. Bone 30(2):337-339.
Parfitt A. 2002b. Targeted and non-targeted bone remodeling: Relationship to BMU origination and progression. Bone(30):1, 5-7.

Parfitt A. 2003. New concepts of bone remodeling: A unified spatial and temporal model with physiologic and pathophysiologic implications. In: Agarwal S, and Stout S, editors. Bone Loss and Osteoporosis: An Anthropological Perspective. New York: Kluwer Academic/Plenum Publishers. p 3-17.

Pearson OM, and Lieberman DE. 2004. The aging of Wolff's “law”: Ontogeny and responses to mechanical loading in cortical bone. American Journal of Physical Anthropology 125(S39):63-99.

Pearson OM, Petersen TR, Sparacello VS, Daneshvari SR, and Grine FE. 2014. Activity, "body shape,' and cross-sectional geometry of the femur and tibia. In: Carlson KJ, and Marchi D, editors. Reconstructing mobility: Environmental, beahvioral, and morphological determinants. New York: Springer.

Peck JJ, and Stout SD. 2007. Intraskeletal variability in bone mass. American Journal of Physical Anthropology 132(1):89-97.

Pfeiffer SK, and Lazenby RA. 1994. Low bone mass in past and present aboriginal populations. In: Draper HH, editor. Advances in Nutritional Research. New York: Plenum Press. p 35-51.

Pho RW. 1981. Malignant giant-cell tumor of the distal end of the radius treated by a free vascularized fibular transplant. JBJS 63(6):877-884.

Pivonka P, Zimak J, Smith DW, Gardiner BS, Dunstan CR, Sims NA, Martin TJ, and Mundy GR. 2008. Model structure and control of bone remodeling: a theoretical study. Bone 43(2):249-263.

Polk J, Demes B, Jungers W, Biknevicius A, Heinrich R, and Runestad J. 2000. A comparison of primate, carnivoran and rodent limb bone cross-sectional properties: Are primates really unique? Journal of Human Evolution 39:297-325.

Prevention CfDCa. 2015. Diabetes Report Card 2014. Atlanta Georgia: Centers for Disease Control and Prevention, US Dept of Health and Human Services.

Pruitt L, Jackson R, Bartells R, and Lehnhard H. 1992. Weight-training effects on bone mineral density in early postmenopausal women. Journal of Bone Mineral Research(7):179-185.

Purves WK, Sadava D, Orians GH, and Heller HC. 2004. Life: the science of biology,. Sunderland: Sinauer Associates.

Qian J-G, Li Z, Zhang H, Bian R, and Zhang S. 2014. Effectiveness of selected fitness exercises on stress of femoral neck using musculoskeletal dynamics simulations and finite element model. Journal of human kinetics 41:59-70.

Quarles L. 2008. Endocrine functions of bone in mineral metabolism regulation. Journal of Clinical Investigation(118):3820-3828.

Raisz L, Wita B, Artis A, Bowen A, Schwartz S, Trahiotis M, Shoukri K, and Smith J. 1996. Comparison of the effects of estrogen alone and estrogen plus androgen on biochemical markers of bone formation and resporption in postmenopausal women. Journal of Clinical Endocrinol Metabolism(81):37-43.

Rang M. 1969. The Growth Plate and its Disorders. Edinburgh: Churchill Livingstone.

Rantalainen T, Nikander R, Heinonen A, Suominen H, and Sievanen H. 2010. Direction-Specific Diaphyseal Geometry and Mineral Mass Distribution of Tibia and Fibula: A pQCT Study of Female Athletes Representing Different Exercise Loading Types. Calified Tissue International 86:447-454.

Rasmussen D. 1998. Effects of chronic nicotine treatment and withdrawal on hypothalamic proopiomelanocortin gene expression and neuroendocrine regulation. Psychoneuroendocrinology(23):245-259.
Rasnick R, Standifird T, Reinbolt JA, Cates HE, and Zhang S. 2016. Knee Joint Loads and Surrounding Muscle Forces during Stair Ascent in Patients with Total Knee Replacement. PLOS ONE 11(6):e0156282.
Rauch F, and Schoenau E. 2001. The developing bone: slave or master of its cells and molecules? Pediatric research 50(3):309-314.
Reeves NM. 2014. Augmenting functional adaptation: Does obesity have a systemic effect on bone strength properties in humans?: University of Tennessee - Knoxville.
Reeves NM, Auerbach BM, and Sylvester AD. 2016. Fluctuating and directional asymmetry in the long bones of captive cotton-top tamarins (Saguinus oedipus). American Journal of Physical Anthropology 160(1):41-51.
Riggs B, Wahner H, Dunn W, Mazess R, Offord K, and III LM. 1981. Differential changes in bone mineral density of the appendicular and axial skeleton with aging. Journal of Clinical Investigation(67):328-335.
Riggs B, Wahner W, Seeman E, Offord K, Dunn W, Mazezz R, Johnson K, and III LM. 1982. Changes in bone mineral density of the proximal femur and spine with aging: differences between the postmenopausal and senile osteoporosis syndromes. Journal of Clinical Investigation(70):716-723.
Riggs BL, Khosla S, and Melton LJI. 2002. Sex steroids and the construction and conservation of the adult skeleton. Endocrine reviews 23(3):279-302.
Riggs BL, Melton LJ, Robb RA, Camp JJ, Atkinson EJ, Peterson JM, Rouleau PA, McCollough CH, Bouxsein ML, and Khosla S. 2004. Population-based study of age and sex differences in bone volumetric density, size, geometry, and structure at different skeletal sites. Journal of Bone and Mineral Research 19(12):1945-1954.
Robling A, Fuchs R, and Burr D. 2014. Mechanical adaptation. In: Burr D, and Allen M, editors. Basic and Applied Bone Biology. New York: Elsevier. p 175-204.
Robling A, Hinant F, Burr D, and Turner CH. 2002. Improved bone structure and strength after long-term mechanical loading is greatest if loading is seperated into short bouts. Journal of Bone and Mineral Research 17:1545-1554.
Robling AG, and Turner CH. 2009. Mechanical signaling for bone modeling and remodeling. Critical Reviews in Eukaryot Gene Expression 19(4):319-338.
Rowe JW, and Kahn RL. 1987. Human aging: usual and successful. Science 237:143-149.
Rubin CT, and Lanyon LE. 1984. Regulation of bone formation by applied dynamic loads. Journal of Bone & Joint Surgery 66:397-402.
Ruff C, and Larsen C. 2014. Long bone structural analyses and the reconstruction of past mobility: A historical review. In: Carlson K, and Marchi D, editors. Reconstructing Mobility. New York: Springer. p 13-30.
Ruff CB. 1987. Structural allometry of the femur and tibia in Hominoidea and Macaca. Folia Primatol 48:9-49.
Ruff CB. 2000a. Body mass prediction from skeletal frame size in elite athletes. American Journal of Physical Anthropology 113(4):507-517.
Ruff CB. 2000b. Body size, body shape, and long bone strength in modern humans. Journal of Human Evolution 38:269-290.

Ruff CB. 2002. Long bone articular and diaphyseal structure in old world monkeys and apes. I: Locomotor effects. American Journal of Physical Anthropology 119:305-342.
Ruff CB. 2003a. Growth in bone strength, body size, and muscle size in a juvenile longitudinal sample. Bone 33(3):317-329.
Ruff CB. 2003b. Long bone articular and diaphyseal structure in Old World monkeys and apes. II: Estimation of body mass. Am J Phys Anthropol 120(1):16-37.
Ruff CB. 2003c. Ontogenetic adaptation to bipedalism: age changes in femoral to humeral length and strength proportions in humans, with a comparison to baboons. J Hum Evol 45(4):317-349.
Ruff CB. 2007. Body size prediction from juvenile skeletal remains. American Journal of Physical Anthropology 133:698-716.
Ruff CB. 2008. Biomechanical Analyses of Archaeological Human Skeletons. Biological Anthropology of the Human Skeleton: John Wiley & Sons, Inc. p 183-206.
Ruff CB, and Hayes WB. 1982. Subperiosteal expansion and cortical remodeling of the human femur and tibia with aging. Science 217(4563):945-948.
Ruff CB, and Hayes WB. 1983a. Cross-sectional geometry of Pecos Pueblo femora and tibiae—A biomechanical investigation: I. Method and general patterns of variation. American Journal of Physical Anthropology 60(3):359-381.
Ruff CB, and Hayes WB. 1983b. Cross-sectional geometry of Pecos Pueblo femora and tibiae: a biomechanical investigation: II. Sex, age, side differences. American Journal of Physical Anthropology 60:383-400.
Ruff CB, Holt B, Niskanen M, Sladek V, Berner M, Garofalo E, Garvin HM, Hora M, Junno J-A, Schuplerova E et al. . 2015. Gradual decline in mobility with the adoption of food production in Europe. Proceedings of the National Academy of Sciences 112(23):7147-7152.
Ruff CB, Holt B, and Trinkaus E. 2006. Who's afraid of the big bad Wolff?: "Wolff's Law" and bone function adaptation. American Journal of Physical Anthropology 129:484-498.
Ruff CB, and Larsen CS. 1990. Postcranial biomechanical adaptations to subsistence strategy changes on the Georgia Coast. In: Larsen CS, editor. The archaeology of Mission Santa Catalina de Guale: 2: biocultural interpretations of a population in transition: Anthropological Papers of the American Museum of Natural History p94-120.
Ruff CB, and Runestad JA. 1992. Primate limb bone structural adaptations. Annual Review of Anthropology 21:407-433.
Ruff CB, Trinkaus E, Walker A, and Larsen CS. 1993. Postcranial robusticity in *Homo.* I: Temporal trends and mechanical interpretation. American Journal of Physical Anthropology 91:21-53.
Ruff CB, Walker A, and Trinkaus E. 1994. Postcranial robusticity in *Homo*. III: ontongeny. American Journal of Physical Anthropology 93:35-54.
Ruff D, and Hayes W. 1988. Sex differences in age-related remodeling of the femur and tibia. Journal of Orthopedic Research(6):886-896.
Salle BL, Rauch F, Travers R, Bouvier R, and Glorieux FH. 2002. Human fetal bone development: histomorphometric evaluation of the proximal femoral metaphysis. Bone 30(6):823-828.
Sarringhaus LA, MacLatchy LM, and Mitani JC. 2016. Long bone cross-sectional properties reflect changes in locomotor behavior in developing. American Journal of Physical Anthropology 160:16-29.

Schaffler M, and Burr D. 1988. Stiffness of compact bone: Effects of porosity and density. Journal of biomechanics(21):13-16.
Schaffler M, Burr D, Jungers W, and Ruff C. 1985. Structural and mechanical indicators of limb specialization in primates. Folia Primatol 45:61-67.
Scheff H, Sprague M, and McGreevy-Nichols S. 2014. Body mechanics: Matching movement to muscles and bones. Experiencing Dance. 2nd ed. Champaign, IL: Human Kinetics. p 9-12.
Scheuer L, and Black S. 2000. Developmental Juvenile Osteology. London: Academic Press.
Schoenau E, and Frost HM. 2002. The "Muscle-Bone Unit" in Children and Adolescents. Calcified Tissue International 70(5):405-407.
Schoenau E, Neu CM, Mokov E, Wassmer G, and Manz F. 2000. Influence of puberty on muscle area and cortical bone area of the forearm in boys and girls. The Journal of clinical endocrinology and metabolism 85(3):1095-1098.
Schuette S, and Linkswiler H. 1982. Effect of CA and P metabolism in humans by adding meat, meat plus milk, or purified proteins plus Ca and P to a low protein diet. Journal of Nutrition (112):338-349.
Sehl ME, and Yates FE. 2001. Kinetics of Human AgingI. Rates of Senescence Between Ages 30 and 70 Years in Healthy People. The Journals of Gerontology: Series A 56(5):B198-B208.
Sellmeyer DE, Stone KL, Sebastian A, Cummings SR, and Group ftSoOFR. 2001. A high ratio of dietary animal to vegetable protein increases the rate of bone loss and the risk of fracture in postmenopausal women. The American journal of clinical nutrition 73(1):118-122.
Shackelford L. 2014. Variation in mobility and anatomical responses in the late Pleistocene. In: Carlson K, and Marchi D, editors. Reconstructing Mobility: Environmental, Behavioral, and Morphological Determinants. New York: Springer. p 153-172.
Shaw C. 2010. 'Putting flesh back onto the bones?' Can we predit soft tissue properties from skeletal and fossil remains? Journal of Human Evolution 59:484-492.
Shaw CN, and Stock JT. 2009a. Habitual throwing and swimming correspond with upper limb diaphyseal strength and shape in modern human athletes. American Journal of Physical Anthropology 140(1):160-172.
Shaw CN, and Stock JT. 2009b. Intensity, repetitiveness, and directionality of habitual adolescent mobility patterns influence the tibial diaphysis morphology of athletes. American Journal of Physical Anthropology 140(1):149-159.
Shaw CN, and Stock JT. 2013. Extreme mobility in the Late Pleistocene? Comparing limb biomechanics among fossil *Homo*, varsity athletes and Holocene foragers. Journal of Human Evolution 64(4):242-249.
Shaw CN, Stock JT, Davies TG, and Ryan TM. 2014. Does the distribution and variation in cortical bone along lower limb diaphyses reflect selection for locomotor economy? In: Carlson KJ, and Damiano M, editors. Reconstructing mobility. New York: Springer. p 49-66.
Shelburne KB, Torry MR, and Pandy MG. 2006. Contributions of muscles, ligaments, and the ground-reaction force to tibiofemoral joint loading during normal gait. Journal of orthopaedic research : official publication of the Orthopaedic Research Society 24(10):1983-1990.

Shepard M, Markolf K, and Dunbar A. 2001. The effects of partial and total interosseous membrane transection on load sharing in the cadver forearm. Journal of Orthopedic Research 19(4):587-592.
Sherman S. 1999. Human aging at the millennium. In: Rosen CJ, Glowacki J, and Bilezikian JP, editors. The Aging Skeleton. San Diego: Academic Press. p 11-18.
Sims N, Dupont S, Krust A, Clement-Lacroix P, Minet D, Resche-Rigon M, Gaillard-Kelly M, and Baron R. 2002. Deletion of estrogen receptors reveals a regulatory role for estrogen receptors-beta in bone remodeling in females but not in males. Bone 30:18-25.
Sissons H. 1955. Experimental study of the effect of radiation on bone growth. In: Mitchell J, Holmes B, and Smith C, editors. Progress in Radiobiology. Edinburgh: Oliver and Boyd. p 436-452.
Sladek V, Berner M, Galeta P, Friedl L, and Kudrnov A. 2010. The effect of midshaft location on the error ranges of femoral and tibial cross-sectional parameters. American Journal of Physical Anthropology 141:325-332.
Slemenda C, Longcope C, Zhou L, Hui S, Peacock M, and Johnston C. 1997. Sex steroids and bone mass in older men. Positive associations with serum estrogens and negative associations with androgens. Journal of Clinical Investigation(100):1755-1759.
Smith EP, Specker B, and Korach KS. 2010. Recent experimental and clinical findings in the skeleton associated with loss of estrogen hormone or estrogen receptor activity. Journal of Steroid Biochemistry and Molecular Biology 118:264-272.
Smith RW, and Walker RR. 1964. Femoral expansion in aging women: Implications for osteoporosis and fractures. Science 145(3628):156-157.
Snowdon D, Kane R, and Beeson W. 1989. Is early natural menopause a biological marker of health and aging? American Journal of Public Health(79):709-714.
Sparacello VS, Marchi D, and Shaw CN. 2014. The Importance of Considering Fibular Robusticity When Inferring the Mobility Patterns of Past Populations. In: Carlson KJ, and Marchi D, editors. Reconstructing Mobility: Environmental, Behavioral, and Morphological Determinants. New Yrok: Springer. p 91-110.
Stern JT. 2000. Climbing to the top: A personal memoir of Australopithecus afarensis. Evolutionary Anthropology: Issues, News, and Reviews 9(3):113-133.
Stinson S, Bogin B, and O'Rourke D. 2012. Growth Variation: Biological and Cultural Factors. In: Sara Stinson BB, Dennis O'Rourke, editor. Human Biology: An Evolutionary and Biocultural Perspective. Second ed: John Wiley & Sons, Inc. p 587-635.
Stock J. 2006. Hunter-gather postcranial robusticity relative to patterns of mobility, climatic adaption, and selectoin for tissue economy. American Journal of Physical Anthropology 91(1):194-204.
Stock JT, and Shaw CN. 2007. Which measures of diaphyseal robusticity are robust? A comparison of external methods of quantifying the strength of long bone diaphyses to cross-sectional geometric properties. Am J Phys Anthropol 134(3):412-423.
Stokes I. 2002. Mechanical effects of skeletal growth. Journal of Musculoskeletal and Neuronal Interactions 2(3):277-280.
Stokes IAF, Spence H, Aronsson DD, and Kilmer N. 1996. Mechanical modulation of vertebral body growth: implications for scoliosis progression. Spine 21(10):1162-1167.
Stout S. 1989. Age markers in the human skeleton. In: MY, editor. Iscan: Springfield: Charles C Thomas. p 195-207.

Summer D, Morbeck M, and Lobick J. 1989. Apparent agerelated bone loss among adult female Gombe chimpanzees. American Journal of Physical Anthropology(79):25-234.
Syed F, and Khosla S. 2005. Mechanisms of sex steroid effects on bone. Biochemical Biophysical Research Communications 328:688-696.
Syed F, and Ng A. 2010. The pathophysiology of the aging skeleton. Current Osteoporos Rep(8):235-240.
Tadic T, Dodig M, Erceg I, Marijanovic I, Mina M, Kalajzic Z, Velonis D, Kronenberg M, Kosher R, Ferrari D et al. . 2002. Overexpression of Dlx5 in chicken calvarial cells accelerates osteoblastic differentiation. Journal of Bone Mineral Research 17:1008-1014.
Takebe K, Nakagawa A, Minami H, Kanazawa H, and Hirohata K. 1984. Role of the fibula in weight-bearing. Clin Orthop Relat Res(184):289-292.
Tanck E, Hannink G, Ruimerman R, Buma P, Burger EH, and Huiskes R. 2006. Cortical bone development under the growth plate is regulated by mechanical load transfer. J Anat 208(1):73-79.
Tardieu C, Glard Y, Garron E, Boulay C, Jouve JL, Dutour O, Boetsch G, and Bollini G. 2006. Relationship between formation of the femoral bicondylar angle and trochlear shape: independence of diaphyseal and epiphyseal growth. Am J Phys Anthropol 130(4):491-500.
Trinkaus E. 1976. The evolution of the hominid femoral diaphysis during the Upper Pleistocene in Europe and the Near East. Z Morphologie und Anthropologie 67:291-319.
Trinkaus E, and Ruff C. 1989. Diaphyseal cross-sectional morphology and biomechanics of the Fond-de-Foret 1 and the Spy 2 femur and tibia. Anthropol Prehist 100:33-42.
Trotter M, and Hixon B. 1974. Sequential changes in weight, density, and precentage ash weight of human skeletons from an early fetal period through old age. Anat Rec 179(1):1-18.
Turner C. 2002. Biomechanics of bone: Determinants of skeletal frailty and bone quality. Osteoporosis International 13:97-104.
Turner C, and Robling A. 2003. Designing exercise regimens to increase bone strength. Exercise Sport Science Review 31(1):45-50.
Turner CH, Robling AG, Duncan CS, and Burr D. 2002. Do bone cells behave like a neuronal network? Calcified Tissue International 70:435-442.
Turner R, Hannon K, Demers L, Buchanan J, and Bell N. 1989. Differential effects of gonadal function on bone histomophometry in male and female rats. Journal of Bone and Mineral Research(4):557-563.
Turner R, Wakley G, and Hannon K. 1990. Differential effects of androgens on cortical bone histomorphometry in gonadectomized male and female rats. Journal of Orthopedic Research(8):612-617.
Ulijaszek SJ, and Lofink H. 2006. Obesity in biocultural perspective. Annual Review of Anthropology 35:337-360.
van der Meulen MCH, and Carter DR. 1999. Mechanical determinants of peak bone mass In: Rosen CJ, Glowacki J, and Bilezikian JP, editors. The Aging Skeleton. San Diego: Academic Press. p 105-114.
Vanderschueren D, Vandenput L, Boonen S, Lindberg MK, Bouillon R, and Ohlsson C. 2004. Androgens and bone. Endocrine reviews 25:389-425.
Venken K, Callewaert F, Boonen S, and Vanderschueren D. 2008. Sex hormones, their receptors and bone health. Osteoporosis international : a journal established as result of cooperation

between the European Foundation for Osteoporosis and the National Osteoporosis Foundation of the USA 19(11):1517-1525.
Vermeulen A, Deslypere J, and Demierleir K. 1989. A new look to the andropause: altered function of he gonadotrophs. Journal of Steriod Biochemistry(32):163-165.
Vestergaard P. 2007. Discrepancies in bone mineral density and fracture risk in patients with type 1 and type 2 diabetes - a meta-analysis. Ostoeporosis International 18(4):427-444.
Villemure I, and Stokes IA. 2009. Growth plate mechanics and mechanobiology. A survey of present understanding. Journal of biomechanics 42(12):1793-1803.
Vincent HK, Raiser SN, and Vincent KR. 2012. The agining muscloskeletal system and obesity-related considerations with exercise. Ageing Research Reviews 11:361-373.
Vogel S. 2013. Comparative Biomechanics: Life's Physical World Princeton, NJ: Princeton University Press.
Wallace BA, and Cumming RG. 2000. Systematic review of randomized trials of the effect of exercise on bone mass in pre- and postmenopausal women. Calcified Tissue International 67:10-18.
Wallace IJ, Tommasini SM, Judex S, Garland T, Jr., and Demes B. 2012. Genetic variations and physical activity as determinants of limb bone morphology: an experimental approach using a mouse model. Am J Phys Anthropol 148(1):24-35.
Wanner JA. 1977. Variations in the anterior patellar groove of the human femur. Am J Phys Anthropol 47(1):99-102.
Ward C. 2013. Postural and locomotor adapation of *Australopithecus* species. In: Reed K, Fleagle J, and Leakey R, editors. The Paleobiology of *Australopithecus*. New York: Springer. p 235-245.
Warren MP. 1999. Hormonal influences on the establishment of peak bone mass. In: Rosen CJ, Glowacki J, and Bilezikian JP, editors. The Aging Skeleton. San Diego: Academic Press. p 115-126.
Weaver C, and Gallant K. 2014a. Nutrition. In: Burr D, and Allen M, editors. Basic and Applied Bone Biology. Amsterdam: Academic Press. p 283-297.
Weaver CM, and Fuchs RK. 2014. Skeletal growth and development. In: Burr DB, and Allen MR, editors. Basic and Applied Bone Biology. Amsterdam: Academic Press. p 245-260.
Weaver CM, and Gallant KMH. 2014b. Nutrition. In: Burr DB, and Allen MR, editors. Basic and Applied Bone Biology. Amsterdam: Academic Press. p 283-297.
Weinmann JP, and Sicher H. 1974. Bone and Bones: Fundamentals of Bone Biology. London: Henry Kimpton.
Welsh L, and Rutherford O. 1996. Hip bone mineral density is improved by high-impact aerobic exercise in postmenopausal women and men over 50 years. European Journal of Applied Physiology and Occupational Physiology(74):511-517.
Wescott DJ. 2006. Effect of mobility on femur midshaft external shape and robusticity. Am J Phys Anthropol 130(2):201-213.
Wilkinson RG, and Pickett KE. 2006. Income inequality and population health: a review and explanation of evidence. Social Science & Medicine 62:1768-1784.
Winter DA. 1990. Biomechanics and motor control of human movement. New York: John Wiley & Sons.
Wise A, Krajnak K, and Kashon M. 1996. Menopause: the aging of multiple pacemakers. Science(273):67-70.
Wolff J. 1892. The Law of Bone Remodeling New York: Springer.

Wong P, Christie J, and Wark J. 2007. The effects of smoking on bone health. Clinical Science(113):233-241.

Woo SLY, Kuei SC, Amiel D, Gomez MA, Hayes WC, White FC, and Akeson WH. 1981. The effect of prolonged physical training on the properties of the long bone: a study of Wolff's law Journal of Bone & Joint Surgery 63:780-787.

Zioupos P, and Currey J. 1998. Changes in the stiffness, strength and toughness of human cortical bone with age. Bone(22):57-66.

Zumoff B, Walsh B, Katz J, Levine L, Rosenfeld R, Kream J, and Weiner H. 1983. Subnormal plasma dehydroepiandrosterone to cortisol ratio in anorexia nervosa: a second hormonal parameter of ontogenic regression. Journal of Clinical Endocrinol Metabolism(56):668-671.

APPENDICES

APPENDIX A
ACTIVITY LEVEL ASSIGNMENT CATEGORIES

Table A.1. Examples of activities, hobbies, and occupations in the final sample by activity level category

	Activity Level Category		
	Light	**Moderate**	**Heavy**
Examples from study sample	Accountant	Nurse	Steel worker
	Secretary	Cook	Coal miner
	Historian	Handyman	Laborer
	Crafting	Delivery man	Factory worker
	Medical transcription	Cycling and boating	Dance teacher
	Radio personality	Basketball	Carpenter
	Bank teller	Military	Construction worker
	Truck driver	Game warden	Machine operator
	Telemarketing	Teacher	Professional wrestler
	Play writing	Electrician	Yard service
	Lawyer	Pharmacist	Iron worker

APPENDIX B
WITHIN BONE UNIVARIATE COMPARISON RESULTS FOR SLICE AND SEX EFFECTS

Table B.1. Results of ANOVA type III models for slice location and sex in the humerus

Source (DF)	Cross-sectional Property						
	Cortical Area (CA)	**Total Area (TA)**	**Medullary Area (MA)**	**Percent Cortical Area (%CA)**	**I_x**	**I_y**	**J**
Slice location (4)	**< 0.0001**	**< 0.0001**	**< 0.0001**	**< 0.0001**	**< 0.0001**	**< 0.0001**	**< 0.0001**
Sex (1)	**< 0.0001**	**< 0.0001**	**< 0.0001**	**0.0024**	**< 0.0001**	**< 0.0001**	**< 0.0001**

Source (DF)	Cross-sectional Property							
	I_{max}	**I_{min}**	**Shape (I_{max}/I_{min})**	**Z_x**	**Z_y**	**Z_p**	**Z_{max}**	**Z_{min}**
Slice location (4)	**< 0.0001**	**< 0.0001**	**< 0.0001**	**< 0.0001**	**< 0.0001**	**< 0.0001**	**< 0.0001**	**< 0.0001**
Sex (1)	**< 0.0001**	**< 0.0001**	0.0640	**< 0.0001**	**< 0.0001**	**< 0.0001**	**< 0.0001**	**< 0.0001**

Significant values ($p < 0.05$) bolded

Table B.2. Results of ANOVA type III models for slice location and sex in the radius

Source (DF)	Cross-sectional Property						
	Cortical Area (CA)	**Total Area (TA)**	**Medullary Area (MA)**	**Percent Cortical Area (%CA)**	**I_x**	**I_y**	**J**
Slice location (4)	**0.0150**	**< 0.0001**	**< 0.0001**	**< 0.0001**	**< 0.0001**	**< 0.0001**	**< 0.0001**
Sex (1)	**< 0.0001**	**< 0.0001**	**< 0.0001**	0.1509	**< 0.0001**	**< 0.0001**	**< 0.0001**

Source (DF)	Cross-sectional Property							
	I_{max}	**I_{min}**	**Shape (I_{max}/I_{min})**	**Z_x**	**Z_y**	**Z_p**	**Z_{max}**	**Z_{min}**
Slice location (4)	**< 0.0001**	**< 0.0001**	**< 0.0001**	**< 0.0001**	**< 0.0001**	**< 0.0001**	**< 0.0001**	**< 0.0001**
Sex (1)	**< 0.0001**	**< 0.0001**	**0.0004**	**< 0.0001**	**< 0.0001**	**< 0.0001**	**< 0.0001**	**< 0.0001**

Significant values ($p < 0.05$) bolded

Table B.3. Results of ANOVA type III models for slice location and sex in the humerus

Source (DF)	Cross-sectional Property						
	Cortical Area (CA)	**Total Area (TA)**	**Medullary Area (MA)**	**Percent Cortical Area (%CA)**	**I_x**	**I_y**	**J**
Slice location (4)	**< 0.0001**	**< 0.0001**	**< 0.0001**	**< 0.0001**	**< 0.0001**	**< 0.0001**	**< 0.0001**
Sex (1)	**< 0.0001**	**< 0.0001**	**< 0.0001**	0.0847	**< 0.0001**	**< 0.0001**	**< 0.0001**

Source (DF)	Cross-sectional Property							
	I_{max}	**I_{min}**	**Shape (I_{max}/I_{min})**	**Z_x**	**Z_y**	**Z_p**	**Z_{max}**	**Z_{min}**
Slice location (4)	**< 0.0001**	**< 0.0001**	**< 0.0001**	**< 0.0001**	**< 0.0001**	**< 0.0001**	**< 0.0001**	**< 0.0001**
Sex (1)	**< 0.0001**	**< 0.0001**	**0.0002**	**< 0.0001**	**< 0.0001**	**< 0.0001**	**< 0.0001**	**< 0.0001**

Significant values ($p < 0.05$) bolded

Table B.4. Results of ANOVA type III models for slice location and sex in the femur

Source (DF)	Cross-sectional Property						
	Cortical Area (CA)	**Total Area (TA)**	**Medullary Area (MA)**	**Percent Cortical Area (%CA)**	**I_x**	**I_y**	**J**
Slice location (4)	**< 0.0001**	**< 0.0001**	**< 0.0001**	**< 0.0001**	**< 0.0001**	**< 0.0001**	**< 0.0001**
Sex (1)	**< 0.0001**	**< 0.0001**	**0.0717**	**0.0050**	**< 0.0001**	**< 0.0001**	**< 0.0001**

Source (DF)	Cross-sectional Property							
	I_{max}	**I_{min}**	**Shape (I_{max}/I_{min})**	**Z_x**	**Z_y**	**Z_p**	**Z_{max}**	**Z_{min}**
Slice location (4)	**< 0.0001**	**< 0.0001**	**< 0.0001**	**< 0.0001**	**< 0.0001**	**< 0.0001**	**< 0.0001**	**< 0.0001**
Sex (1)	**< 0.0001**	**< 0.0001**	**< 0.0001**	**< 0.0001**	**< 0.0001**	**< 0.0001**	**< 0.0001**	**< 0.0001**

Significant values ($p < 0.05$) bolded

Table B.5. Results of ANOVA type III models for slice location and sex in the tibia

Source (DF)	Cross-sectional Property						
	Cortical Area (CA)	**Total Area (TA)**	**Medullary Area (MA)**	**Percent Cortical Area (%CA)**	**I_x**	**I_y**	**J**
Slice location (4)	**< 0.0001**	**< 0.0001**	**< 0.0001**	**< 0.0001**	**< 0.0001**	**< 0.0001**	**< 0.0001**
Sex (1)	**< 0.0001**	**< 0.0001**	**0.0006**	**< 0.0001**	**< 0.0001**	**< 0.0001**	**< 0.0001**

Source (DF)	Cross-sectional Property							
	I_{max}	**I_{min}**	**Shape (I_{max}/I_{min})**	**Z_x**	**Z_y**	**Z_p**	**Z_{max}**	**Z_{min}**
Slice location (4)	**< 0.0001**	**< 0.0001**	**< 0.0001**	**< 0.0001**	**< 0.0001**	**< 0.0001**	**< 0.0001**	**< 0.0001**
Sex (1)	**< 0.0001**	**< 0.0001**	**0.0001**	**< 0.0001**	**< 0.0001**	**< 0.0001**	**< 0.0001**	**< 0.0001**

Significant values ($p < 0.05$) bolded

Table B.6. Results of ANOVA type III models for slice location and sex in the fibula

Source (DF)	Cross-sectional Property						
	Cortical Area (CA)	**Total Area (TA)**	**Medullary Area (MA)**	**Percent Cortical Area (%CA)**	**I_x**	**I_y**	**J**
Slice location (4)	**< 0.0001**	**< 0.0001**	**0.0017**	**< 0.0001**	**< 0.0001**	**< 0.0001**	**< 0.0001**
Sex (1)	**< 0.0001**	**< 0.0001**	**0.1146**	**< 0.0001**	**< 0.0001**	**< 0.0001**	**< 0.0001**

Source (DF)	Cross-sectional Property							
	I_{max}	**I_{min}**	**Shape (I_{max}/I_{min})**	**Z_x**	**Z_y**	**Z_p**	**Z_{max}**	**Z_{min}**
Slice location (4)	**< 0.0001**	**< 0.0001**	**< 0.0001**	**< 0.0001**	**< 0.0001**	**< 0.0001**	**< 0.0001**	**< 0.0001**
Sex (1)	**< 0.0001**	**< 0.0001**	**0.0002**	**< 0.0001**	**< 0.0001**	**< 0.0001**	**< 0.0001**	**< 0.0001**

Significant values ($p < 0.05$) bolded

APPENDIX C
WITHIN BONE PAIRWISE RESULTS FOR SLICE AND SEX

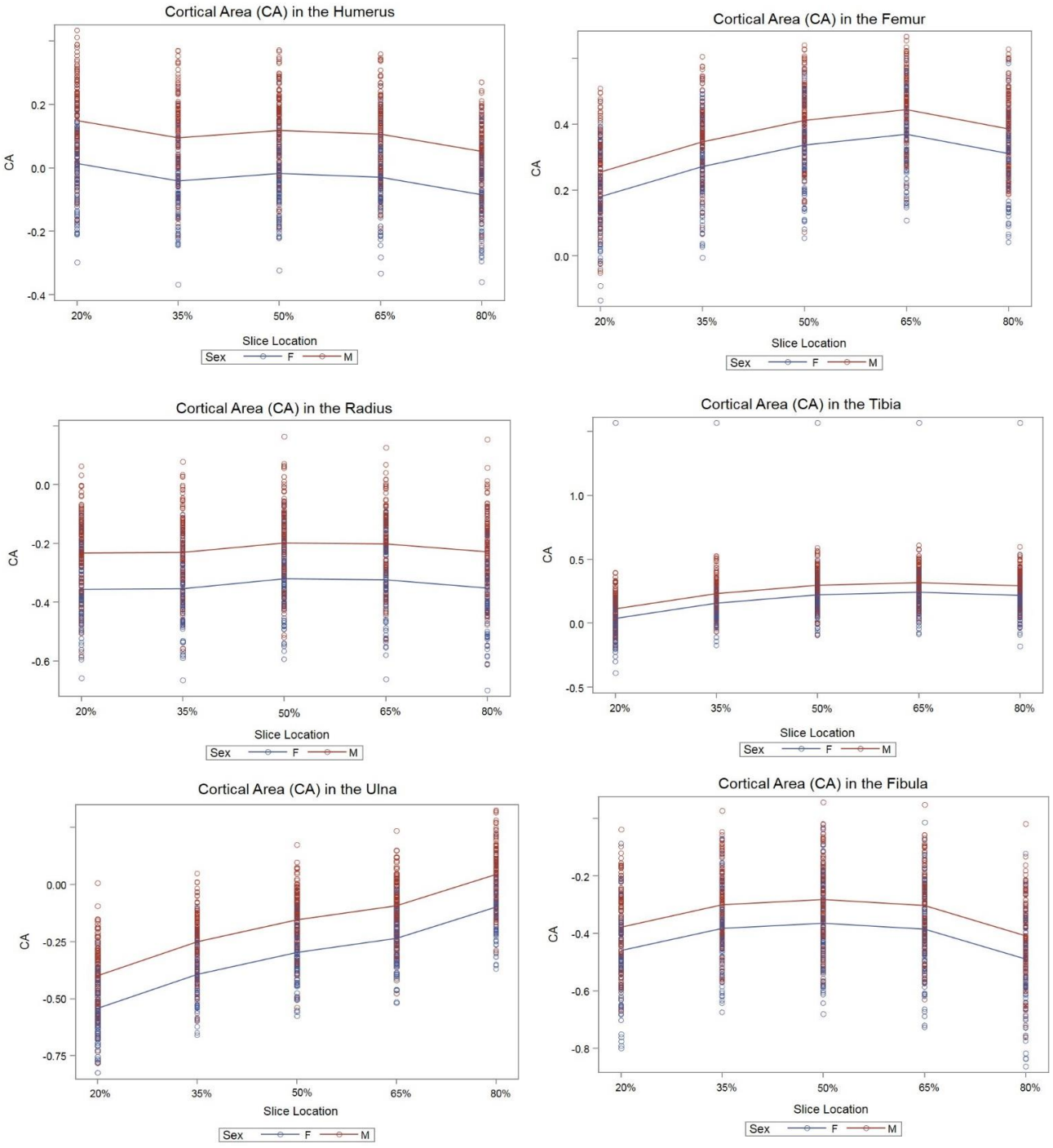

Figure C.1. Cortical area (CA) by sex and slice location within each element
Asterisks **(*)** indicate significant ($p < 0.05$) results in comparisons of means between sexes from post-hoc Least Squares with Tukey-Kramer adjustment for multiple comparisons.

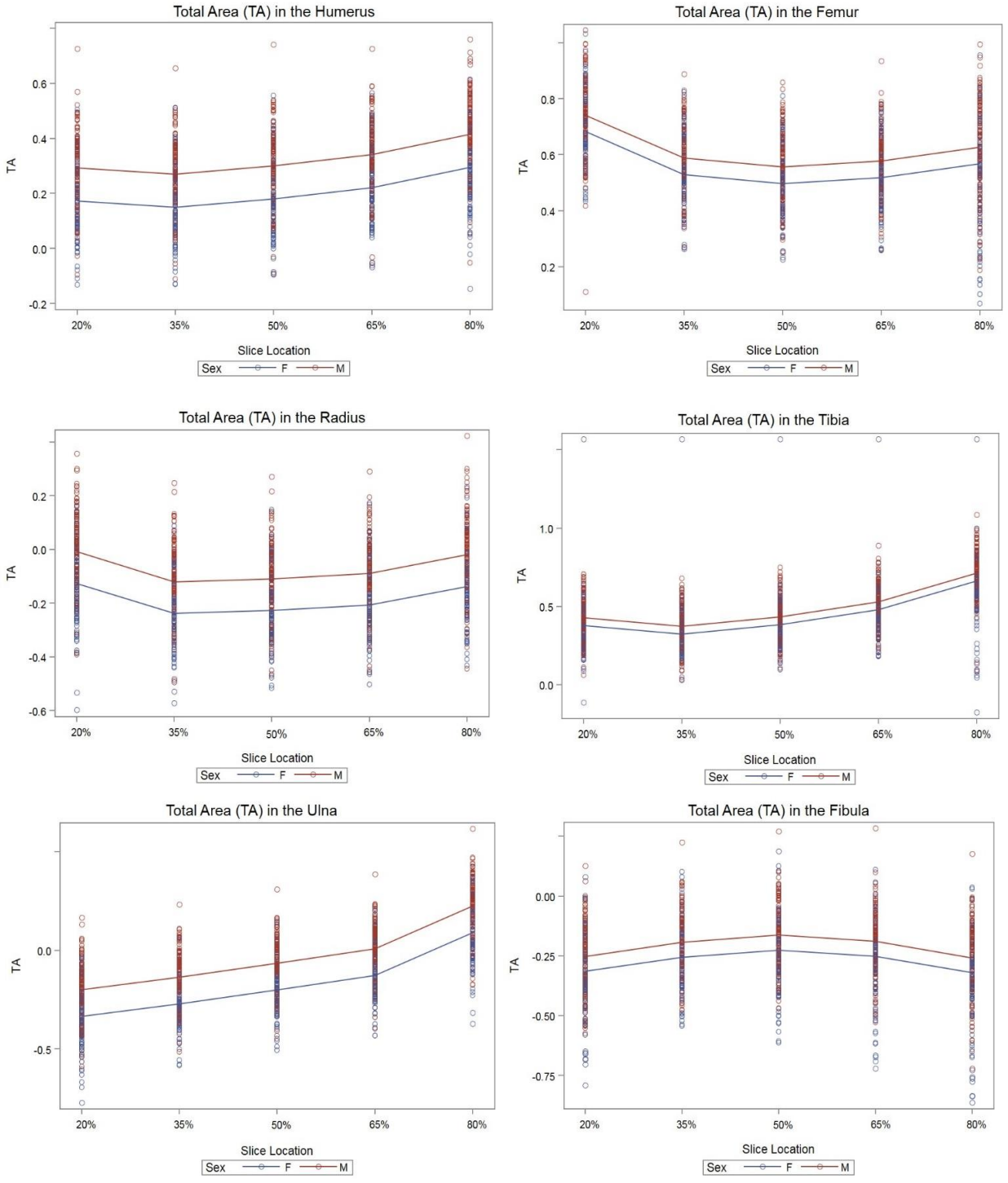

Figure C.2. Total area (TA) by sex and slice location within each element
Asterisks **(*)** indicate significant ($p < 0.05$) results in comparisons of means between sexes from post-hoc Least Squares with Tukey-Kramer adjustment for multiple comparisons.

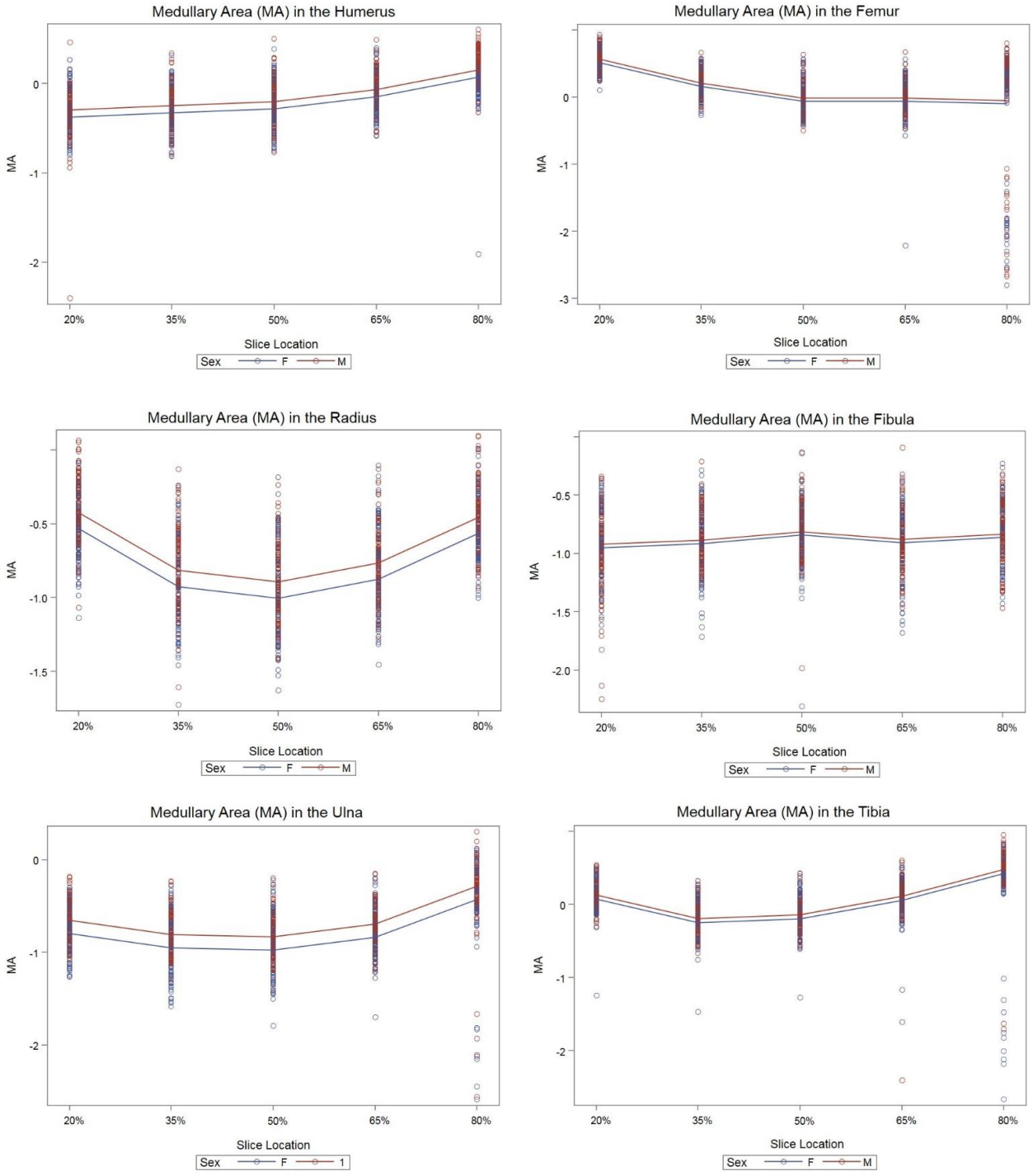

Figure C.3. Medullary area (MA) by sex and slice location within each element
Asterisks **(*)** indicate significant ($p < 0.05$) results in comparisons of means between sexes from post-hoc Least Squares with Tukey-Kramer adjustment for multiple comparisons.

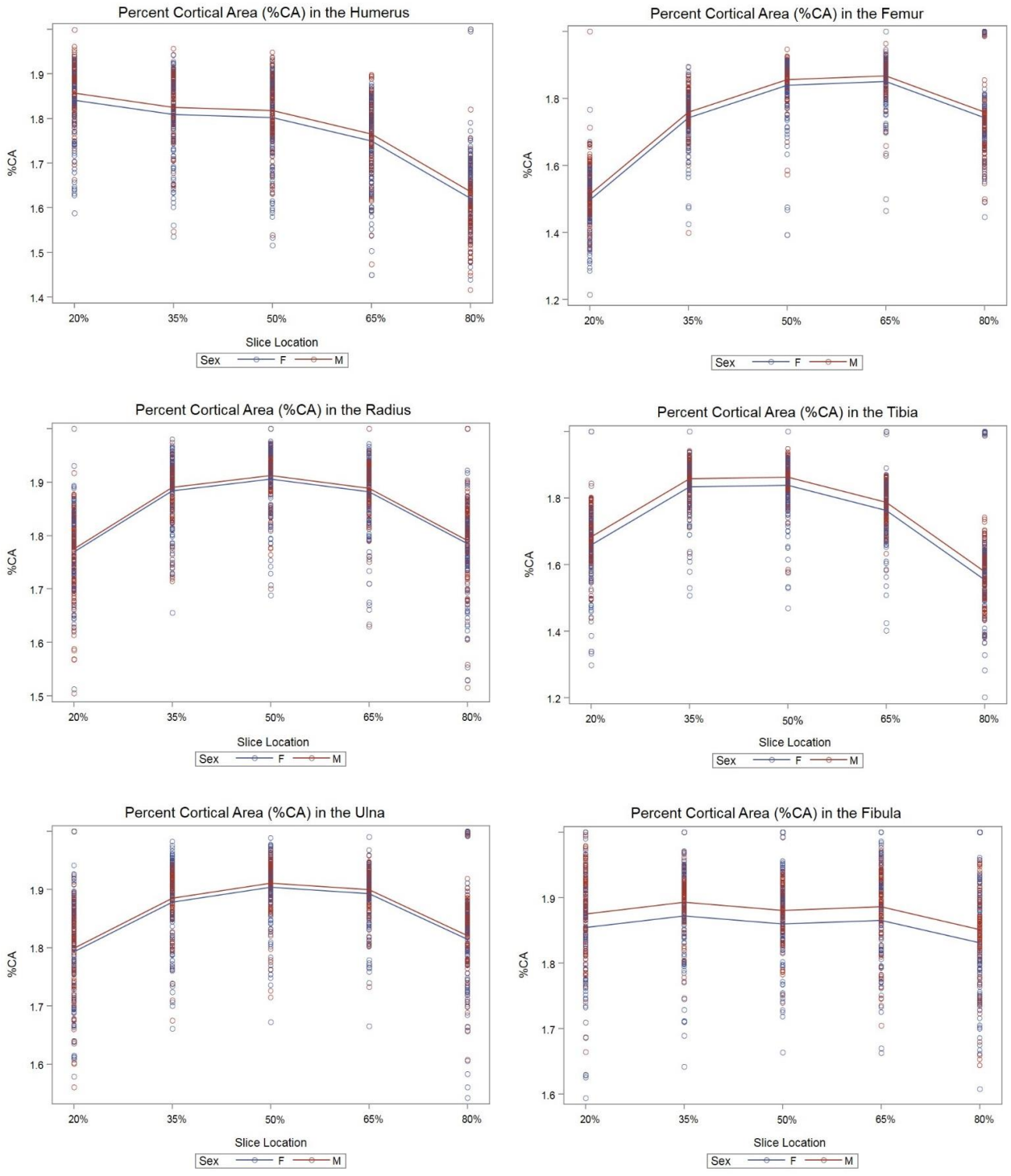

Figure C.4. Percent Cortical Area (%CA) by sex and slice location within each element
Asterisks **(*)** indicate significant ($p < 0.05$) results in comparisons of means between sexes from post-hoc Least Squares with Tukey-Kramer adjustment for multiple comparisons.

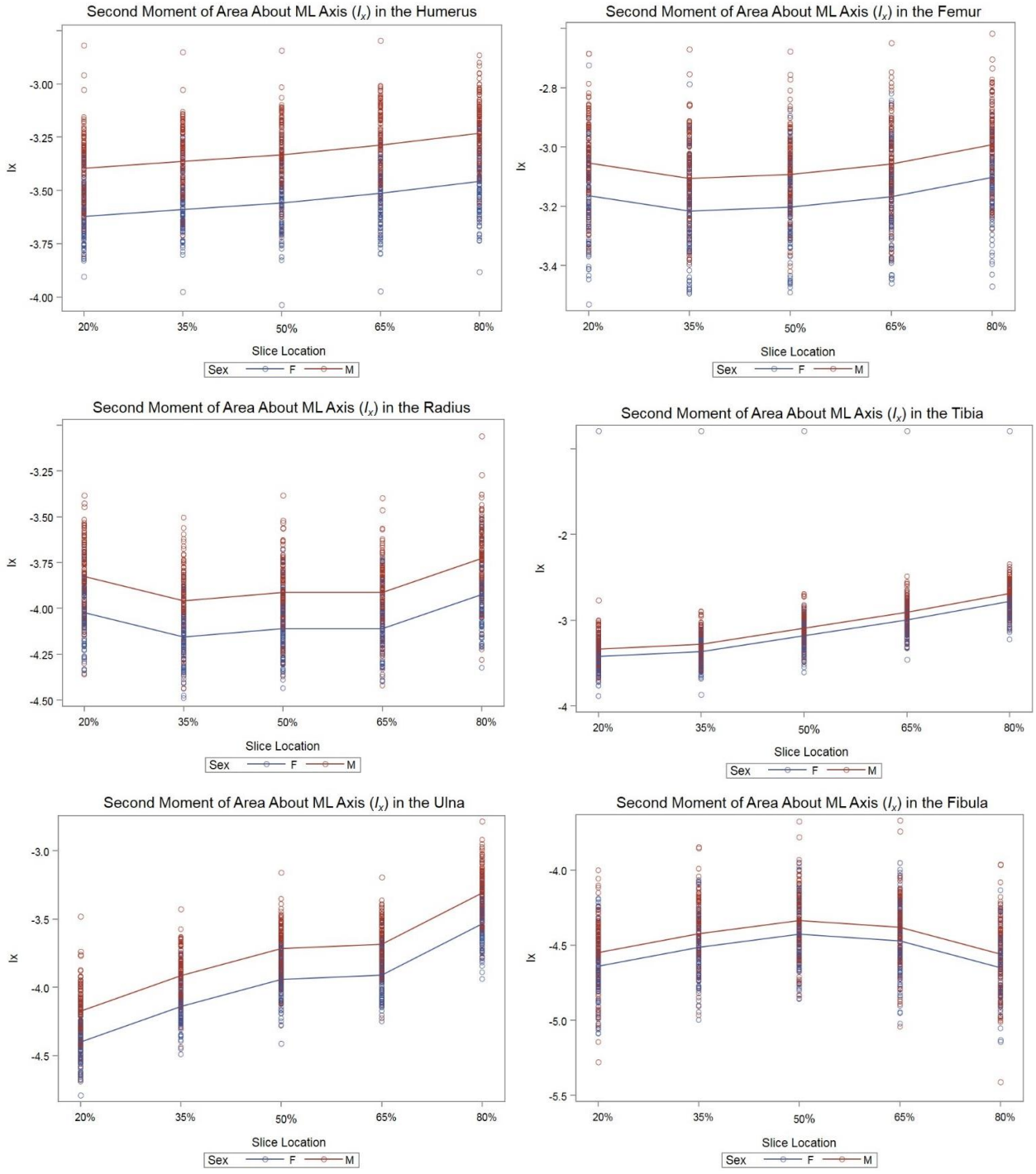

Figure C.5. Second moment of area about the mediolateral (ML) axis (I_x) by sex and slice location within each element

Asterisks **(*)** indicate significant ($p < 0.05$) results in comparisons of means between sexes from post-hoc Least Squares with Tukey-Kramer adjustment for multiple comparisons.

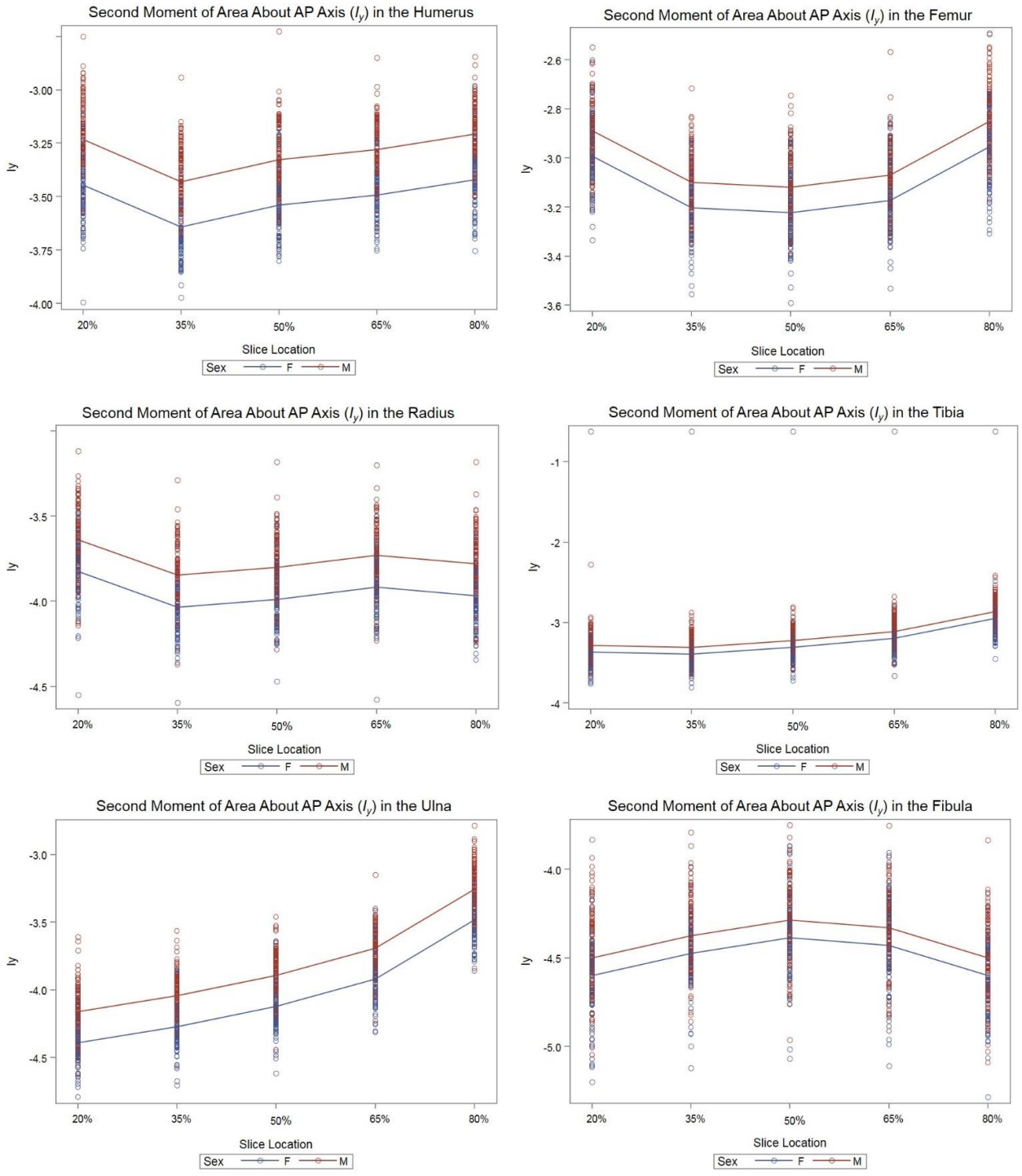

Figure C.6. Second moment of area about the anteroposterior (AP) axis (I_u) by sex and slice location within each element

Asterisks **(*)** indicate significant ($p < 0.05$) results in comparisons of means between sexes from post-hoc Least Squares with Tukey-Kramer adjustment for multiple comparisons.

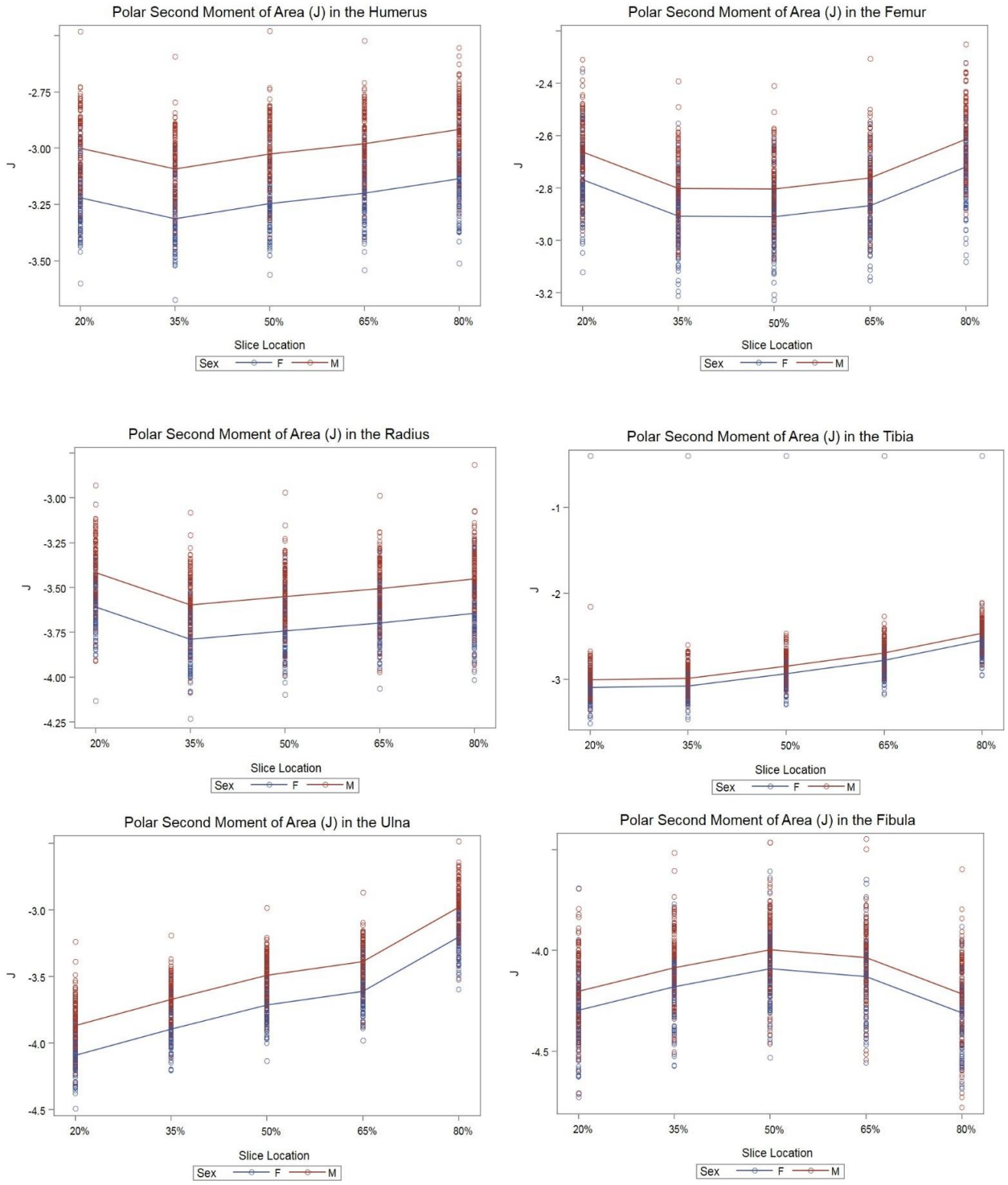

Figure C.7. Polar second moment of area (J) by sex and slice location within each element
Asterisks **(*)** indicate significant ($p < 0.05$) results in comparisons of means between sexes from post-hoc Least Squares with Tukey-Kramer adjustment for multiple comparisons.

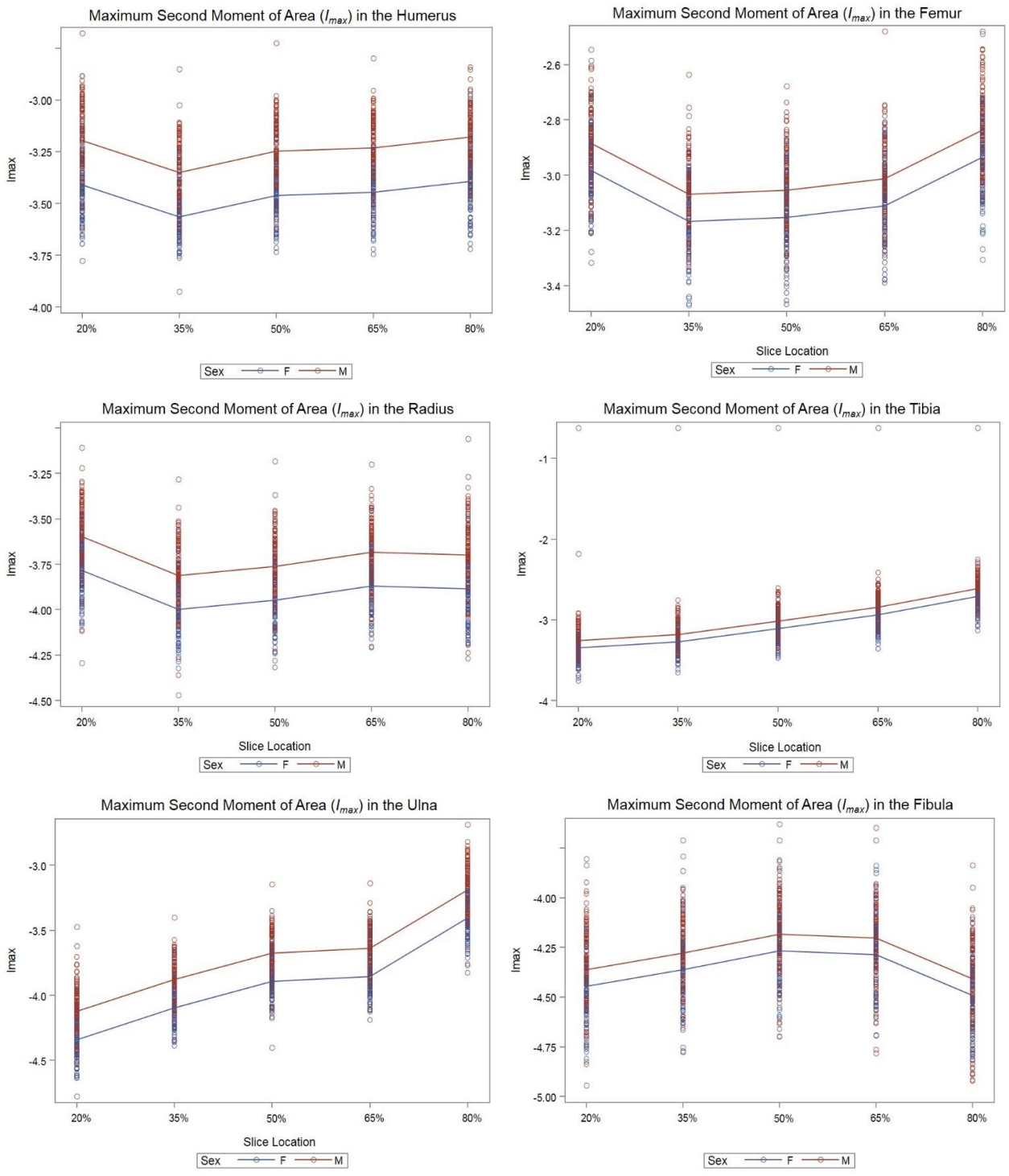

Figure C.8. Maximum second moment of area (I_{max}) by sex and slice location within each element

Asterisks **(*)** indicate significant ($p < 0.05$) results in comparisons of means between sexes from post-hoc Least Squares with Tukey-Kramer adjustment for multiple comparisons.

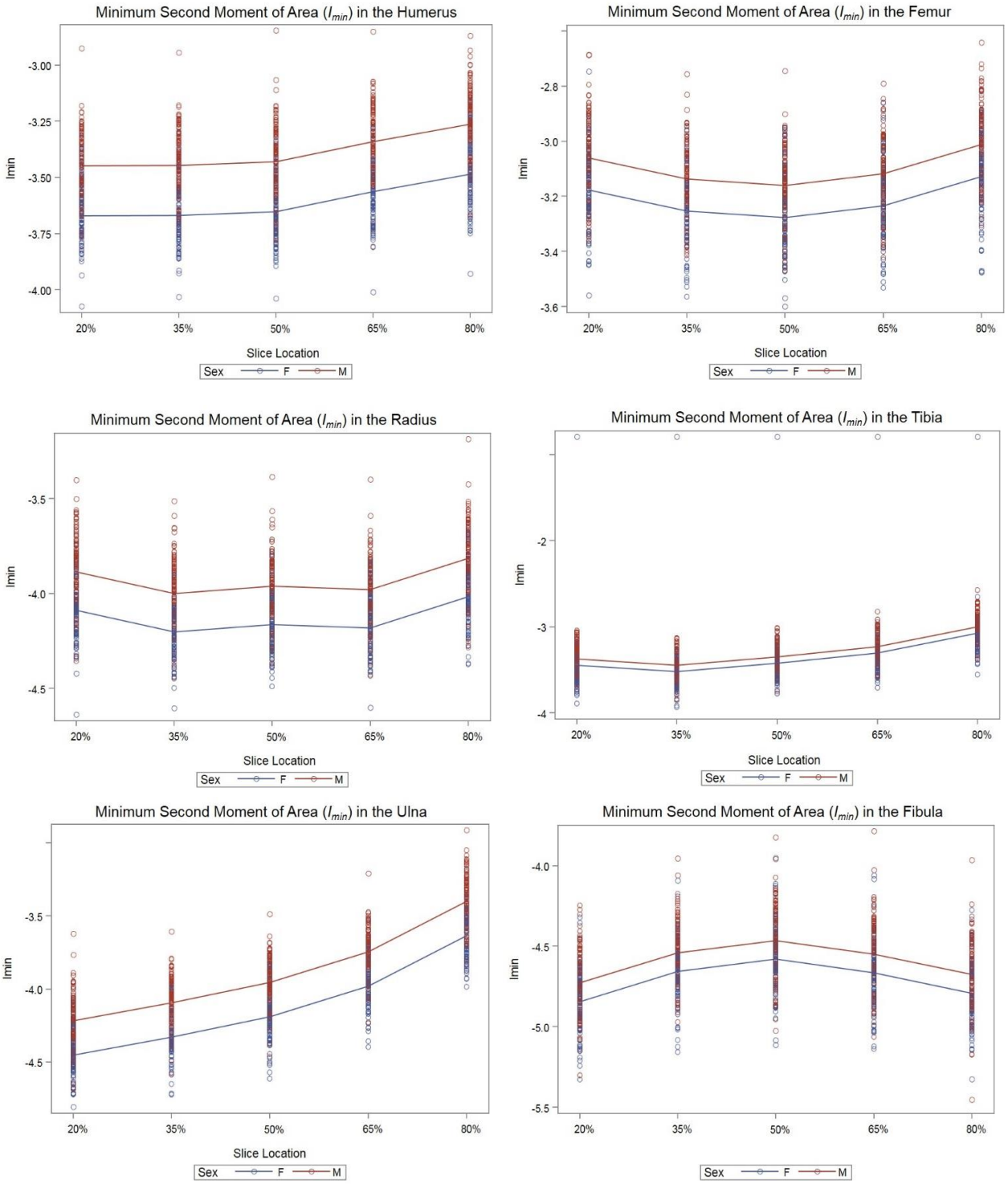

Figure C.9. Minimum second moment of area (I_{min}) by sex and slice location within each element

Asterisks **(*)** indicate significant ($p < 0.05$) results in comparisons of means between sexes from post-hoc Least Squares with Tukey-Kramer adjustment for multiple comparisons.

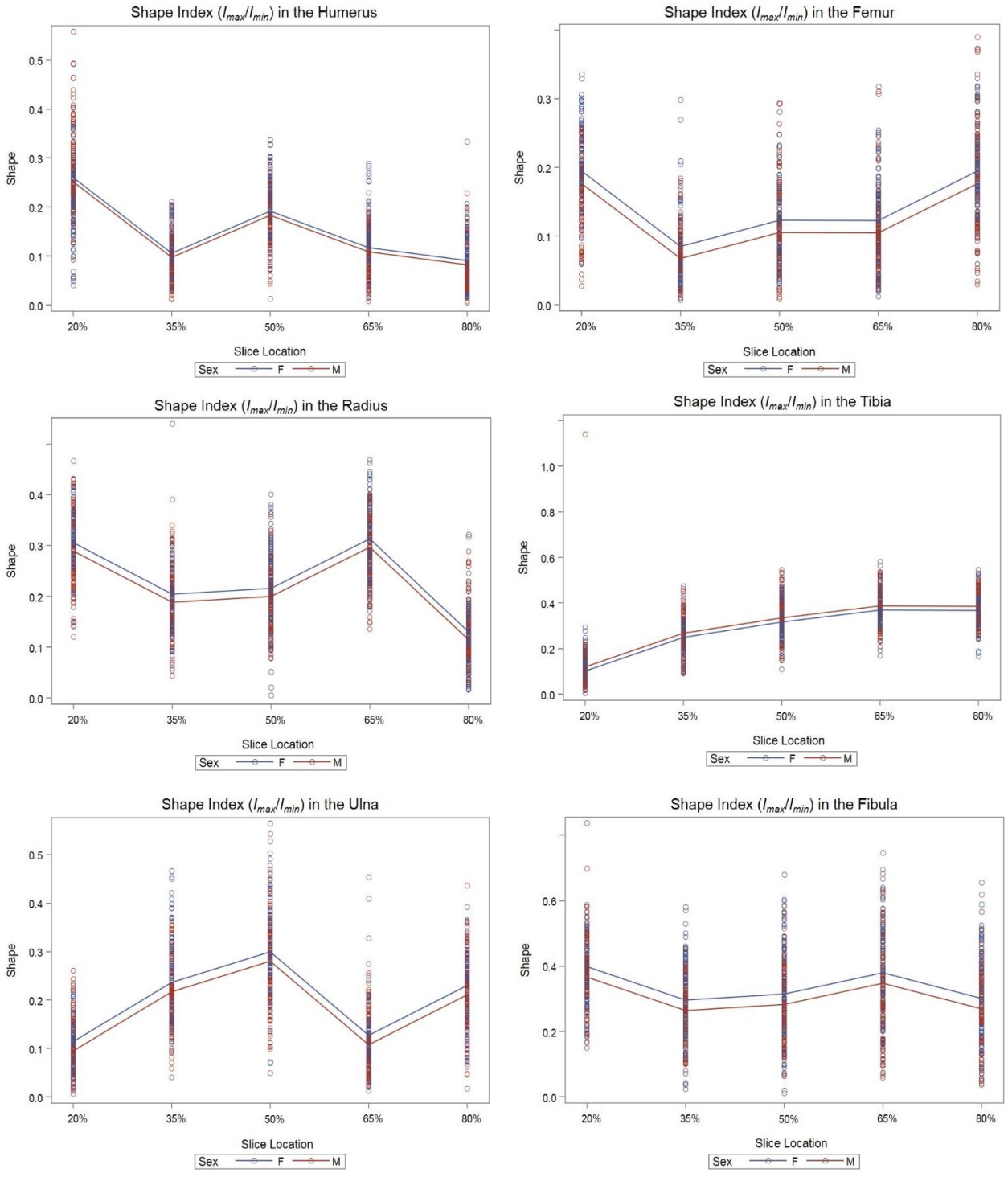

Figure C.10. Shape index by sex and slice location within each element
Asterisks **(*)** indicate significant ($p < 0.05$) results in comparisons of means between sexes from post-hoc Least Squares with Tukey-Kramer adjustment for multiple comparisons.

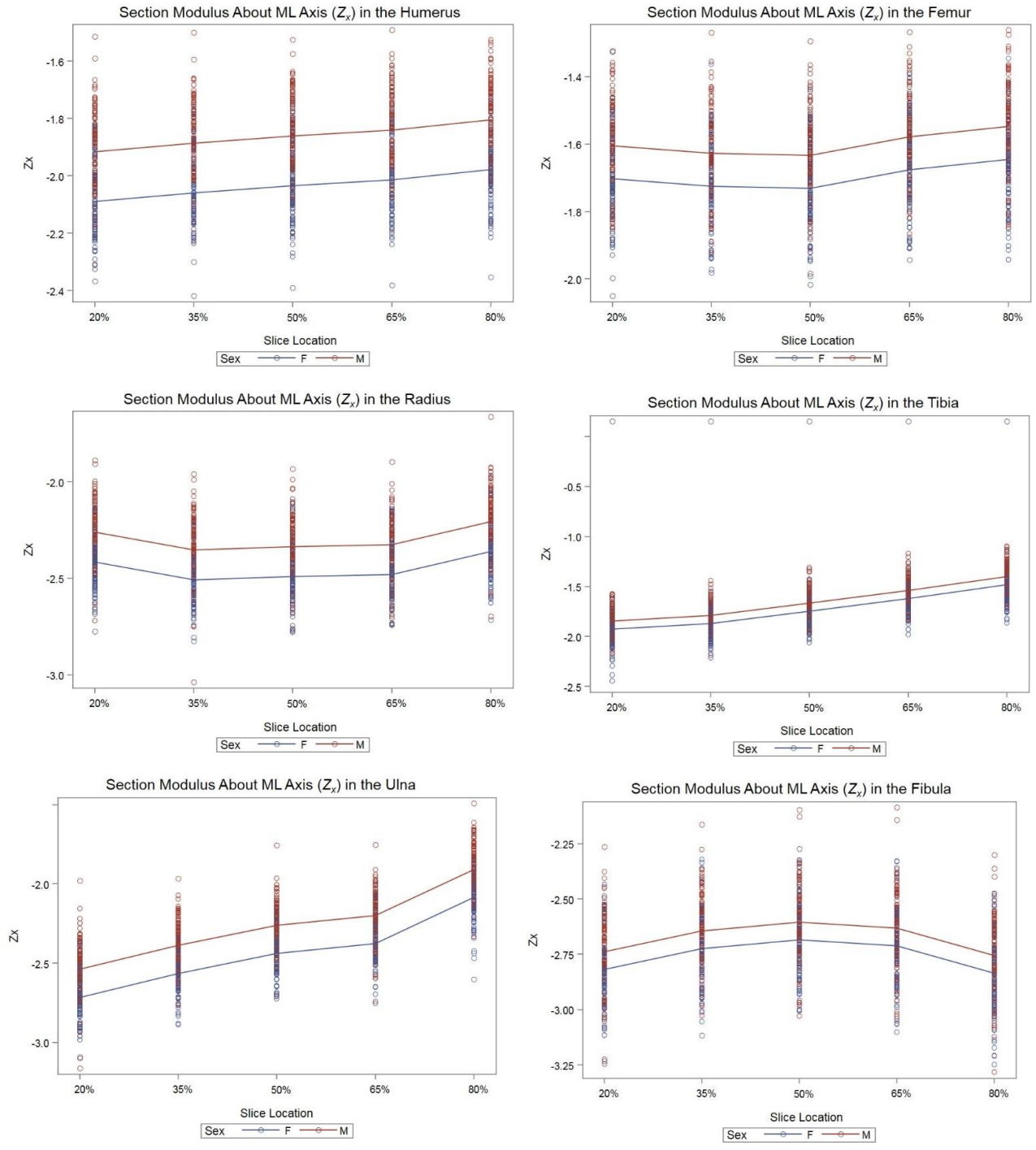

Figure C.11. Section modulus about the mediolateral (ML) axis (Z_x) by sex and slice location within each element

Asterisks **(*)** indicate significant ($p < 0.05$) results in comparisons of means between sexes from post-hoc Least Squares with Tukey-Kramer adjustment for multiple comparisons.

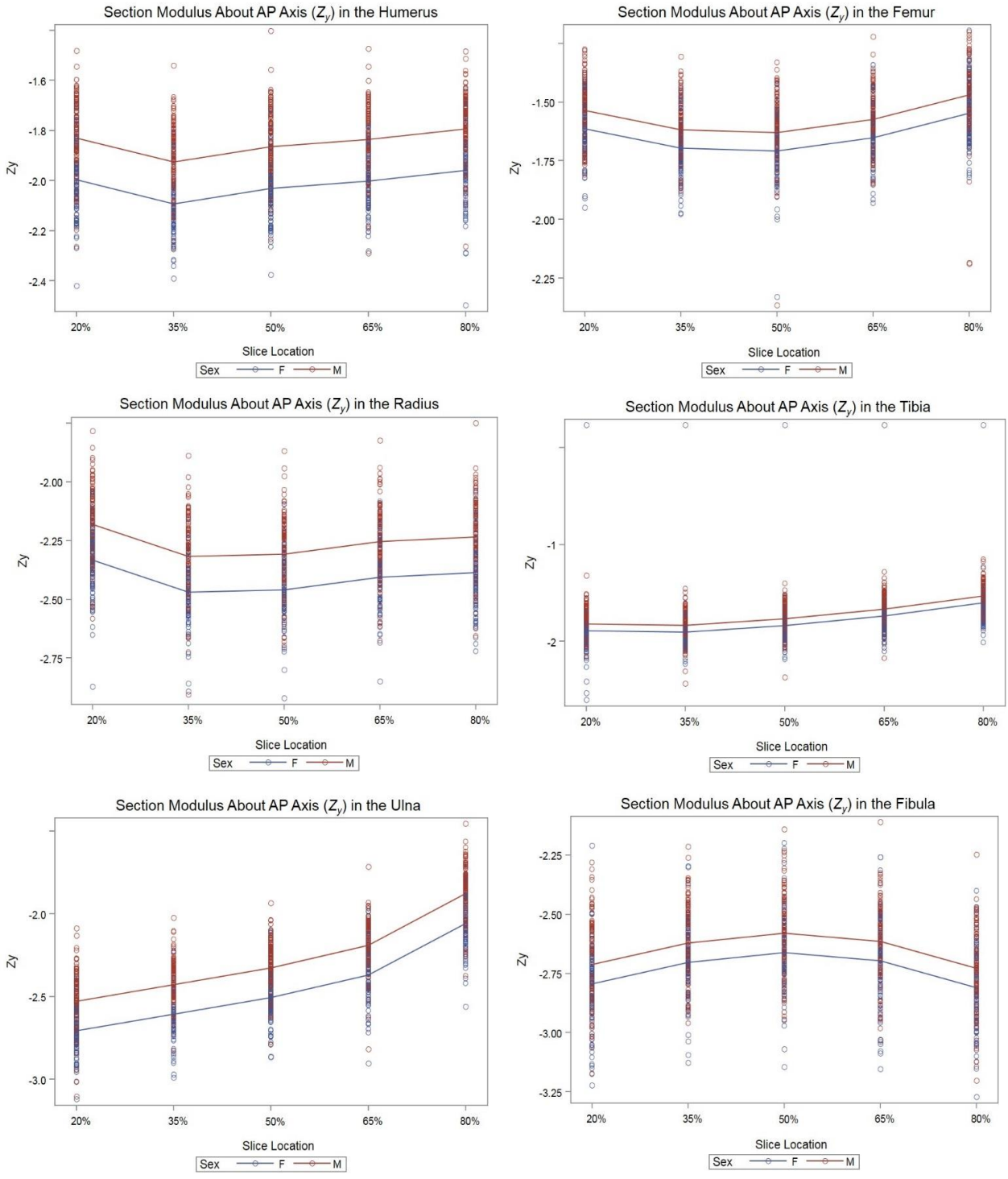

Figure C.12. Section modulus about the anteroposterior (AP) axis (Z_y) by sex and slice location within each element

Asterisks **(*)** indicate significant ($p < 0.05$) results in comparisons of means between sexes from post-hoc Least Squares with Tukey-Kramer adjustment for multiple comparisons.

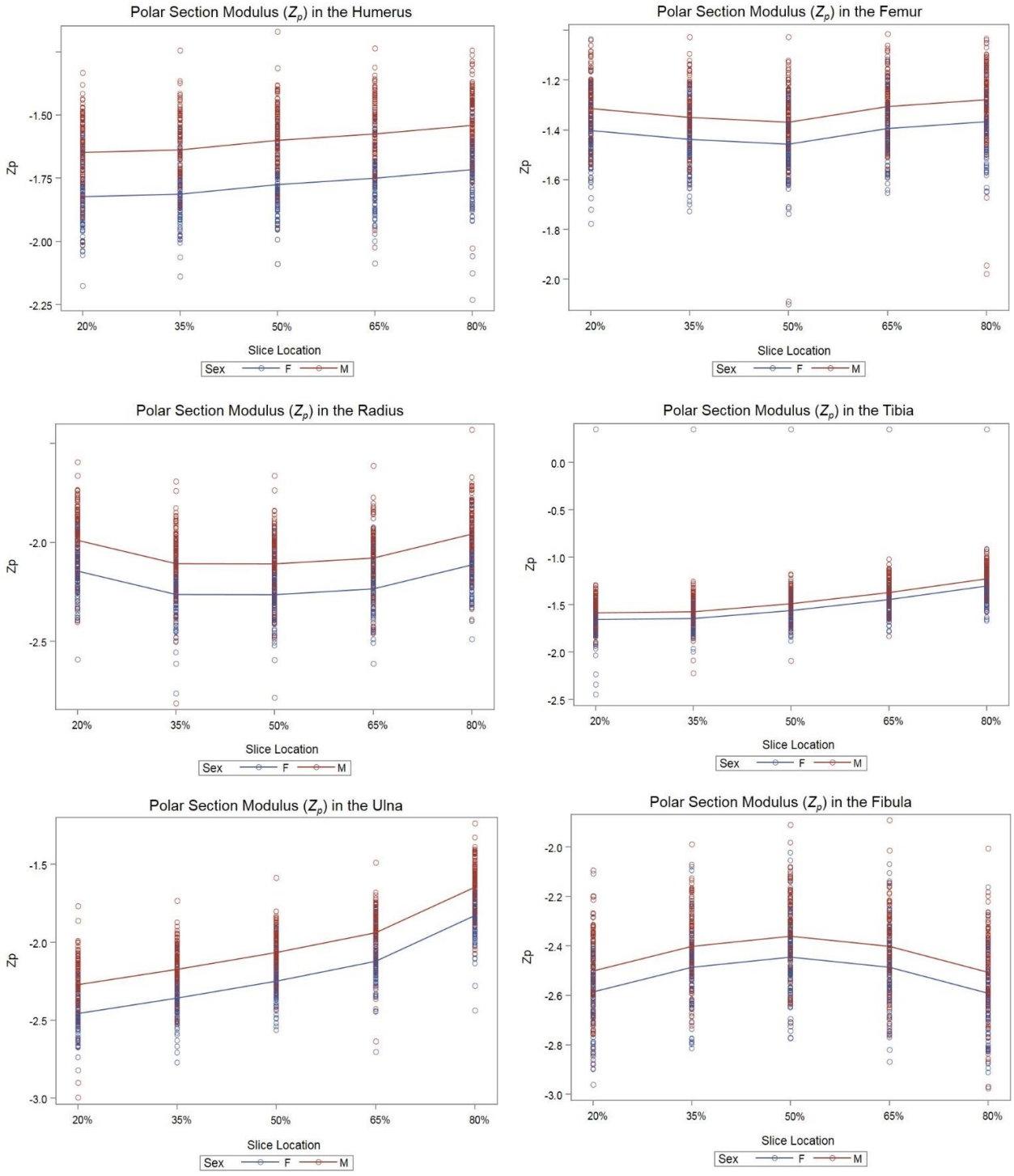

Figure C.13. Polar section modulus (Z_p) by sex and slice location within each element
Asterisks **(*)** indicate significant ($p < 0.05$) results in comparisons of means between sexes from post-hoc Least Squares with Tukey-Kramer adjustment for multiple comparisons.

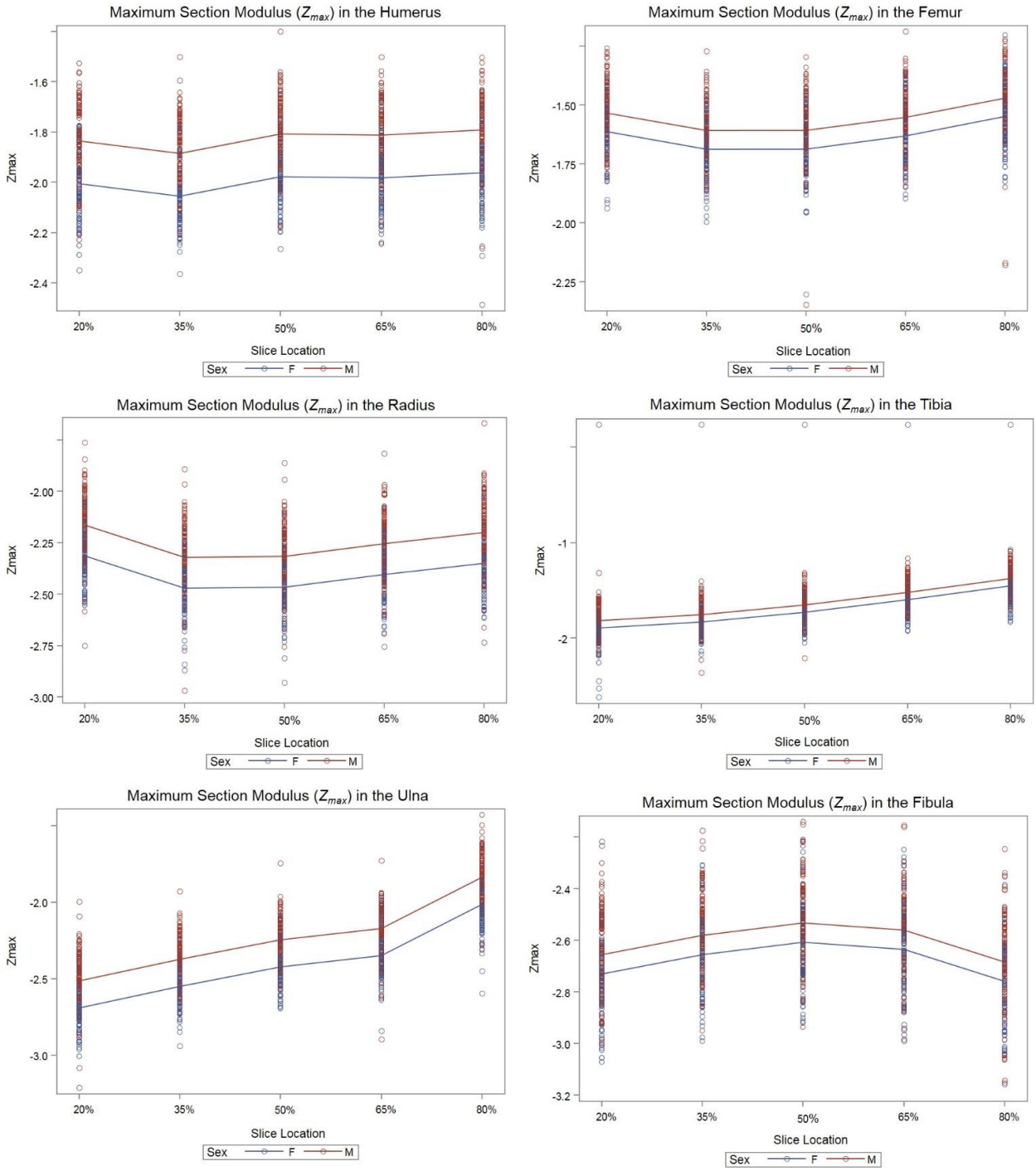

Figure C.14. Maximum section modulus (Z_{max}) by sex and slice location within each element

Asterisks **(*)** indicate significant ($p < 0.05$) results in comparisons of means between sexes from post-hoc Least Squares with Tukey-Kramer adjustment for multiple comparisons.

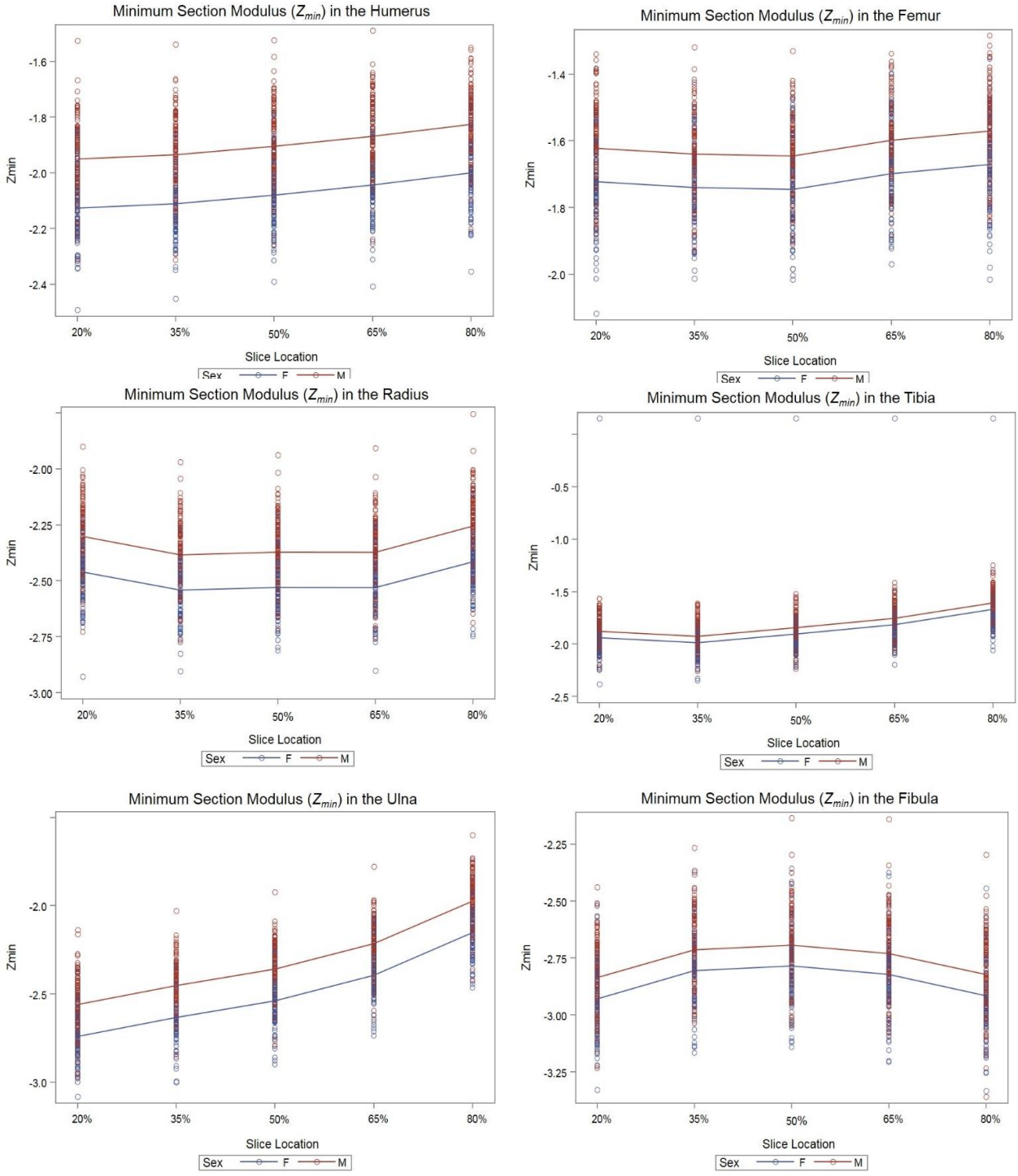

Figure C.15. Minimum section modulus (Z_{min}) by sex and slice location within each element
Asterisks **(*)** indicate significant ($p < 0.05$) results in comparisons of means between sexes from post-hoc Least Squares with Tukey-Kramer adjustment for multiple comparisons.

APPENDIX D
WITHIN BONE UNIVARIATE COMPARISON RESULTS FOR SLICE, SEX, AND AGE EFFECTS

Table D.1. Results of ANOVA type III models for slice location, sex, and age group in the humerus

Source (DF)	Cross-sectional Property						
	Cortical Area (CA)	**Total Area (TA)**	**Medullary Area (MA)**	**Percent Cortical Area (%CA)**	**I_x**	**I_y**	**J**
Slice location (4)	**< 0.0001**	**< 0.0001**	**< 0.0001**	**< 0.0001**	**< 0.0001**	**< 0.0001**	**< 0.0001**
Age group (4)	0.8280	**< 0.0001**	**< 0.0001**	**0.0002**	**0.0155**	**0.0084**	**0.0097**
Sex (1)	**0.0385**	**< 0.0001**	**< 0.0001**	**0.0282**	**< 0.0001**	**< 0.0001**	**< 0.0001**

Source (DF)	Cross-sectional Property							
	I_{max}	**I_{min}**	**Shape (I_{max}/I_{min})**	**Z_x**	**Z_y**	**Z_p**	**Z_{max}**	**Z_{min}**
Slice location (4)	**< 0.0001**	**< 0.0001**	**< 0.0001**	**< 0.0001**	**< 0.0001**	**< 0.0001**	**< 0.0001**	**< 0.0001**
Age group (4)	**0.0136**	**0.0099**	0.6188	**0.0207**	**< 0.0001**	0.0595	**0.0434**	**0.0375**
Sex (1)	**< 0.0001**	**< 0.0001**	**0.0420**	**< 0.0001**	**< 0.0001**	**< 0.0001**	**< 0.0001**	**< 0.0001**

Significant values ($p < 0.05$) bolded

Table D.2. Results of ANOVA type III models for slice location, sex, and age group in the radius

Source (DF)	Cross-sectional Property						
	Cortical Area (CA)	**Total Area (TA)**	**Medullary Area (MA)**	**Percent Cortical Area (%CA)**	**I_x**	**I_y**	**J**
Slice location (4)	**0.0134**	**< 0.0001**	**< 0.0001**	**< 0.0001**	**< 0.0001**	**< 0.0001**	**< 0.0001**
Age group (4)	0.4659	**< 0.0001**	**< 0.0001**	**< 0.0001**	**< 0.0001**	**< 0.0001**	**< 0.0001**
Sex (1)	**< 0.0001**	**< 0.0001**	**< 0.0001**	0.4593	**< 0.0001**	**< 0.0001**	**< 0.0001**

Source (DF)	Cross-sectional Property							
	I_{max}	**I_{min}**	**Shape (I_{max}/I_{min})**	**Z_x**	**Z_y**	**Z_p**	**Z_{max}**	**Z_{min}**
Slice location (4)	**< 0.0001**	**< 0.0001**	**< 0.0001**	**< 0.0001**	**< 0.0001**	**< 0.0001**	**< 0.0001**	**< 0.0001**
Age group (4)	**< 0.0001**	**< 0.0001**	0.7949	**< 0.0001**	**< 0.0001**	**< 0.0001**	**< 0.0001**	**< 0.0001**
Sex (1)	**< 0.0001**	**< 0.0001**	**0.0011**	**< 0.0001**	**< 0.0001**	**< 0.0001**	**< 0.0001**	**< 0.0001**

Significant values ($p < 0.05$) bolded

Table D.3. Results of ANOVA type III models for slice location, sex, and age group in the ulna

Source (DF)	Cross-sectional Property						
	Cortical Area (CA)	**Total Area (TA)**	**Medullary Area (MA)**	**Percent Cortical Area (%CA)**	**I_x**	**I_y**	**J**
Slice location (4)	**< 0.0001**	**< 0.0001**	**< 0.0001**	**< 0.0001**	**< 0.0001**	**< 0.0001**	**< 0.0001**
Age group (4)	0.1009	**< 0.0001**	**< 0.0001**	**< 0.0001**	**< 0.0001**	**< 0.0001**	**< 0.0001**
Sex (1)	**< 0.0001**	**< 0.0001**	**< 0.0001**	0.3650	**< 0.0001**	**< 0.0001**	**< 0.0001**

Source (DF)	Cross-sectional Property							
	I_{max}	**I_{min}**	**Shape (I_{max}/I_{min})**	**Z_x**	**Z_y**	**Z_p**	**Z_{max}**	**Z_{min}**
Slice location (4)	**< 0.0001**	**< 0.0001**	**< 0.0001**	**< 0.0001**	**< 0.0001**	**< 0.0001**	**< 0.0001**	**< 0.0001**
Age group (4)	**< 0.0001**	**< 0.0001**	0.0560	**< 0.0001**	**< 0.0001**	**< 0.0001**	**< 0.0001**	**< 0.0001**
Sex (1)	**< 0.0001**	**< 0.0001**	**< 0.0001**	**< 0.0001**	**< 0.0001**	**< 0.0001**	**< 0.0001**	**< 0.0001**

Significant values ($p < 0.05$) bolded

Table D.4. Results of ANOVA type III models for slice location, sex, and age group in the femur

Source (DF)	Cross-sectional Property						
	Cortical Area (CA)	**Total Area (TA)**	**Medullary Area (MA)**	**Percent Cortical Area (%CA)**	**I_x**	**I_y**	**J**
Slice location (4)	**< 0.0001**	**< 0.0001**	**< 0.0001**	**< 0.0001**	**< 0.0001**	**< 0.0001**	**< 0.0001**
Age group (4)	0.2638	**0.0001**	0.7506	**< 0.0001**	**0.0009**	**0.0002**	**0.0002**
Sex (1)	**< 0.0001**	**< 0.0001**	0.0515	**0.0243**	**< 0.0001**	**< 0.0001**	**< 0.0001**

Source (DF)	Cross-sectional Property							
	I_{max}	**I_{min}**	**Shape (I_{max}/I_{min})**	**Z_x**	**Z_y**	**Z_p**	**Z_{max}**	**Z_{min}**
Slice location (4)	**< 0.0001**	**< 0.0001**	**< 0.0001**	**< 0.0001**	**< 0.0001**	**< 0.0001**	**< 0.0001**	**< 0.0001**
Age group (4)	**< 0.0001**	**0.0018**	0.1648	**0.0248**	**0.0104**	**0.0393**	**0.0105**	**0.0334**
Sex (1)	**< 0.0001**	**< 0.0001**	**< 0.0001**	**< 0.0001**	**< 0.0001**	**< 0.0001**	**< 0.0001**	**< 0.0001**

Significant values ($p < 0.05$) bolded

Table D.5. Results of ANOVA type III models for slice location, sex, and age group in the tibia

Source (DF)	Cross-sectional Property						
	Cortical Area (CA)	**Total Area (TA)**	**Medullary Area (MA)**	**Percent Cortical Area (%CA)**	**I_x**	**I_y**	**J**
Slice location (4)	**< 0.0001**	**< 0.0001**	**< 0.0001**	**< 0.0001**	**< 0.0001**	**< 0.0001**	**< 0.0001**
Age group (4)	**< 0.0001**	**< 0.0001**	**< 0.0001**	**< 0.0001**	**< 0.0001**	**< 0.0001**	**< 0.0001**
Sex (1)	**< 0.0001**	**< 0.0001**	**< 0.0001**	**< 0.0001**	**< 0.0001**	**< 0.0001**	**< 0.0001**

Source (DF)	Cross-sectional Property							
	I_{max}	**I_{min}**	**Shape (I_{max}/I_{min})**	**Z_x**	**Z_y**	**Z_p**	**Z_{max}**	**Z_{min}**
Slice location (4)	**< 0.0001**	**< 0.0001**	**< 0.0001**	**< 0.0001**	**< 0.0001**	**< 0.0001**	**< 0.0001**	**< 0.0001**
Age group (4)	**< 0.0001**	**< 0.0001**	**0.0448**	**< 0.0001**	**< 0.0001**	**< 0.0001**	**< 0.0001**	**< 0.0001**
Sex (1)	**< 0.0001**	**< 0.0001**	**0.0001**	**< 0.0001**	**< 0.0001**	**< 0.0001**	**< 0.0001**	**< 0.0001**

Significant values ($p < 0.05$) bolded

Table D.6. Results of ANOVA type III models for slice location, sex, and age group in the fibula

Source (DF)	Cross-sectional Property						
	Cortical Area (CA)	**Total Area (TA)**	**Medullary Area (MA)**	**Percent Cortical Area (%CA)**	**I_x**	**I_y**	**J**
Slice location (4)	**< 0.0001**	**< 0.0001**	**0.0002**	**< 0.0001**	**< 0.0001**	**< 0.0001**	**< 0.0001**
Age group (4)	0.7898	**< 0.0001**	**< 0.0001**	**< 0.0001**	0.1701	**0.0095**	**0.0383**
Sex (1)	**< 0.0001**	**< 0.0001**	**0.0120**	**< 0.0001**	**< 0.0001**	**< 0.0001**	**< 0.0001**

Source (DF)	Cross-sectional Property							
	I_{max}	**I_{min}**	**Shape (I_{max}/I_{min})**	**Z_x**	**Z_y**	**Z_p**	**Z_{max}**	**Z_{min}**
Slice location (4)	**< 0.0001**	**< 0.0001**	**< 0.0001**	**< 0.0001**	**< 0.0001**	**< 0.0001**	**< 0.0001**	**< 0.0001**
Age group (4)	**0.0347**	0.1172	0.7730	0.1346	**0.0225**	0.0941	0.0849	0.1655
Sex (1)	**< 0.0001**	**< 0.0001**	**0.0001**	**< 0.0001**	**< 0.0001**	**< 0.0001**	**< 0.0001**	**< 0.0001**

Significant values ($p < 0.05$) bolded

APPENDIX E
WITHIN BONE CORTICAL AREA DISTRIBUTION BY SEX AND AGE

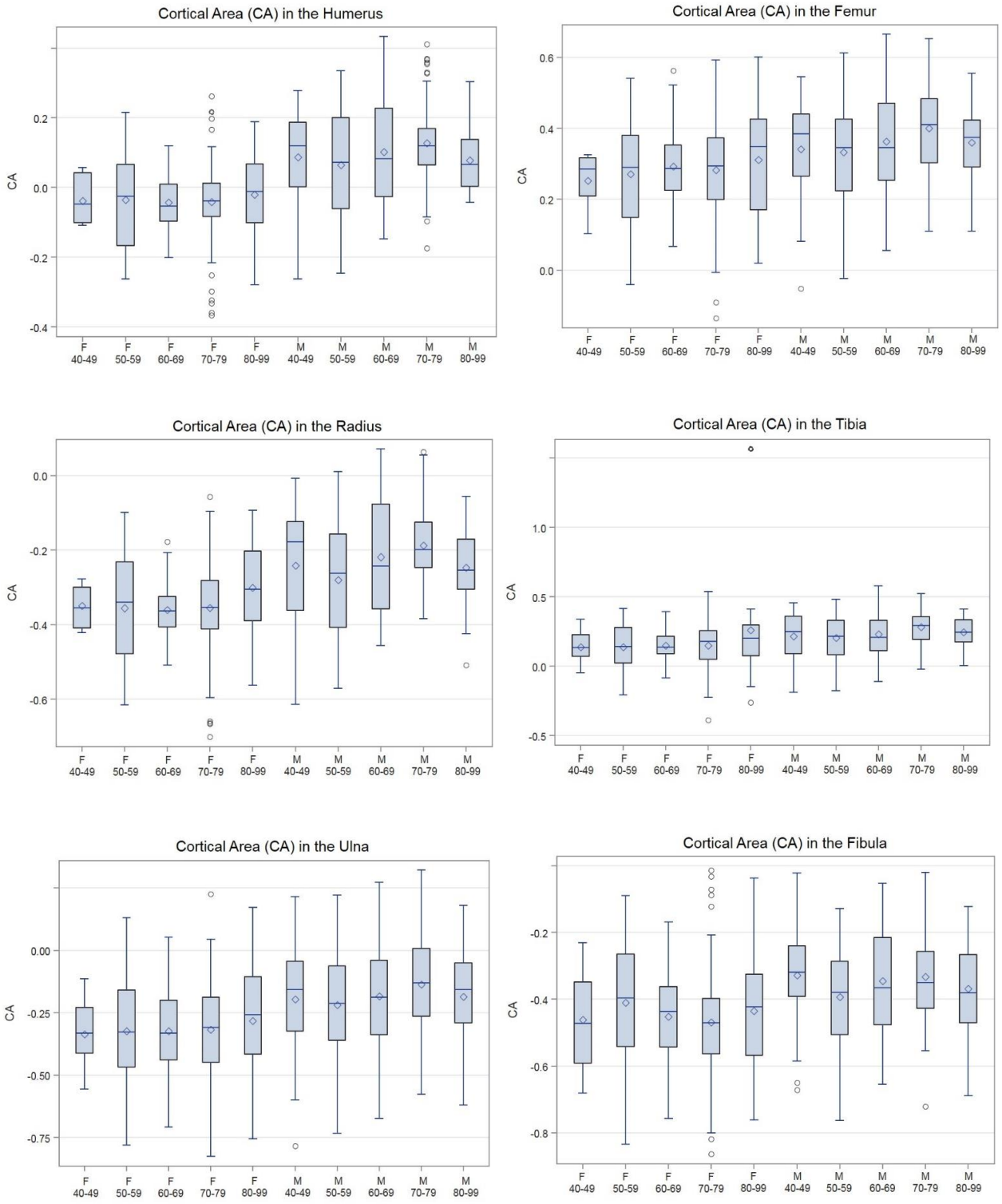

Figure E.1. Cortical area (CA) by sex and age group within each element

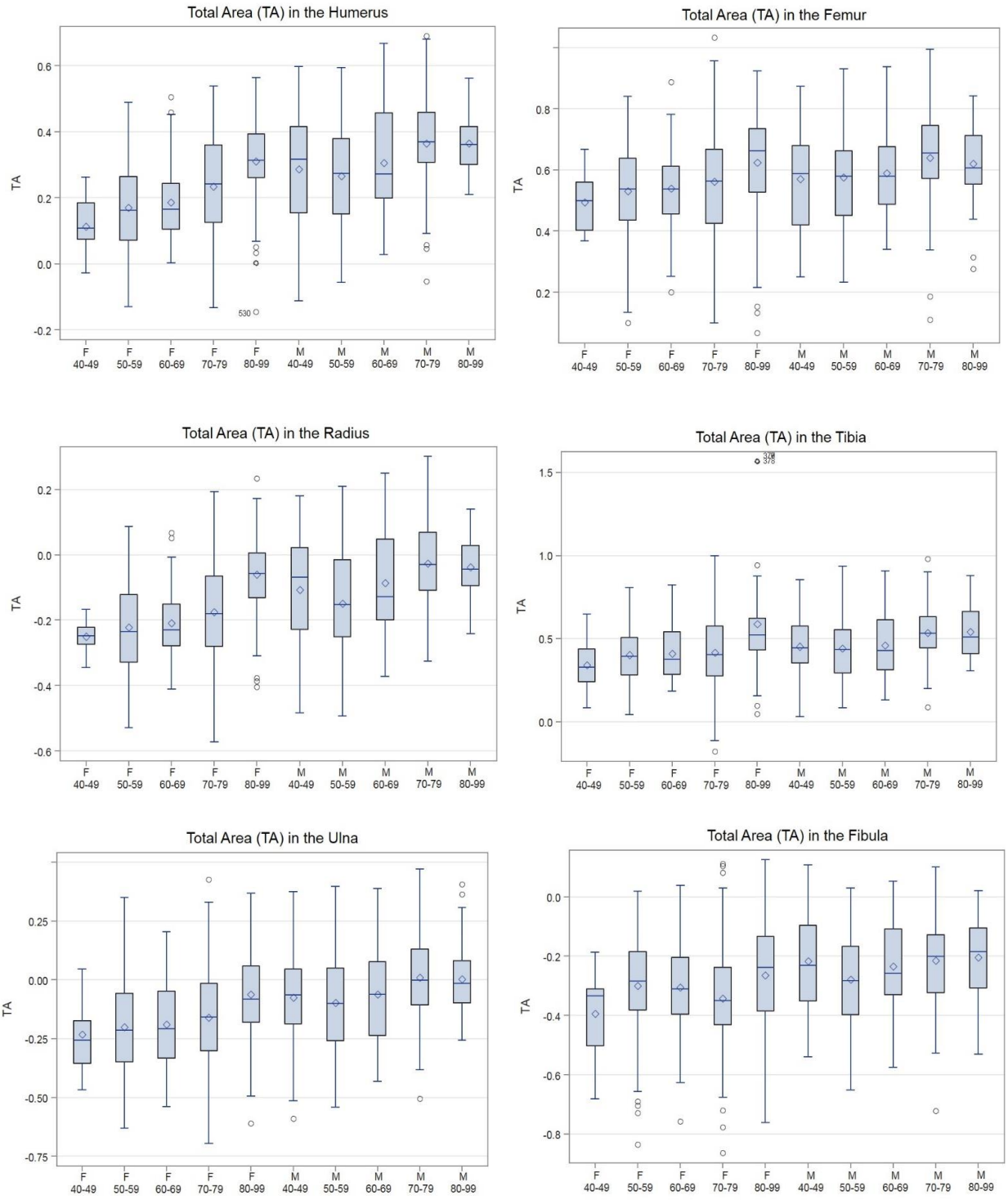

Figure E.2. Total area (TA) by sex and age group within each element

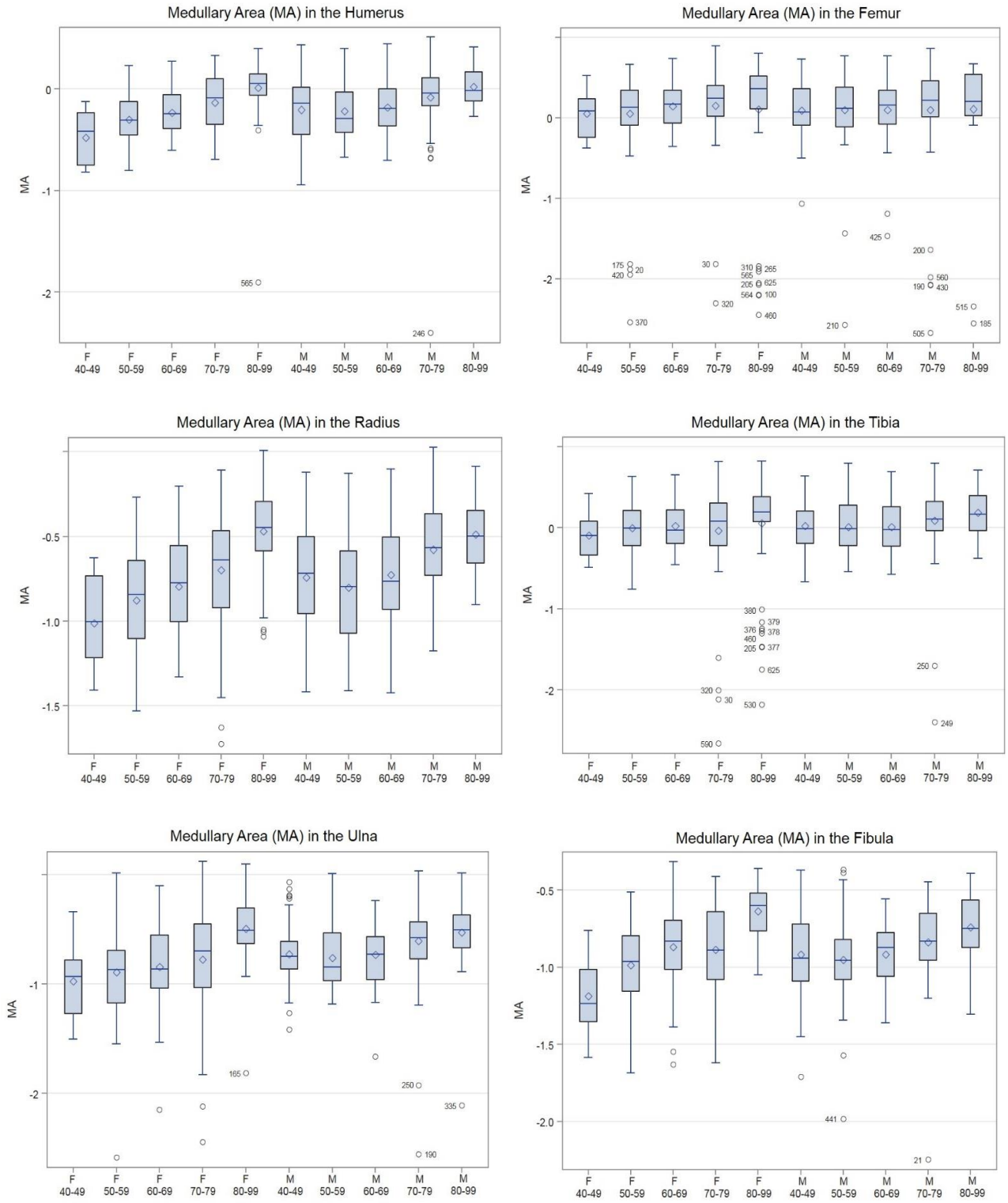

Figure E.3. Medullary area (MA) by sex and age group within each element

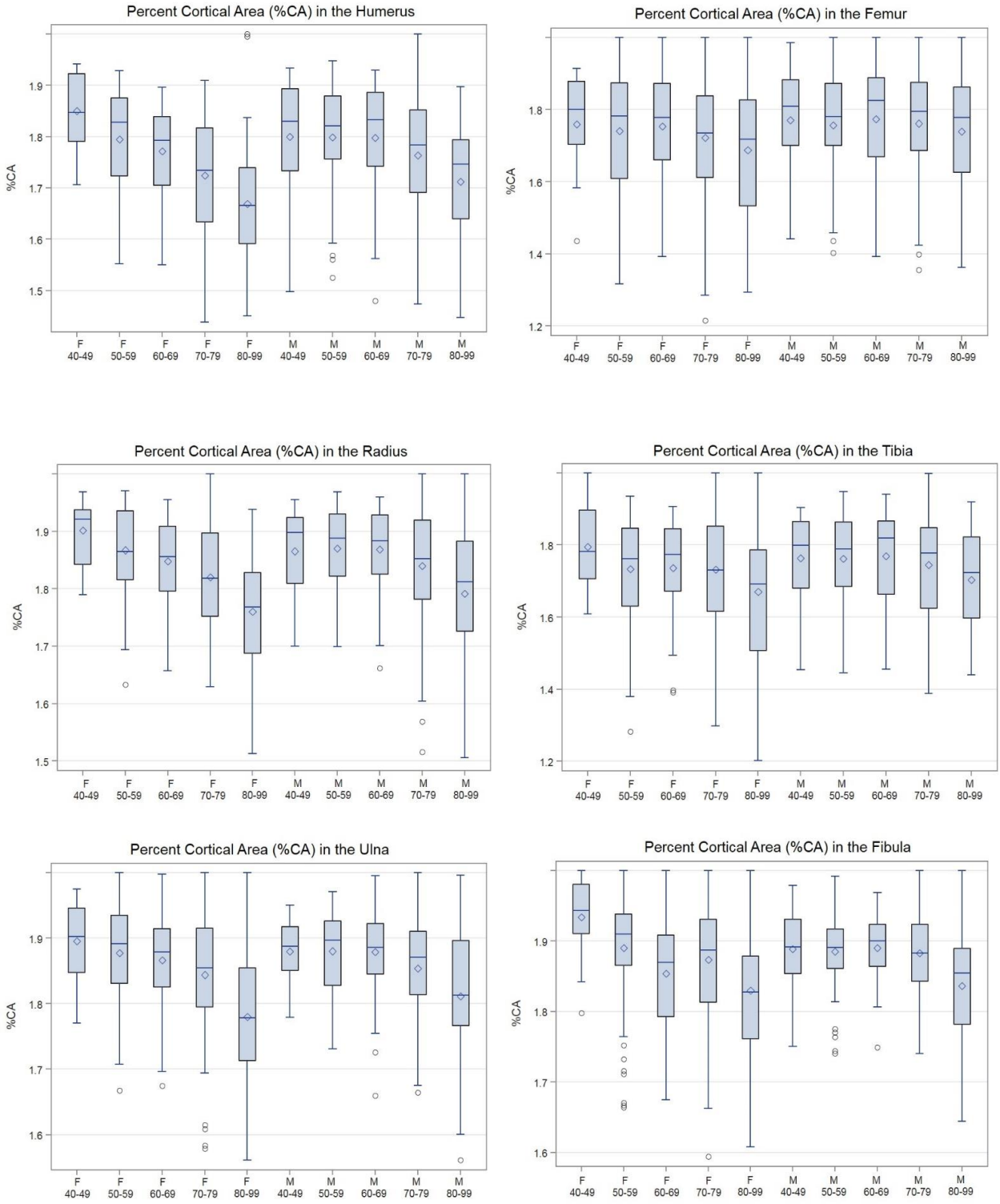

Figure E.4. Percent Cortical Area (%CA) by sex and age group within each element

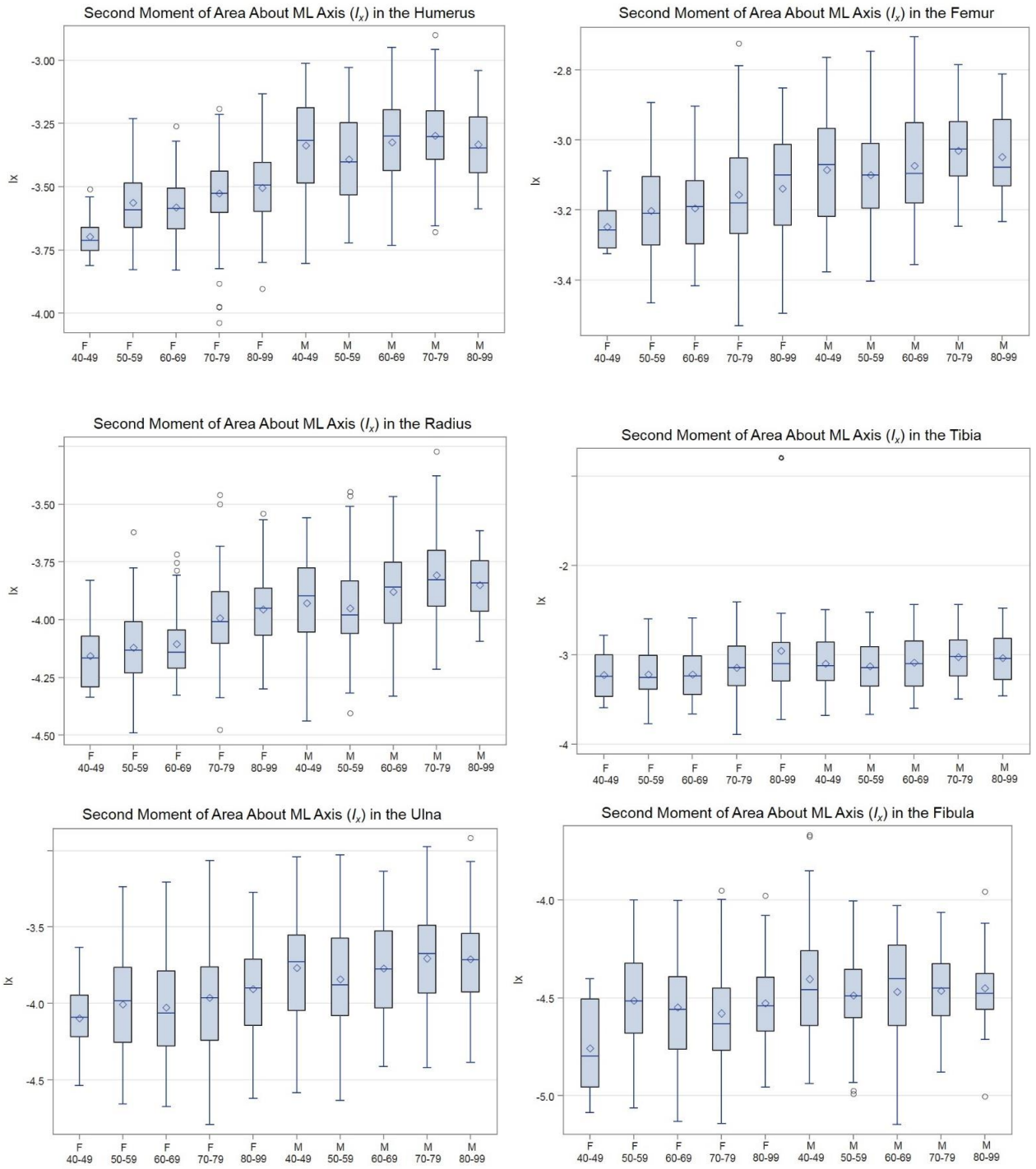

Figure E.5. Second moment of area about the mediolateral (ML) axis (I_x) by sex and age group within each element

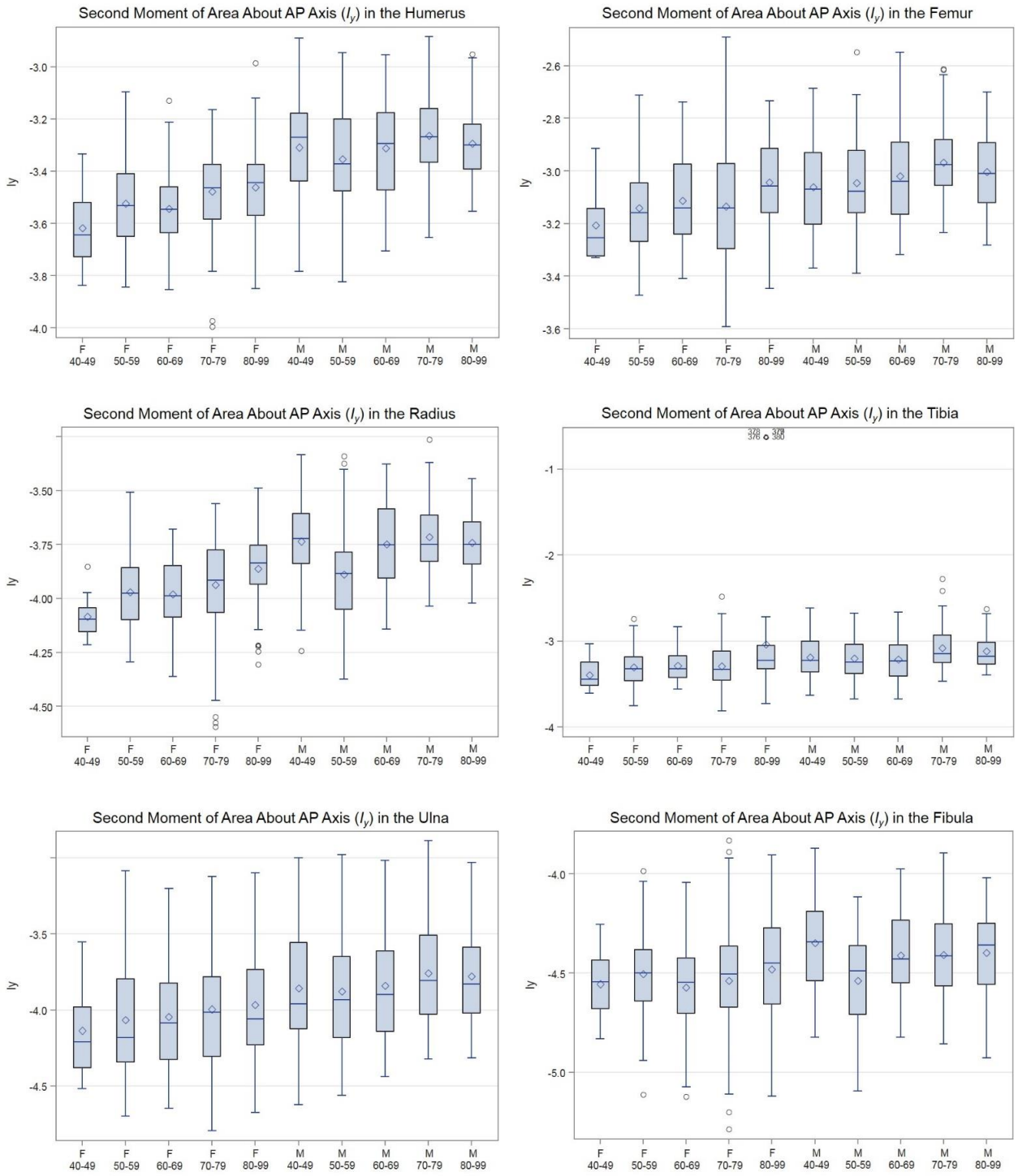

Figure E.6. Second moment of area about the anteroposterior (AP) axis (I_y) by sex and age group within each element

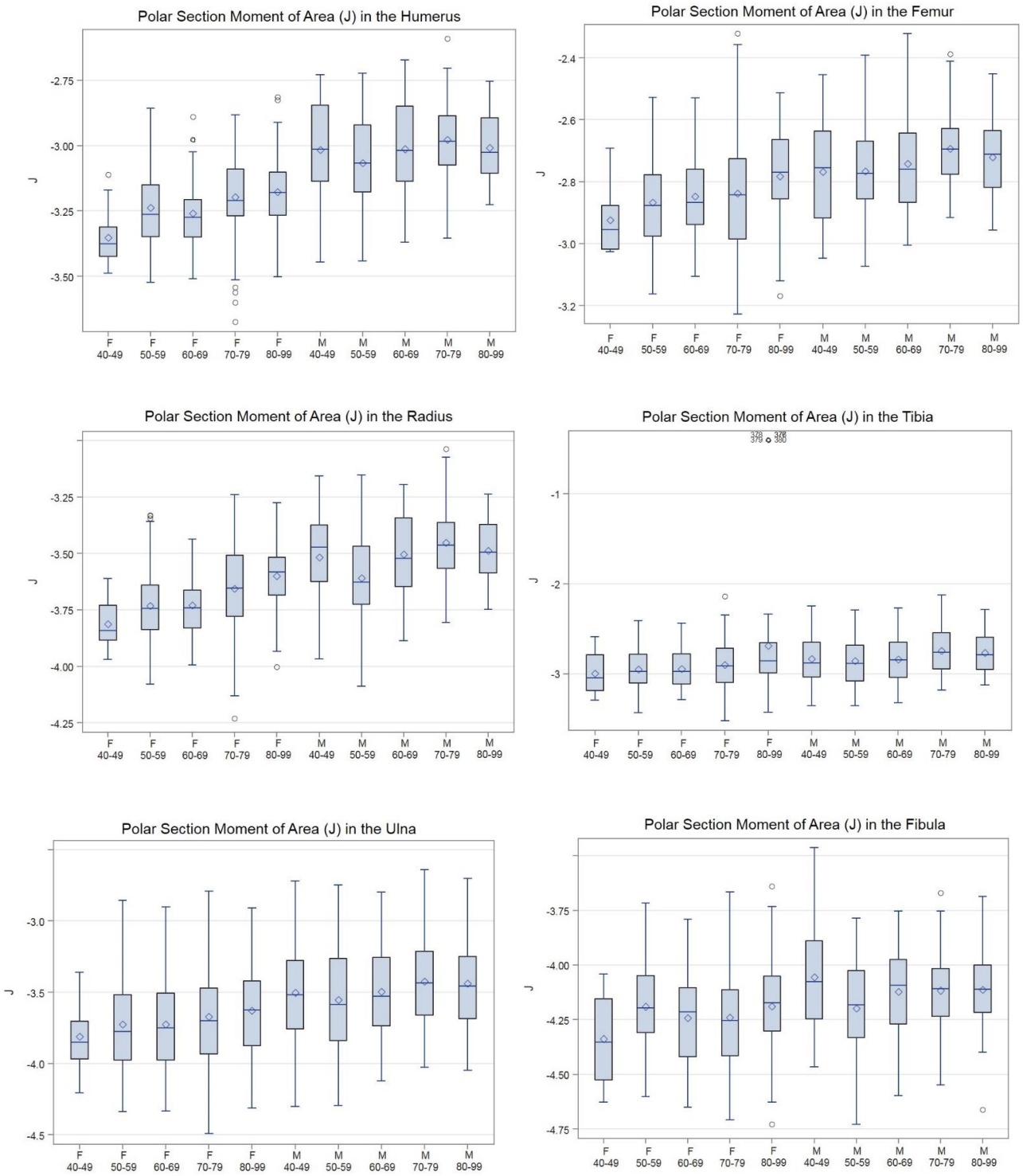

Figure E.7. Polar second moment of area (J) by sex and age group within each element

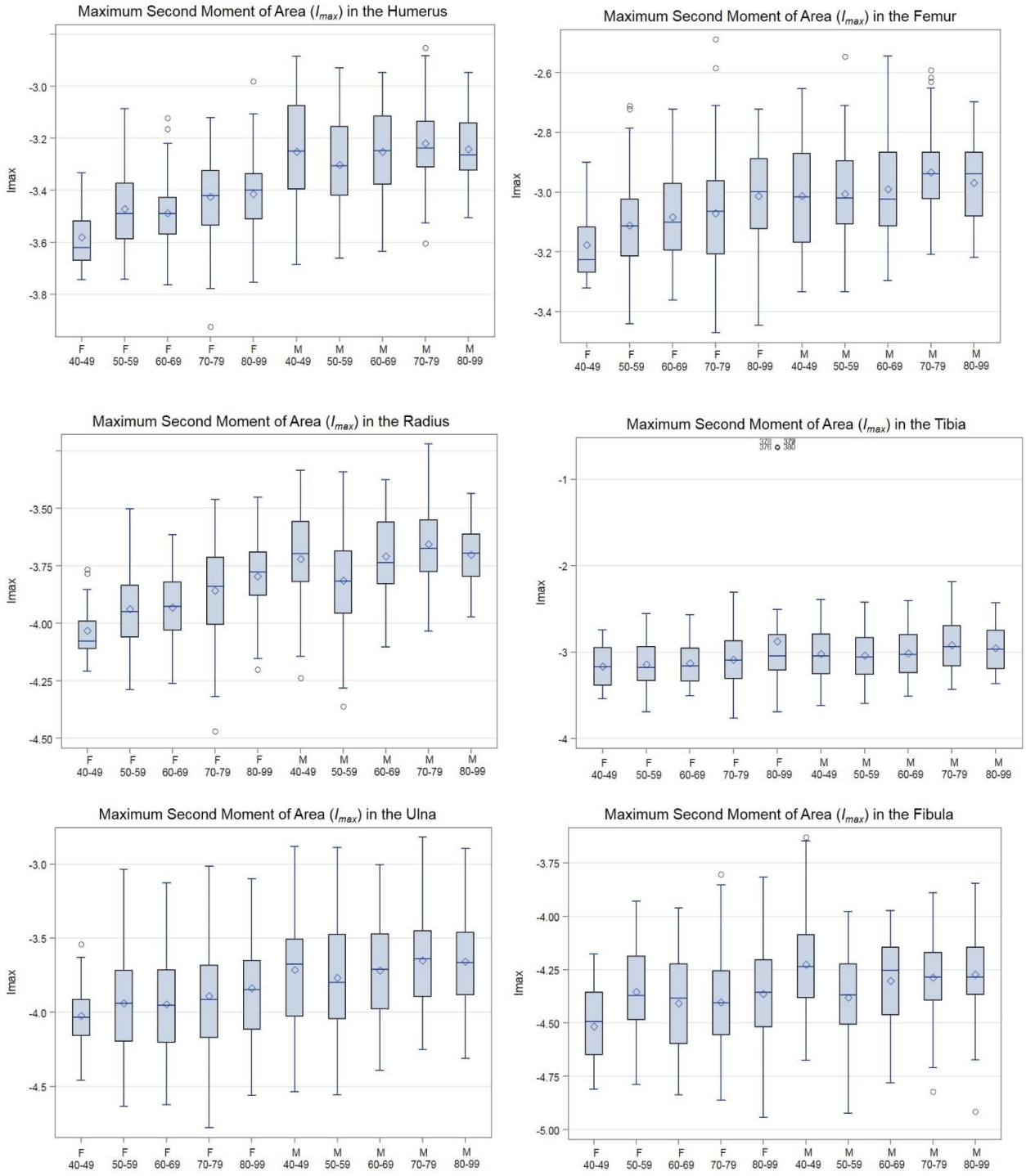

Figure E.8. Maximum second moment of area (I_{max}) by sex and age group within each element

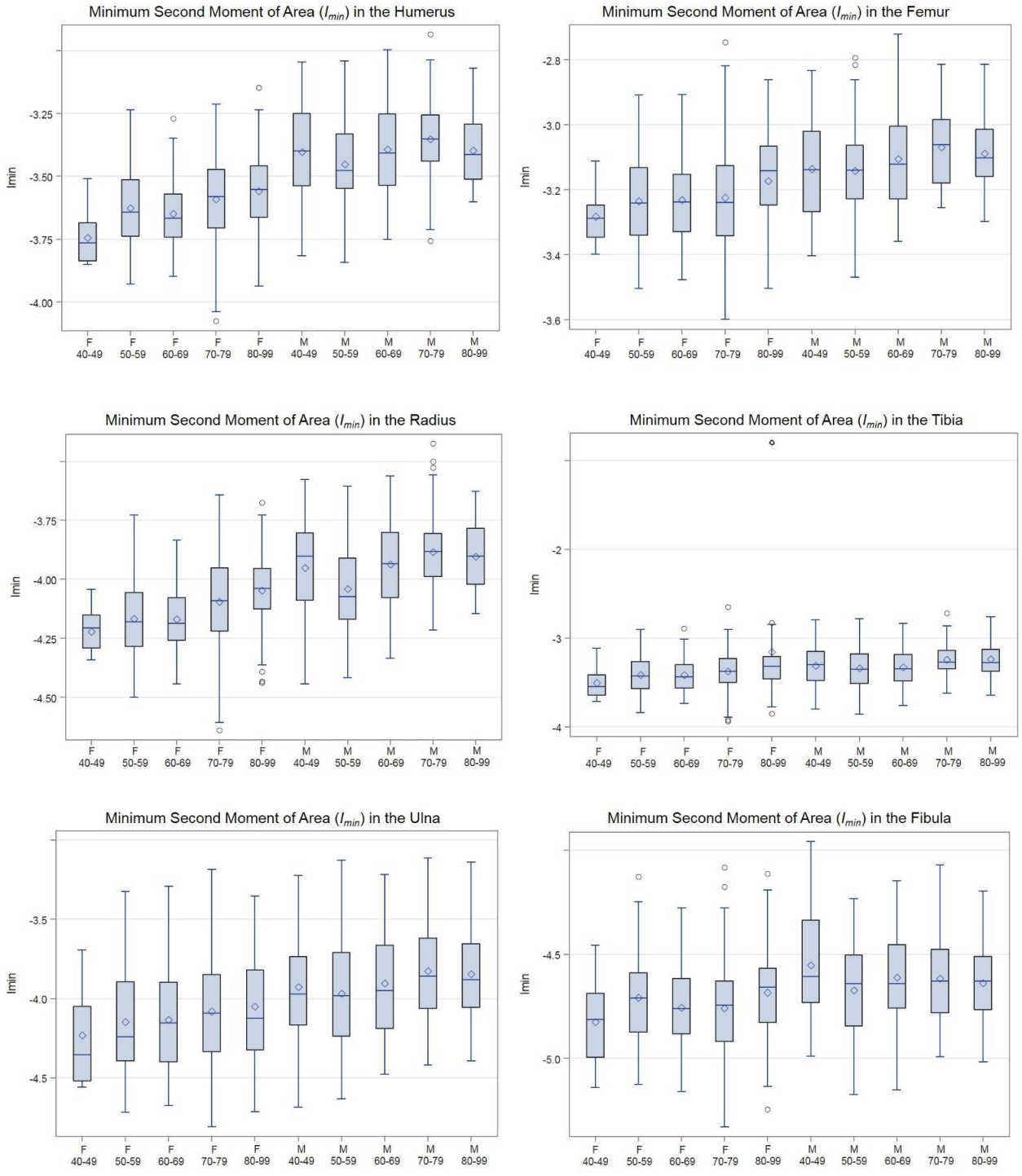

Figure E.9. Minimum second moment of area (I_{min}) by sex and age group within each element

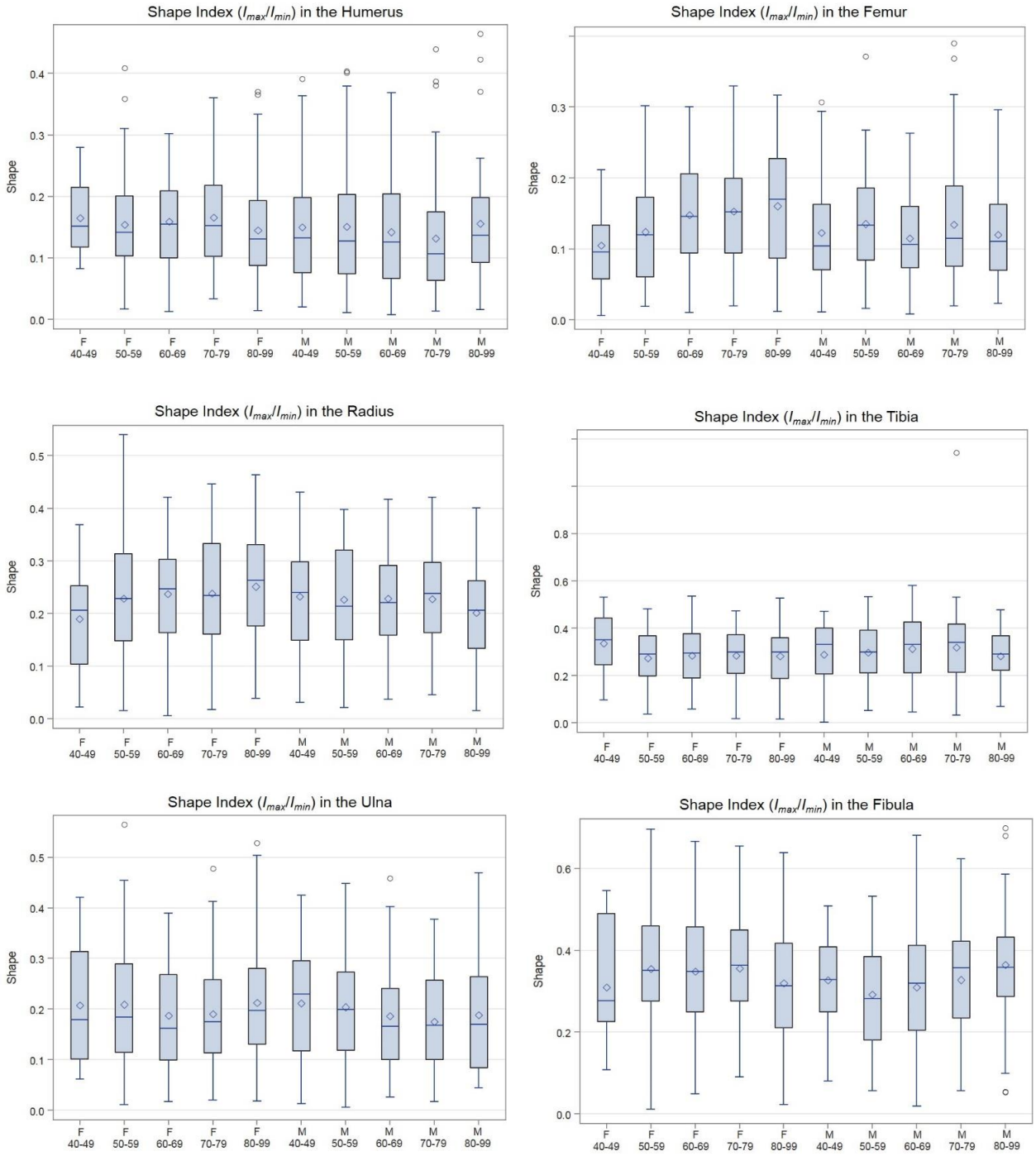

Figure E.10. Shape index (I_{max}/I_{min}) by sex and age group within each element

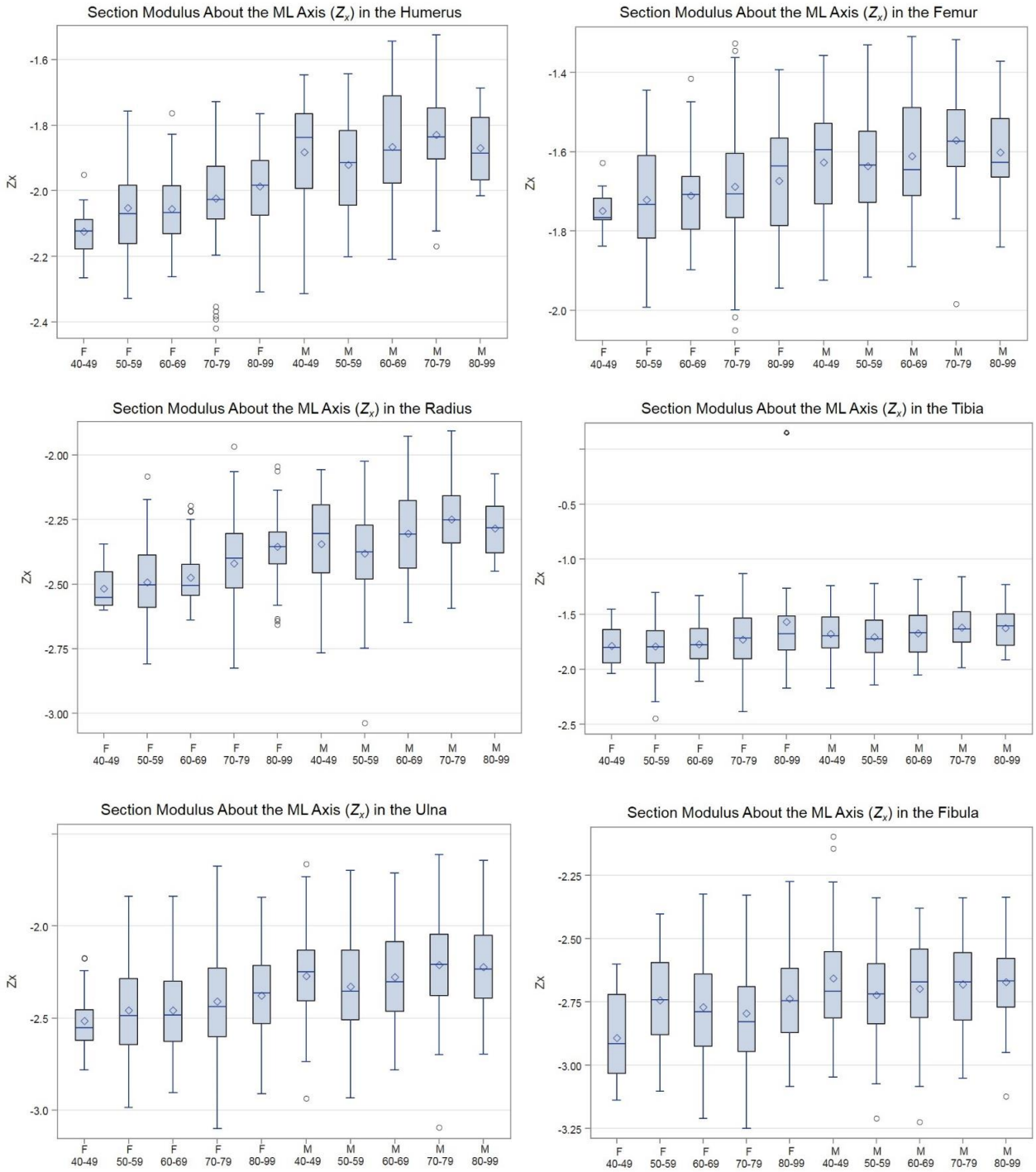

Figure E.11. Section modulus about the mediolateral (ML) axis (Z_x) by sex and age group within each element

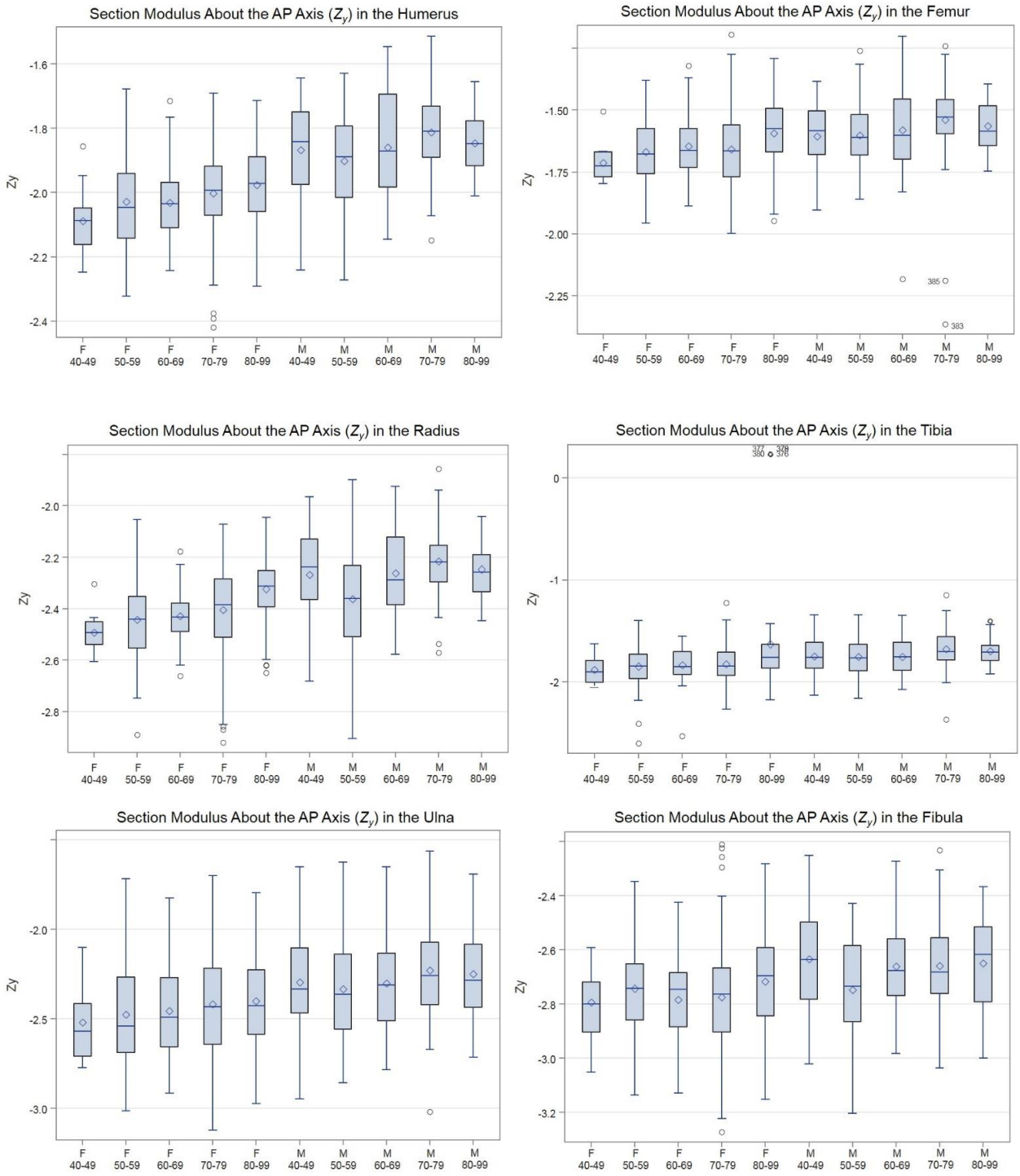

Figure E.12. Section modulus about the anteroposterior (AP) axis (Z_y) by sex and age group within each element

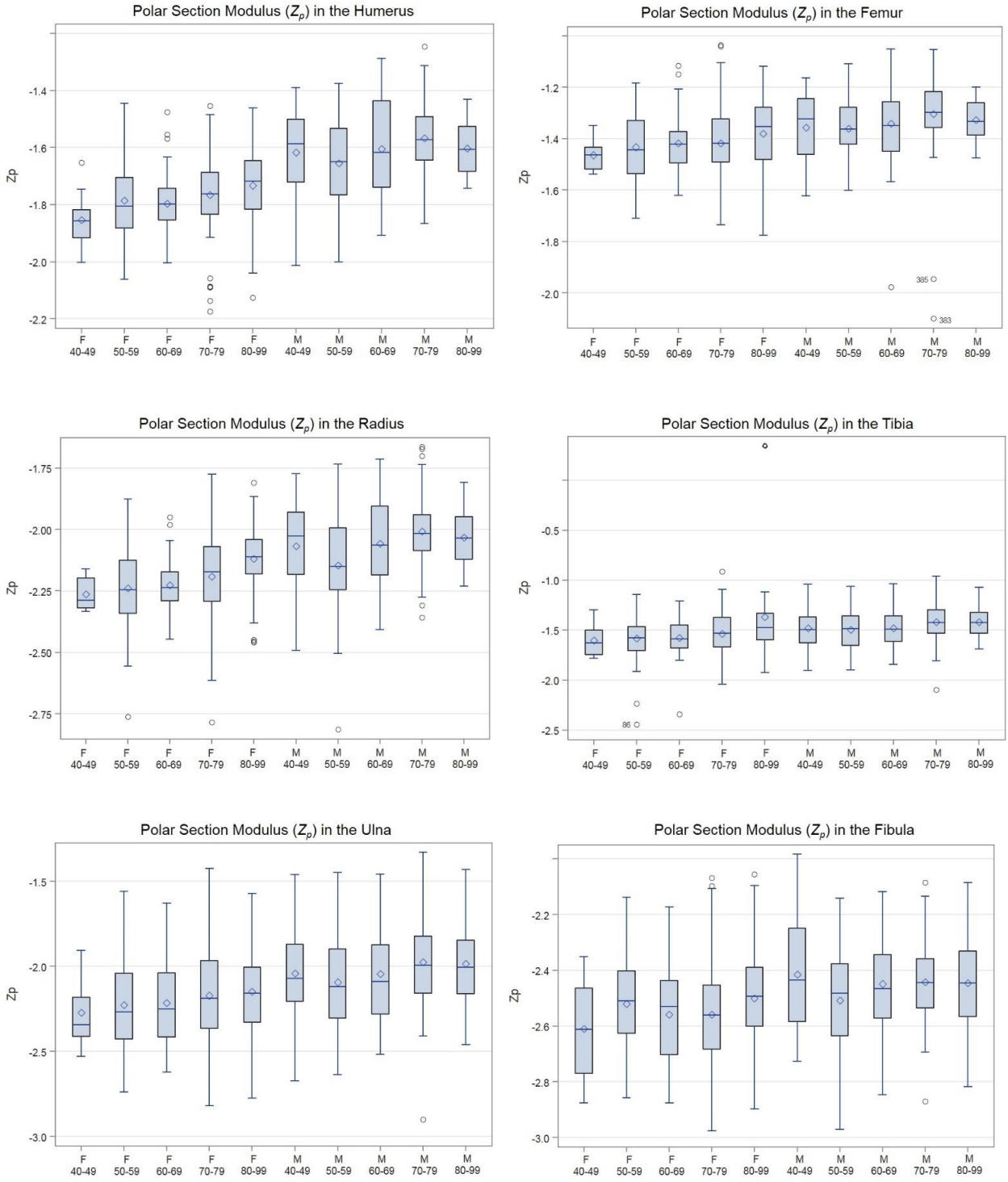

Figure E.13. Polar section modulus (Z_p) by sex and age group within each element

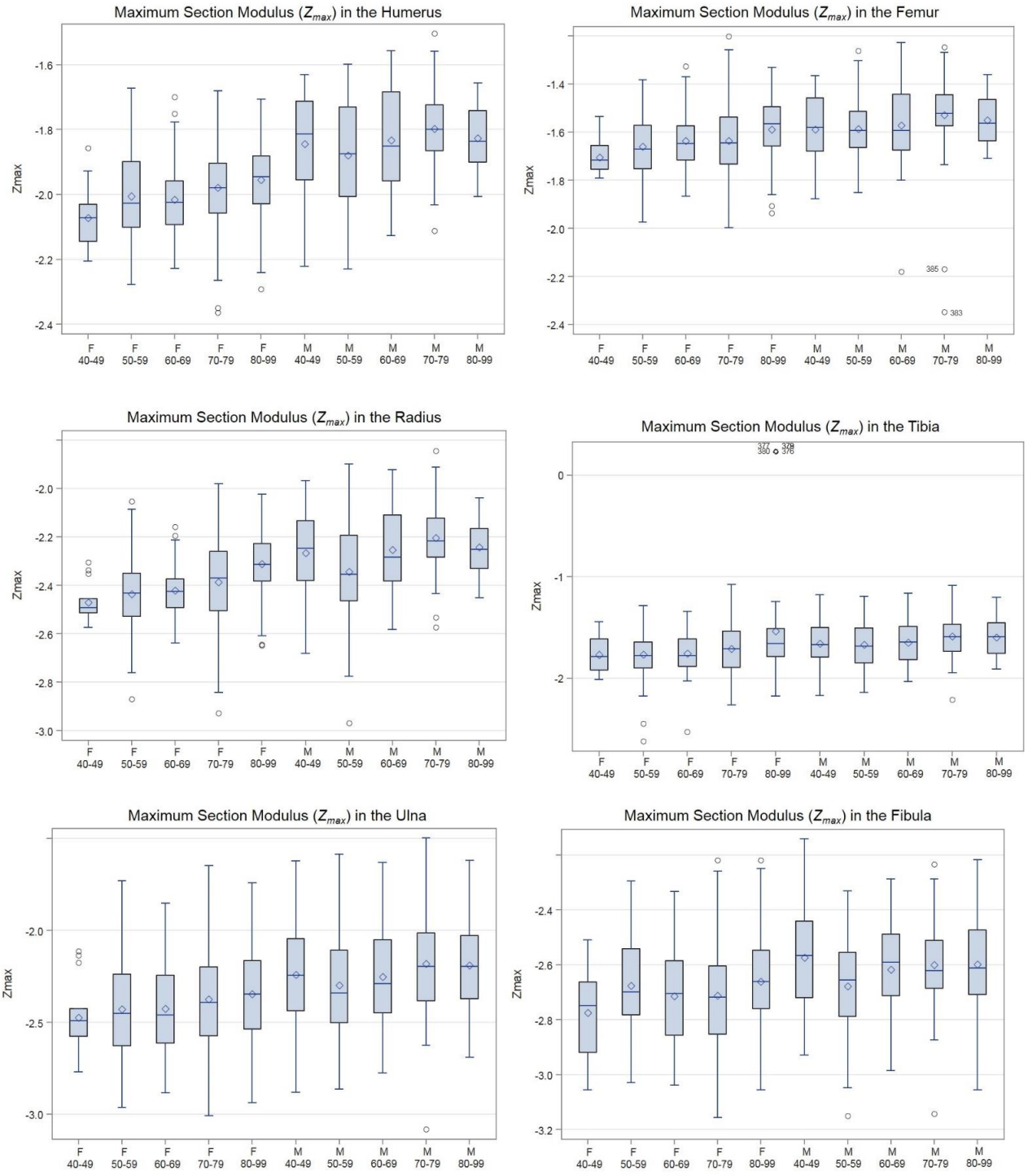

Figure E.14. Maximum section modulus (Z_{max}) by sex and age group within each element

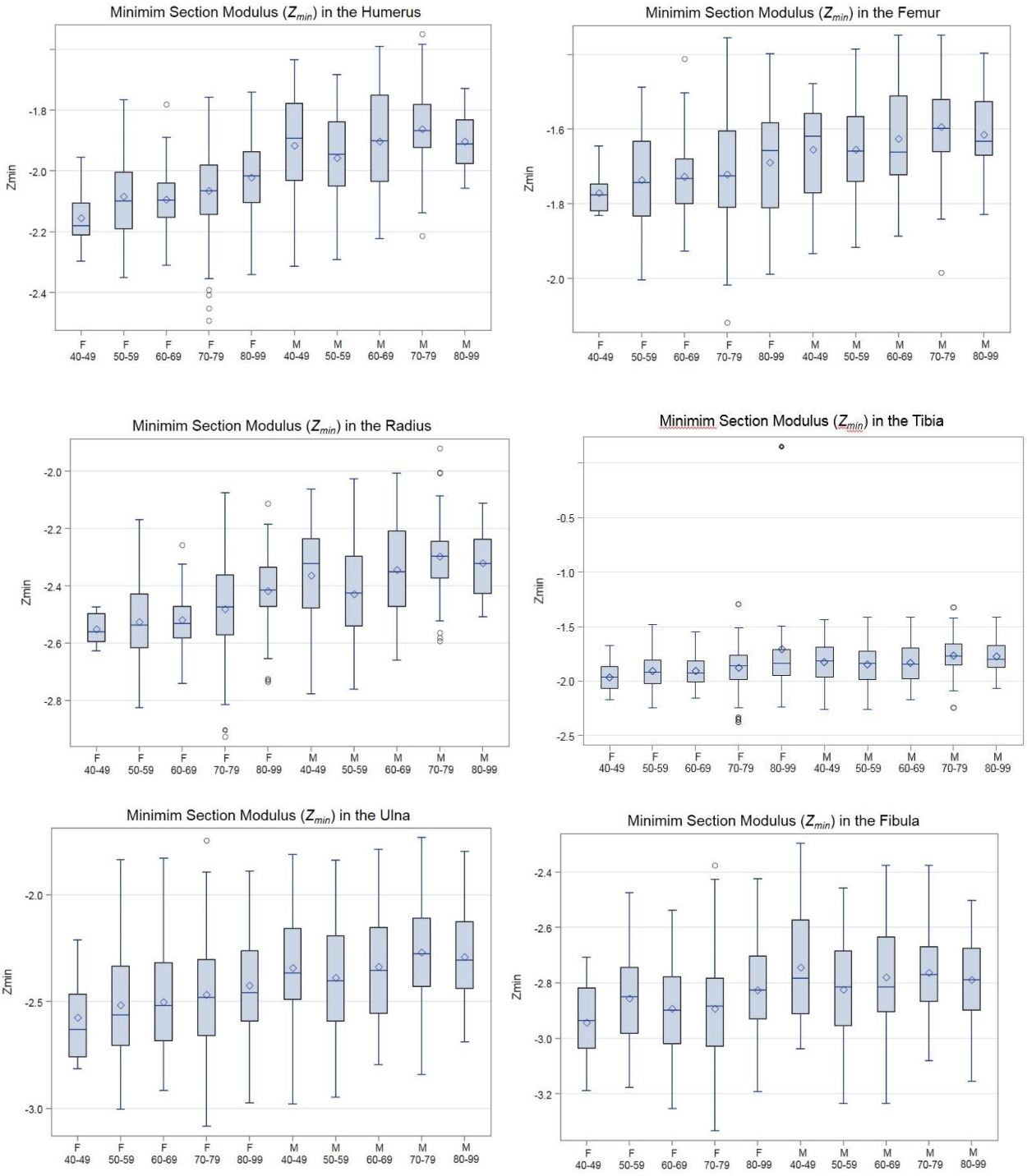

Figure E.15. Minimum section modulus (Z_{min}) by sex and age group within each element

APPENDIX F
WITHIN BONE LEAST SQUARES MEANS COMPARISONS FOR SEX AND AGE GROUP

Table F.1. Cortical area LS means in the upper limb by sex and age

	Humerus		Radius		Ulna	
Age Group	Female	Male	Female	Male	Female	Male
40-49	0.0084	0.1341	-0.2735	-0.1901	-0.2442	-0.1464
50-59	0.0359	0.1231	-0.2746	-0.1999	-0.2419	-0.1406
60-69	0.0045	0.1635	-0.3095	-0.1548	-0.2719	-0.1222
70-79	0.0212	0.1230	-0.2891	-0.1807	-0.2424	-0.1424
80-99	0.0316	0.1111	-0.3126	-0.2106	-0.2847	-0.1499

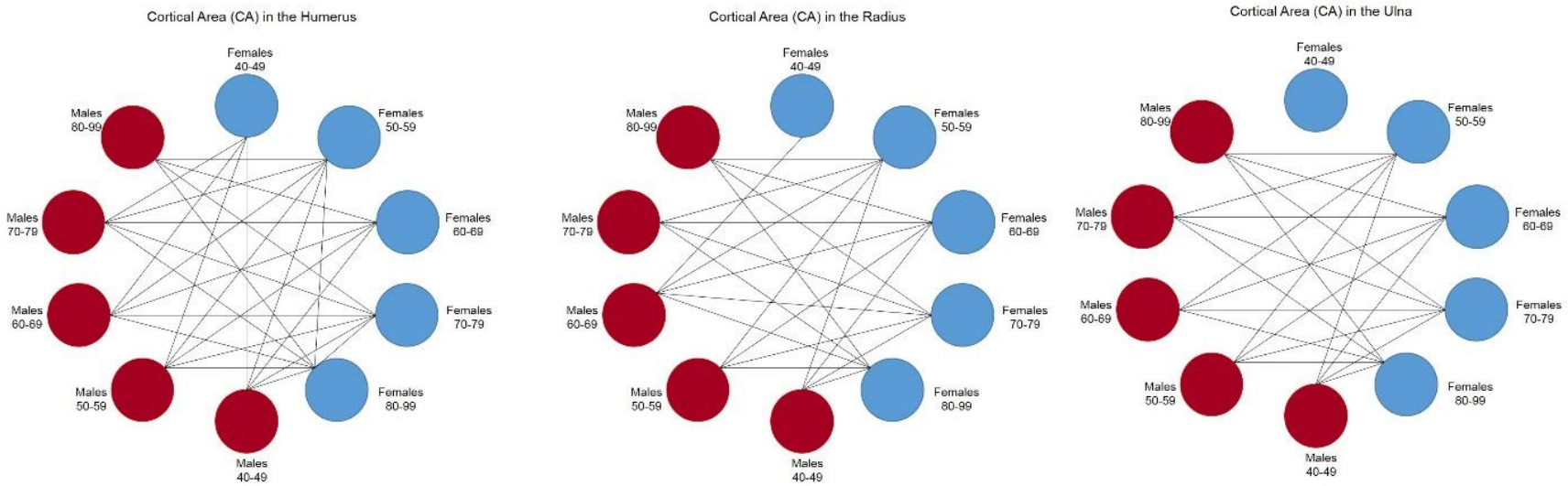

Figure F.1. Results of cortical area LS means comparisons in the upper limb by sex and age
Lines between groups indicate significant ($p < 0.05$) results from post-hoc LS means comparisons with Tukey-Kramer adjustment for multiple comparisons.

Table F.2. Cortical area LS means in the lower limb by sex and age

	Femur		Tibia		Fibula	
Age Group	Female	Male	Female	Male	Female	Male
40-49	0.3613	0.3881	0.1813	0.2425	-0.4090	-0.2643
50-59	0.3472	0.4060	0.2133	0.2602	-0.3083	-0.3194
60-69	0.3399	0.4151	0.1817	0.2687	-0.3898	-0.2828
70-79	0.3409	0.3995	0.2064	0.2879	-0.3833	-0.3358
80-99	0.3173	0.3901	0.3408	0.2708	-0.4216	-0.3399

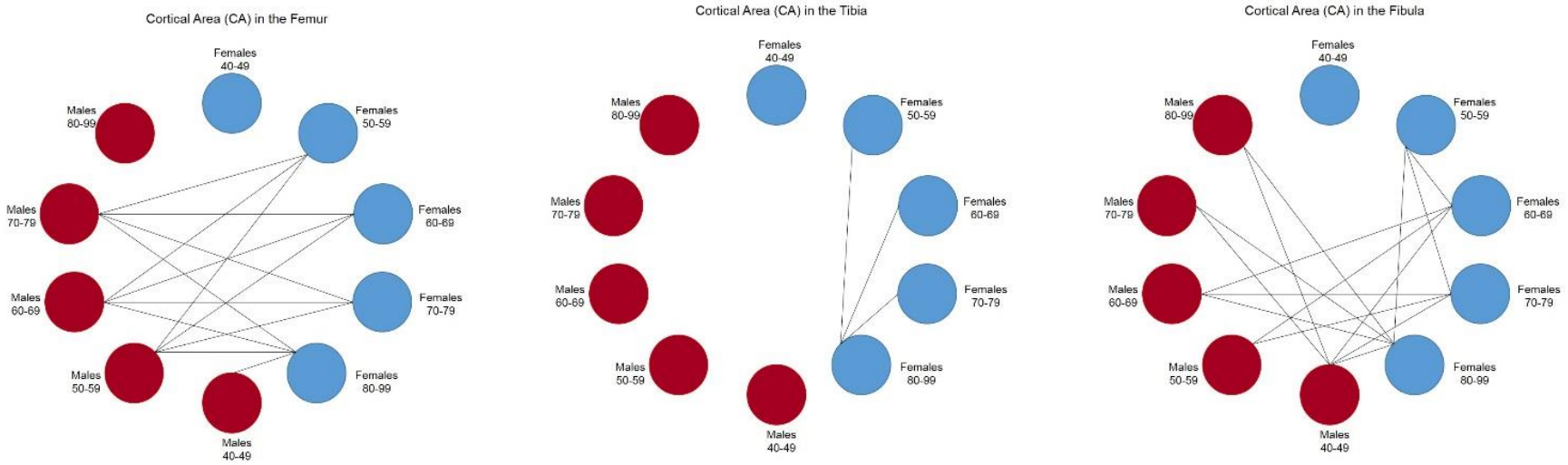

Figure F.2. Results of cortical area LS means comparisons in the lower limb by sex and age
Lines between groups indicate significant ($p < 0.05$) results from post-hoc LS means comparisons with Tukey-Kramer adjustment for multiple comparisons.

Table F.3. Total area LS means in the upper limb by sex and age

	Humerus		Radius		Ulna	
Age Group	Female	Male	Female	Male	Female	Male
40-49	0.1814	0.3384	-0.1525	-0.0517	-0.1310	-0.0216
50-59	0.2400	0.3314	-0.1453	-0.0662	-0.1187	-0.0173
60-69	0.2358	0.3732	-0.1565	-0.0184	-0.1364	.0070
70-79	0.2770	0.3701	-0.1242	-0.0153	-0.0949	.0032
80-99	0.2842	0.3893	-0.0938	-0.0050	-0.0927	.0334

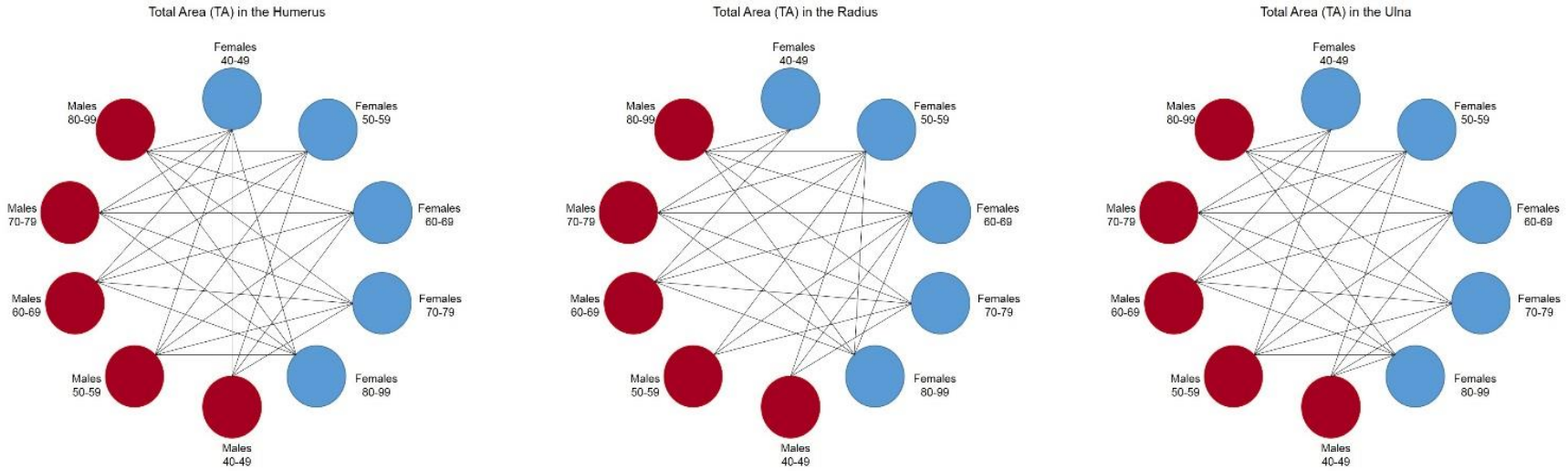

Figure F.3. Results of total area LS means comparisons in the upper limb by sex and age
Lines between groups indicate significant ($p < 0.05$) results from post-hoc LS means comparisons with Tukey-Kramer adjustment for multiple comparisons.

Table F.4. Total area LS means in the lower limb by sex and age group

	Femur		Tibia		Fibula	
Age Group	Female	Male	Female	Male	Female	Male
40-49	0.5800	0.6161	0.4147	0.4776	-0.2885	-0.1501
50-59	0.6077	0.6540	0.4726	0.4954	-0.1981	-0.2082
60-69	0.6075	0.6593	0.4455	0.5098	-0.2444	-0.1703
70-79	0.6244	0.6375	0.4880	0.5430	-0.2349	-0.2074
80-99	0.6099	0.6563	0.6536	0.5539	-0.2232	-0.1797

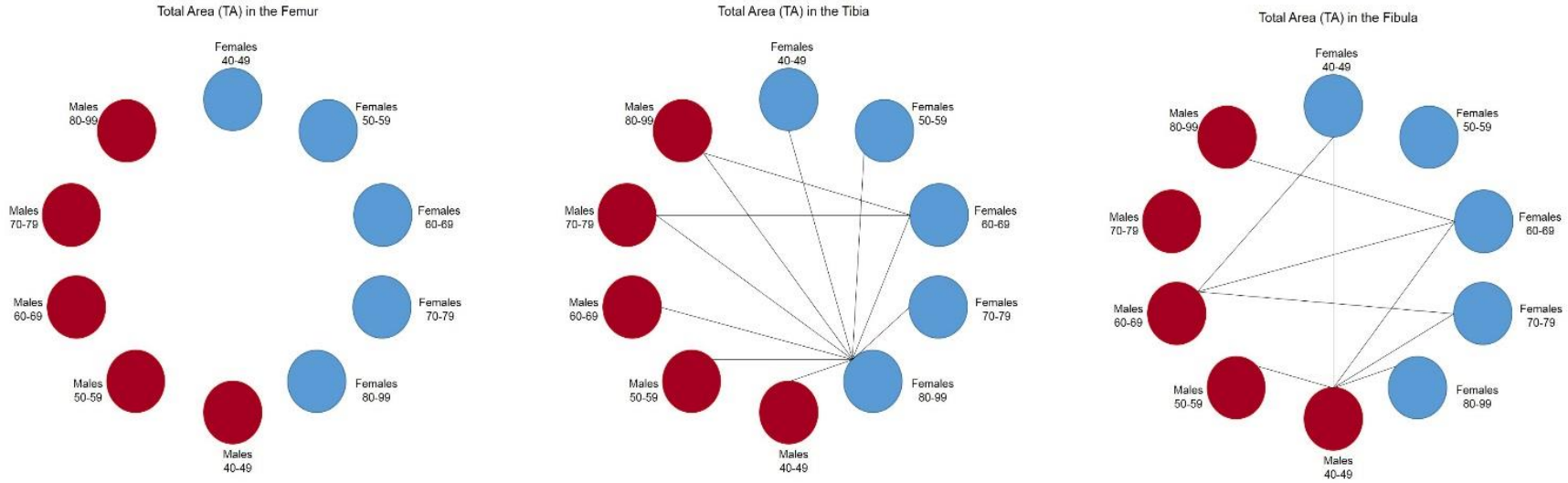

Figure F.4. Results of total area LS means comparisons in the lower limb by sex and age
Lines between groups indicate significant ($p < 0.05$) results from post-hoc LS means comparisons with Tukey-Kramer adjustment for multiple comparisons.

Table F.5. Medullary area LS means in the upper limb by sex and age

	Humerus		Radius		Ulna	
Age Group	Female	Male	Female	Male	Female	Male
40-49	-0.3586	-0.1482	-0.8085	-0.6757	-0.7930	-0.6613
50-59	-0.2268	-0.1384	-0.8028	-0.6978	-0.8009	-0.6531
60-69	-0.1771	-0.1016	-0.7331	-0.6435	-0.7553	-0.6223
70-79	-0.1039	-0.0223	-0.6856	-0.5581	-0.6819	-0.5980
80-99	-0.0132	-0.0436	-0.5283	-0.4721	-0.5764	-0.4736

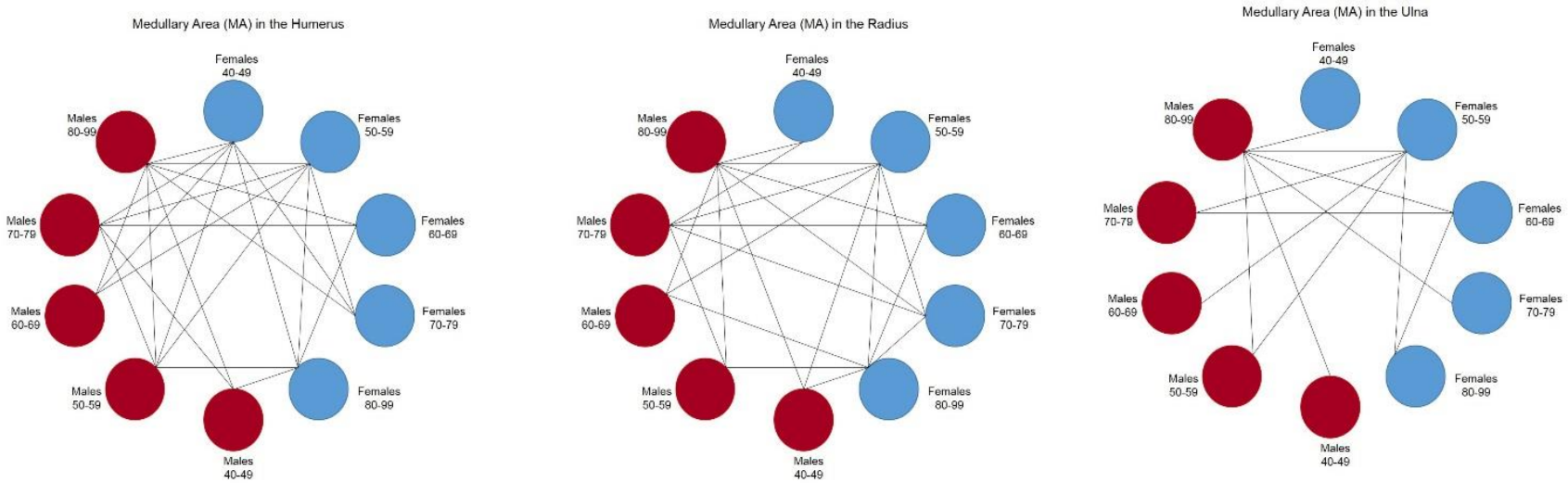

Figure F.5. Results of MA LS means comparisons in the upper limb by sex and age
Lines between groups indicate significant ($p < 0.05$) results from post-hoc LS means comparisons with Tukey-Kramer adjustment for multiple comparisons.

Table F.6. Medullary area LS means in the lower limb by sex and age group

	Femur		Tibia		Fibula	
Age Group	Female	Male	Female	Male	Female	Male
40-49	0.0958	0.1395	-0.0062	0.0784	-0.9440	-0.8440
50-59	0.1595	0.1811	0.0622	0.0805	-0.9182	-0.8923
60-69	0.1889	0.1812	0.0804	0.0921	-0.8440	-0.8500
70-79	0.2393	0.0552	0.1346	0.1436	-0.8317	-0.8241
80-99	0.1105	0.1173	0.0508	0.1918	-0.6784	-0.7379

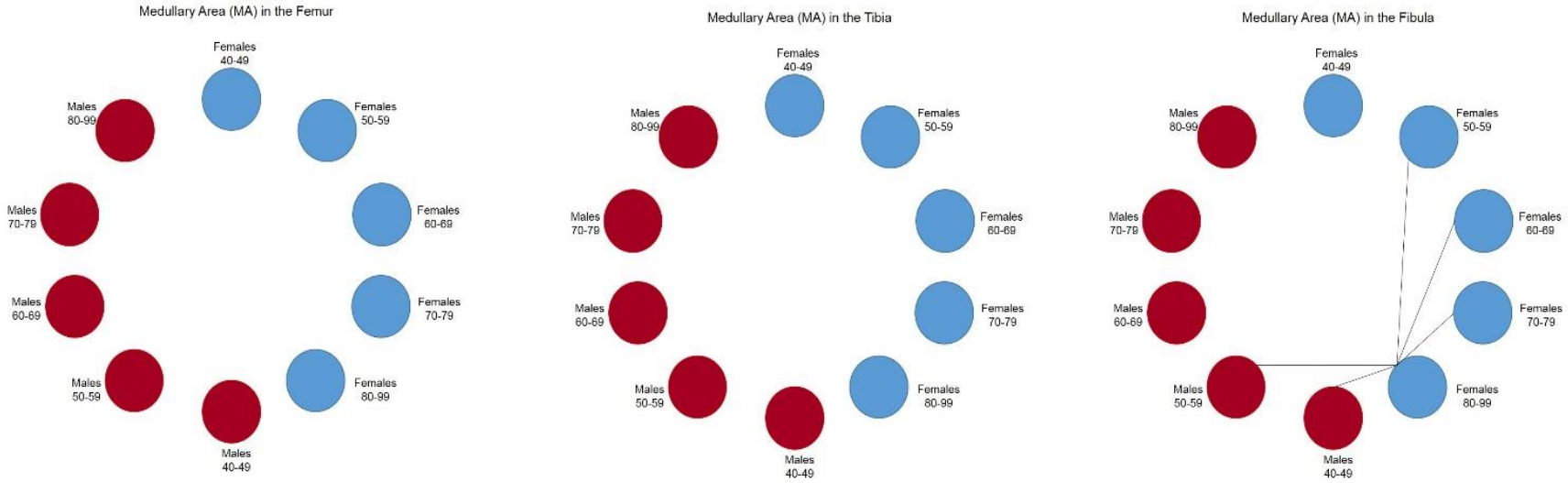

Figure F.6. Results of MA LS means comparisons in the lower limb by sex and age
Lines between groups indicate significant ($p < 0.05$) results from post-hoc LS means comparisons with Tukey-Kramer adjustment for multiple comparisons.

Table F.7. Percent cortical area LS means in the upper limb by sex and age

	Humerus		Radius		Ulna	
Age Group	Female	Male	Female	Male	Female	Male
40-49	1.8270	1.7957	1.8790	1.8615	1.8867	1.8751
50-59	1.7958	1.7917	1.8707	1.8663	1.8768	1.8767
60-69	1.7687	1.7902	1.8470	1.8636	1.8645	1.8706
70-79	1.7442	1.7529	1.8351	1.8345	1.8524	1.8543
80-99	1.6841	1.7217	1.7812	1.7944	1.8080	1.8165

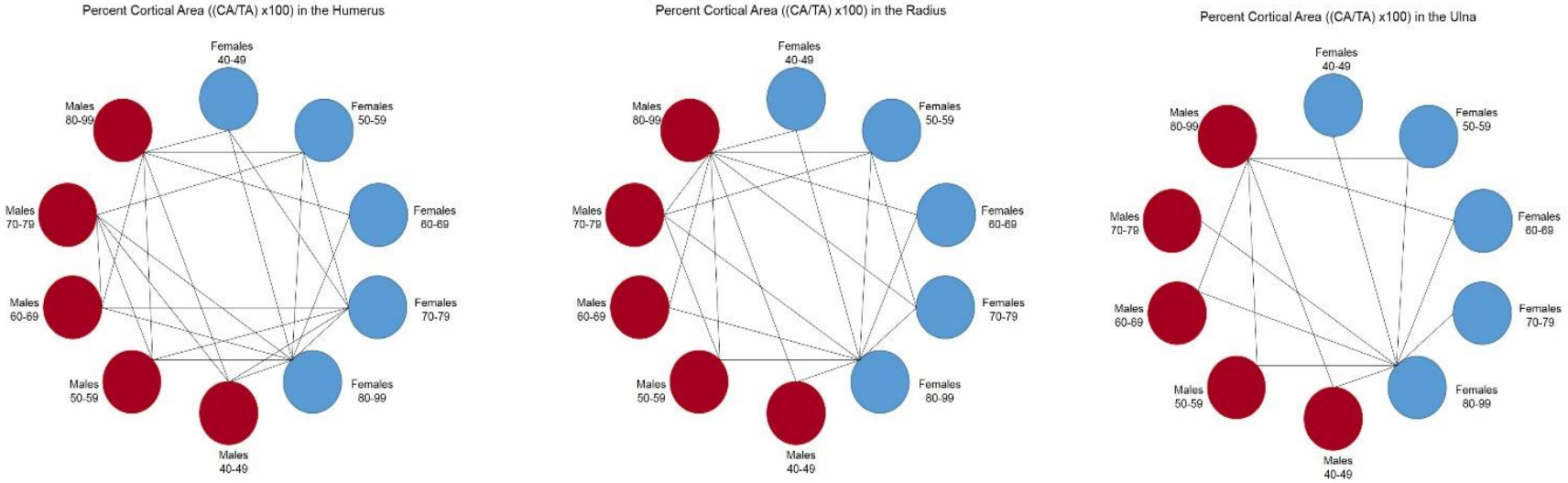

Figure F.7. Results of percent CA LS means comparisons in the upper limb by sex and age
Lines between groups indicate significant ($p < 0.05$) results from post-hoc LS means comparisons with Tukey-Kramer adjustment for multiple comparisons.

Table F.8. Percent cortical area LS means in the lower limb by sex and age

	Femur		Tibia		Fibula	
Age Group	Female	Male	Female	Male	Female	Male
40-49	1.7812	1.7719	1.7666	1.7649	1.8795	1.8857
50-59	1.7395	1.7520	1.7406	1.7647	1.8897	1.8887
60-69	1.7323	1.7557	1.7362	1.7588	1.8546	1.8875
70-79	1.7164	1.7620	1.7184	1.7449	1.8515	1.8715
80-99	1.7074	1.7338	1.6872	1.7169	1.8015	1.8398

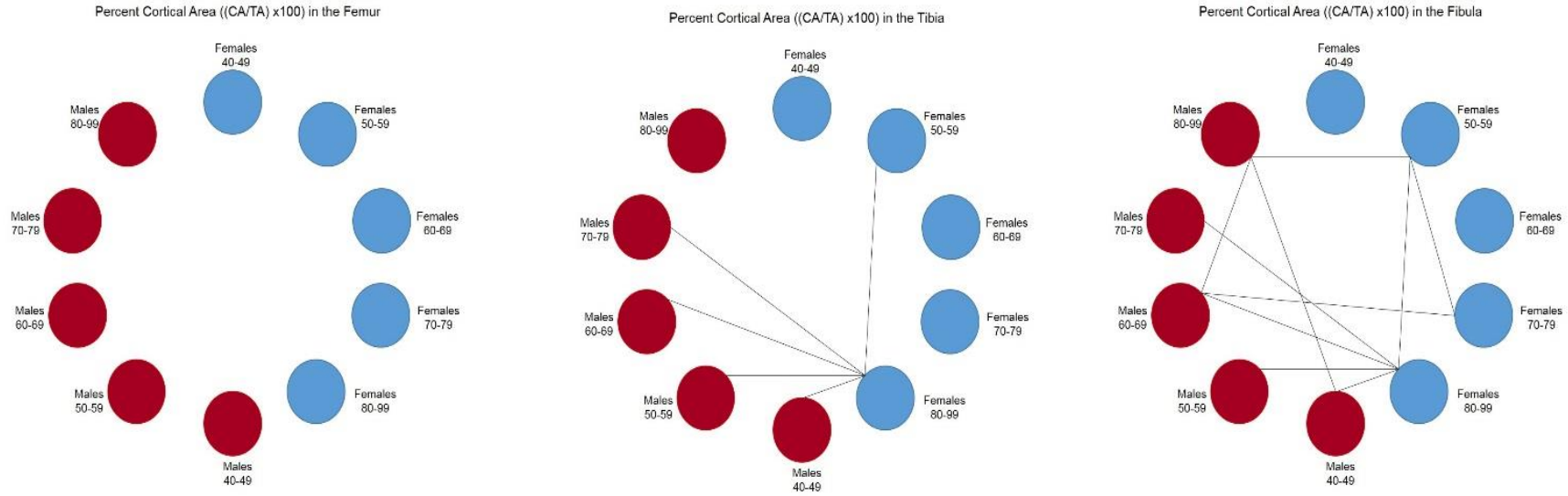

Figure F.8. Results of percent CA LS means comparisons in the lower limb by sex and age
Lines between groups indicate significant ($p < 0.05$) results from post-hoc LS means comparisons with Tukey-Kramer adjustment for multiple comparisons.

Table F.9. I_x LS means in the upper limb by sex and age

	Humerus		Radius		Ulna	
Age Group	Female	Male	Female	Male	Female	Male
40-49	-3.6117	-3.2897	-3.9541	-3.8646	-3.9483	-3.7037
50-59	-3.5021	-3.3281	-3.0443	-3.8569	-3.9247	-3.7673
60-69	-3.5290	-3.2624	-4.0525	-3.8158	-3.9783	-3.7104
70-79	-3.4587	-3.2842	-3.9495	-3.7866	-3.8982	-3.7095
80-99	-3.5294	-3.2834	-3.9742	-3.8148	-3.9171	-3.6684

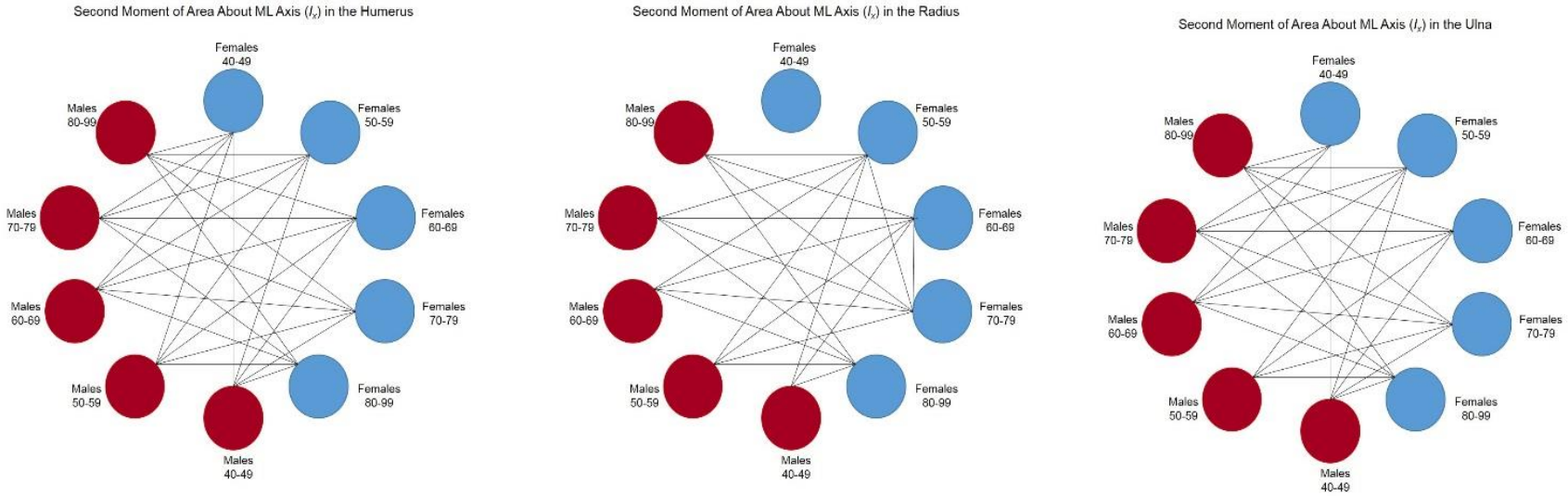

Figure F.9. Results of I_x LS means comparisons in the upper limb by sex and age group
Lines between groups indicate significant ($p < 0.05$) results from post-hoc LS means comparisons with Tukey-Kramer adjustment for multiple comparisons.

Table F.10. I_x LS means in the lower limb by sex and age group

	Femur		Tibia		Fibula	
Age Group	Female	Male	Female	Male	Female	Male
40-49	-3.1424	-3.0335	-3.1677	-3.0906	-4.6579	-4.3350
50-59	-3.1288	-3.0184	-3.1496	-3.0849	-4.3969	-4.3984
60-69	-3.1343	-3.0139	-3.1944	-3.0591	-4.4871	-4.4046
70-79	-3.0928	-3.0252	-3.0987	-3.0184	-4.4929	-4.4710
80-99	-3.1429	-3.0073	-2.8409	-3.0081	-4.5288	-4.4313

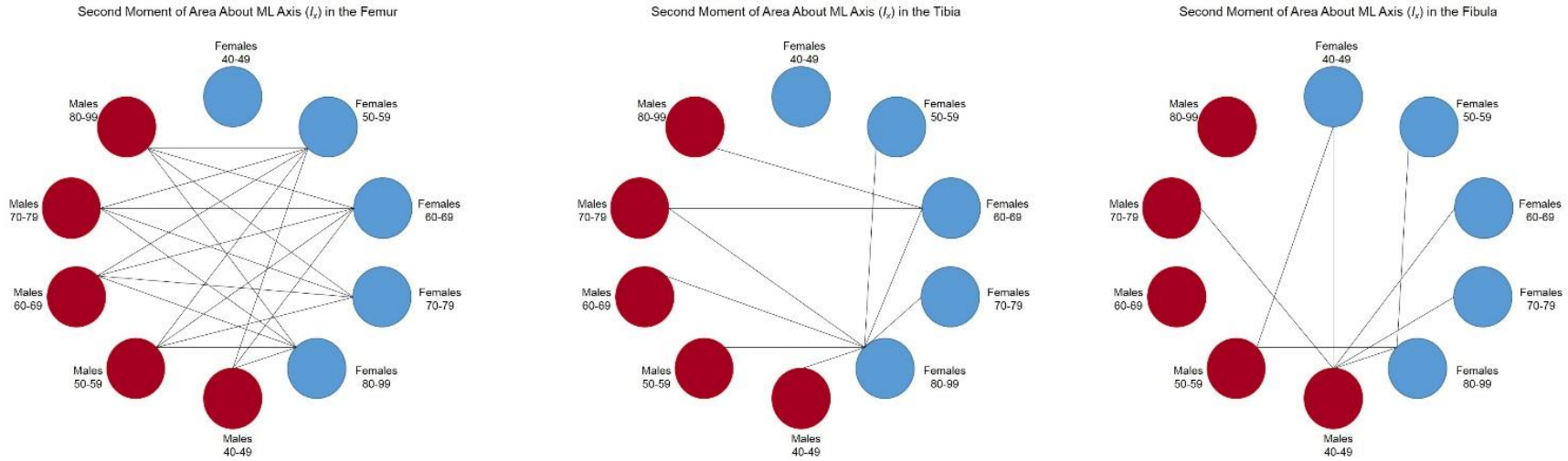

Figure F.10. Results of I_x LS means comparisons in the lower limb by sex and age group
Lines between groups indicate significant ($p < 0.05$) results from post-hoc LS means comparisons with Tukey-Kramer adjustment for multiple comparisons.

Table F.11. I_y LS means in the upper limb by sex and age

	Humerus		Radius		Ulna	
Age Group	Female	Male	Female	Male	Female	Male
40-49	-3.5572	-3.2481	-3.9842	-3.6794	-3.9717	-3.7995
50-59	-3.4651	-3.2859	-3.8972	-3.8029	-3.9788	-3.7894
60-69	-3.4925	-3.2488	-3.9249	-3.6830	-3.9892	-3.7752
70-79	-3.4280	-3.2517	-3.8753	-3.6891	-3.9338	-3.7602
80-99	-3.4929	-3.2420	-3.8830	-3.6896	-3.9889	-3.7496

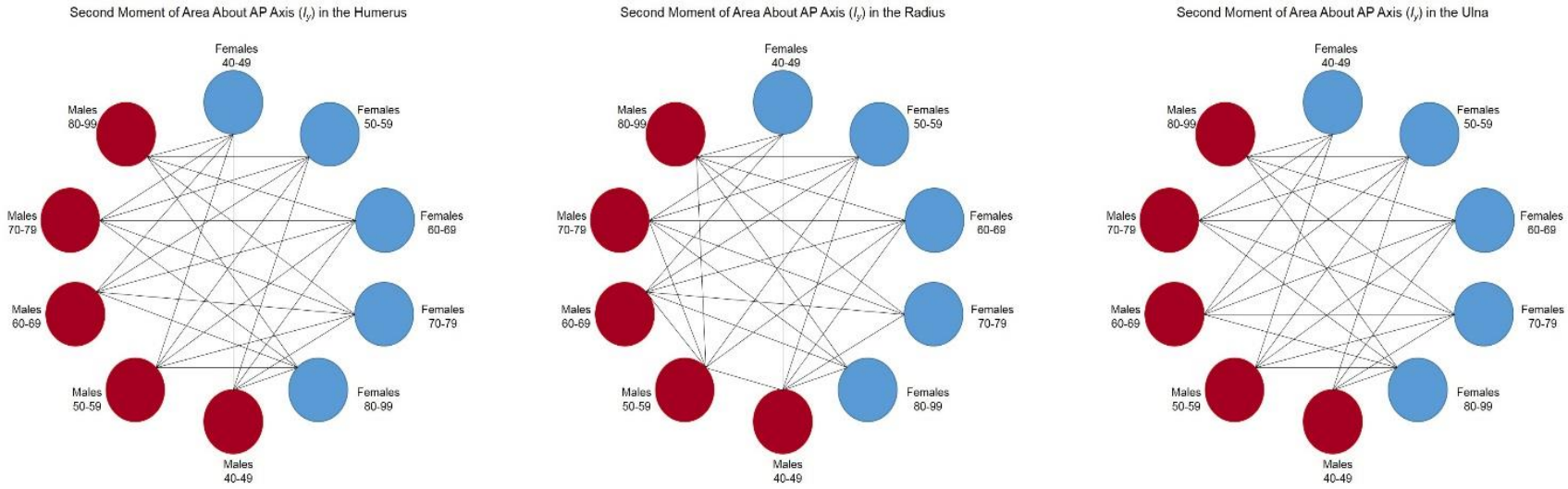

Figure F.11. Results of I_y LS means comparisons in the upper limb by sex and age group
Lines between groups indicate significant ($p < 0.05$) results from post-hoc LS means comparisons with Tukey-Kramer adjustment for multiple comparisons.

Table F.12. I_y LS means in the lower limb by sex and age group

	Femur		Tibia		Fibula	
Age Group	Female	Male	Female	Male	Female	Male
40-49	-3.0967	-3.0169	-3.3597	-3.1693	-4.5208	-4.2501
50-59	-3.0793	-3.9761	-3.2431	-3.1596	-4.4186	-4.4939
60-69	-3.0553	-2.9730	-3.2567	-3.1870	-4.5082	-4.3596
70-79	-3.0958	-2.9538	-3.2585	-3.0708	-4.4847	-4.4187
80-99	-3.0588	-2.9677	-2.9255	-3.0975	-4.4775	-4.3529

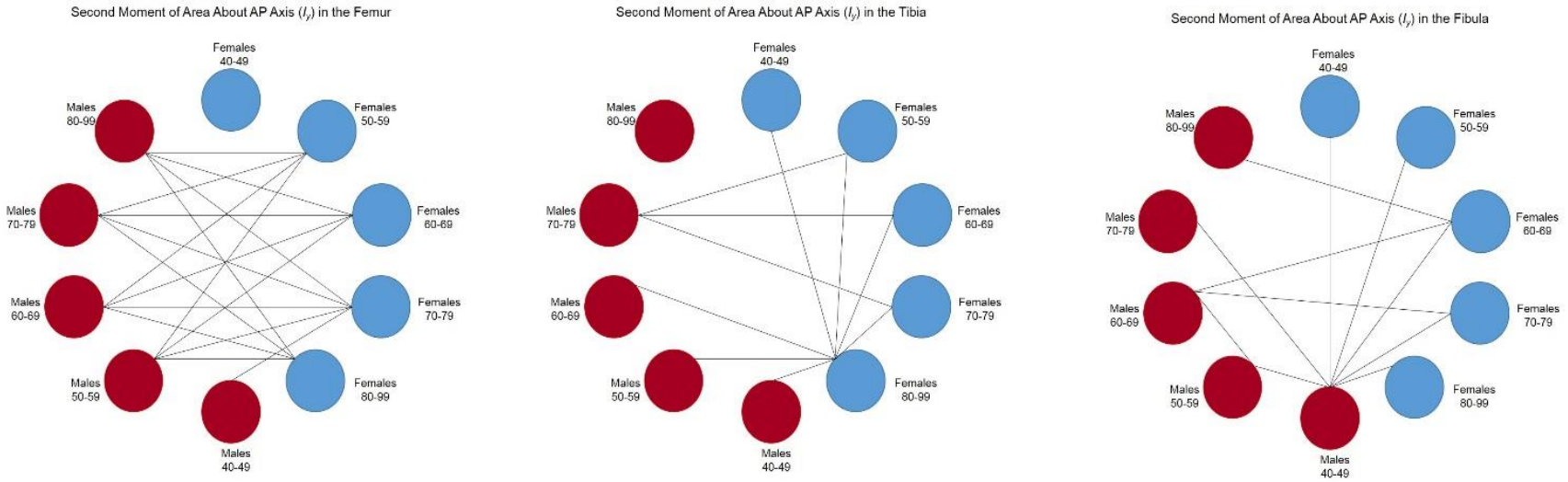

Figure F.12. Results of I_y LS means comparisons in the lower limb by sex and age group
Lines between groups indicate significant ($p < 0.05$) results from post-hoc LS means comparisons with Tukey-Kramer adjustment for multiple comparisons.

Table F.13. Polar section modulus (J) LS means in the upper limb by sex and age

	Humerus		Radius		Ulna	
Age Group	Female	Male	Female	Male	Female	Male
40-49	-3.2807	-2.9626	-3.6656	-3.4562	-3.6522	-3.4429
50-59	-3.1787	-3.0010	-3.6604	-3.5194	-3.6424	-3.4701
60-69	-3.2059	-2.9509	-3.6754	-3.4386	-3.6755	-3.4342
70-79	-3.1385	-2.9631	-3.6048	-3.4282	-3.6080	-3.4272
80-99	-3.2056	-2.9565	-3.6213	-3.4431	-3.6401	-3.4003

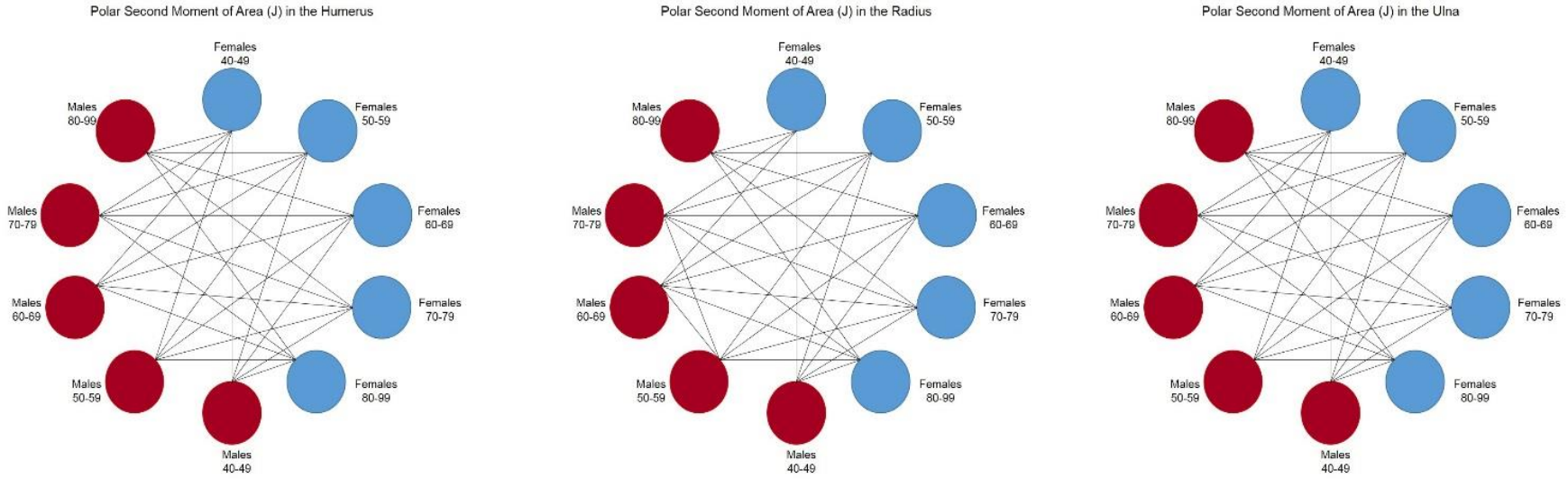

Figure F.13. Results of J LS means comparisons in the upper limb by sex and age
Lines between groups indicate significant ($p < 0.05$) results from post-hoc LS means comparisons with Tukey-Kramer adjustment for multiple comparisons.

Table F.14. Polar section modulus (J) LS means in the lower limb by sex and age

	Femur		Tibia		Fibula	
Age Group	Female	Male	Female	Male	Female	Male
40-49	-2.8151	-2.7199	-2.9500	-2.8218	-4.2745	-3.9738
50-59	-2.7989	-2.6913	-2.8857	-2.8147	-4.0914	-4.1326
60-69	-2.7894	-2.6892	-2.9183	-2.8116	-4.1836	-4.0652
70-79	-2.7887	-2.6839	-2.8643	-2.7381	-4.1733	-4.1243
80-99	-2.7932	-2.6832	-2.5722	-2.7457	-4.1871	-4.0817

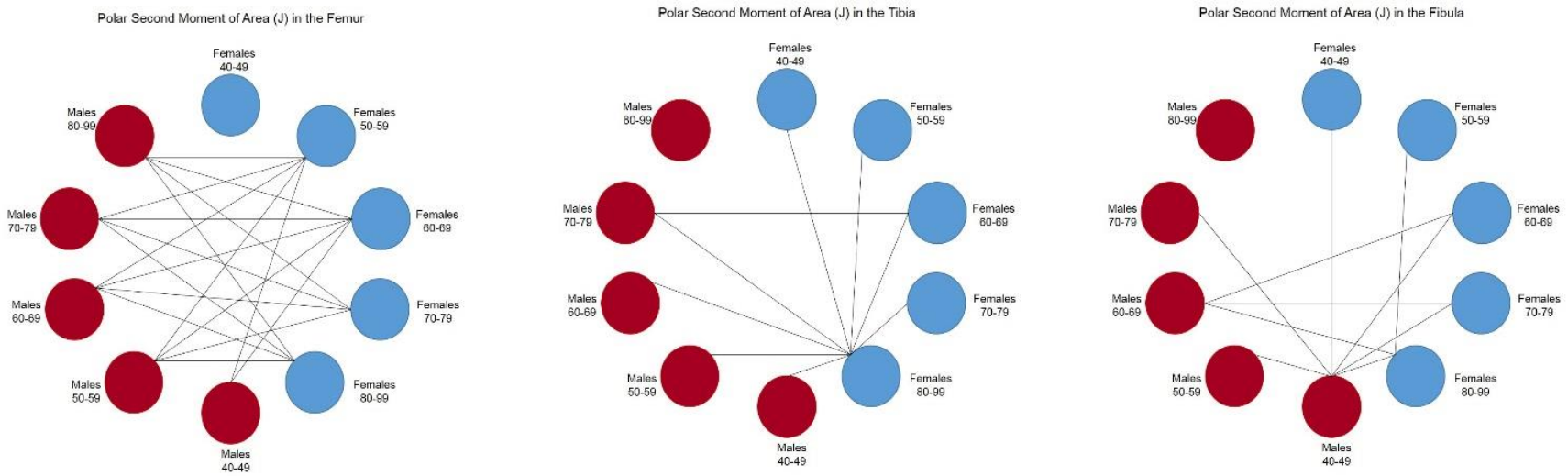

Figure F.14. Results of J LS means comparisons in the lower limb by sex and age
Lines between groups indicate significant ($p < 0.05$) results from post-hoc LS means comparisons with Tukey-Kramer adjustment for multiple comparisons.

Table F.15. I_{max} LS means in the upper limb by sex and age

	Humerus		Radius		Ulna	
Age Group	Female	Male	Female	Male	Female	Male
40-49	-3.5138	-3.1984	-3.8779	-3.6589	-3.8626	-3.6540
50-59	-3.4107	-3.2349	-3.8661	-3.7258	-3.8534	-3.6823
60-69	-3.4353	-3.1902	-3.8776	-3.6426	-3.8955	-3.6548
70-79	-3.3646	-3.2025	-3.8096	-3.6335	-3.8307	-3.6495
80-99	-3.4396	-3.1867	-3.8188	-3.6600	-3.8453	-3.6194

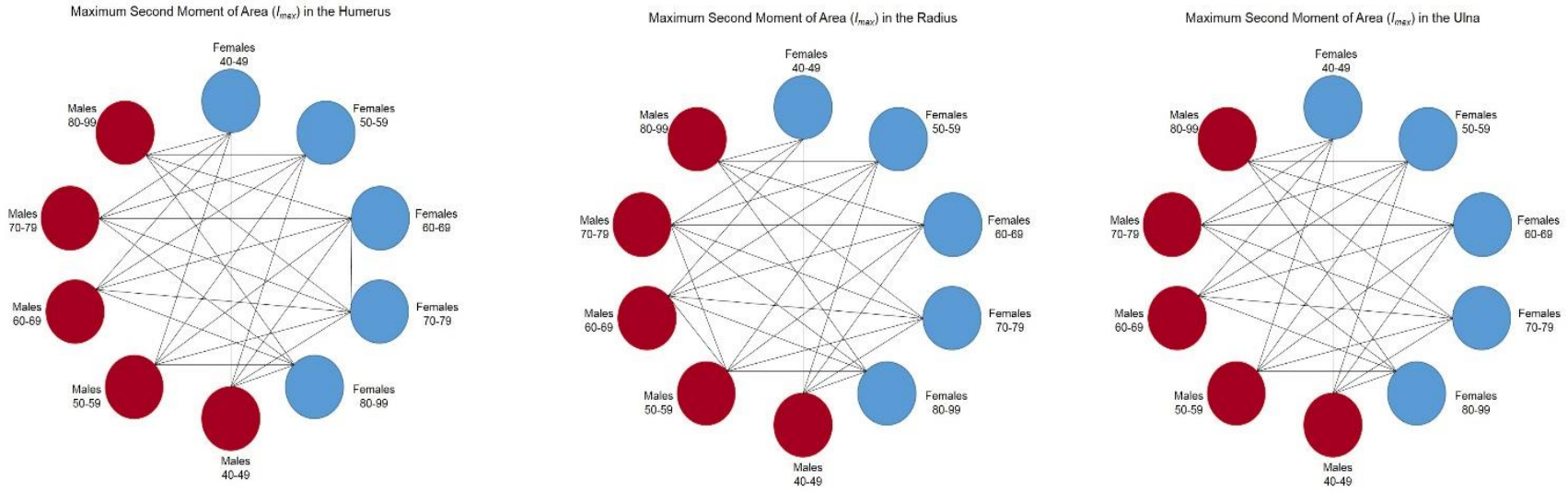

Figure F.15. Results of I_{max} LS means comparisons in the upper limb by sex and age
Lines between groups indicate significant ($p < 0.05$) results from post-hoc LS means comparisons with Tukey-Kramer adjustment for multiple comparisons.

Table F.16. I_{max} LS means in the lower limb by sex and age

	Femur		Tibia		Fibula	
Age Group	Female	Male	Female	Male	Female	Male
40-49	-3.0626	-2.9671	-3.1051	-2.9993	-4.4640	-4.1512
50-59	-3.0454	-2.9322	-3.0680	-2.9923	-4.2589	-4.3171
60-69	-3.0260	-2.9388	-3.1017	-2.9877	-4.3577	-4.2461
70-79	-3.0237	-2.9244	-3.0492	-2.9136	-4.3406	-4.2935
80-99	-3.0205	-2.9295	-2.7584	-2.9312	-4.3556	-4.2474

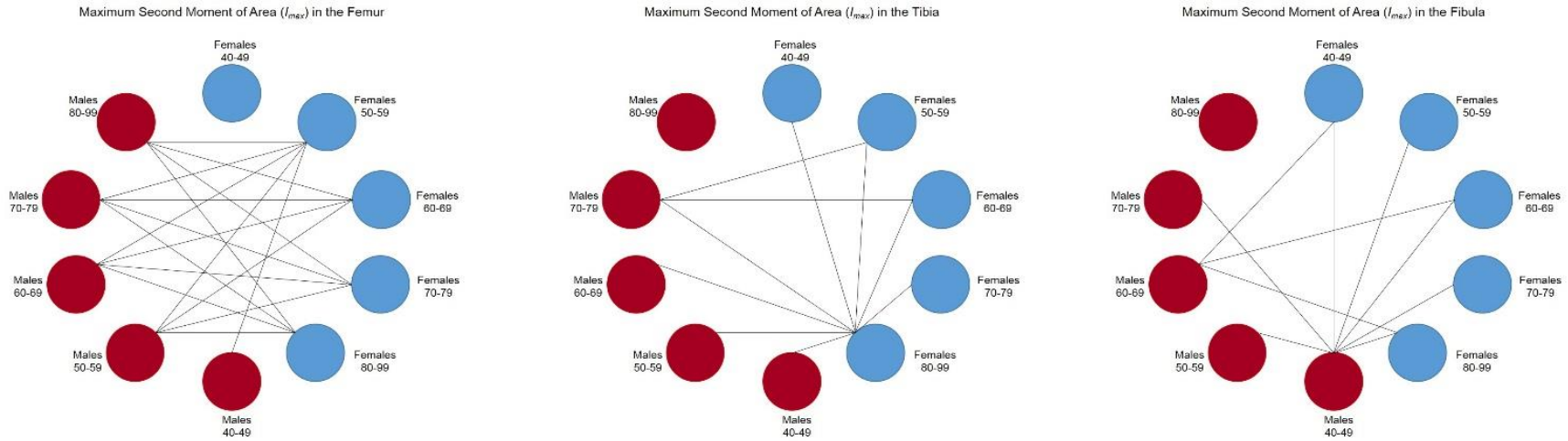

Figure F.16. Results of I_{max} LS means comparisons in the lower limb by sex and age group
Lines between groups indicate significant ($p < 0.05$) results from post-hoc LS means comparisons with Tukey-Kramer adjustment for multiple comparisons.

Table F.17. I_{min} LS means in the upper limb by sex and age

	Humerus		Radius		Ulna	
Age Group	Female	Male	Female	Male	Female	Male
40-49	-3.6639	-3.3472	-4.0878	-3.8908	-4.0733	-3.8657
50-59	-3.5655	-3.3884	-4.0906	-3.9485	-4.0672	-3.8902
60-69	-3.5960	-3.3293	-4.1119	-3.8705	-4.0834	-3.8403
70-79	-3.5354	-3.3411	-4.0375	-3.8583	-4.0117	-3.8307
80-99	-3.5903	-3.3492	-4.0659	-9.8533	-4.0733	-3.8111

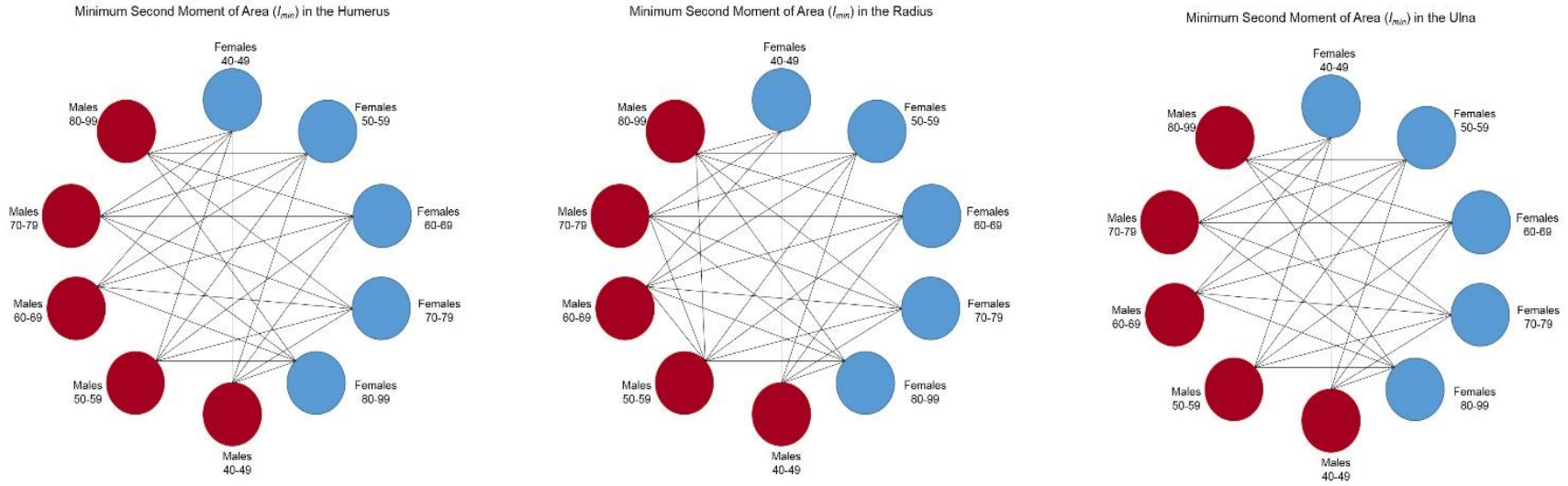

Figure F.17. Results of I_{min} LS means comparisons in the upper limb by sex and age
Lines between groups indicate significant ($p < 0.05$) results from post-hoc LS means comparisons with Tukey-Kramer adjustment for multiple comparisons.

Table F.18. I_{min} LS means in the lower limb by sex and age

	Femur		Tibia		Fibula	
Age Group	Female	Male	Female	Male	Female	Male
40-49	-3.1807	-3.0864	-3.4853	-3.3093	-4.7357	-4.4552
50-59	-3.1655	-3.0651	-3.3623	-3.3042	-4.6005	-4.6028
60-69	-3.1692	-3.0507	-3.3925	-3.3050	-4.6804	-4.5493
70-79	-3.1703	-3.0588	-3.3360	-3.2321	-4.6825	-4.6299
80-99	-3.1866	-3.0489	-3.0405	-3.2141	-4.6961	-4.5984

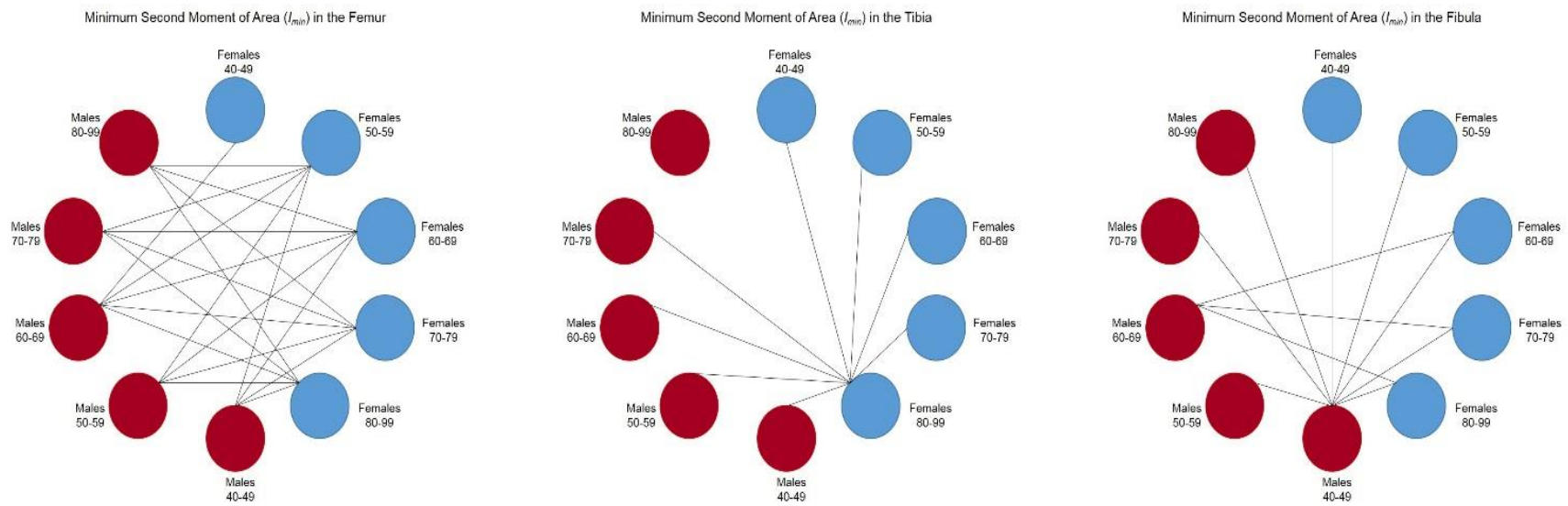

Figure F.18. Results of I_{min} LS means comparisons in the lower limb by sex and age
Lines between groups indicate significant ($p < 0.05$) results from post-hoc LS means comparisons with Tukey-Kramer adjustment for multiple comparisons.

Table F.19. Shape (I_{max}/I_{min}) LS means in the upper limb by sex and age

	Humerus		Radius		Ulna	
Age Group	Female	Male	Female	Male	Female	Male
40-49	0.1501	0.1487	0.2099	0.2318	0.2106	0.2117
50-59	0.1548	0.1535	0.2244	0.2227	0.2137	0.2079
60-69	0.1606	0.1390	0.2343	0.2279	0.1879	0.1854
70-79	0.1708	0.1386	0.2279	0.2248	0.1809	0.1811
80-99	0.1507	0.1625	0.2470	0.1932	0.2279	0.1916

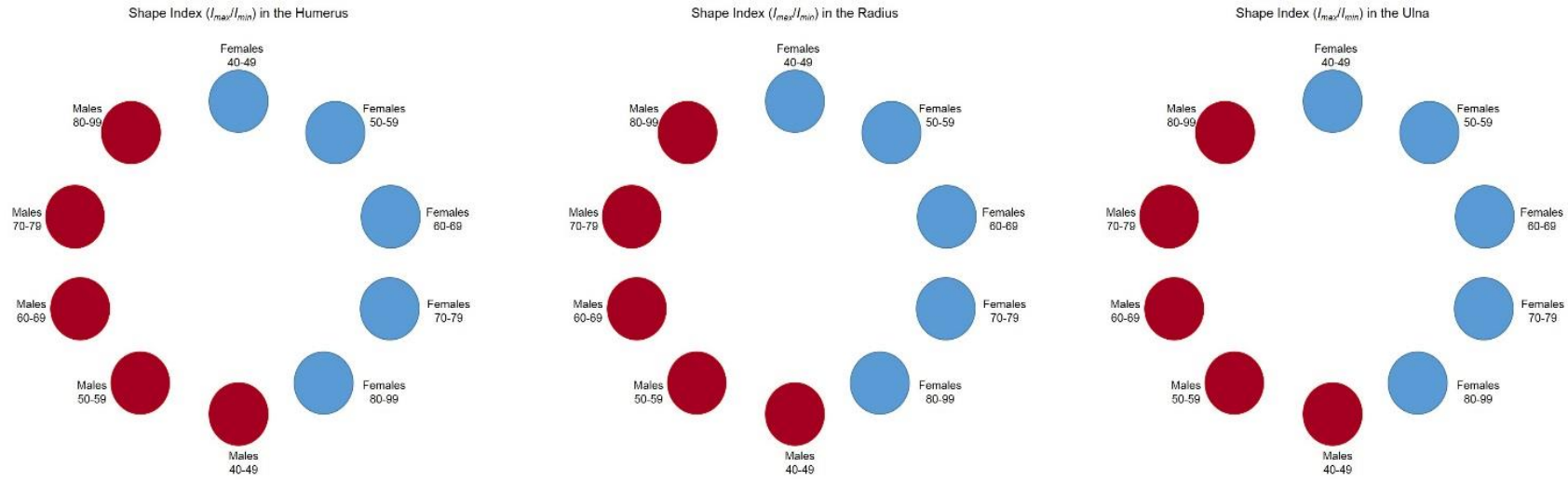

Figure F.19. Results of shape index LS means comparisons in the upper limb by sex and age
Lines between groups indicate significant ($p < 0.05$) results from post-hoc LS means comparisons with Tukey-Kramer adjustment for multiple comparisons.

Table F.20. Shape (I_{max}/I_{min}) LS means in the lower limb by sex and age

	Femur		Tibia		Fibula	
Age Group	Female	Male	Female	Male	Female	Male
40-49	0.1181	0.1193	0.3801	0.3099	0.2717	0.3039
50-59	0.1200	0.1329	0.2942	0.3118	0.3415	0.2856
60-69	0.1431	0.1118	0.2907	0.3171	0.3227	0.3032
70-79	0.1465	0.1344	0.2868	0.3184	0.3418	0.3362
80-99	0.1660	0.1194	0.2821	0.2829	0.3404	0.3509

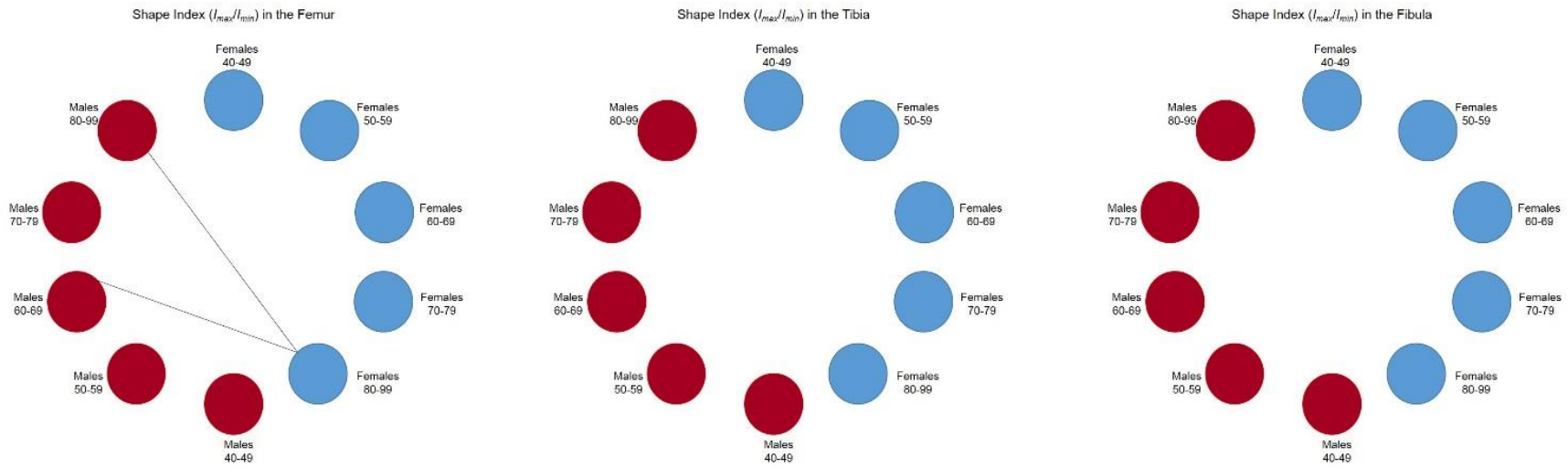

Figure F.20. Results of shape index LS means comparisons in the lower limb by sex and age
Lines between groups indicate significant ($p < 0.05$) results from post-hoc LS means comparisons with Tukey-Kramer adjustment for multiple comparisons.

Table F.21. Z_x LS means in the upper limb by sex and age

	Humerus		Radius		Ulna	
Age Group	Female	Male	Female	Male	Female	Male
40-49	-2.0507	-1.8353	-2.3739	-2.2865	-2.3976	-2.2135
50-59	-1.9865	-1.8580	-2.4105	-2.2920	-2.3758	-2.2513
60-69	-2.0040	-1.8045	-2.4193	-2.2367	-2.4095	-2.2152
70-79	-1.9623	-1.8214	-2.3673	-2.2346	-2.3454	-2.2182
80-99	-2.0088	-1.8289	-2.3737	-2.2465	-2.3913	-2.1849

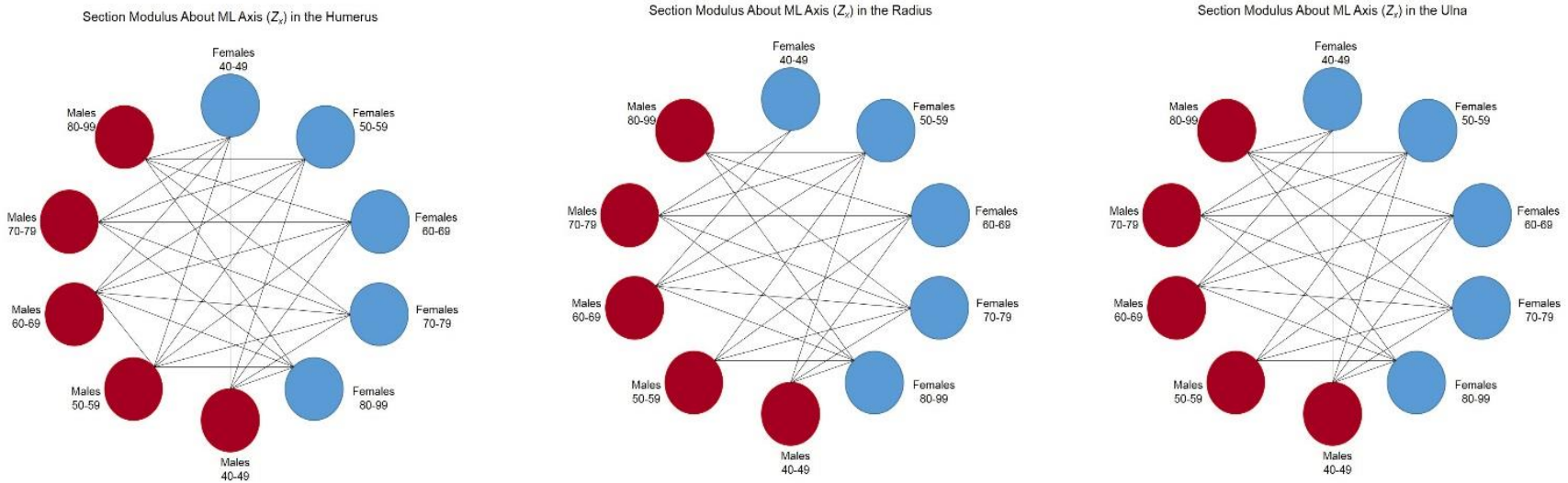

Figure F.21. Results of Z_x LS means comparisons in the upper limb by sex and age
Lines between groups indicate significant ($p < 0.05$) results from post-hoc LS means comparisons with Tukey-Kramer adjustment for multiple comparisons.

Table F.22. Z_x LS means in the lower limb by sex and age group

	Femur		Tibia		Fibula	
Age Group	Female	Male	Female	Male	Female	Male
40-49	-1.6466	-1.5761	-1.7312	-1.6632	-2.8030	-2.5885
50-59	-1.6458	-1.5572	-1.7196	-1.6561	-2.6342	-2.6412
60-69	-1.6529	-1.5520	-1.7442	-1.6393	-2.7090	-2.6330
70-79	-1.6252	-1.5699	-1.6870	-1.6145	-2.7150	-2.6900
80-99	-1.6740	-1.5592	-1.4784	-1.6043	-2.7379	-2.6488

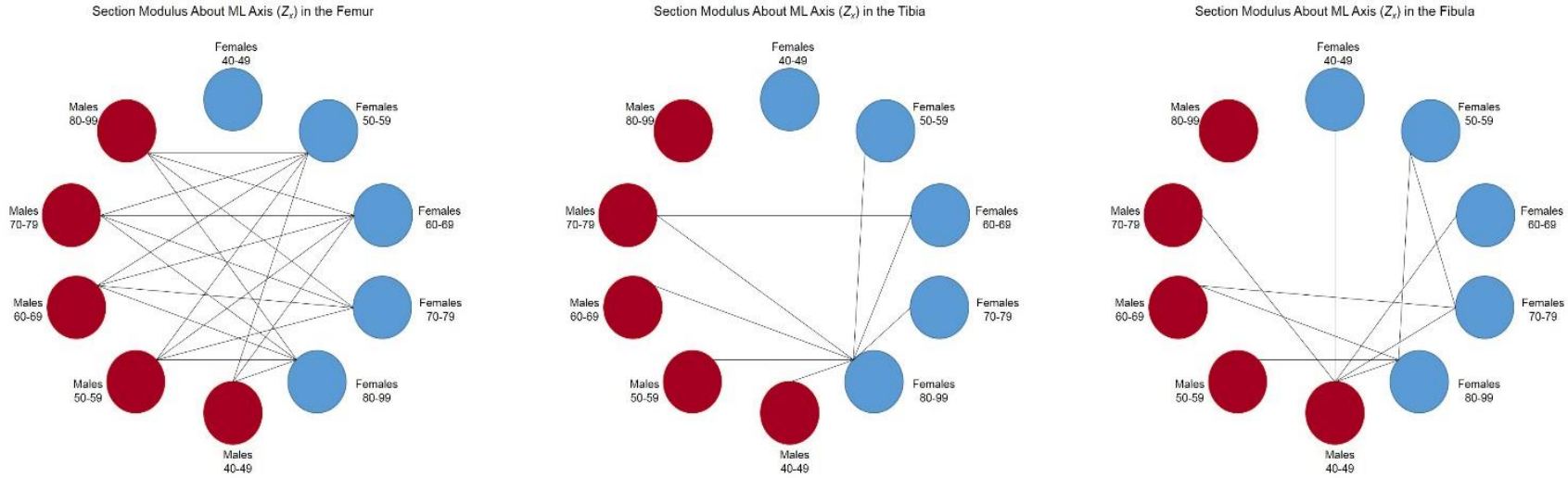

Figure F.22. Results of Z_x LS means comparisons in the lower limb by sex and age group
Lines between groups indicate significant ($p < 0.05$) results from post-hoc LS means comparisons with Tukey-Kramer adjustment for multiple comparisons.

Table F.23. Z_y LS means in the upper limb by sex and age

	Humerus		Radius		Ulna	
Age Group	Female	Male	Female	Male	Female	Male
40-49	-2.0380	-1.8232	-2.3881	-2.2135	-2.3879	-2.2416
50-59	-1.9707	-1.8443	-2.3627	-2.2744	-2.3908	-2.2556
60-69	-1.9878	-1.7994	-2.3736	-2.1936	-2.4012	-2.2395
70-79	-1.9566	-1.8078	-2.3460	-2.1995	-2.3627	-2.2376
80-99	-2.005	-1.8138	-2.3393	-2.2045	-2.4208	-2.2219

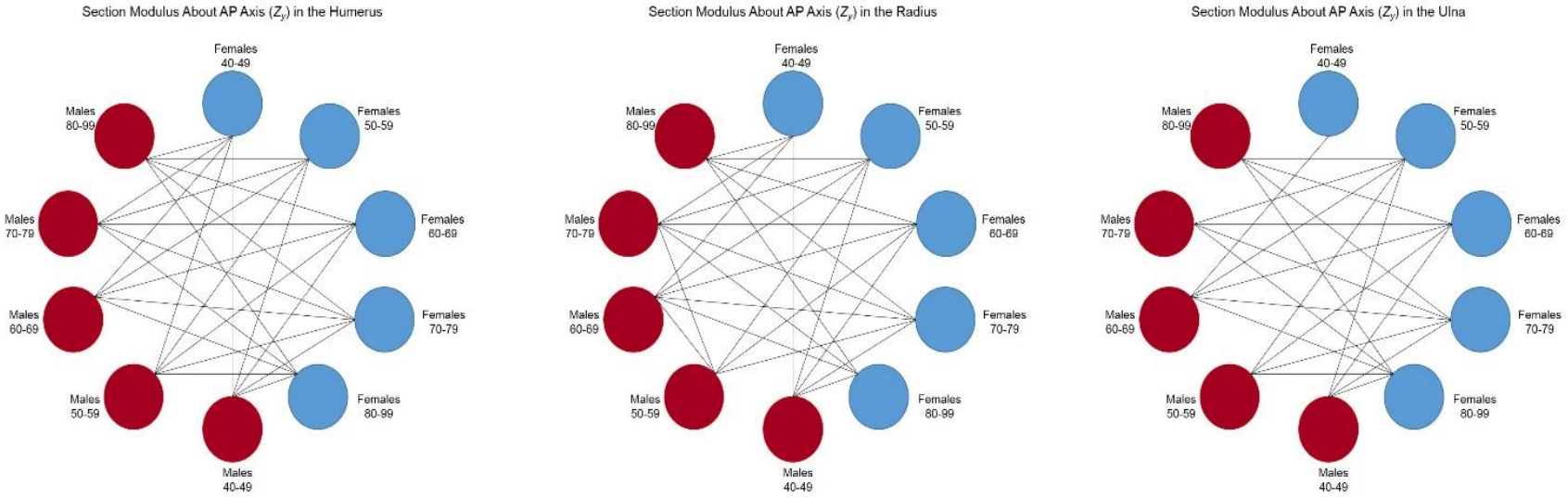

Figure F.23. Results of Z_y LS means comparisons in the upper limb by sex and age
Lines between groups indicate significant ($p < 0.05$) results from post-hoc LS means comparisons with Tukey-Kramer adjustment for multiple comparisons.

Table F.24. Z_y LS means in the lower limb by sex and age group

	Femur		Tibia		Fibula	
Age Group	Female	Male	Female	Male	Female	Male
40-49	-1.5976	-1.5591	-1.8378	-1.7307	-2.7285	-2.5545
50-59	-1.5946	-1.5221	-1.7857	-1.7121	-2.6520	-2.6901
60-69	-1.5891	-1.5231	-1.8075	-1.7225	-2.7243	-2.6040
70-79	-1.6041	-1.5401	-1.7869	-1.6789	-2.7118	-2.6697
80-99	-1.5918	-1.5340	-1.5374	-1.6816	-2.7134	-2.6160

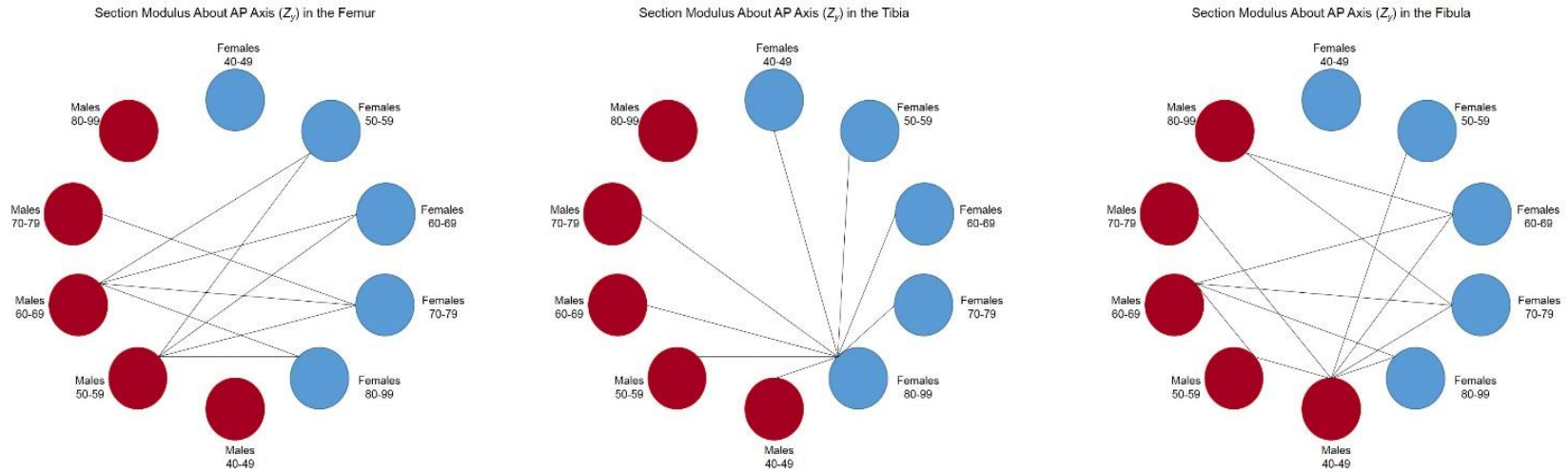

Figure F.24. Results of Z_y LS means comparisons in the lower limb by sex and age
Lines between groups indicate significant ($p < 0.05$) results from post-hoc LS means comparisons with Tukey-Kramer adjustment for multiple comparisons.

Table F.25. Z_p LS means in the upper limb by sex and age

	Humerus		Radius		Ulna	
Age Group	Female	Male	Female	Male	Female	Male
40-49	-1.7984	-1.5738	-2.1389	-2.0125	-2.1490	-1.9848
50-59	-1.7280	-1.5964	-2.1584	-2.0562	-2.1455	-2.0147
60-69	-1.7527	-1.5447	-2.1686	-1.9879	-2.1635	-1.9808
70-79	-1.7132	-1.5596	-2.1351	-1.9910	-2.1076	-1.9818
80-99	-1.7627	-1.5672	-2.1364	-1.9920	-2.1635	-1.9526

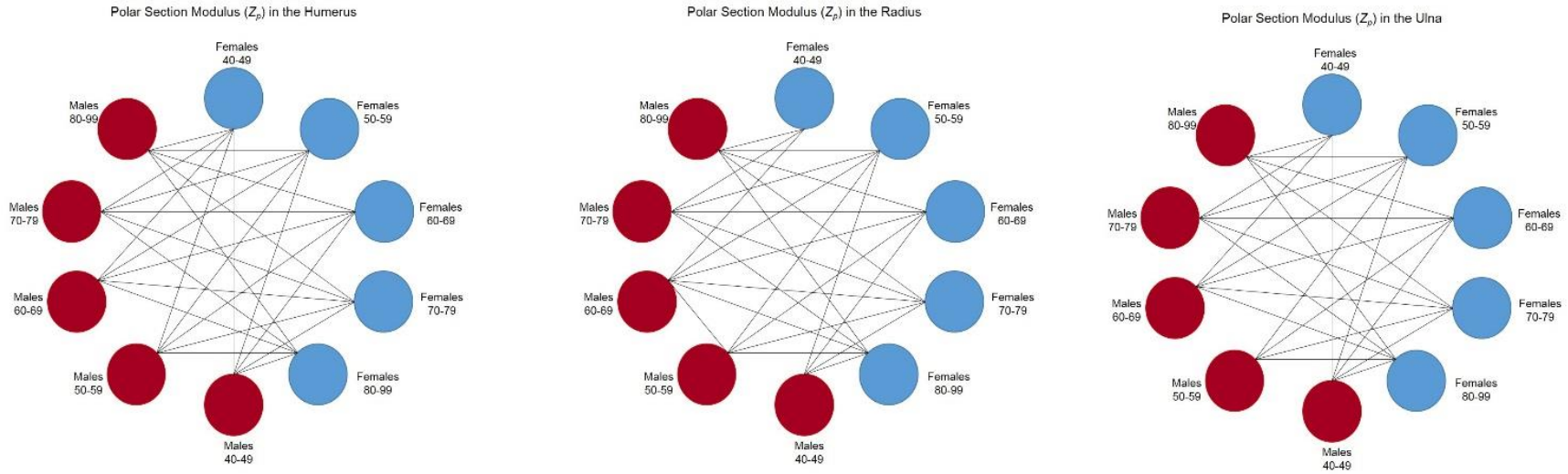

Figure F.25. Results of Z_p LS means comparisons in the upper limb by sex and age
Lines between groups indicate significant ($p < 0.05$) results from post-hoc LS means comparisons with Tukey-Kramer adjustment for multiple comparisons.

Table F.26. Z_p LS means in the lower limb by sex and age group

	Femur		Tibia		Fibula	
Age Group	Female	Male	Female	Male	Female	Male
40-49	-1.3593	-1.3093	-1.5644	-1.4649	-2.5333	-2.3384
50-59	-1.3549	-1.2838	-1.5182	-1.4514	-2.4187	-2.4376
60-69	-1.3610	-1.2833	-1.5453	-1.4446	-2.4959	-2.3881
70-79	-1.3597	-1.3054	-1.4929	-1.4199	-2.4856	-2.4491
80-99	-1.3781	-1.2917	-1.2823	-1.4055	-2.4976	-2.4169

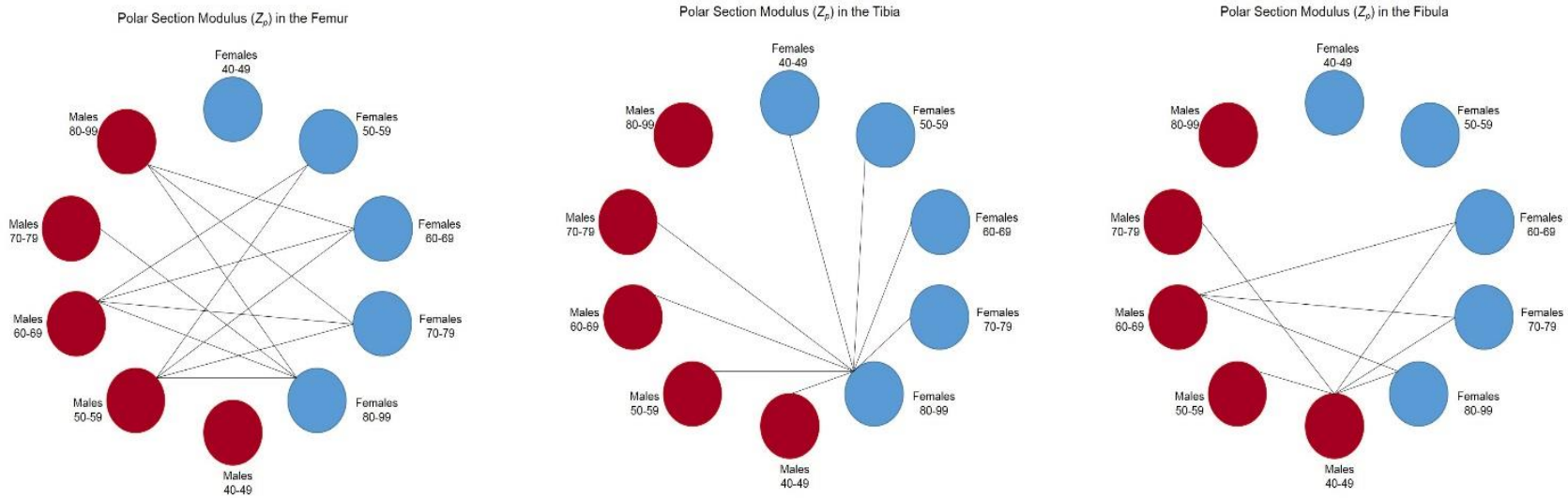

Figure F.26. Results of Z_p LS means comparisons in the lower limb by sex and age
Lines between groups indicate significant ($p < 0.05$) results from post-hoc LS means comparisons with Tukey-Kramer adjustment for multiple comparisons.

Table F.27. Z_{max} LS means in the upper limb by sex and age

	Humerus		Radius		Ulna	
Age Group	Female	Male	Female	Male	Female	Male
40-49	-2.0226	-1.7990	-2.3402	-2.2111	-2.3499	-2.1846
50-59	-1.9458	-1.8195	-2.3578	-2.2570	-2.3457	-2.2171
60-69	-1.9721	-1.7727	-2.3651	-2.1857	-2.3737	-2.1901
70-79	-1.9239	-1.7881	-2.3343	-2.1910	-2.3173	-2.1861
80-99	-1.9840	-1.7860	-2.3299	-2.2041	-2.3578	-2.1582

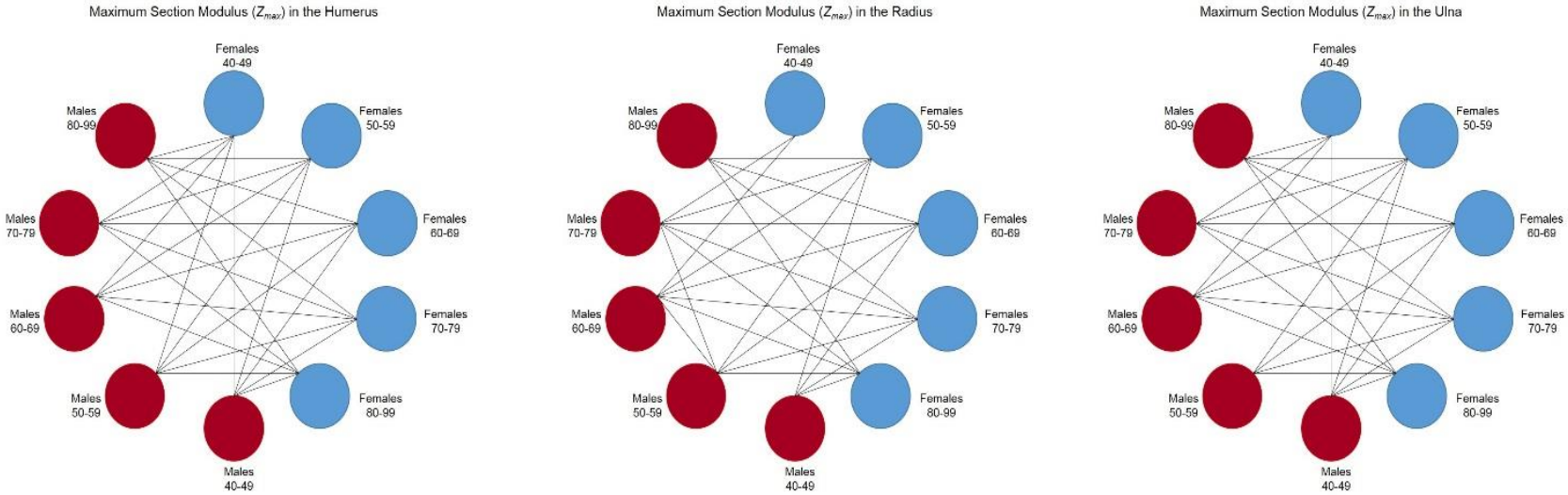

Figure F.27. Results of Z_{max} LS means comparisons in the upper limb by sex and age
Lines between groups indicate significant ($p < 0.05$) results from post-hoc LS means comparisons with Tukey-Kramer adjustment for multiple comparisons.

Table F.28. Z_{max} LS means in the lower limb by sex and age

	Femur		Tibia		Fibula	
Age Group	Female	Male	Female	Male	Female	Male
40-49	-1.5884	-1.5409	-1.7148	-1.6381	-2.7064	-2.5036
50-59	-1.5851	-1.5079	-1.6953	-1.6222	-2.5768	-2.6104
60-69	-1.5809	-1.5151	-1.7248	-1.6153	-2.6587	-2.5579
70-79	-1.5824	-1.5307	-1.6703	-1.5869	-2.6442	-2.6063
80-99	-1.5874	-1.5210	-1.4472	-1.5842	-2.6552	-2.5727

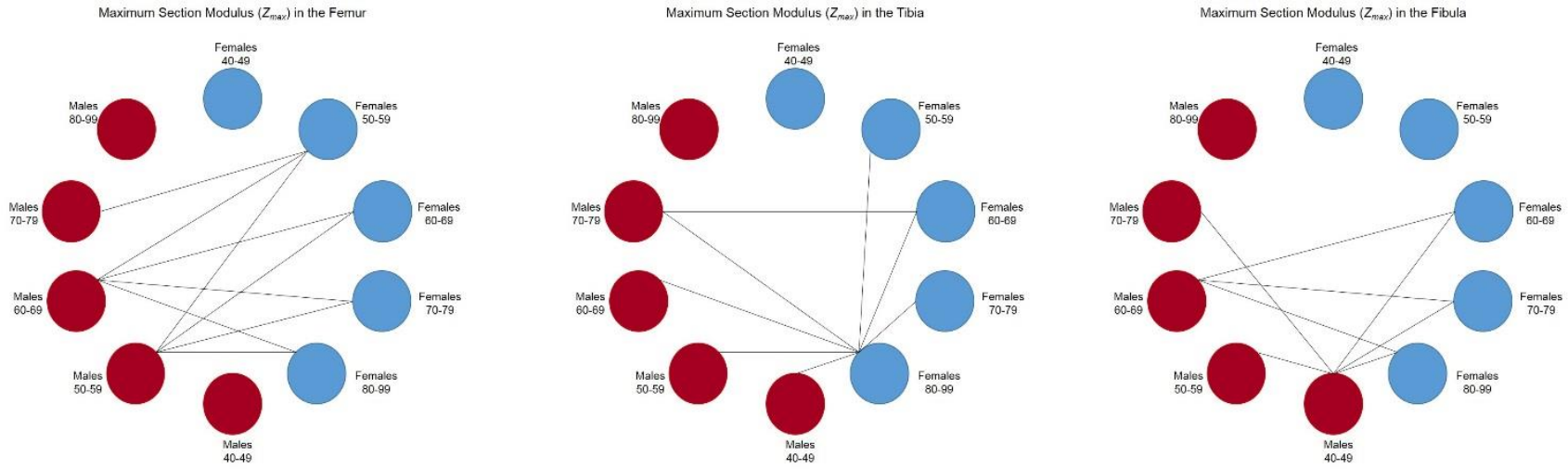

Figure F.28. Results of Z_{max} LS means comparisons in the lower limb by sex and age
Lines between groups indicate significant ($p < 0.05$) results from post-hoc LS means comparisons with Tukey-Kramer adjustment for multiple comparisons.

Table F.29. Z_{min} LS means in the upper limb by sex and age

	Humerus		Radius		Ulna	
Age Group	Female	Male	Female	Male	Female	Male
40-49	-2.0911	-1.8693	-2.4390	-2.3076	-2.4476	-2.2852
50-59	-2.0232	-1.8972	-2.4489	-2.3434	-2.4335	-2.3080
60-69	-2.0471	-1.8411	-2.4652	-2.2777	-2.4529	-2.2724
70-79	-2.0136	-1.8578	-2.4263	-2.2835	-2.4032	-2.2750
80-99	-2.0471	-1.8662	-2.4366	-2.2790	-2.4445	-2.2555

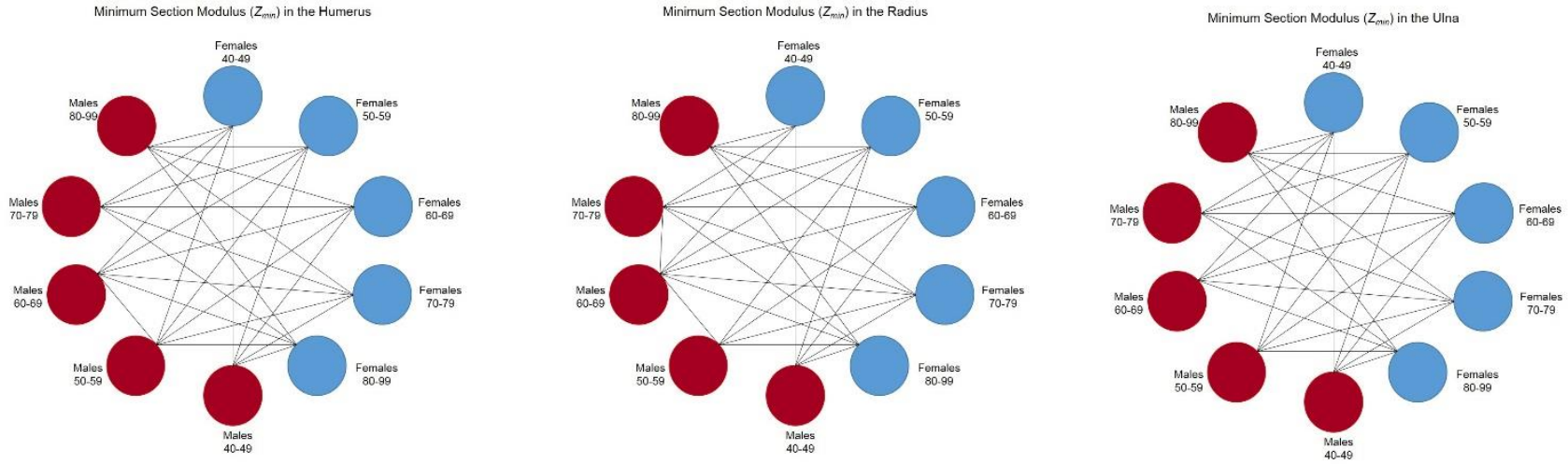

Figure F.29. Results of Z_{min} LS means comparisons in the upper limb by sex and age
Lines between groups indicate significant ($p < 0.05$) results from post-hoc LS means comparisons with Tukey-Kramer adjustment for multiple comparisons.

Table F.30. Z_{min} LS means in the lower limb by sex and age

	Femur		Tibia		Fibula	
Age Group	Female	Male	Female	Male	Female	Male
40-49	-1.6643	-1.6051	-1.9425	-1.8161	-2.8635	-2.6616
50-59	-1.6594	-1.5786	-1.8494	-1.8079	-2.7546	-2.7532
60-69	-1.6682	-1.5682	-1.8821	-1.8022	-2.8255	-2.7168
70-79	-1.6618	-1.5883	-1.8365	-1.7669	-2.8187	-2.7781
80-99	-1.6902	-1.5743	-1.6136	-1.7506	-2.8364	-2.7541

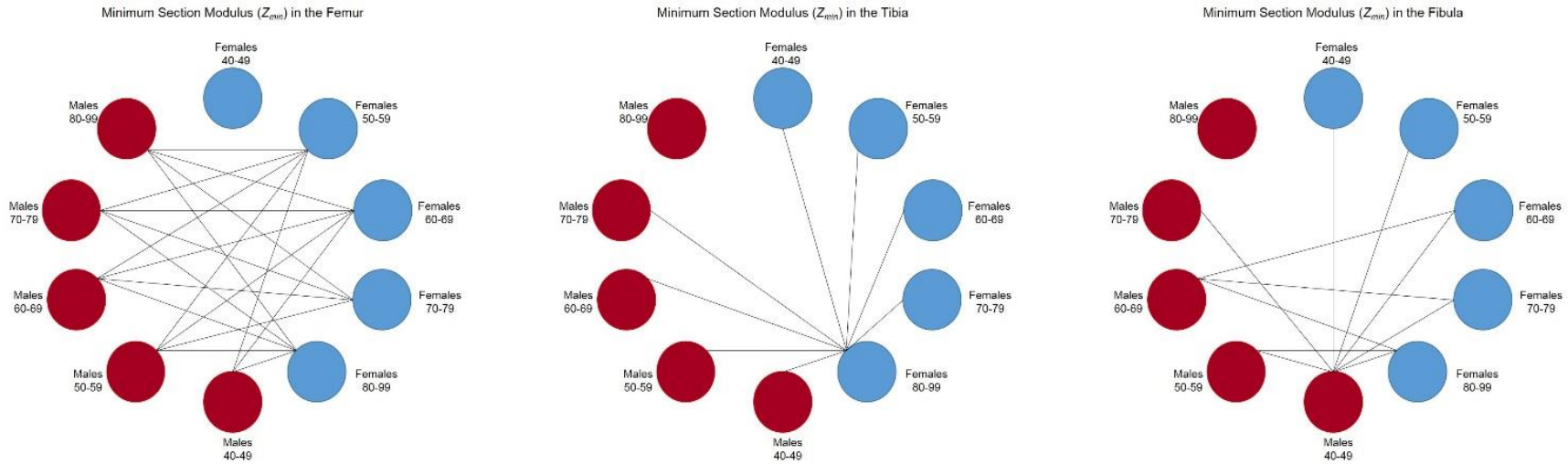

Figure F.30. Results of Z_{min} LS means comparisons in the lower limb by sex and age
Lines between groups indicate significant ($p < 0.05$) results from post-hoc LS means comparisons with Tukey-Kramer adjustment for multiple comparisons.

APPENDIX G
WITHIN BONE UNIVARIATE COMPARISON RESULTS FOR SLICE, AGE, SEX, BMI, ACTIVITY, AND PATHOLOGY EFFECTS

Table G.1. Results of ANOVA type III models for slice location, age, sex, BMI, activity, and pathology group in the humerus

Source (DF)	Cross-sectional Property						
	Cortical Area (CA)	**Total Area (TA)**	**Medullary Area (MA)**	**Percent Cortical Area (%CA)**	**I_x**	**I_y**	**J**
Slice location (4)	**< 0.0001**	**< 0.0001**	**< 0.0001**	**< 0.0001**	**< 0.0001**	**< 0.0001**	**< 0.0001**
Age group (4)	**0.0027**	**< 0.0001**	**< 0.0001**	**< 0.0001**	**0.0140**	0.0943	**0.0259**
Sex (1)	**< 0.0001**	**< 0.0001**	**< 0.0001**	0.3890	**< 0.0001**	**< 0.0001**	**< 0.0001**
BMI group (3)	**< 0.0001**	**< 0.0001**	**< 0.0001**	**0.0026**	**< 0.0001**	**< 0.0001**	**< 0.0001**
Activity level (2)	0.3421	0.4369	0.6804	0.6224	0.3836	0.1554	0.2021
Pathology group (1)	**0.0491**	**0.0012**	**0.0012**	0.1324	**0.0082**	0.1768	**0.0282**
Sex*Age group (4)	**0.0022**	**0.0448**	0.2940	**0.0602**	**0.0007**	**0.0117**	**0.0012**

Source (DF)	Cross-sectional Property							
	I_{max}	**I_{min}**	**Shape (I_{max}/I_{min})**	**Z_x**	**Z_y**	**Z_p**	**Z_{max}**	**Z_{min}**
Slice location (4)	**< 0.0001**	**< 0.0001**	**< 0.0001**	**< 0.0001**	**< 0.0001**	**< 0.0001**	**< 0.0001**	**< 0.0001**
Age group (4)	**0.0316**	**0.0426**	0.9562	**0.0324**	0.0931	0.0753	0.0571	0.1231
Sex (1)	**< 0.0001**	**< 0.0001**	0.2435	**< 0.0001**	**< 0.0001**	**< 0.0001**	**< 0.0001**	**< 0.0001**
BMI group (3)	**< 0.0001**	**< 0.0001**	0.3889	**< 0.0001**	**< 0.0001**	**< 0.0001**	**< 0.0001**	**< 0.0001**
Activity level (2)	0.1104	0.4148	0.0895	0.2436	0.1877	0.2227	0.1187	0.3582
Pathology group (1)	**0.0246**	**0.0581**	0.5233	**0.0038**	**0.0124**	**0.0020**	**0.0017**	**0.0085**
Sex*Age group (4)	**0.0012**	**0.0030**	0.1379	**0.0071**	**0.0232**	**0.0055**	**0.002**	**0.0041**

Significant values ($p < 0.05$) bolded

Table G.2. Results of ANOVA type III models for slice location, age, sex, BMI, activity, and pathology group in the radius

Source (DF)	Cross-sectional Property						
	Cortical Area (CA)	**Total Area (TA)**	**Medullary Area (MA)**	**Percent Cortical Area (%CA)**	**I_x**	**I_y**	**J**
Slice location (4)	**0.0003**	**< 0.0001**	**< 0.0001**	**< 0.0001**	**< 0.0001**	**< 0.0001**	**< 0.0001**
Age group (4)	0.1375	**< 0.0001**	**< 0.0001**	**< 0.0001**	**< 0.0001**	**0.0025**	**0.003**
Sex (1)	**< 0.0001**	**< 0.0001**	**< 0.0001**	0.8153	**< 0.0001**	**< 0.0001**	**< 0.0001**
BMI group (3)	**< 0.0001**	**< 0.0001**	**< 0.0001**	0.0620	**< 0.0001**	**< 0.0001**	**< 0.0001**
Activity level (2)	0.7658	0.8627	0.8718	0.9100	0.4069	0.6971	0.5891
Pathology group (1)	**0.0004**	**0.0036**	0.3092	0.2556	**0.0223**	**0.0241**	**0.0174**
Sex*Age group (4)	**0.0035**	0.0504	0.7200	0.3768	0.1122	**0.0001**	**0.0571**

Source (DF)	Cross-sectional Property							
	I_{max}	**I_{min}**	**Shape (I_{max}/I_{min})**	**Z_x**	**Z_y**	**Z_p**	**Z_{max}**	**Z_{min}**
Slice location (4)	**< 0.0001**	**< 0.0001**	**< 0.0001**	**< 0.0001**	**< 0.0001**	**< 0.0001**	**< 0.0001**	**< 0.0001**
Age group (4)	**0.009**	**0.0002**	0.8245	**0.0049**	**0.0061**	**0.0100**	**0.0127**	**0.0145**
Sex (1)	**< 0.0001**	**< 0.0001**	0.2762	**< 0.0001**	**< 0.0001**	**< 0.0001**	**< 0.0001**	**< 0.0001**
BMI group (3)	**< 0.0001**	**< 0.0001**	0.1916	**< 0.0001**	**< 0.0001**	**< 0.0001**	**< 0.0001**	**< 0.0001**
Activity level (2)	0.5434	0.6211	0.3086	0.7506	0.9668	0.9576	0.9627	0.6914
Pathology group (1)	**0.0399**	**0.0071**	0.4009	**0.0037**	**0.0017**	**0.0016**	**0.0053**	**0.0058**
Sex*Age group (4)	0.0738	**0.0264**	**0.0348**	0.1108	**0.0103**	0.0603	0.0675	0.0217

Significant values ($p < 0.05$) bolded

Table G.3. Results of ANOVA type III models for slice location, age, sex, BMI, activity, and pathology group in the ulna

Source (DF)	Cross-sectional Property						
	Cortical Area (CA)	**Total Area (TA)**	**Medullary Area (MA)**	**Percent Cortical Area (%CA)**	**I_x**	**I_y**	**J**
Slice location (4)	**< 0.0001**	**< 0.0001**	**< 0.0001**	**< 0.0001**	**< 0.0001**	**< 0.0001**	**< 0.0001**
Age group (4)	0.2912	**0.0081**	**< 0.0001**	**< 0.0001**	**0.0391**	0.2638	0.0801
Sex (1)	**< 0.0001**	**< 0.0001**	**< 0.0001**	0.8816	**< 0.0001**	**< 0.0001**	**< 0.0001**
BMI group (3)	**< 0.0001**	**< 0.0001**	**< 0.0001**	**0.0069**	**< 0.0001**	**< 0.0001**	**< 0.0001**
Activity level (2)	0.0966	0.1254	0.4728	0.7434	.05760	0.0559	0.1814
Pathology group (1)	**0.0031**	**0.0309**	0.2891	0.1284	0.4410	0.1093	0.1355
Sex*Age group (4)	0.1260	0.2005	0.8281	0.9299	**0.0222**	0.5233	0.1374

Source (DF)	Cross-sectional Property							
	I_{max}	**I_{min}**	**Shape (I_{max}/I_{min})**	**Z_x**	**Z_y**	**Z_p**	**Z_{max}**	**Z_{min}**
Slice location (4)	**< 0.0001**	**< 0.0001**	**< 0.0001**	**< 0.0001**	**< 0.0001**	**< 0.0001**	**< 0.0001**	**< 0.0001**
Age group (4)	0.1592	**0.0130**	**0.0075**	0.1667	0.5695	0.1753	0.2055	0.1754
Sex (1)	**< 0.0001**	**< 0.0001**	0.3405	**< 0.0001**	**< 0.0001**	**< 0.0001**	**< 0.0001**	**< 0.0001**
BMI group (3)	**< 0.0001**	**< 0.0001**	0.9607	**< 0.0001**	**< 0.0001**	**< 0.0001**	**< 0.0001**	**< 0.0001**
Activity level (2)	0.2948	0.1059	0.7261	0.3856	0.0655	0.1731	0.3009	0.0921
Pathology group (1)	0.0686	0.4150	0.0587	0.1989	0.2237	0.1765	0.0834	0.2109
Sex*Age group (4)	0.2504	0.0688	0.5417	**0.0208**	0.2474	0.0501	0.1063	0.0698

Significant values ($p < 0.05$) bolded

Table G.4. Results of ANOVA type III models for slice location, age, sex, BMI, activity, and pathology group in the femur

Source (DF)	Cross-sectional Property						
	Cortical Area (CA)	**Total Area (TA)**	**Medullary Area (MA)**	**Percent Cortical Area (%CA)**	**I_x**	**I_y**	**J**
Slice location (4)	**< 0.0001**	**< 0.0001**	**< 0.0001**	**< 0.0001**	**< 0.0001**	**< 0.0001**	**< 0.0001**
Age group (4)	0.3120	0.5472	0.8049	0.0948	0.6762	0.4516	0.7408
Sex (1)	**< 0.0001**	**0.0004**	0.6400	0.0580	**< 0.0001**	**< 0.0001**	**< 0.0001**
BMI group (3)	**< 0.0001**	**< 0.0001**	**< 0.0001**	**0.0025**	**< 0.0001**	**< 0.0001**	**< 0.0001**
Activity level (2)	**0.0153**	0.3426	0.4694	0.4914	0.0591	**0.0003**	**0.0036**
Pathology group (1)	0.0941	**0.0114**	0.2919	0.2537	0.1201	0.9237	0.4065
Sex*Age group	0.6757	0.5231	0.3284	0.5025	0.2056	0.2802	0.9957

Source (DF)	Cross-sectional Property							
	I_{max}	**I_{min}**	**Shape (I_{max}/I_{min})**	**Z_x**	**Z_y**	**Z_p**	**Z_{max}**	**Z_{min}**
Slice location (4)	**< 0.0001**	**< 0.0001**	**< 0.0001**	**< 0.0001**	**< 0.0001**	**< 0.0001**	**< 0.0001**	**< 0.0001**
Age group (4)	0.5187	0.8881	0.1098	0.6203	0.6208	0.6704	0.8369	0.7220
Sex (1)	**< 0.0001**	**< 0.0001**	**0.0255**	**< 0.0001**	**< 0.0001**	**< 0.0001**	**< 0.0001**	**< 0.0001**
BMI group (3)	**< 0.0001**	**< 0.0001**	0.3384	**< 0.0001**	**< 0.0001**	**< 0.0001**	**< 0.0001**	**< 0.0001**
Activity level (2)	**0.0219**	**0.0011**	0.5357	**0.0478**	**0.0002**	**0.0006**	**0.004**	**0.0014**
Pathology group (1)	0.3167	0.5706	0.3696	0.1092	0.2465	0.2961	0.2833	0.2741
Sex*Age group	0.8949	0.7376	**0.0017**	0.1483	0.9401	0.7516	0.8394	0.3659

Significant values ($p < 0.05$) bolded

Table G.5. Results of ANOVA type III models for slice location, age, sex, BMI, activity, and pathology group in the tibia

Source (DF)	Cross-sectional Property						
	Cortical Area (CA)	**Total Area (TA)**	**Medullary Area (MA)**	**Percent Cortical Area (%CA)**	**I_x**	**I_y**	**J**
Slice location (4)	**< 0.0001**	**< 0.0001**	**< 0.0001**	**< 0.0001**	**< 0.0001**	**< 0.0001**	**< 0.0001**
Age group (4)	**0.0177**	**< 0.0001**	**0.0291**	**0.0002**	**< 0.0001**	**< 0.0001**	**< 0.0001**
Sex (1)	**0.0385**	0.1780	**0.0198**	**0.0361**	0.2242	**0.0307**	0.1006
BMI group (3)	**< 0.0001**	**< 0.0001**	**< 0.0001**	**< 0.0001**	**0.0080**	**0.0029**	**0.0050**
Activity level (2)	**0.0234**	**0.0045**	0.5029	0.4659	**0.0072**	0.1287	**0.0292**
Pathology group (1)	**0.0482**	**0.0049**	0.2698	0.6223	**0.0229**	0.2609	0.0738
Sex*Age group (4)	**0.0213**	**0.0004**	0.1311	0.9464	**0.0031**	**0.0005**	**0.0018**

Source (DF)	Cross-sectional Property							
	I_{max}	**I_{min}**	**Shape (I_{max}/I_{min})**	**Z_x**	**Z_y**	**Z_p**	**Z_{max}**	**Z_{min}**
Slice location (4)	**< 0.0001**	**< 0.0001**	**< 0.0001**	**< 0.0001**	**< 0.0001**	**< 0.0001**	**< 0.0001**	**< 0.0001**
Age group (4)	**< 0.0001**	**< 0.0001**	**0.0183**	**< 0.0001**	**< 0.0001**	**< 0.0001**	**< 0.0001**	**< 0.0001**
Sex (1)	0.0992	0.1226	0.8883	0.1445	0.0879	0.0887	0.1138	0.1701
BMI group (3)	**0.0017**	**0.0190**	**< 0.0001**	**< 0.0001**	**< 0.0001**	**< 0.0001**	**< 0.0001**	**< 0.0001**
Activity level (2)	**0.0305**	**0.0442**	0.2460	**0.0092**	**0.0413**	**0.0139**	**0.0130**	**0.0316**
Pathology group (1)	0.1055	**0.0430**	0.0896	**0.0308**	0.1622	0.0712	0.1069	**0.0392**
Sex*Age group (4)	**0.0013**	**0.0046**	**0.0443**	**0.0051**	0.0023	**0.0066**	**0.0027**	**0.0075**

Significant values ($p < 0.05$) bolded

Table G.6. Results of ANOVA type III models for slice location, age, sex, BMI, activity, and pathology group in the fibula

Source (DF)	Cross-sectional Property						
	Cortical Area (CA)	**Total Area (TA)**	**Medullary Area (MA)**	**Percent Cortical Area (%CA)**	**I_x**	**I_y**	**J**
Slice location (4)	**< 0.0001**	**< 0.0001**	**0.0036**	**< 0.0001**	**< 0.0001**	**< 0.0001**	**< 0.0001**
Age group (4)	**< 0.0001**	0.4331	**< 0.0001**	**< 0.0001**	**0.0047**	0.2729	0.4793
Sex (1)	**< 0.0001**	**< 0.0001**	0.6022	**0.0076**	**< 0.0001**	**< 0.0001**	**< 0.0001**
BMI group (3)	**< 0.0001**	**< 0.0001**	**< 0.0001**	**0.0047**	**< 0.0001**	**< 0.0001**	**< 0.0001**
Activity level (2)	0.1090	0.1721	0.9273	0.7447	0.1083	0.8287	0.3653
Pathology group (1)	0.9017	0.3177	0.3254	0.2126	0.5522	**0.0004**	0.1007
Sex*Age group (4)	**< 0.0001**	**< 0.0001**	0.5291	0.1002	**0.0038**	**< 0.0001**	**< 0.0001**

Source (DF)	Cross-sectional Property							
	I_{max}	**I_{min}**	**Shape (I_{max}/I_{min})**	**Z_x**	**Z_y**	**Z_p**	**Z_{max}**	**Z_{min}**
Slice location (4)	**< 0.0001**	**< 0.0001**	**< 0.0001**	**< 0.0001**	**< 0.0001**	**< 0.0001**	**< 0.0001**	**< 0.0001**
Age group (4)	0.7528	0.0825	0.1409	**0.0030**	0.4084	0.1418	0.4281	0.0549
Sex (1)	**< 0.0001**	**< 0.0001**	0.6068	**< 0.0001**	**< 0.0001**	**< 0.0001**	**< 0.0001**	**< 0.0001**
BMI group (3)	**< 0.0001**	**< 0.0001**	**0.0009**	**< 0.0001**	**< 0.0001**	**< 0.0001**	**< 0.0001**	**< 0.0001**
Activity level (2)	0.2967	0.1600	**0.0124**	0.0543	0.5508	0.1059	0.0890	0.2682
Pathology group (1)	0.3913	**0.0017**	**0.0021**	0.7734	**0.0085**	0.0838	0.3691	**0.0172**
Sex*Age group (4)	**< 0.0001**	**0.0003**	0.2271	**0.0013**	**< 0.0001**	**< 0.0001**	**< 0.0001**	**0.0003**

Significant values ($p < 0.05$) bolded

APPENDIX H
WITHIN BONE PAIRWISE COMPARISON RESULTS FOR BMI, ACTIVITY, AND PATHOLOGICAL GROUPS

Table H.1. Within bone pairwise comparisons for BMI category for the humerus

Cortical Area (CA)

BMI	< 18.5	18.5-24.9	25.0-29.9	> 30
< 18.5		*	*	*
18.5-24.9	*		*	*
25.0-29.9	*	*		*
> 30	*	*	*	

Total Area (TA)

BMI	< 18.5	18.5-24.9	25.0-29.9	> 30
< 18.5		*	*	*
18.5-24.9	*		*	*
25.0-29.9	*	*		*
> 30	*	*	*	

Medullary Area (MA)

BMI	< 18.5	18.5-24.9	25.0-29.9	> 30
< 18.5		*	*	*
18.5-24.9	*		*	*
25.0-29.9	*	*		*
> 30	*	*	*	

Percent Cortical Area (%CA)

BMI	< 18.5	18.5-24.9	25.0-29.9	> 30
< 18.5		NS	NS	*
18.5-24.9	NS		NS	*
25.0-29.9	NS	NS		*
> 30	*	*	*	

Second Moment of Area About ML Axis (I_x)

BMI	< 18.5	18.5-24.9	25.0-29.9	> 30
< 18.5		*	*	*
18.5-24.9	*		*	*
25.0-29.9	*	*		*
> 30	*	*	*	

Second Moment of Area About AP Axis (I_y)

BMI	< 18.5	18.5-24.9	25.0-29.9	> 30
< 18.5		*	*	*
18.5-24.9	*		*	*
25.0-29.9	*	*		*
> 30	*	*	*	

Polar Second Moment of Area (J)

BMI	< 18.5	18.5-24.9	25.0-29.9	> 30
< 18.5		*	*	*
18.5-24.9	*		*	*
25.0-29.9	*	*		*
> 30	*	*	*	

Maximum Second Moment of Area (I_{max})

BMI	< 18.5	18.5-24.9	25.0-29.9	> 30
< 18.5		*	*	*
18.5-24.9	*		*	*
25.0-29.9	*	*		*
> 30	*	*	*	

Minimum Second Moment of Area (I_{min})

BMI	< 18.5	18.5-24.9	25.0-29.9	> 30
< 18.5		*	*	*
18.5-24.9	*		*	*
25.0-29.9	*	*		*
> 30	*	*	*	

Shape Index (I_{max}/ I_{min})

BMI	< 18.5	18.5-24.9	25.0-29.9	> 30
< 18.5		NS	NS	NS
18.5-24.9	NS		NS	NS
25.0-29.9	NS	NS		NS
> 30	NS	NS	NS	

Section Modulus About ML Axis (Z_x)

BMI	< 18.5	18.5-24.9	25.0-29.9	> 30
< 18.5		*	*	*
18.5-24.9	*		*	*
25.0-29.9	*	*		*
> 30	*	*	*	

Section Modulus About AP Axis (Z_y)

BMI	< 18.5	18.5-24.9	25.0-29.9	> 30
< 18.5		*	*	*
18.5-24.9	*		*	*
25.0-29.9	*	*		*
> 30	*	*	*	

Polar Section Modulus (Z_p)

BMI	< 18.5	18.5-24.9	25.0-29.9	> 30
< 18.5		*	*	*
18.5-24.9	*		*	*
25.0-29.9	*	*		*
> 30	*	*	*	

Maximum Section Modulus (Z_{max})

BMI	< 18.5	18.5-24.9	25.0-29.9	> 30
< 18.5		*	*	*
18.5-24.9	*		*	*
25.0-29.9	*	*		*
> 30	*	*	*	

Minimum Section Modulus (Z_{min})

BMI	< 18.5	18.5-24.9	25.0-29.9	> 30
< 18.5		*	*	*
18.5-24.9	*		*	*
25.0-29.9	*	*		*
> 30	*	*	*	

* indicates significance at $p < 0.05$

Table H.2. Within bone pairwise comparisons for BMI category for the radius

Cortical Area (CA)

BMI	< 18.5	18.5-24.9	25.0-29.9	> 30
< 18.5		*	*	*
18.5-24.9	*		*	*
25.0-29.9	*	*		*
> 30	*	*	*	

Total Area (TA)

BMI	< 18.5	18.5-24.9	25.0-29.9	> 30
< 18.5		*	*	*
18.5-24.9	*		*	*
25.0-29.9	*	*		*
> 30	*	*	*	

Medullary Area (MA)

BMI	< 18.5	18.5-24.9	25.0-29.9	> 30
< 18.5		*	*	*
18.5-24.9	*		*	*
25.0-29.9	*	*		*
> 30	*	*	*	

Percent Cortical Area (%CA)

BMI	< 18.5	18.5-24.9	25.0-29.9	> 30
< 18.5		NS	NS	*
18.5-24.9	NS		NS	*
25.0-29.9	NS	NS		*
> 30	*	*	*	

Second Moment of Area About ML Axis (I_x)

BMI	< 18.5	18.5-24.9	25.0-29.9	> 30
< 18.5		*	*	*
18.5-24.9	*		*	*
25.0-29.9	*	*		*
> 30	*	*	*	

Second Moment of Area About AP Axis (I_y)

BMI	< 18.5	18.5-24.9	25.0-29.9	> 30
< 18.5		*	*	*
18.5-24.9	*		*	*
25.0-29.9	*	*		*
> 30	*	*	*	

Polar Second Moment of Area (J)

BMI	< 18.5	18.5-24.9	25.0-29.9	> 30
< 18.5		*	*	*
18.5-24.9	*		*	*
25.0-29.9	*	*		*
> 30	*	*	*	

Maximum Second Moment of Area (I_{max})

BMI	< 18.5	18.5-24.9	25.0-29.9	> 30
< 18.5		*	*	*
18.5-24.9	*		*	*
25.0-29.9	*	*		*
> 30	*	*	*	

Minimum Second Moment of Area (I_{min})

BMI	< 18.5	18.5-24.9	25.0-29.9	> 30
< 18.5		*	*	*
18.5-24.9	*		*	*
25.0-29.9	*	*		*
> 30	*	*	*	

Shape Index (I_{max}/ I_{min})

BMI	< 18.5	18.5-24.9	25.0-29.9	> 30
< 18.5		NS	NS	NS
18.5-24.9	NS		NS	NS
25.0-29.9	NS	NS		NS
> 30	NS	NS	NS	

Section Modulus About ML Axis (Z_x)

BMI	< 18.5	18.5-24.9	25.0-29.9	> 30
< 18.5		*	*	*
18.5-24.9	*		*	*
25.0-29.9	*	*		*
> 30	*	*	*	

Section Modulus About AP Axis (Z_y)

BMI	< 18.5	18.5-24.9	25.0-29.9	> 30
< 18.5		*	*	*
18.5-24.9	*		*	*
25.0-29.9	*	*		*
> 30	*	*	*	

Polar Section Modulus (Z_p)

BMI	< 18.5	18.5-24.9	25.0-29.9	> 30
< 18.5		*	*	*
18.5-24.9	*		*	*
25.0-29.9	*	*		*
> 30	*	*	*	

Maximum Section Modulus (Z_{max})

BMI	< 18.5	18.5-24.9	25.0-29.9	> 30
< 18.5		*	*	*
18.5-24.9	*		*	*
25.0-29.9	*	*		*
> 30	*	*	*	

Minimum Section Modulus (Z_{min})

BMI	< 18.5	18.5-24.9	25.0-29.9	> 30
< 18.5		*	*	*
18.5-24.9	*		*	*
25.0-29.9	*	*		*
> 30	*	*	*	

* indicates significance at $p < 0.05$

Table H.3. Within bone pairwise comparisons for BMI category for the ulna

Cortical Area (CA)

BMI	< 18.5	18.5-24.9	25.0-29.9	> 30
< 18.5		*	*	*
18.5-24.9	*		*	*
25.0-29.9	*	*		*
> 30	*	*	*	

Minimum Second Moment of Area (I_{min})

BMI	< 18.5	18.5-24.9	25.0-29.9	> 30
< 18.5		*	*	*
18.5-24.9	*		*	*
25.0-29.9	*	*		*
> 30	*	*	*	

Total Area (TA)

BMI	< 18.5	18.5-24.9	25.0-29.9	> 30
< 18.5		*	*	*
18.5-24.9	*		*	*
25.0-29.9	*	*		*
> 30	*	*	*	

Shape Index (I_{max}/ I_{min})

BMI	< 18.5	18.5-24.9	25.0-29.9	> 30
< 18.5		NS	NS	NS
18.5-24.9	NS		NS	NS
25.0-29.9	NS	NS		NS
> 30	NS	NS	NS	

Medullary Area (MA)

BMI	< 18.5	18.5-24.9	25.0-29.9	> 30
< 18.5		*	*	*
18.5-24.9	*		*	*
25.0-29.9	*	*		*
> 30	*	*	*	

Section Modulus About ML Axis (Z_x)

BMI	< 18.5	18.5-24.9	25.0-29.9	> 30
< 18.5		*	*	*
18.5-24.9	*		*	*
25.0-29.9	*	*		*
> 30	*	*	*	

Percent Cortical Area (%CA)

BMI	< 18.5	18.5-24.9	25.0-29.9	> 30
< 18.5		NS	NS	*
18.5-24.9	NS		NS	*
25.0-29.9	NS	NS		*
> 30	*	*	*	

Section Modulus About AP Axis (Z_y)

BMI	< 18.5	18.5-24.9	25.0-29.9	> 30
< 18.5		*	*	*
18.5-24.9	*		*	*
25.0-29.9	*	*		*
> 30	*	*	*	

Second Moment of Area About ML Axis (I_x)

BMI	< 18.5	18.5-24.9	25.0-29.9	> 30
< 18.5		*	*	*
18.5-24.9	*		*	*
25.0-29.9	*	*		*
> 30	*	*	*	

Polar Section Modulus (Z_p)

BMI	< 18.5	18.5-24.9	25.0-29.9	> 30
< 18.5		*	*	*
18.5-24.9	*		*	*
25.0-29.9	*	*		*
> 30	*	*	*	

Second Moment of Area About AP Axis (I_y)

BMI	< 18.5	18.5-24.9	25.0-29.9	> 30
< 18.5		*	*	*
18.5-24.9	*		*	*
25.0-29.9	*	*		*
> 30	*	*	*	

Maximum Section Modulus (Z_{max})

BMI	< 18.5	18.5-24.9	25.0-29.9	> 30
< 18.5		*	*	*
18.5-24.9	*		*	*
25.0-29.9	*	*		*
> 30	*	*	*	

Polar Second Moment of Area (J)

BMI	< 18.5	18.5-24.9	25.0-29.9	> 30
< 18.5		*	*	*
18.5-24.9	*		*	*
25.0-29.9	*	*		*
> 30	*	*	*	

Minimum Section Modulus (Z_{min})

BMI	< 18.5	18.5-24.9	25.0-29.9	> 30
< 18.5		*	*	*
18.5-24.9	*		*	*
25.0-29.9	*	*		*
> 30	*	*	*	

Maximum Second Moment of Area (I_{max})

BMI	< 18.5	18.5-24.9	25.0-29.9	> 30
< 18.5		*	*	*
18.5-24.9	*		*	*
25.0-29.9	*	*		*
> 30	*	*	*	

*indicates significance

Table H.4. Within bone pairwise comparisons for BMI category for the femur

Cortical Area (CA)

BMI	< 18.5	18.5-24.9	25.0-29.9	> 30
< 18.5		*	*	*
18.5-24.9	*		*	*
25.0-29.9	*	*		*
> 30	*	*	*	

Total Area (TA)

BMI	< 18.5	18.5-24.9	25.0-29.9	> 30
< 18.5		*	*	*
18.5-24.9	*		*	*
25.0-29.9	*	*		*
> 30	*	*	*	

Medullary Area (MA)

BMI	< 18.5	18.5-24.9	25.0-29.9	> 30
< 18.5		NS	*	*
18.5-24.9	NS		NS	*
25.0-29.9	*	NS		NS
> 30	*	*	NS	

Percent Cortical Area (%CA)

BMI	< 18.5	18.5-24.9	25.0-29.9	> 30
< 18.5		NS	NS	NS
18.5-24.9	NS		NS	*
25.0-29.9	NS	NS		NS
> 30	NS	*	NS	

Second Moment of Area About ML Axis (I_x)

BMI	< 18.5	18.5-24.9	25.0-29.9	> 30
< 18.5		*	*	*
18.5-24.9	*		*	*
25.0-29.9	*	*		*
> 30	*	*	*	

Second Moment of Area About AP Axis (I_y)

BMI	< 18.5	18.5-24.9	25.0-29.9	> 30
< 18.5		*	*	*
18.5-24.9	*		*	*
25.0-29.9	*	*		*
> 30	*	*	*	

Polar Second Moment of Area (J)

BMI	< 18.5	18.5-24.9	25.0-29.9	> 30
< 18.5		*	*	*
18.5-24.9	*		*	*
25.0-29.9	*	*		*
> 30	*	*	*	

Maximum Second Moment of Area (I_{max})

BMI	< 18.5	18.5-24.9	25.0-29.9	> 30
< 18.5		*	*	*
18.5-24.9	*		*	*
25.0-29.9	*	*		*
> 30	*	*	*	

Minimum Second Moment of Area (I_{min})

BMI	< 18.5	18.5-24.9	25.0-29.9	> 30
< 18.5		*	*	*
18.5-24.9	*		*	*
25.0-29.9	*	*		*
> 30	*	*	*	

Shape Index (I_{max}/ I_{min})

BMI	< 18.5	18.5-24.9	25.0-29.9	> 30
< 18.5		NS	NS	NS
18.5-24.9	NS		NS	NS
25.0-29.9	NS	NS		NS
> 30	NS	NS	NS	

Section Modulus About ML Axis (Z_x)

BMI	< 18.5	18.5-24.9	25.0-29.9	> 30
< 18.5		*	*	*
18.5-24.9	*		*	*
25.0-29.9	*	*		*
> 30	*	*	*	

Section Modulus About AP Axis (Z_y)

BMI	< 18.5	18.5-24.9	25.0-29.9	> 30
< 18.5		*	*	*
18.5-24.9	*		*	*
25.0-29.9	*	*		*
> 30	*	*	*	

Polar Section Modulus (Z_p)

BMI	< 18.5	18.5-24.9	25.0-29.9	> 30
< 18.5		*	*	*
18.5-24.9	*		*	*
25.0-29.9	*	*		*
> 30	*	*	*	

Maximum Section Modulus (Z_{max})

BMI	< 18.5	18.5-24.9	25.0-29.9	> 30
< 18.5		*	*	*
18.5-24.9	*		*	*
25.0-29.9	*	*		*
> 30	*	*	*	

Minimum Section Modulus (Z_{min})

BMI	< 18.5	18.5-24.9	25.0-29.9	> 30
< 18.5		*	*	*
18.5-24.9	*		*	*
25.0-29.9	*	*		*
> 30	*	*	*	

*indicates significance at $p < 0.05$

Table H.5. Within bone pairwise comparisons for BMI category for the tibia

Cortical Area (CA)

BMI	< 18.5	18.5-24.9	25.0-29.9	> 30
< 18.5		*	*	*
18.5-24.9	*		*	*
25.0-29.9	*	*		NS
> 30	*	*	NS	

Total Area (TA)

BMI	< 18.5	18.5-24.9	25.0-29.9	> 30
< 18.5		*	*	*
18.5-24.9	*		*	*
25.0-29.9	*	*		*
> 30	*	*	*	

Medullary Area (MA)

BMI	< 18.5	18.5-24.9	25.0-29.9	> 30
< 18.5		*	*	*
18.5-24.9	*		*	*
25.0-29.9	*	*		*
> 30	*	*	*	

Percent Cortical Area (%CA)

BMI	< 18.5	18.5-24.9	25.0-29.9	> 30
< 18.5		NS	NS	NS
18.5-24.9	NS		*	*
25.0-29.9	NS	*		NS
> 30	NS	*	NS	

Second Moment of Area About ML Axis (I_x)

BMI	< 18.5	18.5-24.9	25.0-29.9	> 30
< 18.5		*	*	*
18.5-24.9	*		*	*
25.0-29.9	*	*		NS
> 30	*	*	NS	

Second Moment of Area About AP Axis (I_y)

BMI	< 18.5	18.5-24.9	25.0-29.9	> 30
< 18.5		*	*	*
18.5-24.9	*		*	*
25.0-29.9	*	*		NS
> 30	*	*	NS	

Polar Second Moment of Area (J)

BMI	< 18.5	18.5-24.9	25.0-29.9	> 30
< 18.5		*	*	*
18.5-24.9	*		*	*
25.0-29.9	*	*		NS
> 30	*	*	NS	

Maximum Second Moment of Area (I_{max})

BMI	< 18.5	18.5-24.9	25.0-29.9	> 30
< 18.5		*	*	*
18.5-24.9	*		*	*
25.0-29.9	*	*		NS
> 30	*	*	NS	

Minimum Second Moment of Area (I_{min})

BMI	< 18.5	18.5-24.9	25.0-29.9	> 30
< 18.5		NS	*	*
18.5-24.9	NS		*	*
25.0-29.9	*	*		NS
> 30	*	*	NS	

Shape Index (I_{max}/ I_{min})

BMI	< 18.5	18.5-24.9	25.0-29.9	> 30
< 18.5		*	*	*
18.5-24.9	*		NS	NS
25.0-29.9	*	NS		NS
> 30	*	NS	NS	

Section Modulus About ML Axis (Z_x)

BMI	< 18.5	18.5-24.9	25.0-29.9	> 30
< 18.5		*	*	*
18.5-24.9	*		*	*
25.0-29.9	*	*		NS
> 30	*	*	NS	

Section Modulus About AP Axis (Z_y)

BMI	< 18.5	18.5-24.9	25.0-29.9	> 30
< 18.5		*	*	*
18.5-24.9	*		*	*
25.0-29.9	*	*		NS
> 30	*	*	NS	

Polar Section Modulus (Z_p)

BMI	< 18.5	18.5-24.9	25.0-29.9	> 30
< 18.5		NS	*	*
18.5-24.9	NS		*	*
25.0-29.9	*	*		NS
> 30	*	*	NS	

Maximum Section Modulus (Z_{max})

BMI	< 18.5	18.5-24.9	25.0-29.9	> 30
< 18.5		*	*	*
18.5-24.9	*		*	*
25.0-29.9	*	*		NS
> 30	*	*	NS	

Minimum Section Modulus (Z_{min})

BMI	< 18.5	18.5-24.9	25.0-29.9	> 30
< 18.5		NS	*	*
18.5-24.9	NS		*	*
25.0-29.9	*	*		NS
> 30	*	*	NS	

* indicates significance at $p < 0.05$

Table H.6. Within bone pairwise comparisons for BMI category for the fibula

Cortical Area (CA)

BMI	< 18.5	18.5-24.9	25.0-29.9	> 30
< 18.5		*	*	*
18.5-24.9	*		*	*
25.0-29.9	*	*		*
> 30	*	*	*	

Total Area (TA)

BMI	< 18.5	18.5-24.9	25.0-29.9	> 30
< 18.5		*	*	*
18.5-24.9	*		*	*
25.0-29.9	*	*		*
> 30	*	*	*	

Medullary Area (MA)

BMI	< 18.5	18.5-24.9	25.0-29.9	> 30
< 18.5		*	*	*
18.5-24.9	*		NS	*
25.0-29.9	*	NS		*
> 30	*	*	*	

Percent Cortical Area (%CA)

BMI	< 18.5	18.5-24.9	25.0-29.9	> 30
< 18.5		NS	NS	NS
18.5-24.9	NS		NS	*
25.0-29.9	NS	NS		*
> 30	NS	*	*	

Second Moment of Area About ML Axis (I_x)

BMI	< 18.5	18.5-24.9	25.0-29.9	> 30
< 18.5		*	*	*
18.5-24.9	*		*	*
25.0-29.9	*	*		*
> 30	*	*	*	

Second Moment of Area About AP Axis (I_y)

BMI	< 18.5	18.5-24.9	25.0-29.9	> 30
< 18.5		*	*	*
18.5-24.9	*		*	*
25.0-29.9	*	*		*
> 30	*	*	*	

Polar Second Moment of Area (J)

BMI	< 18.5	18.5-24.9	25.0-29.9	> 30
< 18.5		*	*	*
18.5-24.9	*		*	*
25.0-29.9	*	*		*
> 30	*	*	*	

Maximum Second Moment of Area (I_{max})

BMI	< 18.5	18.5-24.9	25.0-29.9	> 30
< 18.5		*	*	*
18.5-24.9	*		*	*
25.0-29.9	*	*		*
> 30	*	*	*	

Minimum Second Moment of Area (I_{min})

BMI	< 18.5	18.5-24.9	25.0-29.9	> 30
< 18.5		*	*	*
18.5-24.9	*		*	*
25.0-29.9	*	*		*
> 30	*	*	*	

Shape Index (I_{max}/ I_{min})

BMI	< 18.5	18.5-24.9	25.0-29.9	> 30
< 18.5		NS	*	NS
18.5-24.9	NS		NS	NS
25.0-29.9	*	NS		NS
> 30	NS	NS	NS	

Section Modulus About ML Axis (Z_x)

BMI	< 18.5	18.5-24.9	25.0-29.9	> 30
< 18.5		*	*	*
18.5-24.9	*		*	*
25.0-29.9	*	*		*
> 30	*	*	*	

Section Modulus About AP Axis (Z_y)

BMI	< 18.5	18.5-24.9	25.0-29.9	> 30
< 18.5		*	*	*
18.5-24.9	*		*	*
25.0-29.9	*	*		*
> 30	*	*	*	

Polar Section Modulus (Z_p)

BMI	< 18.5	18.5-24.9	25.0-29.9	> 30
< 18.5		*	*	*
18.5-24.9	*		*	*
25.0-29.9	*	*		*
> 30	*	*	*	

Maximum Section Modulus (Z_{max})

BMI	< 18.5	18.5-24.9	25.0-29.9	> 30
< 18.5		*	*	*
18.5-24.9	*		*	*
25.0-29.9	*	*		*
> 30	*	*	*	

Minimum Section Modulus (Z_{min})

BMI	< 18.5	18.5-24.9	25.0-29.9	> 30
< 18.5		*	*	*
18.5-24.9	*		*	*
25.0-29.9	*	*		*
> 30	*	*	*	

* indicates significance at $p < 0.05$

Table H.7. Within bone pairwise comparisons for activity level in the humerus

Cortical Area (CA)

Activity	Light	Moderate	Heavy
Light		NS	*
Moderate	NS		*
Heavy	*	*	

Total Area (TA)

Activity	Light	Moderate	Heavy
Light		*	*
Moderate	*		*
Heavy	*	*	

Medullary Area (MA)

Activity	Light	Moderate	Heavy
Light		*	*
Moderate	*		*
Heavy	*	*	

Percent Cortical Area (%CA)

Activity	Light	Moderate	Heavy
Light		NS	NS
Moderate	NS		NS
Heavy	NS	NS	

Second Moment of Area About ML Axis (I_x)

Activity	Light	Moderate	Heavy
Light		*	*
Moderate	*		*
Heavy	*	*	

Second Moment of Area About AP Axis (I_y)

Activity	Light	Moderate	Heavy
Light		*	*
Moderate	*		*
Heavy	*	*	

Polar Second Moment of Area (J)

Activity	Light	Moderate	Heavy
Light		*	*
Moderate	*		*
Heavy	*	*	

Maximum Second Moment of Area (I_{max})

Activity	Light	Moderate	Heavy
Light		NS	*
Moderate	NS		*
Heavy	*	*	

Minimum Second Moment of Area (I_{min})

Activity	Light	Moderate	Heavy
Light		*	*
Moderate	*		*
Heavy	*	*	

Shape Index (I_{max}/ I_{min})

Activity	Light	Moderate	Heavy
Light		NS	NS
Moderate	NS		NS
Heavy	NS	NS	

Section Modulus About ML Axis (Z_x)

Activity	Light	Moderate	Heavy
Light		*	*
Moderate	*		*
Heavy	*	*	

Section Modulus About AP Axis (Z_y)

Activity	Light	Moderate	Heavy
Light		NS	*
Moderate	NS		*
Heavy	*	*	

Polar Section Modulus (Z_p)

Activity	Light	Moderate	Heavy
Light		NS	*
Moderate	NS		*
Heavy	*	*	

Maximum Section Modulus (Z_{max})

Activity	Light	Moderate	Heavy
Light		NS	*
Moderate	NS		*
Heavy	*	*	

Minimum Section Modulus (Z_{min})

Activity	Light	Moderate	Heavy
Light		NS	*
Moderate	NS		*
Heavy	*	*	

* indicates significance at $p < 0.05$

Table H.8. Within bone pairwise comparisons for activity level in the radius

Cortical Area (CA)

Activity	Light	Moderate	Heavy
Light		NS	*
Moderate	NS		*
Heavy	*	*	

Total Area (TA)

Activity	Light	Moderate	Heavy
Light		*	*
Moderate	*		*
Heavy	*	*	

Medullary Area (MA)

Activity	Light	Moderate	Heavy
Light		*	*
Moderate	*		*
Heavy	*	*	

Percent Cortical Area (%CA)

Activity	Light	Moderate	Heavy
Light		*	NS
Moderate	*		NS
Heavy	NS	NS	

Second Moment of Area About ML Axis (I_x)

Activity	Light	Moderate	Heavy
Light		*	*
Moderate	*		*
Heavy	*	*	

Second Moment of Area About AP Axis (I_y)

Activity	Light	Moderate	Heavy
Light		NS	*
Moderate	NS		*
Heavy	*	*	

Polar Second Moment of Area (J)

Activity	Light	Moderate	Heavy
Light		*	*
Moderate	*		*
Heavy	*	*	

Maximum Second Moment of Area (I_{max})

Activity	Light	Moderate	Heavy
Light		*	*
Moderate	*		*
Heavy	*	*	

Minimum Second Moment of Area (I_{min})

Activity	Light	Moderate	Heavy
Light		*	*
Moderate	*		*
Heavy	*	*	

Shape Index (I_{max}/ I_{min})

Activity	Light	Moderate	Heavy
Light		NS	NS
Moderate	NS		NS
Heavy	NS	NS	

Section Modulus About ML Axis (Z_x)

Activity	Light	Moderate	Heavy
Light		*	*
Moderate	*		*
Heavy	*	*	

Section Modulus About AP Axis (Z_y)

Activity	Light	Moderate	Heavy
Light		*	*
Moderate	*		*
Heavy	*	*	

Polar Section Modulus (Z_p)

Activity	Light	Moderate	Heavy
Light		*	*
Moderate	*		*
Heavy	*	*	

Maximum Section Modulus (Z_{max})

Activity	Light	Moderate	Heavy
Light		*	*
Moderate	*		*
Heavy	*	*	

Minimum Section Modulus (Z_{min})

Activity	Light	Moderate	Heavy
Light		*	*
Moderate	*		*
Heavy	*	*	

* indicates significance at $p < 0.05$

Table H.9. Within bone pairwise comparisons for activity level in the ulna

Cortical Area (CA)

Activity	Light	Moderate	Heavy
Light		*	*
Moderate	*		*
Heavy	*	*	

Total Area (TA)

Activity	Light	Moderate	Heavy
Light		*	*
Moderate	*		*
Heavy	*	*	

Medullary Area (MA)

Activity	Light	Moderate	Heavy
Light		*	*
Moderate	*		*
Heavy	*	*	

Percent Cortical Area (%CA)

Activity	Light	Moderate	Heavy
Light		NS	NS
Moderate	NS		NS
Heavy	NS	NS	

Second Moment of Area About ML Axis (I_x)

Activity	Light	Moderate	Heavy
Light		*	*
Moderate	*		*
Heavy	*	*	

Second Moment of Area About AP Axis (I_y)

Activity	Light	Moderate	Heavy
Light		*	*
Moderate	*		*
Heavy	*	*	

Polar Second Moment of Area (J)

Activity	Light	Moderate	Heavy
Light		*	*
Moderate	*		*
Heavy	*	*	

Maximum Second Moment of Area (I_{max})

Activity	Light	Moderate	Heavy
Light		*	*
Moderate	*		*
Heavy	*	*	

Minimum Second Moment of Area (I_{min})

Activity	Light	Moderate	Heavy
Light		*	*
Moderate	*		*
Heavy	*	*	

Shape Index (I_{max}/ I_{min})

Activity	Light	Moderate	Heavy
Light		NS	NS
Moderate	NS		NS
Heavy	NS	NS	

Section Modulus About ML Axis (Z_x)

Activity	Light	Moderate	Heavy
Light		*	*
Moderate	*		*
Heavy	*	*	

Section Modulus About AP Axis (Z_y)

Activity	Light	Moderate	Heavy
Light		*	*
Moderate	*		*
Heavy	*	*	

Polar Section Modulus (Z_p)

Activity	Light	Moderate	Heavy
Light		*	*
Moderate	*		*
Heavy	*	*	

Maximum Section Modulus (Z_{max})

Activity	Light	Moderate	Heavy
Light		*	*
Moderate	*		*
Heavy	*	*	

Minimum Section Modulus (Z_{min})

Activity	Light	Moderate	Heavy
Light		*	*
Moderate	*		*
Heavy	*	*	

* indicates significance at $p < 0.05$

Table H.10. Within bone pairwise comparisons for activity level in the femur

Cortical Area (CA)

Activity	Light	Moderate	Heavy
Light		*	*
Moderate	*		*
Heavy	*	*	

Total Area (TA)

Activity	Light	Moderate	Heavy
Light		*	*
Moderate	*		*
Heavy	*	*	

Medullary Area (MA)

Activity	Light	Moderate	Heavy
Light		NS	NS
Moderate	NS		NS
Heavy	NS	NS	

Percent Cortical Area (%CA)

Activity	Light	Moderate	Heavy
Light		NS	NS
Moderate	NS		NS
Heavy	NS	NS	

Second Moment of Area About ML Axis (I_x)

Activity	Light	Moderate	Heavy
Light		*	*
Moderate	*		*
Heavy	*	*	

Second Moment of Area About AP Axis (I_y)

Activity	Light	Moderate	Heavy
Light		NS	*
Moderate	NS		*
Heavy	*	*	

Polar Second Moment of Area (J)

Activity	Light	Moderate	Heavy
Light		NS	*
Moderate	NS		*
Heavy	*	*	

Maximum Second Moment of Area (I_{max})

Activity	Light	Moderate	Heavy
Light		NS	*
Moderate	NS		*
Heavy	*	*	

Minimum Second Moment of Area (I_{min})

Activity	Light	Moderate	Heavy
Light		NS	*
Moderate	NS		*
Heavy	*	*	

Shape Index (I_{max}/ I_{min})

Activity	Light	Moderate	Heavy
Light		NS	NS
Moderate	NS		NS
Heavy	NS	NS	

Section Modulus About ML Axis (Z_x)

Activity	Light	Moderate	Heavy
Light		*	*
Moderate	*		*
Heavy	*	*	

Section Modulus About AP Axis (Z_y)

Activity	Light	Moderate	Heavy
Light		NS	*
Moderate	NS		*
Heavy	*	*	

Polar Section Modulus (Z_p)

Activity	Light	Moderate	Heavy
Light		NS	*
Moderate	NS		*
Heavy	*	*	

Maximum Section Modulus (Z_{max})

Activity	Light	Moderate	Heavy
Light		NS	*
Moderate	NS		*
Heavy	*	*	

Minimum Section Modulus (Z_{min})

Activity	Light	Moderate	Heavy
Light		NS	*
Moderate	NS		*
Heavy	*	*	

* indicates significance at $p < 0.05$

Table H.11. Within bone pairwise comparisons for activity level in the tibia

Cortical Area (CA)

Activity	Light	Moderate	Heavy
Light		*	*
Moderate	*		NS
Heavy	*	NS	

Total Area (TA)

Activity	Light	Moderate	Heavy
Light		*	*
Moderate	*		NS
Heavy	*	NS	

Medullary Area (MA)

Activity	Light	Moderate	Heavy
Light		NS	*
Moderate	NS		NS
Heavy	*	NS	

Percent Cortical Area (%CA)

Activity	Light	Moderate	Heavy
Light		NS	NS
Moderate	NS		NS
Heavy	NS	NS	

Second Moment of Area About ML Axis (I_x)

Activity	Light	Moderate	Heavy
Light		*	*
Moderate	*		NS
Heavy	*	NS	

Second Moment of Area About AP Axis (I_y)

Activity	Light	Moderate	Heavy
Light		*	*
Moderate	*		NS
Heavy	*	NS	

Polar Second Moment of Area (J)

Activity	Light	Moderate	Heavy
Light		*	*
Moderate	*		NS
Heavy	*	NS	

Maximum Second Moment of Area (I_{max})

Activity	Light	Moderate	Heavy
Light		*	*
Moderate	*		NS
Heavy	*	NS	

Minimum Second Moment of Area (I_{min})

Activity	Light	Moderate	Heavy
Light		*	*
Moderate	*		NS
Heavy	*	NS	

Shape Index (I_{max}/ I_{min})

Activity	Light	Moderate	Heavy
Light		NS	NS
Moderate	NS		NS
Heavy	NS	NS	

Section Modulus About ML Axis (Z_x)

Activity	Light	Moderate	Heavy
Light		*	*
Moderate	*		NS
Heavy	*	NS	

Section Modulus About AP Axis (Z_y)

Activity	Light	Moderate	Heavy
Light		*	*
Moderate	*		NS
Heavy	*	NS	

Polar Section Modulus (Z_p)

Activity	Light	Moderate	Heavy
Light		*	*
Moderate	*		NS
Heavy	*	NS	

Maximum Section Modulus (Z_{max})

Activity	Light	Moderate	Heavy
Light		*	*
Moderate	*		NS
Heavy	*	NS	

Minimum Section Modulus (Z_{min})

Activity	Light	Moderate	Heavy
Light		*	*
Moderate	*		NS
Heavy	*	NS	

* indicates significance at $p < 0.05$

Table H.12. Within bone pairwise comparisons for activity level in the fibula

Cortical Area (CA)

Activity	Light	Moderate	Heavy
Light		NS	*
Moderate	NS		*
Heavy	*	*	

Total Area (TA)

Activity	Light	Moderate	Heavy
Light		*	*
Moderate	*		*
Heavy	*	*	

Medullary Area (MA)

Activity	Light	Moderate	Heavy
Light		NS	*
Moderate	NS		NS
Heavy	*	NS	

Percent Cortical Area (%CA)

Activity	Light	Moderate	Heavy
Light		NS	NS
Moderate	NS		NS
Heavy	NS	NS	

Second Moment of Area About ML Axis (I_x)

Activity	Light	Moderate	Heavy
Light		NS	*
Moderate	NS		NS
Heavy	*	NS	

Second Moment of Area About AP Axis (I_y)

Activity	Light	Moderate	Heavy
Light		NS	*
Moderate	NS		*
Heavy	*	*	

Polar Second Moment of Area (J)

Activity	Light	Moderate	Heavy
Light		NS	*
Moderate	NS		*
Heavy	*	*	

Maximum Second Moment of Area (I_{max})

Activity	Light	Moderate	Heavy
Light		*	*
Moderate	*		NS
Heavy	*	NS	

Minimum Second Moment of Area (I_{min})

Activity	Light	Moderate	Heavy
Light		NS	*
Moderate	NS		*
Heavy	*	*	

Shape Index (I_{max}/ I_{min})

Activity	Light	Moderate	Heavy
Light		NS	NS
Moderate	NS		*
Heavy	NS	*	

Section Modulus About ML Axis (Z_x)

Activity	Light	Moderate	Heavy
Light		*	*
Moderate	*		*
Heavy	*	*	

Section Modulus About AP Axis (Z_y)

Activity	Light	Moderate	Heavy
Light		NS	*
Moderate	NS		*
Heavy	*	*	

Polar Section Modulus (Z_p)

Activity	Light	Moderate	Heavy
Light		*	*
Moderate	*		*
Heavy	*	*	

Maximum Section Modulus (Z_{max})

Activity	Light	Moderate	Heavy
Light		*	*
Moderate	*		*
Heavy	*	*	

Minimum Section Modulus (Z_{min})

Activity	Light	Moderate	Heavy
Light		NS	*
Moderate	NS		*
Heavy	*	*	

* indicates significance at $p < 0.05$

Table H.13. Within bone pairwise comparisons for activity level in the humerus

Cortical Area (CA)

	Mean	Sig.
Pathological Group	0.087302	*
Healthy Group	0.011054	

Total Area (TA)

	Mean	Sig.
Pathological Group	0.31275	*
Healthy Group	0.235862	

Medullary Area (MA)

	Mean	Sig.
Pathological Group	-0.12028	*
Healthy Group	-0.20472	

Percent Cortical Area (%CA)

	Mean	Sig.
Pathological Group	1.775191	NS
Healthy Group	1.774927	

Second Moment of Area About ML Axis (I_x)

	Mean	Sig.
Pathological Group	-3.38079	*
Healthy Group	-3.47129	

Second Moment of Area About AP Axis (I_y)

	Mean	Sig.
Pathological Group	-3.35795	*
Healthy Group	-3.43375	

Polar Second Moment of Area (J)

	Mean	Sig.
Pathological Group	-3.06378	*
Healthy Group	-3.14754	

Maximum Second Moment of Area (I_{max})

	Mean	Sig.
Pathological Group	-3.29696	*
Healthy Group	-3.38162	

Minimum Second Moment of Area (I_{min})

	Mean	Sig.
Pathological Group	-3.45061	*
Healthy Group	-3.53272	

Shape Index (I_{max}/ I_{min})

	Mean	Sig.
Pathological Group	0.153647	NS
Healthy Group	0.151094	

Section Modulus About ML Axis (Z_x)

	Mean	Sig.
Pathological Group	-1.895682	*
Healthy Group	-1.979798	

Section Modulus About AP Axis (Z_y)

	Mean	Sig.
Pathological Group	-1.882526	*
Healthy Group	-1.962938	

Polar Section Modulus (Z_p)

	Mean	Sig.
Pathological Group	-1.633338	*
Healthy Group	-1.719597	

Maximum Section Modulus (Z_{max})

	Mean	Sig.
Pathological Group	-1.855684	*
Healthy Group	-1.941950	

Minimum Section Modulus (Z_{min})

	Mean	Sig.
Pathological Group	-1.934247	*
Healthy Group	-2.06215	

Degrees of freedom = 514; critical value = 2.77835
* Significant at $p < 0.05$

Table H.14. Within bone pairwise comparisons for activity level in the radius

Cortical Area (CA)

	Mean	Sig.
Pathological Group	-0.221494	*
Healthy Group	-0.308969	

Total Area (TA)

	Mean	Sig.
Pathological Group	-0.079552	*
Healthy Group	-0.154401	

Medullary Area (MA)

	Mean	Sig.
Pathological Group	-0.69301	*
Healthy Group	-0.74839	

Percent Cortical Area (%CA)

	Mean	Sig.
Pathological Group	1.858058	*
Healthy Group	1.845432	

Second Moment of Area About ML Axis (I_x)

	Mean	Sig.
Pathological Group	-3.92302	*
Healthy Group	-3.99363	

Second Moment of Area About AP Axis (I_y)

	Mean	Sig.
Pathological Group	-3.78508	*
Healthy Group	-3.88503	

Polar Second Moment of Area (J)

	Mean	Sig.
Pathological Group	-3.54265	*
Healthy Group	-3.62804	

Maximum Second Moment of Area (I_{max})

	Mean	Sig.
Pathological Group	-3.74714	*
Healthy Group	-3.82962	

Minimum Second Moment of Area (I_{min})

	Mean	Sig.
Pathological Group	-3.97538	*
Healthy Group	-4.06495	

Shape Index (I_{max}/ I_{min})

	Mean	Sig.
Pathological Group	0.235326	NS
Healthy Group	0.228244	

Section Modulus About ML Axis (Z_x)

	Mean	Sig.
Pathological Group	-2.32401	*
Healthy Group	-2.40397	

Section Modulus About AP Axis (Z_y)

	Mean	Sig.
Pathological Group	-2.27426	*
Healthy Group	-2.36753	

Polar Section Modulus (Z_p)

	Mean	Sig.
Pathological Group	-2.06981	*
Healthy Group	-2.16103	

Maximum Section Modulus (Z_{max})

	Mean	Sig.
Pathological Group	-2.26923	*
Healthy Group	-2.35648	

Minimum Section Modulus (Z_{min})

	Mean	Sig.
Pathological Group	-2.363874	*
Healthy Group	-2.447907	

Degrees of freedom = 514; critical value = 2.77835
* Significant at $p < 0.05$

Table H.15. Within bone pairwise comparisons for activity level in the ulna

Cortical Area (CA)

	Mean	Sig.
Pathological Group	-0.192183	*
Healthy Group	-0.277415	

Total Area (TA)

	Mean	Sig.
Pathological Group	-0.062491	*
Healthy Group	-0.134648	

Medullary Area (MA)

	Mean	Sig.
Pathological Group	-0.69338	*
Healthy Group	-0.76067	

Percent Cortical Area (%CA)

	Mean	Sig.
Pathological Group	1.870308	*
Healthy Group	1.857233	

Second Moment of Area About ML Axis (I_x)

	Mean	Sig.
Pathological Group	-3.83447	*
Healthy Group	-3.90684	

Second Moment of Area About AP Axis (I_y)

	Mean	Sig.
Pathological Group	-3.88920	*
Healthy Group	-3.97015	

Polar Second Moment of Area (J)

	Mean	Sig.
Pathological Group	-3.55154	*
Healthy Group	-3.63005	

Maximum Second Moment of Area (I_{max})

	Mean	Sig.
Pathological Group	-3.76391	*
Healthy Group	-3.84785	

Minimum Second Moment of Area (I_{min})

	Mean	Sig.
Pathological Group	-3.97208	*
Healthy Group	-4.04224	

Shape Index (I_{max}/ I_{min})

	Mean	Sig.
Pathological Group	0.208173	NS
Healthy Group	0.194390	

Section Modulus About ML Axis (Z_x)

	Mean	Sig.
Pathological Group	-2.30584	*
Healthy Group	-2.38105	

Section Modulus About AP Axis (Z_y)

	Mean	Sig.
Pathological Group	-2.32507	*
Healthy Group	-2.40147	

Polar Section Modulus (Z_p)

	Mean	Sig.
Pathological Group	-2.07239	*
Healthy Group	-2.14897	

Maximum Section Modulus (Z_{max})

	Mean	Sig.
Pathological Group	-2.27453	*
Healthy Group	-2.35478	

Minimum Section Modulus (Z_{min})

	Mean	Sig.
Pathological Group	-2.365868	*
Healthy Group	-2.439692	

Degrees of freedom = 514; critical value = 2.77835

* Significant at $p < 0.05$

Table H.16. Within bone pairwise comparisons for activity level in the femur

Cortical Area (CA)

	Mean	Sig.
Pathological Group	0.370458	*
Healthy Group	0.307980	

Total Area (TA)

	Mean	Sig.
Pathological Group	0.631571	*
Healthy Group	0.561290	

Medullary Area (MA)

	Mean	Sig.
Pathological Group	0.17917	*
Healthy Group	0.07902	

Percent Cortical Area (%CA)

	Mean	Sig.
Pathological Group	1.746690	NS
Healthy Group	1.738887	

Second Moment of Area About ML Axis (I_x)

	Mean	Sig.
Pathological Group	-3.075523	*
Healthy Group	-3.142601	

Second Moment of Area About AP Axis (I_y)

	Mean	Sig.
Pathological Group	-3.04324	*
Healthy Group	-3.08359	

Polar Second Moment of Area (J)

	Mean	Sig.
Pathological Group	-2.754418	*
Healthy Group	-2.807409	

Maximum Second Moment of Area (I_{max})

	Mean	Sig.
Pathological Group	-2.99751	*
Healthy Group	-3.04852	

Minimum Second Moment of Area (I_{min})

	Mean	Sig.
Pathological Group	-3.125371	*
Healthy Group	-3.181473	

Shape Index (I_{max}/ I_{min})

	Mean	Sig.
Pathological Group	0.132949	NS
Healthy Group	0.127865	

Section Modulus About ML Axis (Z_x)

	Mean	Sig.
Pathological Group	-1.606745	*
Healthy Group	-1.672940	

Section Modulus About AP Axis (Z_y)

	Mean	Sig.
Pathological Group	-1.573086	*
Healthy Group	-1.632250	

Polar Section Modulus (Z_p)

	Mean	Sig.
Pathological Group	-1.332701	*
Healthy Group	-1.394943	

Maximum Section Modulus (Z_{max})

	Mean	Sig.
Pathological Group	-1.561125	*
Healthy Group	-1.620457	

Minimum Section Modulus (Z_{min})

	Mean	Sig.
Pathological Group	-1.929469	*
Healthy Group	-1.690758	

Degrees of freedom = 514; critical value = 2.77835
* Significant at $p < 0.05$

Table H.17. Within bone pairwise comparisons for activity level in the tibia

Cortical Area (CA)		
	Mean	Sig.
Pathological Group	0.24439	*
Healthy Group	0.19573	

Minimum Second Moment of Area (I_{min})		
	Mean	Sig.
Pathological Group	-3.30333	NS
Healthy Group	-3.33383	

Total Area (TA)		
	Mean	Sig.
Pathological Group	0.49966	*
Healthy Group	0.45056	

Shape Index (I_{max}/ I_{min})		
	Mean	Sig.
Pathological Group	0.288129	NS
Healthy Group	0.284737	

Medullary Area (MA)		
	Mean	Sig.
Pathological Group	0.09107	*
Healthy Group	0.00915	

Section Modulus About ML Axis (Z_x)		
	Mean	Sig.
Pathological Group	-1.66720	*
Healthy Group	-1.70929	

Percent Cortical Area (%CA)		
	Mean	Sig.
Pathological Group	1.745175	NS
Healthy Group	1.744722	

Section Modulus About AP Axis (Z_y)		
	Mean	Sig.
Pathological Group	-1.74233	NS
Healthy Group	-1.76984	

Second Moment of Area About ML Axis (I_x)		
	Mean	Sig.
Pathological Group	-3.09119	NS
Healthy Group	-3.12962	

Polar Section Modulus (Z_p)		
	Mean	Sig.
Pathological Group	-1.46965	NS
Healthy Group	-1.50362	

Second Moment of Area About AP Axis (I_y)		
	Mean	Sig.
Pathological Group	-3.19341	NS
Healthy Group	-3.20917	

Maximum Section Modulus (Z_{max})		
	Mean	Sig.
Pathological Group	-1.64896	NS
Healthy Group	-1.67960	

Polar Second Moment of Area (J)		
	Mean	Sig.
Pathological Group	-2.83267	NS
Healthy Group	-2.86122	

Minimum Section Modulus (Z_{min})		
	Mean	Sig.
Pathological Group	-1.80891	NS
Healthy Group	-1.84850	

Maximum Second Moment of Area (I_{max})		
	Mean	Sig.
Pathological Group	-3.01859	NS
Healthy Group	-3.04570	

Degrees of freedom = 514; critical value = 2.77835
* Significant at $p < 0.05$

Table H.18. Within bone pairwise comparisons for activity level in the fibula

Cortical Area (CA)

	Mean	Sig.
Pathological Group	-0.332365	*
Healthy Group	-0.406124	

Minimum Second Moment of Area (I_{min})

	Mean	Sig.
Pathological Group	-4.63671	*
Healthy Group	-4.68138	

Total Area (TA)

	Mean	Sig.
Pathological Group	-0.209081	*
Healthy Group	-0.268416	

Shape Index (I_{max}/ I_{min})

	Mean	Sig.
Pathological Group	0.34995	*
Healthy Group	0.32444	

Medullary Area (MA)

	Mean	Sig.
Pathological Group	-0.87105	NS
Healthy Group	-0.89127	

Section Modulus About ML Axis (Z_x)

	Mean	Sig.
Pathological Group	-2.66211	*
Healthy Group	-2.74380	

Percent Cortical Area (%CA)

	Mean	Sig.
Pathological Group	1.876716	*
Healthy Group	1.862292	

Section Modulus About AP Axis (Z_y)

	Mean	Sig.
Pathological Group	-2.67700	*
Healthy Group	-2.72173	

Second Moment of Area About ML Axis (I_x)

	Mean	Sig.
Pathological Group	-4.42838	*
Healthy Group	-4.52245	

Polar Section Modulus (Z_p)

	Mean	Sig.
Pathological Group	-2.44672	*
Healthy Group	-2.50490	

Second Moment of Area About AP Axis (I_y)

	Mean	Sig.
Pathological Group	-4.45090	NS
Healthy Group	-4.47912	

Maximum Section Modulus (Z_{max})

	Mean	Sig.
Pathological Group	-2.60263	*
Healthy Group	-2.66747	

Polar Second Moment of Area (J)

	Mean	Sig.
Pathological Group	-4.12163	*
Healthy Group	-4.18417	

Minimum Section Modulus (Z_{min})

	Mean	Sig.
Pathological Group	-2.78147	*
Healthy Group	-2.83422	

Maximum Second Moment of Area (I_{max})

	Mean	Sig.
Pathological Group	-4.28676	*
Healthy Group	-4.35695	

Degrees of freedom = 514; critical value = 2.77835
* Significant at $p < 0.05$

APPENDIX I
WITHIN LIMB PAIRWISE COMPARISON RESULTS FOR THE UPPER LIMB

Table I.1. Cortical Area (CA) pairwise comparisons by slice location in the upper limb

20% of bone length

Bone	Humerus	Radius	Ulna
Humerus		*	*
Radius	*		*
Ulna	*	*	

35% of bone length

Bone	Humerus	Radius	Ulna
Humerus		*	*
Radius	*		NS
Ulna	*	NS	

50% of bone length

Bone	Humerus	Radius	Ulna
Humerus		*	*
Radius	*		*
Ulna	*	*	

65% of bone length

Bone	Humerus	Radius	Ulna
Humerus		*	*
Radius	*		*
Ulna	*	*	

80% of bone length

Bone	Humerus	Radius	Ulna
Humerus		*	NS
Radius	*		*
Ulna	NS	*	

* indicates significance at p <0.05

Table I.2. Total Area (TA) pairwise comparisons by slice location in the upper limb

20% of bone length

Bone	Humerus	Radius	Ulna
Humerus		*	*
Radius	*		*
Ulna	*	*	

35% of bone length

Bone	Humerus	Radius	Ulna
Humerus		*	*
Radius	*		NS
Ulna	*	NS	

50% of bone length

Bone	Humerus	Radius	Ulna
Humerus		*	*
Radius	*		*
Ulna	*	*	

65% of bone length

Bone	Humerus	Radius	Ulna
Humerus		*	*
Radius	*		*
Ulna	*	*	

80% of bone length

Bone	Humerus	Radius	Ulna
Humerus		*	*
Radius	*		*
Ulna	*	*	

* indicates significance at p <0.05

Table I.3. Medullary Area (MA) pairwise comparisons by slice location in the upper limb

20% of bone length

Bone	Humerus	Radius	Ulna
Humerus		*	*
Radius	*		*
Ulna	*	*	

35% of bone length

Bone	Humerus	Radius	Ulna
Humerus		*	*
Radius	*		NS
Ulna	*	NS	

50% of bone length

Bone	Humerus	Radius	Ulna
Humerus		*	*
Radius	*		*
Ulna	*	*	

65% of bone length

Bone	Humerus	Radius	Ulna
Humerus		*	*
Radius	*		*
Ulna	*	*	

80% of bone length

Bone	Humerus	Radius	Ulna
Humerus		*	*
Radius	*		*
Ulna	*	*	

* indicates significance at p <0.05

Table I.4. Percent Cortical Area ((CA/TA) x 100) pairwise comparisons by slice location in the upper limb

20% of bone length

Bone	Humerus	Radius	Ulna
Humerus		*	*
Radius	*		*
Ulna	*	*	

35% of bone length

Bone	Humerus	Radius	Ulna
Humerus		*	*
Radius	*		NS
Ulna	*	NS	

50% of bone length

Bone	Humerus	Radius	Ulna
Humerus		*	*
Radius	*		NS
Ulna	*	NS	

65% of bone length

Bone	Humerus	Radius	Ulna
Humerus		*	*
Radius	*		NS
Ulna	*	NS	

80% of bone length

Bone	Humerus	Radius	Ulna
Humerus		*	*
Radius	*		*
Ulna	*	*	

* indicates significance at p <0.05

Table I.5. Second moment area about ML axis (I_x) pairwise comparisons by slice location in the upper limb

20% of bone length

Bone	Humerus	Radius	Ulna
Humerus		*	*
Radius	*		*
Ulna	*	*	

35% of bone length

Bone	Humerus	Radius	Ulna
Humerus		*	*
Radius	*		NS
Ulna	*	NS	

50% of bone length

Bone	Humerus	Radius	Ulna
Humerus		*	*
Radius	*		*
Ulna	*	*	

65% of bone length

Bone	Humerus	Radius	Ulna
Humerus		*	*
Radius	*		*
Ulna	*	*	

80% of bone length

Bone	Humerus	Radius	Ulna
Humerus		*	*
Radius	*		*
Ulna	*	*	

* indicates significance at p <0.05

Table I.6. Second moment area about AP axis (I_y) pairwise comparisons by slice location in the upper limb

20% of bone length

Bone	Humerus	Radius	Ulna
Humerus		*	*
Radius	*		*
Ulna	*	*	

35% of bone length

Bone	Humerus	Radius	Ulna
Humerus		*	*
Radius	*		*
Ulna	*	*	

50% of bone length

Bone	Humerus	Radius	Ulna
Humerus		*	*
Radius	*		*
Ulna	*	*	

65% of bone length

Bone	Humerus	Radius	Ulna
Humerus		*	*
Radius	*		NS
Ulna	*	NS	

80% of bone length

Bone	Humerus	Radius	Ulna
Humerus		*	*
Radius	*		*
Ulna	*	*	

* indicates significance at p <0.05

Table I.7. Polar section moment of area (J) pairwise comparisons by slice location in the upper limb

20% of bone length

Bone	Humerus	Radius	Ulna
Humerus		*	*
Radius	*		*
Ulna	*	*	

35% of bone length

Bone	Humerus	Radius	Ulna
Humerus		*	*
Radius	*		*
Ulna	*	*	

50% of bone length

Bone	Humerus	Radius	Ulna
Humerus		*	*
Radius	*		*
Ulna	*	*	

65% of bone length

Bone	Humerus	Radius	Ulna
Humerus		*	*
Radius	*		*
Ulna	*	*	

80% of bone length

Bone	Humerus	Radius	Ulna
Humerus		*	*
Radius	*		*
Ulna	*	*	

* indicates significance at p <0.05

Table I.8. Maximum second moment area (I_{max}) pairwise comparisons by slice location in the upper limb

20% of bone length

Bone	Humerus	Radius	Ulna
Humerus		*	*
Radius	*		*
Ulna	*	*	

35% of bone length

Bone	Humerus	Radius	Ulna
Humerus		*	*
Radius	*		*
Ulna	*	*	

50% of bone length

Bone	Humerus	Radius	Ulna
Humerus		*	*
Radius	*		*
Ulna	*	*	

65% of bone length

Bone	Humerus	Radius	Ulna
Humerus		*	*
Radius	*		NS
Ulna	*	NS	

80% of bone length

Bone	Humerus	Radius	Ulna
Humerus		*	NS
Radius	*		*
Ulna	NS	*	

* indicates significance at p <0.05

Table I.9. Minimum second moment area (I_{min}) pairwise comparisons by slice location in the upper limb

20% of bone length

Bone	Humerus	Radius	Ulna
Humerus		*	*
Radius	*		*
Ulna	*	*	

35% of bone length

Bone	Humerus	Radius	Ulna
Humerus		*	*
Radius	*		*
Ulna	*	*	

50% of bone length

Bone	Humerus	Radius	Ulna
Humerus		*	*
Radius	*		NS
Ulna	*	NS	

65% of bone length

Bone	Humerus	Radius	Ulna
Humerus		*	*
Radius	*		*
Ulna	*	*	

80% of bone length

Bone	Humerus	Radius	Ulna
Humerus		*	*
Radius	*		*
Ulna	*	*	

* indicates significance at p <0.05

Table I.10. Shape index (I_{max}/ I_{min}) pairwise comparisons by slice location in the upper limb

20% of bone length

Bone	Humerus	Radius	Ulna
Humerus		*	*
Radius	*		*
Ulna	*	*	

35% of bone length

Bone	Humerus	Radius	Ulna
Humerus		*	*
Radius	*		*
Ulna	*	*	

50% of bone length

Bone	Humerus	Radius	Ulna
Humerus		*	*
Radius	*		*
Ulna	*	*	

65% of bone length

Bone	Humerus	Radius	Ulna
Humerus		*	NS
Radius	*		*
Ulna	NS	*	

80% of bone length

Bone	Humerus	Radius	Ulna
Humerus		*	*
Radius	*		*
Ulna	*	*	

* indicates significance at p <0.05

Table I.11. Section modulus about ML axis (Z_x) pairwise comparisons by slice location in the upper limb

20% of bone length

Bone	Humerus	Radius	Ulna
Humerus		*	*
Radius	*		*
Ulna	*	*	

35% of bone length

Bone	Humerus	Radius	Ulna
Humerus		*	*
Radius	*		*
Ulna	*	*	

50% of bone length

Bone	Humerus	Radius	Ulna
Humerus		*	*
Radius	*		*
Ulna	*	*	

65% of bone length

Bone	Humerus	Radius	Ulna
Humerus		*	*
Radius	*		*
Ulna	*	*	

80% of bone length

Bone	Humerus	Radius	Ulna
Humerus		*	*
Radius	*		*
Ulna	*	*	

* indicates significance at p <0.05

Table I.12. Section modulus about AP axis (Z_y) pairwise comparisons by slice location in the upper limb

20% of bone length

Bone	Humerus	Radius	Ulna
Humerus		*	*
Radius	*		*
Ulna	*	*	

35% of bone length

Bone	Humerus	Radius	Ulna
Humerus		*	*
Radius	*		*
Ulna	*	*	

50% of bone length

Bone	Humerus	Radius	Ulna
Humerus		*	*
Radius	*		NS
Ulna	*	NS	

65% of bone length

Bone	Humerus	Radius	Ulna
Humerus		*	*
Radius	*		*
Ulna	*	*	

80% of bone length

Bone	Humerus	Radius	Ulna
Humerus		*	*
Radius	*		*
Ulna	*	*	

* indicates significance at p <0.05

Table I.13. Polar section modulus (Z_p) pairwise comparisons by slice location in the upper limb

20% of bone length

Bone	Humerus	Radius	Ulna
Humerus		*	*
Radius	*		*
Ulna	*	*	

35% of bone length

Bone	Humerus	Radius	Ulna
Humerus		*	*
Radius	*		*
Ulna	*	*	

50% of bone length

Bone	Humerus	Radius	Ulna
Humerus		*	*
Radius	*		*
Ulna	*	*	

65% of bone length

Bone	Humerus	Radius	Ulna
Humerus		*	*
Radius	*		*
Ulna	*	*	

80% of bone length

Bone	Humerus	Radius	Ulna
Humerus		*	*
Radius	*		*
Ulna	*	*	

* indicates significance at p <0.05

Table I.14. Maximum section modulus (Z_{max}) pairwise comparisons by slice location in the upper limb

20% of bone length

Bone	Humerus	Radius	Ulna
Humerus		*	*
Radius	*		*
Ulna	*	*	

35% of bone length

Bone	Humerus	Radius	Ulna
Humerus		*	*
Radius	*		*
Ulna	*	*	

50% of bone length

Bone	Humerus	Radius	Ulna
Humerus		*	*
Radius	*		*
Ulna	*	*	

65% of bone length

Bone	Humerus	Radius	Ulna
Humerus		*	*
Radius	*		*
Ulna	*	*	

80% of bone length

Bone	Humerus	Radius	Ulna
Humerus		*	*
Radius	*		*
Ulna	*	*	

* indicates significance at p <0.05

Table I.15. Maximum section modulus (Z_{min}) pairwise comparisons by slice location in the upper limb

20% of bone length

Bone	Humerus	Radius	Ulna
Humerus		*	*
Radius	*		*
Ulna	*	*	

35% of bone length

Bone	Humerus	Radius	Ulna
Humerus		*	*
Radius	*		*
Ulna	*	*	

50% of bone length

Bone	Humerus	Radius	Ulna
Humerus		*	*
Radius	*		NS
Ulna	*	NS	

65% of bone length

Bone	Humerus	Radius	Ulna
Humerus		*	*
Radius	*		*
Ulna	*	*	

80% of bone length

Bone	Humerus	Radius	Ulna
Humerus		*	*
Radius	*		*
Ulna	*	*	

* indicates significance at $p < 0.05$

APPENDIX J
WITHIN LIMB PAIRWISE COMPARISON RESULTS FOR THE LOWER LIMB

Table J.1. Cortical Area (CA) pairwise comparisons by slice location in the lower limb

20% of bone length

Bone	Femur	Tibia	Fibula
Femur		*	*
Tibia	*		*
Fibula	*	*	

35% of bone length

Bone	Femur	Tibia	Fibula
Femur		*	*
Tibia	*		*
Fibula	*	*	

50% of bone length

Bone	Femur	Tibia	Fibula
Femur		*	*
Tibia	*		*
Fibula	*	*	

65% of bone length

Bone	Femur	Tibia	Fibula
Femur		*	*
Tibia	*		*
Fibula	*	*	

80% of bone length

Bone	Femur	Tibia	Fibula
Femur		*	*
Tibia	*		*
Fibula	*	*	

* indicates significance at p <0.05

Table J.2. Total Area (TA) pairwise comparisons by slice location in the lower limb

20% of bone length

Bone	Femur	Tibia	Fibula
Femur		*	*
Tibia	*		*
Fibula	*	*	

35% of bone length

Bone	Femur	Tibia	Fibula
Femur		*	*
Tibia	*		*
Fibula	*	*	

50% of bone length

Bone	Femur	Tibia	Fibula
Femur		*	*
Tibia	*		*
Fibula	*	*	

65% of bone length

Bone	Femur	Tibia	Fibula
Femur		*	*
Tibia	*		*
Fibula	*	*	

80% of bone length

Bone	Femur	Tibia	Fibula
Femur		*	*
Tibia	*		*
Fibula	*	*	

* indicates significance at p <0.05

Table J.3. Medullary Area (MA) pairwise comparisons by slice location in the lower limb

20% of bone length

Bone	Femur	Tibia	Fibula
Femur		*	*
Tibia	*		*
Fibula	*	*	

35% of bone length

Bone	Femur	Tibia	Fibula
Femur		*	*
Tibia	*		*
Fibula	*	*	

50% of bone length

Bone	Femur	Tibia	Fibula
Femur		*	*
Tibia	*		*
Fibula	*	*	

65% of bone length

Bone	Femur	Tibia	Fibula
Femur		*	*
Tibia	*		*
Fibula	*	*	

80% of bone length

Bone	Femur	Tibia	Fibula
Femur		*	*
Tibia	*		*
Fibula	*	*	

* indicates significance at p <0.05

Table J.4. Percent Cortical Area ((CA/TA) x 100) pairwise comparisons by slice location in the lower limb

20% of bone length

Bone	Femur	Tibia	Fibula
Femur		*	*
Tibia	*		*
Fibula	*	*	

35% of bone length

Bone	Femur	Tibia	Fibula
Femur		*	*
Tibia	*		*
Fibula	*	*	

50% of bone length

Bone	Femur	Tibia	Fibula
Femur		NS	*
Tibia	NS		*
Fibula	*	*	

65% of bone length

Bone	Femur	Tibia	Fibula
Femur		*	*
Tibia	*		*
Fibula	*	*	

80% of bone length

Bone	Femur	Tibia	Fibula
Femur		*	*
Tibia	*		*
Fibula	*	*	

* indicates significance at p <0.05

Table J.5. Second moment area about ML axis (I_x) pairwise comparisons by slice location in the lower limb

20% of bone length

Bone	Femur	Tibia	Fibula
Femur		*	*
Tibia	*		*
Fibula	*	*	

35% of bone length

Bone	Femur	Tibia	Fibula
Femur		*	*
Tibia	*		*
Fibula	*	*	

50% of bone length

Bone	Femur	Tibia	Fibula
Femur		NS	*
Tibia	NS		*
Fibula	*	*	

65% of bone length

Bone	Femur	Tibia	Fibula
Femur		*	*
Tibia	*		*
Fibula	*	*	

80% of bone length

Bone	Femur	Tibia	Fibula
Femur		*	*
Tibia	*		*
Fibula	*	*	

* indicates significance at p <0.05

Table J.6. Second moment area about AP axis (I_y) pairwise comparisons by slice location in the lower limb

20% of bone length

Bone	Femur	Tibia	Fibula
Femur		*	*
Tibia	*		*
Fibula	*	*	

35% of bone length

Bone	Femur	Tibia	Fibula
Femur		*	*
Tibia	*		*
Fibula	*	*	

50% of bone length

Bone	Femur	Tibia	Fibula
Femur		*	*
Tibia	*		*
Fibula	*	*	

65% of bone length

Bone	Femur	Tibia	Fibula
Femur		*	*
Tibia	*		*
Fibula	*	*	

80% of bone length

Bone	Femur	Tibia	Fibula
Femur		NS	*
Tibia	NS		*
Fibula	*	*	

* indicates significance at p <0.05

Table J.7. Polar section moment of area (J) pairwise comparisons by slice location in the lower limb

20% of bone length

Bone	Femur	Tibia	Fibula
Femur		*	*
Tibia	*		*
Fibula	*	*	

35% of bone length

Bone	Femur	Tibia	Fibula
Femur		*	*
Tibia	*		*
Fibula	*	*	

50% of bone length

Bone	Femur	Tibia	Fibula
Femur		*	*
Tibia	*		*
Fibula	*	*	

65% of bone length

Bone	Femur	Tibia	Fibula
Femur		*	*
Tibia	*		*
Fibula	*	*	

80% of bone length

Bone	Femur	Tibia	Fibula
Femur		*	*
Tibia	*		*
Fibula	*	*	

* indicates significance at p <0.05

Table J.8. Maximum second moment area (I_{max}) pairwise comparisons by slice location in the lower limb

20% of bone length

Bone	Femur	Tibia	Fibula
Femur		*	*
Tibia	*		*
Fibula	*	*	

35% of bone length

Bone	Femur	Tibia	Fibula
Femur		*	*
Tibia	*		*
Fibula	*	*	

50% of bone length

Bone	Femur	Tibia	Fibula
Femur		*	*
Tibia	*		*
Fibula	*	*	

65% of bone length

Bone	Femur	Tibia	Fibula
Femur		*	*
Tibia	*		*
Fibula	*	*	

80% of bone length

Bone	Femur	Tibia	Fibula
Femur		*	*
Tibia	*		*
Fibula	*	*	

* indicates significance at p <0.05

Table J.9. Minimum second moment area (I_{min}) pairwise comparisons by slice location in the lower limb

20% of bone length

Bone	Femur	Tibia	Fibula
Femur		*	*
Tibia	*		*
Fibula	*	*	

35% of bone length

Bone	Femur	Tibia	Fibula
Femur		*	*
Tibia	*		*
Fibula	*	*	

50% of bone length

Bone	Femur	Tibia	Fibula
Femur		*	*
Tibia	*		*
Fibula	*	*	

65% of bone length

Bone	Femur	Tibia	Fibula
Femur		*	*
Tibia	*		*
Fibula	*	*	

80% of bone length

Bone	Femur	Tibia	Fibula
Femur		NS	*
Tibia	NS		*
Fibula	*	*	

* indicates significance at p <0.05

Table J.10. Shape index (I_{max}/ I_{min}) pairwise comparisons by slice location in the lower limb

20% of bone length

Bone	Femur	Tibia	Fibula
Femur		*	*
Tibia	*		*
Fibula	*	*	

35% of bone length

Bone	Femur	Tibia	Fibula
Femur		*	*
Tibia	*		NS
Fibula	*	NS	

50% of bone length

Bone	Femur	Tibia	Fibula
Femur		*	*
Tibia	*		*
Fibula	*	*	

65% of bone length

Bone	Femur	Tibia	Fibula
Femur		*	*
Tibia	*		NS
Fibula	*	NS	

80% of bone length

Bone	Femur	Tibia	Fibula
Femur		*	*
Tibia	*		*
Fibula	*	*	

* indicates significance at p <0.05

Table J.11. Section modulus about ML axis (Z_x) pairwise comparisons by slice location in the lower limb

20% of bone length

Bone	Femur	Tibia	Fibula
Femur		*	*
Tibia	*		*
Fibula	*	*	

35% of bone length

Bone	Femur	Tibia	Fibula
Femur		*	*
Tibia	*		*
Fibula	*	*	

50% of bone length

Bone	Femur	Tibia	Fibula
Femur		NS	*
Tibia	NS		*
Fibula	*	*	

65% of bone length

Bone	Femur	Tibia	Fibula
Femur		*	*
Tibia	*		*
Fibula	*	*	

80% of bone length

Bone	Femur	Tibia	Fibula
Femur		*	*
Tibia	*		*
Fibula	*	*	

* indicates significance at p <0.05

Table J.12. Section modulus about AP axis (Z_y) pairwise comparisons by slice location in the lower limb

20% of bone length

Bone	Femur	Tibia	Fibula
Femur		*	*
Tibia	*		*
Fibula	*	*	

35% of bone length

Bone	Femur	Tibia	Fibula
Femur		*	*
Tibia	*		*
Fibula	*	*	

50% of bone length

Bone	Femur	Tibia	Fibula
Femur		*	*
Tibia	*		*
Fibula	*	*	

65% of bone length

Bone	Femur	Tibia	Fibula
Femur		*	*
Tibia	*		*
Fibula	*	*	

80% of bone length

Bone	Femur	Tibia	Fibula
Femur		*	*
Tibia	*		*
Fibula	*	*	

* indicates significance at p <0.05

Table J.13. Polar section modulus (Z_p) pairwise comparisons by slice location in the lower limb

20% of bone length

Bone	Femur	Tibia	Fibula
Femur		*	*
Tibia	*		*
Fibula	*	*	

35% of bone length

Bone	Femur	Tibia	Fibula
Femur		*	*
Tibia	*		*
Fibula	*	*	

50% of bone length

Bone	Femur	Tibia	Fibula
Femur		*	*
Tibia	*		*
Fibula	*	*	

65% of bone length

Bone	Femur	Tibia	Fibula
Femur		*	*
Tibia	*		*
Fibula	*	*	

80% of bone length

Bone	Femur	Tibia	Fibula
Femur		*	*
Tibia	*		*
Fibula	*	*	

* indicates significance at p <0.05

Table J.14. Maximum section modulus (Z_{max}) pairwise comparisons by slice location in the lower limb

20% of bone length

Bone	Femur	Tibia	Fibula
Femur		*	*
Tibia	*		*
Fibula	*	*	

35% of bone length

Bone	Femur	Tibia	Fibula
Femur		*	*
Tibia	*		*
Fibula	*	*	

50% of bone length

Bone	Femur	Tibia	Fibula
Femur		*	*
Tibia	*		*
Fibula	*	*	

65% of bone length

Bone	Femur	Tibia	Fibula
Femur		NS	*
Tibia	NS		*
Fibula	*	*	

80% of bone length

Bone	Femur	Tibia	Fibula
Femur		*	*
Tibia	*		*
Fibula	*	*	

* indicates significance at p <0.05

Table J.15. Maximum section modulus (Z_{min}) pairwise comparisons by slice location in the lower limb

20% of bone length

Bone	Femur	Tibia	Fibula
Femur		*	*
Tibia	*		*
Fibula	*	*	

35% of bone length

Bone	Femur	Tibia	Fibula
Femur		*	*
Tibia	*		*
Fibula	*	*	

50% of bone length

Bone	Femur	Tibia	Fibula
Femur		*	*
Tibia	*		*
Fibula	*	*	

65% of bone length

Bone	Femur	Tibia	Fibula
Femur		*	*
Tibia	*		*
Fibula	*	*	

80% of bone length

Bone	Femur	Tibia	Fibula
Femur		NS	*
Tibia	NS		*
Fibula	*	*	

* indicates significance at $p < 0.05$

APPENDIX K
BETWEEN LIMB PAIRWISE COMPARISON RESULTS FOR DISTAL LIMB ELEMENTS

Table K.1. Cortical Area (CA) pairwise comparisons by slice location in distal limb elements

20% of bone length

Bone	Radius	Ulna	Tibia	Fibula
Radius		*	*	*
Ulna	*		*	*
Tibia	*	*		*
Fibula	*	*	*	

35% of bone length

Bone	Radius	Ulna	Tibia	Fibula
Radius		NS	*	*
Ulna	NS		*	NS
Tibia	*	*		*
Fibula	*	NS	*	

50% of bone length

Bone	Radius	Ulna	Tibia	Fibula
Radius		*	*	*
Ulna	*		*	*
Tibia	*	*		*
Fibula	*	*	*	

65% of bone length

Bone	Radius	Ulna	Tibia	Fibula
Radius		*	*	*
Ulna	*		*	*
Tibia	*	*		*
Fibula	*	*	*	

80% of bone length

Bone	Radius	Ulna	Tibia	Fibula
Radius		*	*	*
Ulna	*		*	*
Tibia	*	*		*
Fibula	*	*	*	

* indicates significance at p <0.05

Table K.2. Total Area (TA) pairwise comparisons by slice location in distal limb elements

20% of bone length

Bone	Radius	Ulna	Tibia	Fibula
Radius		*	*	*
Ulna	*		*	NS
Tibia	*	*		*
Fibula	*	NS	*	

35% of bone length

Bone	Radius	Ulna	Tibia	Fibula
Radius		NS	*	*
Ulna	NS		*	NS
Tibia	*	*		*
Fibula	*	NS	*	

50% of bone length

Bone	Radius	Ulna	Tibia	Fibula
Radius		*	*	NS
Ulna	*		*	*
Tibia	*	*		*
Fibula	NS	*	*	

65% of bone length

Bone	Radius	Ulna	Tibia	Fibula
Radius		*	*	*
Ulna	*		*	*
Tibia	*	*		*
Fibula	*	*	*	

80% of bone length

Bone	Radius	Ulna	Tibia	Fibula
Radius		*	*	*
Ulna	*		*	*
Tibia	*	*		*
Fibula	*	*	*	

* indicates significance at p <0.05

Table K.3. Medullary Area (MA) pairwise comparisons by slice location in distal limb elements

20% of bone length

Bone	Radius	Ulna	Tibia	Fibula
Radius		*	*	*
Ulna	*		*	*
Tibia	*	*		*
Fibula	*	*	*	

35% of bone length

Bone	Radius	Ulna	Tibia	Fibula
Radius		NS	*	NS
Ulna	NS		*	*
Tibia	*	*		*
Fibula	NS	*	*	

50% of bone length

Bone	Radius	Ulna	Tibia	Fibula
Radius		*	*	*
Ulna	*		*	NS
Tibia	*	*		*
Fibula	*	NS	*	

65% of bone length

Bone	Radius	Ulna	Tibia	Fibula
Radius		NS	*	*
Ulna	NS		*	*
Tibia	*	*		*
Fibula	*	*	*	

80% of bone length

Bone	Radius	Ulna	Tibia	Fibula
Radius		*	*	*
Ulna	*		*	*
Tibia	*	*		*
Fibula	*	*	*	

* indicates significance at p <0.05

Table K.4. Percent Cortical Area ((CA/TA) x 100) pairwise comparisons by slice location in distal limb elements

20% of bone length

Bone	Radius	Ulna	Tibia	Fibula
Radius		*	*	*
Ulna	*		*	*
Tibia	*	*		*
Fibula	*	*	*	

35% of bone length

Bone	Radius	Ulna	Tibia	Fibula
Radius		NS	*	NS
Ulna	NS		*	NS
Tibia	*	*		*
Fibula	NS	NS	*	

50% of bone length

Bone	Radius	Ulna	Tibia	Fibula
Radius		NS	*	*
Ulna	NS		*	*
Tibia	*	*		*
Fibula	*	*	*	

65% of bone length

Bone	Radius	Ulna	Tibia	Fibula
Radius		NS	*	NS
Ulna	NS		*	NS
Tibia	*	*		*
Fibula	NS	NS	*	

80% of bone length

Bone	Radius	Ulna	Tibia	Fibula
Radius		*	*	*
Ulna	*		*	NS
Tibia	*	*		*
Fibula	*	NS	*	

* indicates significance at p <0.05

Table K.5. Second moment area about ML axis (I_x) pairwise comparisons by slice location in distal limb elements

20% of bone length

Bone	Radius	Ulna	Tibia	Fibula
Radius		*	*	*
Ulna	*		*	*
Tibia	*	*		*
Fibula	*	*	*	

35% of bone length

Bone	Radius	Ulna	Tibia	Fibula
Radius		NS	*	*
Ulna	NS		*	*
Tibia	*	*		*
Fibula	*	*	*	

50% of bone length

Bone	Radius	Ulna	Tibia	Fibula
Radius		*	*	*
Ulna	*		*	*
Tibia	*	*		*
Fibula	*	*	*	

65% of bone length

Bone	Radius	Ulna	Tibia	Fibula
Radius		*	*	*
Ulna	*		*	*
Tibia	*	*		*
Fibula	*	*	*	

80% of bone length

Bone	Radius	Ulna	Tibia	Fibula
Radius		*	*	*
Ulna	*		*	*
Tibia	*	*		*
Fibula	*	*	*	

* indicates significance at p <0.05

Table K.6. Second moment area about AP axis (I_y) pairwise comparisons by slice location in distal limb elements

20% of bone length

Bone	Radius	Ulna	Tibia	Fibula
Radius		*	*	*
Ulna	*		*	*
Tibia	*	*		*
Fibula	*	*	*	

35% of bone length

Bone	Radius	Ulna	Tibia	Fibula
Radius		*	*	*
Ulna	*		*	*
Tibia	*	*		*
Fibula	*	*	*	

50% of bone length

Bone	Radius	Ulna	Tibia	Fibula
Radius		*	*	*
Ulna	*		*	*
Tibia	*	*		*
Fibula	*	*	*	

65% of bone length

Bone	Radius	Ulna	Tibia	Fibula
Radius		NS	*	*
Ulna	NS		*	*
Tibia	*	*		*
Fibula	*	*	*	

80% of bone length

Bone	Radius	Ulna	Tibia	Fibula
Radius		*	*	*
Ulna	*		*	*
Tibia	*	*		*
Fibula	*	*	*	

* indicates significance at p <0.05

Table K.7. Polar section moment of area (J) pairwise comparisons by slice location in distal limb elements

20% of bone length

Bone	Radius	Ulna	Tibia	Fibula
Radius		*	*	*
Ulna	*		*	*
Tibia	*	*		*
Fibula	*	*	*	

35% of bone length

Bone	Radius	Ulna	Tibia	Fibula
Radius		*	*	*
Ulna	*		*	*
Tibia	*	*		*
Fibula	*	*	*	

50% of bone length

Bone	Radius	Ulna	Tibia	Fibula
Radius		*	*	*
Ulna	*		*	*
Tibia	*	*		*
Fibula	*	*	*	

65% of bone length

Bone	Radius	Ulna	Tibia	Fibula
Radius		*	*	*
Ulna	*		*	*
Tibia	*	*		*
Fibula	*	*	*	

80% of bone length

Bone	Radius	Ulna	Tibia	Fibula
Radius		*	*	*
Ulna	*		*	*
Tibia	*	*		*
Fibula	*	*	*	

* indicates significance at p <0.05

Table K.8. Maximum second moment area (I_{max}) pairwise comparisons by slice location in distal limb elements

20% of bone length

Bone	Radius	Ulna	Tibia	Fibula
Radius		*	*	*
Ulna	*		*	*
Tibia	*	*		*
Fibula	*	*	*	

35% of bone length

Bone	Radius	Ulna	Tibia	Fibula
Radius		*	*	*
Ulna	*		*	*
Tibia	*	*		*
Fibula	*	*	*	

50% of bone length

Bone	Radius	Ulna	Tibia	Fibula
Radius		*	*	*
Ulna	*		*	*
Tibia	*	*		*
Fibula	*	*	*	

65% of bone length

Bone	Radius	Ulna	Tibia	Fibula
Radius		NS	*	*
Ulna	NS		*	*
Tibia	*	*		*
Fibula	*	*	*	

80% of bone length

Bone	Radius	Ulna	Tibia	Fibula
Radius		*	*	*
Ulna	*		*	*
Tibia	*	*		*
Fibula	*	*	*	

* indicates significance at p <0.05

Table K.9. Minimum second moment area (I_{min}) pairwise comparisons by slice location in distal limb elements

20% of bone length

Bone	Radius	Ulna	Tibia	Fibula
Radius		*	*	*
Ulna	*		*	*
Tibia	*	*		*
Fibula	*	*	*	

35% of bone length

Bone	Radius	Ulna	Tibia	Fibula
Radius		*	*	*
Ulna	*		*	*
Tibia	*	*		*
Fibula	*	*	*	

50% of bone length

Bone	Radius	Ulna	Tibia	Fibula
Radius		NS	*	*
Ulna	NS		*	*
Tibia	*	*		*
Fibula	*	*	*	

65% of bone length

Bone	Radius	Ulna	Tibia	Fibula
Radius		*	*	*
Ulna	*		*	*
Tibia	*	*		*
Fibula	*	*	*	

80% of bone length

Bone	Radius	Ulna	Tibia	Fibula
Radius		*	*	*
Ulna	*		*	*
Tibia	*	*		*
Fibula	*	*	*	

* indicates significance at p <0.05

Table K.10. Shape index (I_{max}/ I_{min}) pairwise comparisons by slice location in distal limb elements

20% of bone length

Bone	Radius	Ulna	Tibia	Fibula
Radius		*	*	*
Ulna	*		NS	*
Tibia	*	NS		*
Fibula	*	*	*	

35% of bone length

Bone	Radius	Ulna	Tibia	Fibula
Radius		*	*	*
Ulna	*		*	*
Tibia	*	*		NS
Fibula	*	*	NS	

50% of bone length

Bone	Radius	Ulna	Tibia	Fibula
Radius		*	*	*
Ulna	*		*	NS
Tibia	*	*		*
Fibula	*	NS	*	

65% of bone length

Bone	Radius	Ulna	Tibia	Fibula
Radius		*	*	*
Ulna	*		*	*
Tibia	*	*		NS
Fibula	*	*	NS	

80% of bone length

Bone	Radius	Ulna	Tibia	Fibula
Radius		*	*	*
Ulna	*		*	*
Tibia	*	*		*
Fibula	*	*	*	

* indicates significance at p <0.05

Table K.11. Section modulus about ML axis (Z_x) pairwise comparisons by slice location in distal limb elements

20% of bone length

Bone	Radius	Ulna	Tibia	Fibula
Radius		*	*	*
Ulna	*		*	*
Tibia	*	*		*
Fibula	*	*	*	

35% of bone length

Bone	Radius	Ulna	Tibia	Fibula
Radius		*	*	*
Ulna	*		*	*
Tibia	*	*		*
Fibula	*	*	*	

50% of bone length

Bone	Radius	Ulna	Tibia	Fibula
Radius		*	*	*
Ulna	*		*	*
Tibia	*	*		*
Fibula	*	*	*	

65% of bone length

Bone	Radius	Ulna	Tibia	Fibula
Radius		*	*	*
Ulna	*		*	*
Tibia	*	*		*
Fibula	*	*	*	

80% of bone length

Bone	Radius	Ulna	Tibia	Fibula
Radius		*	*	*
Ulna	*		*	*
Tibia	*	*		*
Fibula	*	*	*	

* indicates significance at p <0.05

Table K.12. Section modulus about AP axis (Z_y) pairwise comparisons by slice location in distal limb elements

20% of bone length

Bone	Radius	Ulna	Tibia	Fibula
Radius		*	*	*
Ulna	*		*	*
Tibia	*	*		*
Fibula	*	*	*	

35% of bone length

Bone	Radius	Ulna	Tibia	Fibula
Radius		*	*	*
Ulna	*		*	*
Tibia	*	*		*
Fibula	*	*	*	

50% of bone length

Bone	Radius	Ulna	Tibia	Fibula
Radius		NS	*	*
Ulna	NS		*	*
Tibia	*	*		*
Fibula	*	*	*	

65% of bone length

Bone	Radius	Ulna	Tibia	Fibula
Radius		*	*	*
Ulna	*		*	*
Tibia	*	*		*
Fibula	*	*	*	

80% of bone length

Bone	Radius	Ulna	Tibia	Fibula
Radius		*	*	*
Ulna	*		*	*
Tibia	*	*		*
Fibula	*	*	*	

* indicates significance at p <0.05

Table K.13. Polar section modulus (Z_p) pairwise comparisons by slice location in distal limb elements

20% of bone length

Bone	Radius	Ulna	Tibia	Fibula
Radius		*	*	*
Ulna	*		*	*
Tibia	*	*		*
Fibula	*	*	*	

35% of bone length

Bone	Radius	Ulna	Tibia	Fibula
Radius		*	*	*
Ulna	*		*	*
Tibia	*	*		*
Fibula	*	*	*	

50% of bone length

Bone	Radius	Ulna	Tibia	Fibula
Radius		*	*	*
Ulna	*		*	*
Tibia	*	*		*
Fibula	*	*	*	

65% of bone length

Bone	Radius	Ulna	Tibia	Fibula
Radius		*	*	*
Ulna	*		*	*
Tibia	*	*		*
Fibula	*	*	*	

80% of bone length

Bone	Radius	Ulna	Tibia	Fibula
Radius		*	*	*
Ulna	*		*	*
Tibia	*	*		*
Fibula	*	*	*	

* indicates significance at p <0.05

Table K.14. Maximum section modulus (Z_{max}) pairwise comparisons by slice location in distal limb elements

20% of bone length

Bone	Radius	Ulna	Tibia	Fibula
Radius		*	*	*
Ulna	*		*	*
Tibia	*	*		*
Fibula	*	*	*	

35% of bone length

Bone	Radius	Ulna	Tibia	Fibula
Radius		*	*	*
Ulna	*		*	*
Tibia	*	*		*
Fibula	*	*	*	

50% of bone length

Bone	Radius	Ulna	Tibia	Fibula
Radius		*	*	*
Ulna	*		*	*
Tibia	*	*		*
Fibula	*	*	*	

65% of bone length

Bone	Radius	Ulna	Tibia	Fibula
Radius		*	*	*
Ulna	*		*	*
Tibia	*	*		*
Fibula	*	*	*	

80% of bone length

Bone	Radius	Ulna	Tibia	Fibula
Radius		*	*	*
Ulna	*		*	*
Tibia	*	*		*
Fibula	*	*	*	

* indicates significance at p <0.05

Table K.15. Maximum section modulus (Z_{min}) pairwise comparisons by slice location in distal limb elements

20% of bone length

Bone	Radius	Ulna	Tibia	Fibula
Radius		*	*	*
Ulna	*		*	*
Tibia	*	*		*
Fibula	*	*	*	

35% of bone length

Bone	Radius	Ulna	Tibia	Fibula
Radius		*	*	*
Ulna	*		*	*
Tibia	*	*		*
Fibula	*	*	*	

50% of bone length

Bone	Radius	Ulna	Tibia	Fibula
Radius		NS	*	*
Ulna	NS		*	*
Tibia	*	*		*
Fibula	*	*	*	

65% of bone length

Bone	Radius	Ulna	Tibia	Fibula
Radius		*	*	*
Ulna	*		*	*
Tibia	*	*		*
Fibula	*	*	*	

80% of bone length

Bone	Radius	Ulna	Tibia	Fibula
Radius		*	*	*
Ulna	*		*	*
Tibia	*	*		*
Fibula	*	*	*	

* indicates significance at $p < 0.05$

VITA

Alice Fazlollah Gooding was born outside of Atlanta, Georgia. She completed her B.A. in Anthropology, Critical Theory, and Social Justice in 2008 at Occidental College in Los Angeles, California. She began her graduate career in anthropology at the University of Georgia, earning at M.S. in Archaeological Resource Management in 2011. During her time at UGA, Alice was a graduate teaching assistant in the Medical College of Georgia's gross anatomy lab. She then moved to Knoxville, Tennessee to pursue a doctorate in biological anthropology at the University of Tennessee. She earned her Ph.D. in December 2017. During her tenure in graduate school, Alice was a graduate teaching assistant for introductory courses in osteology and biological anthropology. She served as the volunteer coordinator for the UT Forensic Anthropology Center for two years. Alice is now an Assistant Professor of Anthropology at Kennesaw State University in Kennesaw, Georgia where she continues to pursue her research and teaching goals.